Non-cooperative game theoretical control for green and efficient energy communities

Nicola Mignoni

Non-cooperative Game Theoretical Control for Green and Efficient Energy Communities

Thesis submitted for the degree of Philosophiae Doctor

Department of Electrical and Information Engineering
Politecnico di Bari

Tutors
Prof. Engr. *Mariagrazia Dotoli*
Prof. Engr. *Raffaele Carli*

2025

La borsa di dottorato è stata cofinanziata con risorse del Programma Operativo Nazionale Ricerca e Innovazione 2014-2020, risorse FSE REACT-EU Azione IV.4 "Dottorati e contratti di ricerca su tematiche dell'innovazione" e Azione IV.5 "Dottorati su tematiche Green"

Dissertation submitted for the degree of *Philosophiae Doctor* in Electrical and Information Engineering (XXXVII cycle)

Title:
Non-cooperative Game Theoretical Control for Green and Efficient Energy Communities

Ph.D. Candidate:
Nicola Mignoni, Politecnico di Bari (Bari, Italy)

Tutors:
Prof. Engr. *Mariagrazia Dotoli*, Politecnico di Bari (Bari, Italy)
Prof. Engr. *Raffaele Carli*, Politecnico di Bari (Bari, Italy)

Coordinator:
Prof. Engr. *Mario Carpentieri*, Politecnico di Bari (Bari, Italy)

External Reviewers:
Prof. Engr. *Valeriy Vyatkin*, Aalto University (Espoo, Finland)
Prof. Engr. *Johan Driesen*, KU Leuven (Leuven, Belgium).

Last version:
February 19, 2025

Abstract

Energy communities are socially driven initiatives that emphasize collective participation in energy production, distribution, and consumption. Differently from smart grids, which focus on the infrastructural and technological side, energy communities are concerned with the market and economical incentive design, aiming at guaranteeing a socially, environmentally, and economically sustainable energy grid. Thus, the study of energy communities is tightly intertwined with the analysis of the behavior that arises when several agents are faced with conflicting needs and resource scarcity. Non-cooperative game theory has proved to be a solid tool for tackling the challenge of optimally controlling energy communities: this dissertation aims to contribute to the topic by addressing aspects such as transactive market design, plug-in electric vehicles (PEVs) integration, and learning-based decision-making.

In particular, the first part explores the economical and operational design of energy communities from the *transactive* perspective. Such a term refers to relational patterns between two or more agents that are based on "transactions", i.e., on the exchange of one or more commodities or services. Such a setup can be effectively studied under the lens of game theory since any transaction, in order to be successful, requires two or more parties to agree on the quantities to be exchanged. Energy markets are perfectly suitable to be considered as transactive environments, because of the ubiquitous need that agents have to exchange energy. In particular, the analysis focuses on the modelling of energy communities with independent and selfish agents, as well as the subsequent design of decentralized and distributed schemes for the equilibrium seeking of the arising non-cooperative game.

Among the diverse actors that characterize the modern energy community, PEVs are the ones that, in the last decade, have caused a consistent push towards a more decentralized and dynamic energy market system. This is due to their inherent unpredictability with respect to their energy demand, which serves the purpose of recharging their batteries. Such a unilateral energy exchange gives rise to the V1G-based energy market. However, being equipped with storage devices, PEVs can be considered as non-static ESSs, which can be used by the grid operators for tasks such as voltage and frequency regulation, but also by prosumers and actors that can experience temporary energy surpluses. Such a bilateral exchange is captured by the V2B and – in the most general sense – V2X protocols. The second part of this dissertation frames PEVs as non-cooperative agents, which participate in the energy market with the aim of recharging their batteries in the most economically efficient way, or providing temporary storage service for a fee.

The two aforementioned research directions frame the agents in the energy community as rational entities, whose prerogatives are described by an optimization problem constituted by a certain cost function to minimize and operational constraints to satisfy. Such an approach is reasonable when modelling a perfectly rational entity, e.g., control systems that solely follow its instructions. However, as many grid actors are backed by the decisions and actions made by people, the perfect "rationality assumption" becomes unrealistic: people are often driven by habits and belief systems that do not necessarily yield the "optimal" decisions. The third part collects the result of a work-in-progress which aims at defining a *learning-based* equilibrium – and its related seeking methods – where the agents' behavior is not modelled by an optimization problem, where its objective expresses some cost (utility) to minimize (maximize), but through a neural network. The idea is to capture behavioral patterns on the basis of existing data, representing the agents' response to the environment and the other players' strategies.

"Iam enim coeperam velle videri sapiens plenus poena mea et non flebam, insuper et inflabar scientia."

Agustinus, *Confessiones*

"Il faut imaginer Sisyphe heureux."

A. Camus, *Le Mythe de Sisyphe*

Contents

Preface

This thesis is submitted in partial fulfilment of the requirements for the degree of *Philosophiae Doctor* in Electrical and Information Engineering at the *Politecnico di Bari*. This work was supported by the Italian Ministry of Research through PON "Ricerca e Innovazione" 2014-2020, REACT-EU Azione IV.5: "*Dottorati su Tematiche Green*".

The research presented in this dissertation was conducted at the Decision and Control Laboratory of Politecnico di Bari, under the supervision of Profs. Mariagrazia Dotoli and Raffaele Carli, between January 2022 and December 2024.

The content of the present dissertation is original; when using excerpts from other literature sources, references are duly inserted. The majority of the content of the Thesis comprises the research work that has been published, is in press, or is under review, where I feature among the primary – i.e., first or second – authors. Professors **Mariagrazia Dotoli** and **Raffaele Carli** feature as authors in all the publications referenced in this Preface, where they mostly contributed during the modelling, conceptualization, and proofreading, providing constant supervision and feedback over all the research literature here referenced.

In introducing the topic of this Thesis, a review [1] and a book chapter [9], both submitted for publication, have been partially used in Chapter , which serves as the introduction of this work, providing the context of each Chapter, as well as describing the conceptual subdivision of each Part of this dissertation. In particular, reference [9] has been written in collaboration with Dr. **Paolo Scarabaggio** (Politecnico di Bari, Bari, Italy).

Chapters 2 and 5 are based on [10] and [2], respectively, which have been developed together with Dr. **Juan Piazuelo-Martinez**, Prof. **Carlos Ocampo-Martinez** (both from UPC Barcelona, Barcelona, Spain), and Prof. **Nicanor Quijano** (UniAndes, Bogotá, Colombia). They contributed to conceptualization and modelling phases, and provided decisive support on the technical aspects of population games and evolutionary dynamics, while I worked on the conceptualization, energy community model and the implementation of the numerical results. Chapters 3 and 4 heavily rely on [11], [3], and [12], [4], where I contributed on the several aspects of the articles in their entirety.

Finally, Chapters 6 and 7, based on [13] and [14] have been developed in collaboration with Dr. **Paolo Scarabaggio** (Politecnico di Bari, Bari, Italy), where he mainly contributed to the modelling and numerical results, while I worked on the final development of the conceptualization of the learning-based approach and the subsequent equilibrium seeking solutions.

An effort has been made with the aim of keeping the general notation consistent throughout the Chapters. In order to ease the reading, each Chapter is equipped with its own *Notation* paragraph, in order to preserve the locality of specific symbols employed for the purposes of the Chapter at hand. Shorter proofs have been left as part of the Chapters, while the longer ones have been deferred to Appendix A for the interested reader.

Albeit my research project had its focus on multi-agent systems applications for energy communities, I was fortunate enough to be left free to pursue "side quests", spanning photovoltaics [5], [15] and agrivoltaics [6], transportation [16] and logistic systems [17], [7], games [8], variational inequalities [18], scientometrics [19], and diverse applications of game theoretical methods [20].

The full list of research works is reported hereafter.

List of Papers Written by the Author

International Journal Articles

[1] Scarabaggio, P., Mignoni, N., Carli, R., *et al.*, "Control of energy storage systems in power networks: A review from the perspectives of grid services," *Annual Reviews in Control*, (**under review**).

[2] Martinez-Piazuelo, J., Mignoni, N., Carli, R., Ocampo-Martinez, C., Quijano, N., and Dotoli, M., "Real-time power allocation for plug-in electric vehicles via event-triggered evolutionary dynamics," *Applied Energy*, (**under review**).

[3] Mignoni, N., Scarabaggio, P., Carli, R., and Dotoli, M., "Control frameworks for transactive energy storage services in energy communities," *Control Engineering Practice*, vol. 130, p. 105 364, 2023.

[4] Mignoni, N., Carli, R., and Dotoli, M., "Distributed noncooperative mpc for energy scheduling of charging and trading electric vehicles in energy communities," *IEEE Transactions on Control Systems Technology*, 2023.

[5] Mignoni, N., Carli, R., and Dotoli, M., "Layout optimization for photovoltaic panels in solar power plants via a minlp approach," *IEEE Transactions on Automation Science and Engineering*, 2023.

[6] Mignoni, N., Carli, R., and Dotoli, M., "Controlling tilt orientation for optimal crop shading and power generation in agrivoltaic plants," *IEEE Transactions on Control Systems Technology*, (**under review**).

[7] Mignoni, N., Scarabaggio, P., Carli, R., and Dotoli, M., "A framework for the automated and optimal design of vertical lift modules," *IEEE Transactions on System, Man, and Cybernetics*, (**2nd review round**).

[8] Mignoni, N., Carli, R., and Dotoli, M., "Optimal decision strategies for the generalized cuckoo card game," *IEEE Transactions on Games*, vol. 16, no. 1, pp. 185–194, 2023.

Book Chapters

[9] Mignoni, N., Scarabaggio, P., Carli, R., and Dotoli, M., *An overview on non-centralized control of multi-energy systems for the optimal operations of energy communities*, Energy Systems Integration for Multi-Energy Systems From Operation to Planning in the Green Energy Context. Springer, (**in press**).

International Conference Proceedings

[10] Mignoni, N., Martinez-Piazuelo, J., Carli, R., Ocampo-Martinez, C., Quijano, N., and Dotoli, M., "A game-theoretical control framework for transactive energy trading in energy communities," in *2024 European Control Conference (ECC)*, IEEE, 2024, pp. 786–791.

[11] Mignoni, N., Scarabaggio, P., Carli, R., and Dotoli, M., "Game theoretical control frameworks for multiple energy storage services in energy communities," in *2022 8th International Conference on Control, Decision and Information Technologies (CoDIT)*, IEEE, vol. 1, 2022, pp. 1580–1585.

[12] Mignoni, N., Carli, R., and Dotoli, M., "A noncooperative stochastic rolling horizon control framework for v1g and v2b scheduling in energy communities," in *2023 European Control Conference (ECC)*, IEEE, 2023, pp. 1–6.

[13] Scarabaggio, P., Mignoni, N., Carli, R., and Dotoli, M., "Equilibrium seeking in learning-based noncooperative nash games," in *2024 IEEE Conference on Decision and Control*, IEEE, (**in press**).

[14] Scarabaggio, P., Mignoni, N., Carli, R., and Dotoli, M., "Model predictive control with recursive multi-step input convex lipschitz neural networks: An application to smart buildings," in *2024 IEEE International Conference on Systems, Man, and Cybernetics (SMC)*, IEEE, 2024.

[15] Mignoni, N., Carli, R., and Dotoli, M., "An optimization tool for displacing photovoltaic arrays in polygonal areas," in *IEEE EUROCON 2023-20th International Conference on Smart Technologies*, IEEE, 2023, pp. 573–578.

[16] Mignoni, N., Scarabaggio, P., Carli, R., and Dotoli, M., "A compact convex quadratically constrained formulation for a class of delivery schedule problems," in *2024 IEEE Conference on Decision and Control*, IEEE, (**in press**).

[17] Mignoni, N., Scarabaggio, P., Carli, R., and Dotoli, M., "Optimizing debris recycling in space manufacturing and logistics: A conceptual model," in *12th International Conference on Interoperability for Enterprise Systems and Applications*, (**in press**).

[18] Mignoni, N., Rahimi Baghbadorani, R., Mohajerin Esfahani, P., Carli, R., Dotoli, M., and Grammatico, S., "`monviso`: A python package for solving monotone variational inequalities," in *2025 European Control Conference (ECC)*, IEEE, (**under review**).

[19] Mignoni, N., Scarabaggio, P., Carli, R., and Dotoli, M., "A markowitz optimization approach for automating the italian research quality monitoring and evaluation," in *2024 IEEE 20th International Conference on Automation Science and Engineering (CASE)*, IEEE, 2024, pp. 1741–1746.

[20] Mignoni, N., Scarabaggio, P., Marina Caselli, S., Carli, R., and Dotoli, M., "Generalized nash equilibrium seeking for crop mix selection in sustainable agriculture," in *2024 IEEE International Humanitarian Technologies Conference (IHTC)*, IEEE, 2024.

Acknowledgements

Around 3 years ago, I started my PhD almost on a whim, when, right out of graduate school, one tries to figure out what to do with their own life.

I crossed paths with many people during these 36 months, all of them leaving something that, somehow, made me a better researcher and (hopefully) a better person. Profs. Mariagrazia Dotoli and Raffaele Carli decided to have me as a PhD student, putting more faith in me than I probably have in myself. I want to thank both of them for all the support, guidance, patience, and academic freedom they granted me during these years.

I'm grateful to have met all the people who passed through the Decision and Control Laboratory (D&C Lab) at Politecnico di Bari, the research group that hosted me during my PhD, and in particular, I want to thank Dr. Paolo Scarabaggio for being a tireless and conscientious colleague and friend, at the common denominator of most of the activities I carried out at the D&C Lab.

Between April and September 2024, I had the privilege of visiting the Delft Center for System (DCSC) and Control at TU Delft, The Netherlands, under the supervision of Prof. Sergio Grammatico. I want to thank him for the hospitality and the productive discussions. A warm thanks goes to all the people I met during those months for the technical conversations, laughs, beers, foosball games, and for having made Delft a place where I left a piece of my heart.

During November 2024 I was honored to visit the *Departament d'Enginyeria de Sistemes, Automàtica i Informàtica Industrial* (ESAII) at UPC Barcelona, Spain, under the supervision of Prof. Carlos Ocampo-Martinez, who can seamlessly and effectively merge technical insights and hilarious jokes in the same sentence. I want to thank him for this opportunity, and the fruitful and fun conversations during those weeks in Spain. Some work of this thesis has been developed with Juan Martinez-Piazuelo: I want to thank him for being the best colleague one can hope for and for his hospitality during my stay in Barcelona.

A special thank goes to all the members of the IEEE RAS Student Activities Committee, which I was honored to be part of, as well as the IEEE RAS staff. With many of them, I shared both the stressful and the happy moments during the CASE24 and ICRA40 conferences that put me out of my comfort zone of being a "lab rat" and reminded me of what it means to be part of a volunteering reality.

Postremo sed non minimum, my family and closest friends have always been a discreet but ever-present reference, always at reach for support and advice. I want to thank them for gently nudging me in the right direction when frustration and tiredness can get the better of me.

Acronyms

ADALM accelerated distributed augmented Lagrangian method. 6, 46, 47, 55, 56, 58, 59, 63, 64

ADMM alternating direction method of multipliers. 5, 12, 18

ALM augmented Lagrangian method. 31, 32, 34, 55

CESS cloud energy storage system. 25, 26

CEV charging electric vehicle. 47, 48, 49, 50, 51, 53, 54, 56, 57, 59, 61, 63

DMPC distributed model predictive control. 47

EGT evolutionary game theory. 69, 70, 71

ER energy retailer. 6, 12, 16, 20, 27, 28, 68, 70, 71, 81

ESS energy storage system. 17, 20, 21, 24, 25, 26, 27, 28, 29, 36, 38, 39, 49, 103

GNE generalized Nash equilibrium. 5, 11, 12, 15, 16, 19, 21, 30, 31, 54, 55, 57

GNEP generalized Nash equilibrium problem. 5, 6, 11, 12, 14, 15, 16, 17, 18, 19, 21, 30, 31, 45, 46, 54, 55

HDS hybrid dynamical system. 72, 79, 80

HVAC heating, ventilation, and air conditioning. 7, 99

LBE learning-based equilibrium. 92, 93, 94

ML machine learning. 87, 88

MPC model predictive control. 6, 7, 46, 47, 53, 57, 59, 61, 64, 98, 99, 100, 102, 103, 104, 105

NE Nash equilibrium. 3, 6, 54, 70, 77, 80, 87, 89

NEP Nash equilibrium problem. 89

NN neural network. 7, 99, 101, 102, 103, 104

PEV plug-in electric vehicle. 2, 5, 6, 16, 45, 46, 47, 49, 50, 51, 53, 54, 58, 59, 60, 61, 63, 64

SD standard deviation. 81

SE shared economy. 25

TEV trading electric vehicle. 47, 48, 49, 51, 52, 53, 54, 56, 57, 59, 61, 62, 63, 64

TN truncated normal. 60

VESS virtual energy storage system. 25, 26

vGNE variational generalized Nash equilibrium. 15, 16, 19

VI variational inequality. 31, 55

VPP virtual power plant. 25

Chapter 1

Introduction

The transition from wood and animal power to coal during the Industrial Revolution marked a historical shift in energy consumption, driven by the need for more efficient and scalable energy sources as economies industrialized. This transition laid the groundwork for modern energy systems, where coal became the dominant energy source, facilitating advancements in energy generation and transportation technologies [1]. The discovery of oil and natural gas further transformed the energy landscapes, particularly in the twentieth century, as these resources became integral to transportation and household energy needs [2]. The last milestone in the evolution of the energy infrastructure is constituted by the shift from the traditional heat/coal-based centralized systems to a distributed and multi-source grid.

This is the current step where research and engineering efforts focus on ensuring a smooth transition. In fact, among the several concerns affecting international decisions for the medium-long term, the energy transition is one of the most discussed matters. The effort that has been made [3], as well as the ones *in fieri* [4], principally aim at the efficiency of the power grid, its reliability and, most importantly, its overall environmental sustainability. The latter, in particular, regards one of the objectives of net-zero greenhouse emissions by 2050. However, the desire of developing a greener and clean grid infrastructure is not the only force pushing towards change. The proliferation of cheaper and alternative generation sources, such as eolic and photovoltaic, is enabling their adoption by both energy companies and private citizens, attracted by the grid-independence, and consequent economic advantages, that those technologies bring [5]. Fully implementing such a transition project comes with numerous difficulties, both research-wise and from a practical engineering standpoint, as it involves the simultaneous advancements of a diverse, and often unrelated, knowledge domain.

Differently from the traditional "few-retailers to multiple-users" architecture, where the main focus was put on the mere electrical design aspect, the modern paradigm comprise multiple and diverse energy actors. The natural question, then, arises: *how do we coordinate them to ensure an operational feasible working state?* Such a research proposition sparked the interest of the control community on the matter of energy systems [6]. Until this point, the control issues that were tackled regarded the more “classic” problems of, e.g., stability and frequency control [7, Part 3]. Now, instead, the non-centralized design of the grid introduces new challenges and problems: demand-side management [8], pricing mechanisms [9], and market design [10] are just few of the issues that can be effectively tackled through control and automation techniques. The common denominator for all of those is the need of distributing a limited resource, i.e., energy, among agents whose prerogatives are non-symmetrical, and are characterized by a more or less extended degree of independence. Game theory provides the tools for analyzing such a scenario, where the competitiveness and selfishness of the actors constituting the modern energy grid is not non-negligible [11]. In the following, we explore the aspects at the intersection of such topics, providing the needed context of this dissertation.

1.1 *Energy Communities*: the New Energy Infrastructure Paradigm

One of the fundamental landmarks in the evolution of the energy infrastructure was the advent of the *smart grid*, whose earliest mentions in the scientific literature date back to the early 2010s [12]. A smart grid can be described as an electric power grid infrastructure that integrates digital technology to enhance the efficiency, reliability, and sustainability of electricity supply. While the traditional grid structure comprises a central power

retailer that feeds the network in a top-down approach, smart grids are comprised by i) non-coal based energy sources, such as, e.g., photovoltaic, eolic, hydroelectric sources; ii) intermittent energy sources and demands; iii) grid agents that are able to both feed from the main grid, but also independently produce energy, possibly re-injecting surplus back in the main grid. Such a description is not exhaustive, but it covers the main aspects that differentiate smart grid from the older paradigm. The first two points are strictly related, as the majority of renewable resources, albeit cleaner, suffer from the impossibility of providing a constant output. This issues can be effectively tackled by the use of storage system, capable of stocking energy during off-peak periods and releasing them when the demand surpasses the generation. The third point highlights a fundamental aspect of smart grids, i.e., the independence of grid actors equipped with local and private production means. These are referred to as *prosumers* – from the crasis of *producers* and *consumers* – and constitute the element that characterize the inherent dynamism of smart grids. Like prosumers, PEVs are a further agent that is characterized by independence and intermittent demand, instead of generation. The proliferation of PEVs in the modern urban environment enriches the smart grid landscape, as their ever-growing numbers makes satisfying their demand a non-trivial task.

Such a grid structure has been studied for more than a decade, and many successful deployments prove the goodness of such concept. From the earliest implementations, such as the Italian *Telegestore* [13], to the Smart Grid Project promoted by the American Recovery and Reinvestment Act [14], they constitute a trend that is in continuous grow, as witnessed by their market value [15]. During the last few years, a new conceptualization has start to be investigated by the research community, which is commonly known as *energy community* [16]. While they both represent innovative approaches to modernizing energy systems, they bear differences in scope, functionality, and objectives. A smart grid encompass the electrical infrastructure need to realize a grid network that reflects the aforementioned description. In contrast, energy communities are socially driven initiatives that emphasize collective participation in energy production, distribution, and consumption. These communities often operate as a local, decentralized energy hub where members collaborate to generate and share energy, frequently – but not solely – from renewable sources [17]. Energy communities prioritize local empowerment, economic benefits, and sustainability by encouraging citizen engagement and promoting energy autonomy [18]. While smart grids focus on optimizing large-scale energy infrastructure through technological advancements, energy communities center on fostering a cooperative model of energy governance at the community level. Despite these differences, smart grids and energy communities indeed complement each other: the integration of smart grid technologies into energy communities can enhance their functionality if appropriate mechanism design pattern are developed with the aim of improving the collective welfare [19]. In other terms, smart grids provide the technical foundation that empowers energy communities to thrive, demonstrating the potential for these two concepts to coexist and mutually reinforce sustainable energy transitions. With respect to the well-known sustainability pillars, energy communities delve into the social one by focusing on the aggregate impact that the single agents have on the entire system. This is not merely measured in terms of economic performance, but also with respect to crucial metrics such as carbon emission, traffic congestion, and development indicators such as *benessere equo e sostenibile*[1]. On such premises, it becomes evident that the traditional tools used to study smart grids are not always suitable to tackle problems whose social component often overpass the technological one.

[1]"Fair and sustainable welfare" is an index developed by ISTAT (Italian National Institute of Statistics) and CNEL (National Council of Economy and Labour) to assess societal progress beyond traditional economic measures like GDP. It incorporates social and environmental dimensions, highlighting the importance of well-being and sustainability in evaluating quality of life.

1.2 Selfishness, Robustness, and Rationality in Non-cooperative Environments

A set of problems that are tangent to multiple disciplines, such as economics, behavioral science, mathematics, and computer science deals with finding a solution to a situation where two or more involved party make decisions that affect the outcome of the others. More often than not, this kind of interaction brings unwanted effect to the other parties, resulting in situation of *conflict*. The collective of tools, methods, and technique that study such problems constitute the broad field of *game theory*. From the seminal work of Nash in 1952 [20], important progresses have been made with the common goal of finding ways to resolve scenarios where the decision of the players involved are intertwined. Such a resolution is concretely sought by looking for *equilibria*, i.e., states where the all the players do not change their strategy any longer. Albeit several equilibrium concepts have been developed, the most employed and studied one is the NE. Informally, its states than an equilibrium solution is reached when all agents' *best response* stop deviating anymore. The best response is the best solution each player can come up with, given the current strategy all other players are taking. The reason that makes the NE the most popular equilibrium concept is the inherent fundamental assumption that players always behave selfishly. This pessimistic view of their behavior guarantees a certain degree of robustness, as it accounts for the worst case for the collective well-being. Considering agents driven by their best response also implies the former to be perfectly rational, i.e., capable of always making the optimal choice, give the current circumstances. When modelling human behavior, such an assumption becomes restrictive. Several alternatives set-ups, where the players' rationality is considered as "bounded", exists; notable examples are evolutionary games [21].

From its definition, it can be seen how equilbria in game theory are congruent to the ones that are studied in the theory of dynamical systems. However, differently from those where – even for strongly non-linear system – computational tools effectively come in aid, determining (at least one) game equilibrium is (generally) a hard problem: in one of the most famous results in the field it was shown to be NP-hard [22]. Moreover, not all games have a NE: a typical elementary example is tic-tac-toe. Apart from side cases such as potential games [23], where results for calculating Nash equilibria are available, the current way to tackle such a problem is through the variational inequality theory [24]. Only game classes can be equivalently reformulated via such a theory; in the majority of cases the available tools are "best efforts" methods. Some of them will be discussed in the following Chapters, which consists of iterative methods whose convergence point can be proved to be an equilibrium. Nonetheless, their characterization is somehow suitable for networked applications, such as energy communities, as they allow, in some case, distributed resolution schemes that do not require the central coordinators or computation nodes.

1.3 Non-cooperative Game Theory for the Energy Community Design and Operations

The previous Section provided a condensed panoramic on non-cooperative game theory, in order to lay out the motivation of its adoption in the context of energy communities. As discussed in Section 1.2, energy communities capture the more social aspect of the smart grid infrastructure. Concretely, this resolves in the study of market structures, price dynamics, and incentive mechanisms. The non-cooperative game-theoretical framework is particularly suited for such a task. It is important to mention, however, that cooperative frameworks have been employed in the energy community realm [25]. Here, the goal is to construct a *stable* coalition of players, whose collective payoff is distributed through a suitable *characteristic function*, in such a way that no player has any incentive to leave their current coalition and join another [26]. The non-cooperative perspective is a particular case of the non-cooperative one, where all coalitions are comprised by a single

player. One of the downsides of extending the discussion to non-sigleton coalitions is the inherent combinatorial complexity of finding *stable* coalitions [27]. The most employed metrics for evaluating the nature of a coalition, e.g., the Shapely value and the nucleolus [28], heavily rely on evaluations over sets of coalitions, which are inherently combinatorial structures.

Since energy communities are dramatically affected by scalability requirements, such an approach is not ideal. Albeit the variational tools mentioned in Section 1.2 do not always capture the entire set of equilibria a general game has, they present desirable properties when applied to networked systems, as in the case of the grid infrastructure. First, it is generally desirable to maximize the amount of computation that can be performed locally, i.e., by the grid agents themselves. This mainly serves three purposes: i) it offers grid agents a certain degree of privacy [29], ii) it allows for scalable applications by not burdening central computation nodes [30], and iii) it makes the community resilient against failures [31]. The first point refers to the need for agents to exchange information in order to allow the feasible operational state of the grid. This occurs since many grid elements are affected by the collective of all the decisions agents make. A typical example is the use of shared storage systems, where it must be ensured that the overall amount of injected energy does not exceed its capacity. Either through peer-to-peer communication, or by relying on a central aggregator, agents are compelled to make part of their decisions public. Large amounts of data on energy consumption and production can map the behavioral pattern of energy actors, possibly allowing malicious entities to exploit such information to damage the single agent, as well as the entire grid [32]. When the exchange of information is unavoidable, several techniques based on obfuscation and encryption have been researched: notable examples that have been integrated into the game-theoretical realm are differential privacy [33] and blockchain-based frameworks [34]. The second point presents a further deleterious aspect of the centralization of information, i.e., the burden that the computational nodes are loaded with. Due to the ubiquitous spread of internet-of-things-based devices, the number of actors populating the energy community reaches non-negligible numbers. In such a scenario, accentrating computational tasks becomes a hardly efficient solution. Federated learning [35] is one of the possible solutions that researchers in the machine-learning community adopt to localize the training process – being the most computationally intense one – locally, i.e., on the devices living on the *edge*. Equilibrium-seeking algorithms, especially when designed following the variational framework, allow for concentrating most of the load on the agents themselves, reserving only a smaller fraction to central nodes, if the algorithm at hand requires it. Closely related to the previous one, the third point stresses the low tolerance to faults that centralized systems have. When critical workload is concentrated in a single *point of failure*, it becomes hard for the system to recover after a malfunction, affecting either the node itself or the communication channels. Some recovery schemes have been developed, most of them relying on quick algorithms that can select a new central node, in case the existing one becomes unresponsive [36]. Such solutions, however, do not tackle the problem at its root.

These three aspects that have been discussed so far constitute a further motivation for the adoption of game-theoretical tools in the context of energy communities. Apart from the need to characterize selfish and – to some extent – rational agents, architectural and infrastructural needs can not be neglected, as they represent the first landmark for ensuring the transition from purely researched ideas to concrete implementations. Non-cooperative game theory does not act as a unifying tool for tackling all of those issues, mostly because the energy community, with its underlying grid structure, is a large collection of diverse subsystems, whose numerous combinations give rise to the specific applicative case at hand. This dissertation collocates itself among the research works that aim to develop frameworks for the optimal design and operation of energy communities. In this context, the *optimality* refers to being able to simultaneously tackle the open challenges so far discussed through the lens of non-cooperative game theory, from capturing the social aspects of selfish behavior, to the privacy, scalability, and resilience that the modern energy infrastructure requires.

1.4 Contributions and Positioning of the Thesis

The content of this dissertation revolves around the application of non-cooperative game-theoretical concepts to the operational and design aspect of energy communities, with a particular focus on the market structure and the consequent interaction between all the grids agents, that are considered as selfish agents, each one equipped with their own local constraints to be satisfied and costs to be minimized.

These premises are the common denominator of the research directions that constitute the baseline of this Thesis.

- *Part I*: the first Part of the dissertation explores the energy market under the so-called *transactive* perspective, i.e., on the iteration between selfish agents whose prerogatives are accomplished through the buying and selling of common goods, i.e., energy.
- *Part II*: in this Part, we discuss PEVs, which are the energy community agents that, among the others, are characterized by a challenging degree of dynamism, as they represent intermittent loads for the grid operator, but also possible energy buffer – when inactive – for prosumers.
- *Part III*: the last Part of the dissertation represents a work-in-progress on the characterization of the energy communities' agents as selfish actors with possibly limited rationality, where we try to capture their behavior through neural networks – instead of optimization problems – and characterize the subsequent learning-based equilibrium.

The results presented in this Thesis represent the collection of the research work carried out by the authors and published in as journal articles and conference proceedings, as detailed in the Preface. The three main Parts that comprise the Thesis, as described in the following.

1.4.1 Energy Communities' Actors as Transactive Agents

The term *transactive* references a relational pattern, between two or more agents, that is based on "transactions", i.e., on the exchange of one or more commodities or services. It can be noticed immediately how such a setup can be effectively studied under the lens of game theory, since any transaction, in order to be successful, requires two or more parties to agree on the quantities to be exchanged. Energy markets are perfectly suitable to be considered as transactive environments, due to the ubiquitous need agents have for exchanging energy. Part I explores this research direction, by investigating energy community models whose operational equilibrium point can be efficiently through suitable seeking algorithms.

Several works [37] modeled energy transactions among community members and a single retailer as a GNEPs, but only considered constraint-based couplings and bipartite graph topologies, where centralized coordination is needed to reach a feasible transaction scheduling. Building on this, **Chapter 2** generalizes to cost functions coupled through aggregate price-dependent demands, arbitrary graph structures for transactions, and multiple selfish energy retailers. A distributed algorithm based on Gauss-Seidel ADMM is developed for GNE computation, with a reformulated two-block iterative process allowing parallel execution. Sufficient conditions on cost and pricing functions ensure strong monotonicity of the pseudo-gradient mapping, guaranteeing algorithm convergence and practical design guidance for energy community management.

Chapter 2 considers both the commodity quantity and their prices as quantities to be determined. However, in the current energy market structure, prices are generally fixed – e.g., by contracts, – or can be represented as functions of the exchanged energy. Such a scenario is discussed in **Chapter 3**, which introduces a novel transactive control framework to optimize energy management and sharing within a community comprising prosumers with unique demands and renewable generation, alongside service-oriented

energy storage providers that store surplus energy for a fee. The control problem focuses on scheduling energy activities through an economy-driven mechanism, enhancing supply efficiency for prosumers while creating sustainable business models for storage providers. An energy retailer, supplying conventional power, enables prosumers to trade energy with the main grid. Using a game-theoretical formulation, the chapter defines both coordinated and uncoordinated control schemes, suited to different communication architectures, and validates them through numerical/simulations in realistic scenarios. Compared to centralized methods, these approaches demonstrate superior computational performance.

1.4.2 Non-cooperative Plug-in Electric Vehicles for V1G and V2B

Among the diverse actors that characterize the modern energy community, PEVs are the ones that, in the last decade, have caused a consistent push towards a more decentralized and dynamic energy market system. This is due to their inherent unpredictability with respect to their energy demand, which serves the purpose of recharging their batteries. Such a unilateral energy exchange gives rise to the V1G-based energy market. However, being equipped with storage devices, PEVs can be considered as non-static ESSs, which can be used by the grid operators for tasks such as voltage and frequency regulation, but also by prosumers and actors that can experience temporary energy surpluses. Such a bilateral exchange is captured by the V2B and – in the most general sense – V2X protocols. This Part frames PEVs as non-cooperative agents, which participate in the energy market with the aim of recharging their batteries in the most economically efficient way, or providing temporary storage service for a fee.

Building on such a premise, and leveraging the extensive data collected by modern PEVs, this last aspect is investigated in **Chapter 4**. Here, a novel and scalable stochastic MPC method is proposed to enable prosumers to leverage long-parked PEVs as energy buffers, while simultaneously accommodating the charging needs of active PEVs. The control problem is modeled as a GNEP, solved using variational inequality theory and a distributed framework based on the ADALM, with proven sufficient conditions for convergence. The proposed MPC framework is validated through numerical simulations in realistic scenarios [38], [39].

Regarding the more traditional V1G framework, an innovative approach is introduced in **Chapter 5**, Differently from the classical setup, which equips each agent with an optimization problem to solve, here a novel hybrid event-triggered control system [40], based on population dynamics [21], is proposed. The aim is to dynamically allocate power to a fleet of PEVs supplied by a single ER with limited power. The proposed model-free real-time control strategy ensures compliance with operational constraints and achieves a stable equilibrium where all connected PEVs are fully charged, even under unknown and nonlinear battery dynamics. Using precedence functions to represent economic and performance indicators, the method seeks a NE in power allocation, enabling PEVs to adjust charging rates based on designed incentives. Additionally, the hybrid system accounts for practical events such as arrivals, departures, and charging completion. The effectiveness of the strategy is demonstrated through a numerical case study involving random PEVs' arrivals, departures, and power needs.

1.4.3 Towards Behavioral Equilibrium Seeking in Energy Communities

So far, the two aforementioned research directions frame the agents in the energy community as rational entities, whose prerogatives are described by an optimization problem constituted by a certain cost function to minimize and operational constraints to satisfy. Such an approach is reasonable when modelling a perfectly rational entity, e.g., a control system that solely follows its instructions. However, as many of the grid actors are backed by the decisions and actions made by people, the perfect "rationality assumption" becomes unrealistic: people are often driven by habits and belief systems which not necessarily yield the "optimal" decisions. This Part collects the result of a work-in-progress which aims at defining a *learning-based* equilibrium – and its related

seeking methods – where the agents' behavior is not modelled by an optimization problem, where its objective expresses some cost (utility) to minimize (maximize), but through a neural network. The idea is to capture behavioral patterns on the basis of existing data, representing the agents' response to the environment and the other players' strategies.

In particular, **Chapter 6** begins by addressing the growing complexity of agents' behavior and the practical need for convex cost functions to represent them. We integrate the effectiveness of game-theoretic frameworks in resolving conflicts over shared resources with the ability of DNNs to approximate complex agents' behavior. Departing from traditional approaches, we do not define cost functions as direct representations of agents' goals, but instead use DNNs to approximate their response actions. Under a technical assumption on DNN weights, we establish the existence and, with additional assumptions, the uniqueness of an equilibrium. To compute equilibria, we propose two fixed-point iteration algorithms and prove their convergence. These findings are applied to a non-cooperative community of smart energy users operating under a dynamic time-of-use pricing scheme.

The discussion in Chapter 6 serves the purpose of laying down the foundational aspects of the learning-based equilibrium-seeking concept. A more hands-on perspective is provided in **Chapter 7** where, building on [41], a recursive multi-step learning-based dynamical modeling framework is employed for controlling dynamic systems. By imposing constraints on the NN structure and weights, the resulting model remains convex and continuous, enabling its use in defining convex MPC problems. Unlike [42] and [43], which rely on multi-shot predictions, our approach offers two key advantages: the convexity of the MPC optimization problem eliminates issues with local minima, and the simpler recursive multi-step architecture reduces the computational complexity of model identification. Tested on a real-world smart HVAC system in Ballen Marina, Samso, Denmark, the method effectively maintains room temperature within comfort constraints while minimizing energy consumption.

References

[1] Bhutada, G., "The 200-year history of mankind's energy transitions," in *World Economic Forum*, 2022.

[2] Sørensen, B., "A history of renewable energy technology," *Energy policy*, vol. 19, no. 1, pp. 8–12, 1991.

[3] Kanellakis, M., Martinopoulos, G., and Zachariadis, T., "European energy policy—a review," *Energy Policy*, vol. 62, pp. 1020–1030, 2013.

[4] Fetting, C., "The european green deal," *ESDN report*, vol. 53, 2020.

[5] Ram, M., Child, M., Aghahosseini, A., Bogdanov, D., Lohrmann, A., and Breyer, C., "A comparative analysis of electricity generation costs from renewable, fossil fuel and nuclear sources in g20 countries for the period 2015-2030," *Journal of Cleaner Production*, 2018. DOI: 10.1016/J.JCLEPRO.2018.07.159.

[6] Samad, T. and Annaswamy, A., "Controls for smart grids: Architectures and applications," *Proceedings of the IEEE*, vol. 105, pp. 2244–2261, 2017. DOI: 10.1109/JPROC.2017.2707326.

[7] Kundur, P., "Power system stability," *Power system stability and control*, vol. 10, pp. 7–1, 2007.

[8] Palensky, P. and Dietrich, D., "Demand side management: Demand response, intelligent energy systems, and smart loads," *IEEE Transactions on Industrial Informatics*, vol. 7, pp. 381–388, 2011. DOI: 10.1109/TII.2011.2158841.

[9] Ma, J., Deng, J., Song, L., and Han, Z., "Incentive mechanism for demand side management in smart grid using auction," *IEEE Transactions on Smart Grid*, vol. 5, pp. 1379–1388, 2014. DOI: 10.1109/TSG.2014.2302915.

[10] Bandeiras, F., Gomes, Á., Gomes, M., and Coelho, P., "Exploring energy trading markets in smart grid and microgrid systems and their implications for sustainability in smart cities," *Energies*, 2023. DOI: 10.3390/en16020801.

[11] Saad, W., Han, Z., Poor, H., and Başar, T., "Game-theoretic methods for the smart grid: An overview of microgrid systems, demand-side management, and smart grid communications," *IEEE Signal Processing Magazine*, vol. 29, pp. 86–105, 2012. DOI: 10.1109/MSP.2012.2186410.

[12] Shahidehpour, M., "Editorial," *IEEE Transactions on Smart Grid*, vol. 1, no. 1, pp. 1–2, 2010. DOI: 10.1109/TSG.2010.2048171.

[13] Botte, B., Cannatelli, V., and Rogai, S., "The telegestore project in enel's metering system," in *CIRED 2005-18th International Conference and Exhibition on Electricity Distribution*, IET, 2005, pp. 1–4.

[14] Bender, D. A., Byrne, R. H., and Borneo, D. R., "Arra energy storage demonstration projects: Lessons learned and recommendations," Sandia National Lab.(SNL-NM), Albuquerque, NM (United States); Sandia ..., Tech. Rep., 2015.

[15] Brown, M. A. and Zhou, S., "Smart-grid policies: An international review," *Advances in Energy Systems: The Large-scale renewable energy integration challenge*, pp. 127–147, 2019.

[16] Ceglia, F., Esposito, P., Marrasso, E., and Sasso, M., "From smart energy community to smart energy municipalities: Literature review, agendas and pathways," *Journal of Cleaner Production*, vol. 254, p. 120 118, 2020. DOI: 10.1016/j.jclepro.2020.120118.

[17] Lowitzsch, J., Hoicka, C. E., and Tulder, F. J. van, "Renewable energy communities under the 2019 european clean energy package–governance model for the energy clusters of the future?" *Renewable and Sustainable Energy Reviews*, vol. 122, p. 109 489, 2020.

[18] Devine-Wright, P., *Renewable energy and the public*.

[19] Mengelkamp, E., Gärttner, J., Rock, K., Kessler, S., Orsini, L., and Weinhardt, C., "Designing microgrid energy markets: A case study: The brooklyn microgrid," *Applied energy*, vol. 210, pp. 870–880, 2018.

[20] Nash Jr, J. F., "Equilibrium points in n-person games," *Proceedings of the national academy of sciences*, vol. 36, no. 1, pp. 48–49, 1950.

[21] Sandholm, W. H., *Population games and evolutionary dynamics*. MIT Press, 2010.

[22] Daskalakis, C., Goldberg, P. W., and Papadimitriou, C. H., "The complexity of computing a nash equilibrium," *Communications of the ACM*, vol. 52, no. 2, pp. 89–97, 2009.

[23] Monderer, D. and Shapley, L. S., "Potential games," *Games and economic behavior*, vol. 14, no. 1, pp. 124–143, 1996.

[24] Scutari, G., Palomar, D. P., Facchinei, F., and Pang, J.-S., "Convex optimization, game theory, and variational inequality theory," *IEEE Signal Processing Magazine*, vol. 27, no. 3, pp. 35–49, 2010.

[25] Loni, A. and Parand, F.-A., "A survey of game theory approach in smart grid with emphasis on cooperative games," in *2017 IEEE International Conference on Smart Grid and Smart Cities (ICSGSC)*, IEEE, 2017, pp. 237–242.

[26] Branzei, R., Dimitrov, D., and Tijs, S., *Models in cooperative game theory*. Springer Science & Business Media, 2008, vol. 556.

[27] Curiel, I., *Cooperative game theory and applications: cooperative games arising from combinatorial optimization problems*. Springer Science & Business Media, 2013, vol. 16.

[28] Winter, E., "The shapley value," *Handbook of game theory with economic applications*, vol. 3, pp. 2025–2054, 2002.

[29] Van Aubel, P., Colesky, M., Hoepman, J.-H., Poll, E., and Montes Portela, C., "Privacy by design for local energy communities," 2018.

[30] Dolatabadi, M., Siano, P., and Soroudi, A., "Assessing the scalability and privacy of energy communities by using a large-scale distributed and parallel real-time optimization," *IEEE Access*, vol. 10, pp. 69 771–69 787, 2022.

[31] Wang, J., Garifi, K., Baker, K., *et al.*, "Optimal renewable resource allocation and load scheduling of resilient communities," *Energies*, vol. 13, p. 5683, 2020. DOI: 10.3390/en13215683.

[32] Singh, S. and Yassine, A., "Mining energy consumption behavior patterns for households in smart grid," *IEEE Transactions on Emerging Topics in Computing*, vol. 7, pp. 404–419, 2019. DOI: 10.1109/TETC.2017.2692098.

[33] Zhang, L., Zhu, T., Xiong, P., Zhou, W., and Yu, P. S., "More than privacy: Adopting differential privacy in game-theoretic mechanism design," *ACM Computing Surveys (CSUR)*, vol. 54, no. 7, pp. 1–37, 2021.

[34] Moniruzzaman, M., Yassine, A., and Benlamri, R., "Blockchain and cooperative game theory for peer-to-peer energy trading in smart grids," *International Journal of Electrical Power & Energy Systems*, vol. 151, p. 109 111, 2023.

[35] Su, Z., Wang, Y., Luan, T. H., *et al.*, "Secure and efficient federated learning for smart grid with edge-cloud collaboration," *IEEE Transactions on Industrial Informatics*, vol. 18, no. 2, pp. 1333–1344, 2021.

[36] Mackin, E. and Patterson, S., "Submodular optimization for consensus networks with noise-corrupted leaders," *IEEE Transactions on Automatic Control*, vol. 64, pp. 3054–3059, 2017. DOI: 10.1109/tac.2018.2874306.

[37] Mignoni, N., Scarabaggio, P., Carli, R., and Dotoli, M., "Control frameworks for transactive energy storage services in energy communities," *Control Engineering Practice*, vol. 130, p. 105 364, 2023.

[38] Melbourne - Open Data Portal, C. of. "On-street car parking sensor data - 2017." (), [Online]. Available: https://data.melbourne.vic.gov.au/Transport/On-street-Car-Parking-Sensor-Data-2017/u9sa-j86i. (accessed: 22.01.2022).

[39] "Electric vehicles database." ((Accessed: 21.01.2022)), [Online]. Available: https://ev-database.org/.

[40] Goebel, R., Sanfelice, R. G., and Teel, A. R., *Hybrid Dynamical Systems: Modeling, Stability, and Robustness*. Princeton University Press, 2012.

[41] Wang, Z., Pravin, P., and Wu, Z., "Input convex lipschitz RNN: A fast and robust approach for engineering tasks," *arXiv preprint arXiv:2401.07494*, 2024.

[42] Chen, Y., Shi, Y., and Zhang, B., "Optimal control via neural networks: A convex approach," in *7th International Conference on Learning Representations, ICLR 2019*, 2019.

[43] Bünning, F., Schalbetter, A., Aboudonia, A., Badyn, M. H. de, Heer, P., and Lygeros, J., "Input convex neural networks for building MPC," in *Learning for Dynamics and Control*, PMLR, 2021, pp. 251–262.

Part I: Energy Communities' Actors as Transactive Agents

Chapter 2

A Game-Theoretical Control Framework for Transactive Energy Trading in Energy Communities

Abstract

Under the umbrella of non-cooperative game theory, we formulate a transactive energy framework to model and control energy communities comprised of heterogeneous agents including (yet not limited to) prosumers, energy storage systems, and energy retailers. The underlying control task is defined as a GNEP, which must be solved in a distributed fashion. To solve the GNEP, we formulate a Gauss-Seidel-type alternating direction method of multipliers algorithm, which is guaranteed to converge under strongly monotone pseudo-gradient mappings. As such, we provide sufficient conditions on the private cost and energy pricing functions of the community members, so that the strong monotonicity of the overall pseudo-gradient is ensured. Finally, the proposed framework and the effectiveness of the solution method are illustrated through a numerical simulation.

Contents

2.1 Introduction

As the advent of distributed energy resource technologies has increased the independence of grid actors from central power providers [1], the problem of efficiently controlling the overall operational apparatus has not yet thoroughly been solved. Renewable energy sources, such as photovoltaic, eolic, and hydropower, have opened up the path to dynamic energy communities, whose members (nodes) are not merely passive loads, but active agents capable of steering the dynamics of the energy market, e.g., prosumers and energy storage systems (ESSs) [2]. Given that market dynamics often stimulate selfish behaviors, the community members can be modelled as non-cooperative agents characterized by private objectives and operational constraints, which are tightly coupled to the decisions of the remaining actors. Therefore, non-cooperative game theory [3] is a powerful tool to model, design, and analyze energy communities, and the concept of GNE [4] yields a reasonable solution for the underlying multi-agent decision-making task. Furthermore, the modern architecture of energy communities, whose members are often geographically distant, calls for non-centralized algorithmic approaches, able to take over the limitations of centralized frameworks, such as low scalability and privacy weaknesses.

The problem of distributed GNE computation in multi-agent systems has recently received significant attention [5]–[8], and its role in energy communities has been studied both from the classical and evolutionary game theoretical perspectives [9]–[11]. In fact, in our previous work [12], we formulate the control task of the energy community as a GNEP,

where the agents' decisions correspond to energy transactions between prosumers, ESSs, and a single ER. Nonetheless, the modelling in [12] only considers inter-agent couplings through the constraints and not through the private cost functions of the community members, and the allowed energy transactions are ruled by a particular bipartite graph topology.

Motivated by these previous works, in this Chapter, we extend the framework in [12] to a more general energy market setup, where the community members have private cost functions coupled with each other through the monetary price at which each member sells its energy. Besides, these energy prices are allowed to be dependent on aggregate demands, thus coupling the decisions of multiple community members. Moreover, the inter-agent energy transactions and communication are ruled by an arbitrarily connected and undirected graph, and we take in the (multiple) ERs as active participants in the energy community, characterizing them with their own objectives to pursue selfishly. To solve the underlying GNEP in a distributed fashion, we leverage the results in [8] to formulate a Gauss-Seidel-type alternating direction method of multipliers (ADMM) distributed GNE computation algorithm. Note that, although Gauss-Seidel-type methods tend to converge faster than Jacobi-type ones [7], [8], the former requires ordered sequential computations which would not suitably scale for large energy communities. To overcome such a drawback, we reformulate the underlying GNEP in an equivalent form, and we solve it following a two-block iterative process, i.e., energy transactions computation and energy prices update, where each block can be executed in parallel over the energy community regardless of the total number of members. Finally, as the main technical contribution, we provide sufficient conditions on the private cost and energy pricing functions to ensure the strong monotonicity of the overall pseudo-gradient mapping, which is in turn a sufficient condition to guarantee the convergence of the considered ADMM-type algorithm. As such, the provided sufficient conditions are useful in the management of energy communities, as the cost and pricing functions can be designed to ensure convergence to a GNE.

2.2 Notation and Preliminaries

Let $\mathbb{R}$, $\mathbb{R}_{\geq 0}$, $\mathbb{R}_{>0}$ denote the sets of real, non-negative real, and positive real numbers, respectively. Let $\mathbb{Z}_{\geq a}$ be the set of integers not less than $a \in \mathbb{Z}_{\geq 1}$, and let $\mathbb{B} := \{0, 1\}$ be the set of binary numbers. Given a set $\mathcal{S} = \{1, 2, \ldots, N\}$, with $N \in \mathbb{Z}_{\geq 2}$, and a set of matrices $\mathbf{Z}_1, \mathbf{Z}_2, \ldots, \mathbf{Z}_N$, with $\mathbf{Z}_i \in \mathbb{R}^{n_i \times m}$, let

$$\operatorname{col}\left(\mathbf{Z}_i\right)_{i\in\mathcal{S}} = \left[\mathbf{Z}_1^\top, \mathbf{Z}_2^\top, \ldots, \mathbf{Z}_N^\top\right]^\top \in \mathbb{R}^{\left(\sum_{i\in\mathcal{S}} n_i\right)\times m}.$$

Namely, $\operatorname{col}(\cdot)_{i\in\mathcal{S}}$ denotes the column stack operation ordered by the set $\mathcal{S}$, and the natural ordering of the elements in $\mathcal{S}$ is preserved in the concatenation. Similarly, for a set of square matrices $\mathbf{Z}_1, \mathbf{Z}_2, \ldots, \mathbf{Z}_N$, we let $\operatorname{diag}(\mathbf{Z}_i)_{i\in\mathcal{S}}$ denote the (block) diagonal stack operation ordered by the set $\mathcal{S}$. Moreover, given any subset $\hat{\mathcal{S}} \subseteq \mathcal{S}$, the natural ordering of $\mathcal{S}$ is preserved in $\hat{\mathcal{S}}$ and $\phi_{\hat{\mathcal{S}}} \colon \hat{\mathcal{S}} \to \{1, 2, \ldots, |\hat{\mathcal{S}}|\}$ yields the relative natural ordering of the elements of $\hat{\mathcal{S}}$. Namely, if $\mathcal{S} = \{1, 2, 3, 4, 5\}$ and $\hat{\mathcal{S}} = \{2, 4, 5\}$, then $\phi_{\hat{\mathcal{S}}}(2) = 1$, $\phi_{\hat{\mathcal{S}}}(4) = 2$, and $\phi_{\hat{\mathcal{S}}}(5) = 3$. Given a symmetric matrix $\mathbf{S}$, we let $\lambda_{\max}(\mathbf{S})$ denote the maximum eigenvalue of $\mathbf{S}$, and $\mathbf{S} \succeq 0$ denotes that $\mathbf{S}$ is positive semi-definite. Throughout the Chapter, $\|\cdot\|$ and $\|\cdot\|_\infty$ denote the Euclidean and infinity norms, respectively, and $|\cdot|$ yields the cardinality when applied to a set. Operators ∇ and D yield the gradient and Jacobian matrix when applied to differentiable scalar-valued and vector-valued functions, respectively (we view gradients as column vectors by default). Besides, a subindex is included to ∇ and D when specifying partial differentiation. Given a scalar-valued function $f \colon \mathcal{D} \to \mathbb{R}$ and some $\theta \in \mathbb{R}_{>0}$, we say that $f(\cdot)$ is θ-strongly convex if it holds that $g(\mathbf{z}) = f(\mathbf{z}) - (\theta/2)\mathbf{z}^\top\mathbf{z}$ is convex for every $\mathbf{z} \in \mathcal{D}$. Given a vector-valued function $\mathbf{h} \colon \mathcal{D} \to \mathbb{R}^m$ with domain $\mathcal{D} \subseteq \mathbb{R}^m$, we say that $\mathbf{h}(\cdot)$ is L-Lipschitz continuous if there exists some $L \in \mathbb{R}_{>0}$ such that $\|\mathbf{h}(\mathbf{z}) - \mathbf{h}(\tilde{\mathbf{z}})\| \leq L\|\mathbf{z} - \tilde{\mathbf{z}}\|$, for all $\mathbf{z}, \tilde{\mathbf{z}} \in \mathcal{D}$; we say that $\mathbf{h}(\cdot)$ is monotone if $(\mathbf{h}(\mathbf{z}) - \mathbf{h}(\tilde{\mathbf{z}}))^\top(\mathbf{z} - \tilde{\mathbf{z}}) \geq 0$, for all $\mathbf{z}, \tilde{\mathbf{z}} \in \mathcal{D}$; and we say that $\mathbf{h}(\cdot)$ is μ-strongly

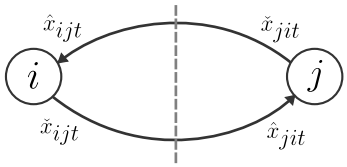

Figure 2.1: Schematic overview of the energy transaction between agents i and j at time t. For the transaction to be attainable, the agreement constraints $\hat{x}_{ijt} = \check{x}_{jit}$ and $\check{x}_{ijt} = \hat{x}_{jit}$ must hold.

monotone if there exists a $\mu \in \mathbb{R}_{>0}$ such that $(\mathbf{h}(\mathbf{z}) - \mathbf{h}(\tilde{\mathbf{z}}))^\top (\mathbf{z} - \tilde{\mathbf{z}}) \geq \mu \|\mathbf{z} - \tilde{\mathbf{z}}\|^2$, for all $\mathbf{z}, \tilde{\mathbf{z}} \in \mathcal{D}$. If $\mathbf{h}(\cdot)$ is continuously differentiable, then a sufficient and necessary condition for μ-strong monotonicity is that $\mathrm{D}\,\mathbf{h}(\mathbf{z}) + \mathrm{D}\,\mathbf{h}(\mathbf{z})^\top - 2\mu\mathbf{I}_m \succeq 0$, for all $\mathbf{z} \in \mathcal{D}$. Throughout the Chapter, $\mathbf{I}_n$ is the $n \times n$ identity matrix, $\mathbf{1}_n$ ($\mathbf{0}_n$) is the column vector with n ones (zeros), $\mathbf{0}_{n\times m}$ is the $n \times m$ matrix of zeros, and $\otimes$ denotes the Kronecker product. Finally, $\mathcal{U}[a, b]$ is the uniform random distribution over $[a, b] \subset \mathbb{R}$.

2.3 Problem Statement

Consider an energy community with $N \in \mathbb{Z}_{\geq 2}$ agents indexed by the set $\mathcal{A} = \{1, 2, \ldots, N\}$. The interaction and communication among agents is characterized by the connected[1] and undirected graph $\mathcal{G} = (\mathcal{A}, \mathcal{E})$, where the agents correspond to the nodes, and $\mathcal{E} \subset \mathcal{A} \times \mathcal{A}$ is the set of edges (by convention we assume that there are no self-loops, i.e., $(i, i) \notin \mathcal{E}$, for all $i \in \mathcal{A}$). If $(i, j) \in \mathcal{E}$, then, we say that agents $i, j \in \mathcal{A}$ are neighbors and thus can interact and communicate with each other, and since $\mathcal{G}$ is undirected, $(i, j) \in \mathcal{E} \Leftrightarrow (j, i) \in \mathcal{E}$. Hence, we denote $\mathcal{A}_i = \{j \in \mathcal{A} \colon (i, j) \in \mathcal{E}\}$ as the set of neighbors of agent i, and we let $N_i = |\mathcal{A}_i|$ ($N_i \geq 1$ due to the connectivity of $\mathcal{G}$).

In the considered energy community, every agent $i \in \mathcal{A}$ is allowed to trade energy with its neighbors over $T \in \mathbb{Z}_{\geq 1}$ ordered time slots $t_1 < t_2 < \cdots < t_T$, where t_k represents a generic time slot and $k \in \mathcal{T} = \{1, 2, \ldots, T\}$. As such, for all $(i, j, t) \in \mathcal{A} \times \mathcal{A}_i \times \mathcal{T}$, let $\hat{x}_{ijt} \in \mathbb{R}_{\geq 0}$ denote the energy that agent i buys from agent j at time t, let $\check{x}_{ijt} \in \mathbb{R}_{\geq 0}$ denote the energy that agent i sells to agent j at time t, and let $p_{ijt} \in \mathbb{R}_{\geq 0}$ denote the monetary price at which agent i sells its energy to agent j at time t. An illustrative overview is provided in Fig. 2.1. Clearly, for an energy trade to be attainable, it is necessary that $\hat{x}_{ijt} = \check{x}_{jit}$ and $\check{x}_{ijt} = \hat{x}_{jit}$, i.e., agents must agree on their energy exchanges. Let z be a placeholder notation for either $\hat{x}$, $\check{x}$, or p, and define the vectorization given by

$$\begin{aligned} \mathbf{z}_{ij} &= \operatorname{col}(z_{ijt})_{t\in\mathcal{T}} \in \mathbb{R}^T \\ \mathbf{z}_i &= \operatorname{col}(\mathbf{z}_{ij})_{j\in\mathcal{A}_i} \in \mathbb{R}^{n_i} \\ \mathbf{z} &= \operatorname{col}(\mathbf{z}_i)_{i\in\mathcal{A}} \in \mathbb{R}^n \\ \mathbf{z}_{-i} &= \operatorname{col}(\mathbf{z}_{ji})_{j\in\mathcal{A}_i} \in \mathbb{R}^{n_i}, \end{aligned} \tag{2.1}$$

where $n_i = TN_i$ and $n = \sum_{i\in\mathcal{A}} n_i$. That is, the vectors $\hat{\mathbf{x}}_{ij}$, $\check{\mathbf{x}}_{ij}$, $\mathbf{p}_{ij}$, $\hat{\mathbf{x}}_i$, $\check{\mathbf{x}}_i$, $\mathbf{p}_i$, $\hat{\mathbf{x}}$, $\check{\mathbf{x}}$, $\mathbf{p}$, $\hat{\mathbf{x}}_{-i}$, $\check{\mathbf{x}}_{-i}$, and $\mathbf{p}_{-i}$, are all constructed following the ordering in (2.1). Namely, $\hat{\mathbf{x}}_i$ ($\check{\mathbf{x}}_i$) yields the energy that agent i buys from (sells to) its neighbors, $\hat{\mathbf{x}}_{-i}$ ($\check{\mathbf{x}}_{-i}$) yields the energy that the neighbors of agent i buy from (sell to) agent i, and $\mathbf{p}_{-i}$ yields the energy selling prices that the neighbors of agent i offer to agent i. Under the considered framework, every agent $i \in \mathcal{A}$ is thus responsible for computing its own decision $(\hat{\mathbf{x}}_i, \check{\mathbf{x}}_i, \mathbf{p}_i)$ subject to the constraints given by

$$(\hat{\mathbf{x}}_i, \check{\mathbf{x}}_i) \in \mathcal{X}_i \tag{2.2a}$$
$$\hat{\mathbf{x}}_i = \check{\mathbf{x}}_{-i} \tag{2.2b}$$
$$\check{\mathbf{x}}_i = \hat{\mathbf{x}}_{-i} \tag{2.2c}$$
$$\mathbf{p}_i \in \mathbb{R}^{n_i}_{\geq 0}. \tag{2.2d}$$

[1] If the graph were disconnected, then each connected component could be treated as a separate energy community.

Here, $\mathcal{X}_i \subseteq \mathbb{R}^{2n_i}_{\geq 0}$ defines the local energy-related constraint set of agent i, and the constraints in (2.2b)-(2.2c) impose an agreement between neighboring agents regarding their energy trades. Therefore, the decision of agent i is feasible only if $(\hat{\mathbf{x}}_i, \check{\mathbf{x}}_i, \mathbf{p}_i) \in \Omega_i\left(\hat{\mathbf{x}}_{-i}, \check{\mathbf{x}}_{-i}\right) \times \mathbb{R}^{n_i}_{\geq 0}$, with

$$\Omega_i\left(\hat{\mathbf{x}}_{-i}, \check{\mathbf{x}}_{-i}\right) = \left\{ (\hat{\mathbf{x}}_i, \check{\mathbf{x}}_i) \in \mathcal{X}_i \colon \begin{array}{l} \hat{\mathbf{x}}_i = \check{\mathbf{x}}_{-i} \\ \check{\mathbf{x}}_i = \hat{\mathbf{x}}_{-i} \end{array} \right\}.$$

Consequently, the set of feasible collective decisions for the entire energy community is given by $\Omega \times \mathbb{R}^{n}_{\geq 0}$, where

$$\Omega = \left\{ (\hat{\mathbf{x}}, \check{\mathbf{x}}) \in \prod_{i \in \mathcal{A}} \mathcal{X}_i \colon \hat{\mathbf{x}} = \mathbf{B}\check{\mathbf{x}} \right\}.$$

Here, $\mathbf{B} = \operatorname{col}\left(\mathbf{B}_i\right)_{i \in \mathcal{A}} \in \mathbb{B}^{n \times n}$, and $\mathbf{B}_i \in \mathbb{B}^{n_i \times n}$ is the (unique) matrix that satisfies $\mathbf{z}_{-i} = \mathbf{B}_i \mathbf{z}$, for any placeholder $z \in \{\hat{x}, \check{x}, p\}$ and all $i \in \mathcal{A}$. More precisely, $\mathbf{B}_i$ has the block structure given by $\mathbf{B}_i = \begin{bmatrix} \mathbf{B}_{i1} & \mathbf{B}_{i2} & \cdots & \mathbf{B}_{iN} \end{bmatrix}$, where

$$\mathbf{B}_{ij} = \begin{cases} \mathbf{0}_{n_i \times n_j}, & \text{if } j \notin \mathcal{A}_i \\ \mathbf{W}_{ij} \otimes \mathbf{I}_T, & \text{if } j \in \mathcal{A}_i, \end{cases}$$

and $\mathbf{W}_{ij} \in \mathbb{B}^{N_i \times N_j}$ is the matrix that has a 1 at the $(\text{row} = \phi_{\mathcal{A}_i}(j), \text{column} = \phi_{\mathcal{A}_j}(i))$ position and a 0 elsewhere, i.e., $\mathbf{W}_{ij} = \mathbf{e}_{\phi_{\mathcal{A}_i}(j)} \mathbf{e}^{\top}_{\phi_{\mathcal{A}_j}(i)}$, where $\mathbf{e}_k$ is k-th column of $\mathbf{I}_n$.

Remark 2.3.1

We highlight that matrix $\mathbf{B}$ is both symmetric and orthogonal, i.e., $\mathbf{B} = \mathbf{B}^{\top}$ and $\mathbf{B}^{\top}\mathbf{B} = \mathbf{I}_n$ (thus, $\mathbf{B}$ defines an involution: $\mathbf{B}\mathbf{B} = \mathbf{I}_n$). To show the first claim, note that $\mathbf{B}_{ij} = \mathbf{B}^{\top}_{ji}$, for all $i, j \in \mathcal{A}$. For the second claim, observe that, by construction and symmetry, all rows and columns of $\mathbf{B}$ are linearly independent, and each row and column of $\mathbf{B}$ has exactly one non-zero element, which is equal to 1. Therefore, all the rows and columns of $\mathbf{B}$ are orthonormal vectors.

Based on the considered framework, every agent $i \in \mathcal{A}$ computes its own decision $(\hat{\mathbf{x}}_i, \check{\mathbf{x}}_i, \mathbf{p}_i)$ to simultaneously solve the optimization problems (OPs) given by

$$\min_{\hat{\mathbf{x}}_i, \check{\mathbf{x}}_i} f_i\left(\hat{\mathbf{x}}_i, \check{\mathbf{x}}_i, \mathbf{p}_i, \mathbf{p}_{-i}\right) \text{ s.t. } (\hat{\mathbf{x}}_i, \check{\mathbf{x}}_i) \in \Omega_i\left(\hat{\mathbf{x}}_{-i}, \check{\mathbf{x}}_{-i}\right) \tag{2.3a}$$

$$\min_{\mathbf{p}_i} \frac{\rho_i}{2} \left\| \mathbf{p}_i - \mathbf{g}_i\left(\hat{\mathbf{x}}_{-i}\right) \right\|^2 \text{ s.t. } \mathbf{p}_i \in \mathbb{R}^{n_i}. \tag{2.3b}$$

Here, $f_i \colon \mathbb{R}^{4n_i}_{\geq 0} \to \mathbb{R}$ is the local cost function of agent i, $\rho_i \in \mathbb{R}_{>0}$ is a weighting parameter, and $\mathbf{g}_i \colon \mathbb{R}^{n_i}_{\geq 0} \to \mathbb{R}^{n_i}_{\geq 0}$ is the (non-negative) local pricing function of agent i. Note that the unique solution of the OP in (2.3b) is $\mathbf{p}_i = \mathbf{g}_i\left(\hat{\mathbf{x}}_{-i}\right)$ and the constraint $\mathbf{p}_i \in \mathbb{R}^{n_i}_{\geq 0}$ is enforced by the co-domain of $\mathbf{g}_i(\cdot)$ (we define such a computation as an OP for convenience). Hence, solving the OP in (2.3a) yields the energy transactions that agent i should execute to minimize its operational costs $f_i(\cdot, \cdot, \cdot, \cdot)$, whilst solving the OP in (2.3b) yields the energy-selling prices of agent i. Besides, notice that for a single agent i the OP in (2.3a) is coupled to the OP in (2.3b) through $\mathbf{p}_i$, while for multiple agents the OPs in (2.3) are coupled to each other through $\hat{\mathbf{x}}_{-i}$, $\check{\mathbf{x}}_{-i}$, and $\mathbf{p}_{-i}$. As such, simultaneously solving the OPs in (2.3) for every agent $i \in \mathcal{A}$ is equivalent to solving the GNEP stated in Definition 2.3.1.

Definition 2.3.1

The GNEP for the energy community is to compute a collective decision $(\hat{\mathbf{x}}^*, \check{\mathbf{x}}^*, \mathbf{p}^*) \in \Omega \times \mathbb{R}^{n}_{\geq 0}$ such that

$$f_i\left(\hat{\mathbf{x}}^*_i, \check{\mathbf{x}}^*_i, \mathbf{p}^*_i, \mathbf{p}^*_{-i}\right) \leq f_i\left(\hat{\mathbf{x}}_i, \check{\mathbf{x}}_i, \mathbf{p}^*_i, \mathbf{p}^*_{-i}\right)$$
$$\left\| \mathbf{p}^*_i - \mathbf{g}_i\left(\hat{\mathbf{x}}^*_{-i}\right) \right\|^2 \leq \left\| \mathbf{p}_i - \mathbf{g}_i\left(\hat{\mathbf{x}}^*_{-i}\right) \right\|^2,$$

for all $(\hat{\mathbf{x}}_i, \check{\mathbf{x}}_i) \in \Omega_i \left(\hat{\mathbf{x}}^*_{-i}, \check{\mathbf{x}}^*_{-i}\right)$, *all* $\mathbf{p}_i \in \mathbb{R}^{n_i}_{\geq 0}$, *and all* $i \in \mathcal{A}$. *Such a collective decision* $(\hat{\mathbf{x}}^*, \check{\mathbf{x}}^*, \mathbf{p}^*)$ *is termed as a GNE for the energy community.*

Namely, the GNEP is the task of computing a GNE, which is a collective (feasible) decision $(\hat{\mathbf{x}}^*, \check{\mathbf{x}}^*, \mathbf{p}^*)$ where no agent can further decrease its local costs by unilaterally deviating from the GNE. In that sense, a GNE is a self-enforceable agreement among the energy community.

Throughout the Chapter, we impose Standing Assumption 2.3.1.

Assumption 2.3.1

For all $i \in \mathcal{A}$, *the functions* $f_i(\cdot,\cdot,\cdot,\cdot)$ *and* $\mathbf{g}_i(\cdot)$ *are continuously differentiable,* $f_i(\cdot,\cdot,\mathbf{p}_i,\mathbf{p}_{-i})$ *is (jointly) convex for every fixed* $(\mathbf{p}_i,\mathbf{p}_{-i})$, *and* $\nabla_{\hat{\mathbf{x}}_i} f_i\left(\hat{\mathbf{x}}_i,\check{\mathbf{x}}_i,\cdot,\cdot\right)$ *and* $\nabla_{\check{\mathbf{x}}_i} f_i\left(\hat{\mathbf{x}}_i,\check{\mathbf{x}}_i,\cdot,\cdot\right)$ *are* $\hat{L}_i$*-Lipschitz continuous and* $\check{L}_i$*-Lipschitz continuous for every fixed* $(\hat{\mathbf{x}}_i,\check{\mathbf{x}}_i)$, *respectively. Moreover, the pseudo-gradient*

$$\mathbf{q}\left(\hat{\mathbf{x}},\check{\mathbf{x}},\mathbf{p}\right) = \begin{bmatrix} \operatorname{col}\left(\nabla_{\hat{\mathbf{x}}_i} f_i\left(\hat{\mathbf{x}}_i,\check{\mathbf{x}}_i,\mathbf{p}_i,\mathbf{p}_{-i}\right)\right)_{i\in\mathcal{A}} \\ \operatorname{col}\left(\nabla_{\check{\mathbf{x}}_i} f_i\left(\hat{\mathbf{x}}_i,\check{\mathbf{x}}_i,\mathbf{p}_i,\mathbf{p}_{-i}\right)\right)_{i\in\mathcal{A}} \\ \operatorname{col}\left(\rho_i\left(\mathbf{p}_i - \mathbf{g}_i(\hat{\mathbf{x}}_{-i})\right)\right)_{i\in\mathcal{A}} \end{bmatrix} \in \mathbb{R}^{3n}$$

is μ*-strongly monotone. Finally,* Ω *is a closed convex set with a non-empty relative interior.*

Furthermore, in Proposition 2.3.1 we provide sufficient conditions on the functions $f_i(\cdot,\cdot,\cdot,\cdot)$ and $\mathbf{g}_i(\cdot)$ to guarantee the μ-strong monotonicity of the pseudo-gradient $\mathbf{q}(\cdot,\cdot,\cdot)$.

Proposition 2.3.1

Suppose that every agent $i \in \mathcal{A}$ *has functions* $f_i(\cdot,\cdot,\cdot,\cdot)$ *and* $\mathbf{g}_i(\cdot)$ *of the form*

$$\begin{aligned} f_i\left(\hat{\mathbf{x}}_i,\check{\mathbf{x}}_i,\mathbf{p}_i,\mathbf{p}_{-i}\right) &= \psi_i\left(\hat{\mathbf{x}}_i,\check{\mathbf{x}}_i\right) + \mathbf{p}_{-i}^\top \hat{\mathbf{x}}_i - \mathbf{p}_i^\top \check{\mathbf{x}}_i \\ \mathbf{g}_i\left(\hat{\mathbf{x}}_{-i}\right) &= \mathbf{Q}_i \hat{\mathbf{x}}_{-i} + \mathbf{r}_i, \end{aligned} \tag{2.4}$$

where $\psi_i \colon \mathbb{R}^{2n_i}_{\geq 0} \to \mathbb{R}$ *is twice continuously differentiable and* θ_i*-strongly convex in all its arguments,* $\mathbf{Q}_i \in \mathbb{R}^{n_i \times n_i}_{\geq 0}$, *and* $\mathbf{r}_i \in \mathbb{R}^{n_i}_{\geq 0}$. *Moreover, denote*

$$\underline{\theta} = \min_{i\in\mathcal{A}} \theta_i, \qquad \overline{\lambda} = \max_{i\in\mathcal{A}} \lambda_{\max}\left(\mathbf{Q}_i^\top \mathbf{Q}_i\right),$$

and let $\rho_i = \rho \in \mathbb{R}_{>0}$, *for all* $i \in \mathcal{A}$. *If there exists a* $\mu \in (0,\rho)$ *such that*

$$\underline{\theta} - \mu \geq \frac{\max\left\{2,\, \rho^2 \overline{\lambda}\right\}}{\rho - \mu}, \tag{2.5}$$

then the pseudo-gradient $\mathbf{q}(\cdot,\cdot,\cdot)$ *is* μ*-strongly monotone.*

The proof is reported in Appendix A.1 We remark that (2.4) encompasses commonly employed objectives and pricing schemas, where the former collects the local operational costs, while the latter includes aggregative pricing functions as illustrated in Section 2.5.

In this Chapter, we focus on the so-called variational GNE (vGNE), which is a particular type of GNE that can be linked to the solution of an underlying variational inequality [13].

Definition 2.3.2

A collective decision $(\hat{\mathbf{x}}^*, \check{\mathbf{x}}^*, \mathbf{p}^*)$ *is a vGNE if* $(\hat{\mathbf{x}}^*, \check{\mathbf{x}}^*, \mathbf{p}^*) \in \mathrm{SOL}\left(\Omega \times \mathbb{R}^n_{\geq 0}, \mathbf{q}(\cdot,\cdot,\cdot)\right)$, *where* $\mathrm{SOL}\left(\Omega \times \mathbb{R}^n_{\geq 0}, \mathbf{q}(\cdot,\cdot,\cdot)\right)$ *denotes the set of solutions of the variational inequality* $\mathrm{VI}\left(\Omega \times \mathbb{R}^n_{\geq 0}, \mathbf{q}(\cdot,\cdot,\cdot)\right)$ *defined as: find* $(\hat{\mathbf{x}}^*, \check{\mathbf{x}}^*, \mathbf{p}^*) \in \Omega \times \mathbb{R}^n_{\geq 0}$ *such that*

$$\begin{bmatrix} \hat{\mathbf{x}} - \hat{\mathbf{x}}^* \\ \check{\mathbf{x}} - \check{\mathbf{x}}^* \\ \mathbf{p} - \mathbf{p}^* \end{bmatrix}^\top \mathbf{q}\left(\hat{\mathbf{x}}^*, \check{\mathbf{x}}^*, \mathbf{p}^*\right) \geq 0, \quad \forall (\hat{\mathbf{x}}, \check{\mathbf{x}}, \mathbf{p}) \in \Omega \times \mathbb{R}^n_{\geq 0}.$$

Under Standing Assumption 2.3.1, it follows that there exists a unique vGNE for the considered energy community [13, Theorem 2.3.3]. Besides, from [4, Theorem 3.9] it holds that every vGNE is also a GNE (yet the converse is not true in general). Consequently, computing a vGNE is sufficient to solve the GNEP of Definition 2.3.1.

We now proceed to describe the three types of agents we consider in the energy community: ERs, prosumers, and ESSs. Nonetheless, we highlight that other types of agents might also fit the considered framework, e.g., PEVs, and energy hubs. The number of agents of each type and the topology of the graph $\mathcal{G}$ are arbitrary as long as the non-emptiness of the feasible set $\Omega \times \mathbb{R}^n_{\geq 0}$ is guaranteed according to Standing Assumption 2.3.1.

Energy Retailers

ERs constitute the traditional power providers in centralized distribution networks, being mainly characterized by thermal-based production plants, and thus able to serve medium-to-large districts. Their presence is still relevant in the modern energy community since they can provide almost-steady power throughput, and hence compensate for the intermittent generation by renewable-based sources. Therefore, ERs are active grid agents, collected in the set $\mathcal{R} \subset \mathcal{G}$, so that each ER $i \in \mathcal{R}$ is characterized by an outward energy availability $\check{a}_{it} \in \mathbb{R}_{\geq 0}$, i.e., the maximum aggregate energy that can be sold to the agents in $\mathcal{A}_i$ at time $t \in \mathcal{T}$, and a maximum inward energy availability $\hat{a}_{it} \in \mathbb{R}_{\geq 0}$, i.e., the maximum aggregate energy that can be absorbed from neighboring agents in $\mathcal{A}_i$ at time $t \in \mathcal{T}$. As such, each ER's local constraints set is given by

$$\mathcal{X}_i = \left\{ (\hat{\mathbf{x}}_i, \check{\mathbf{x}}_i) \in \mathbb{R}^{2n_i}_{\geq 0} : \begin{array}{l} \mathbf{I}_2 \otimes \mathbf{1}^\top_{N_i} \otimes \mathbf{I}_T \begin{bmatrix} \check{\mathbf{x}}_i \\ \hat{\mathbf{x}}_i \end{bmatrix} \leq \begin{bmatrix} \check{\mathbf{a}}_i \\ \hat{\mathbf{a}}_i \end{bmatrix} \\ \hat{x}_{ijt} \leq \overline{\hat{x}}_{ijt},\ \check{x}_{ijt} \leq \overline{\check{x}}_{ijt} \\ \forall j \in \mathcal{A}_i, t \in \mathcal{T} \end{array} \right\}, \tag{2.6}$$

for all $i \in \mathcal{R}$, with $\hat{\mathbf{a}}_i := \mathrm{col}(\hat{a}_{it})_{t\in\mathcal{T}}$ and $\check{\mathbf{a}}_i := \mathrm{col}(\check{a}_{it})_{t\in\mathcal{T}}$. Namely, the constraints set in (2.6) ensure that the aggregate energy inflow and outflow of a ER do not exceed its respective availability.

Prosumers

The backbone of the modern energy community is composed of prosumers, which are grid agents equipped with their own means of generation in addition to their local energy demand. Often, those private sources are renewable, e.g., eolic, photovoltaic, or hydroelectric, with a gross power production capable of fulfilling domestic energy requirements for industrial appliances. Hence, let us indicate the prosumer set with $\mathcal{P} \subset \mathcal{A}$, with each $i \in \mathcal{P}$ being characterized by the difference between its local energy generation and demand $\delta_{it} \in [\underline{\delta}_i, \overline{\delta}_i] \subset \mathbb{R}$. Namely, for $\delta_{it} = 0$, the i-th prosumer is capable of exact self-sustenance, while for $\delta_{it} > 0$ and $\delta_{it} < 0$, the i-th prosumer has an energy *deficit* and *surplus*, respectively. Therefore, $\underline{\delta}_i$ and $\overline{\delta}_i$ indicate the maximum demand and generation that prosumer i can attain, respectively. For every prosumer, its interactions with its neighbors aim at ensuring its overall energy balance. Therefore, the

i-th prosumer's local constraints set is defined as

$$\mathcal{X}_i = \left\{ (\hat{\mathbf{x}}_i, \check{\mathbf{x}}_i) \in \mathbb{R}^{2n_i}_{\geq 0} : \begin{array}{l} \mathbf{1}_{N_i}^\top \otimes \mathbf{I}_T(\check{\mathbf{x}}_i - \hat{\mathbf{x}}_i) = \boldsymbol{\delta}_i \\ \hat{x}_{ijt} \leq \overline{\hat{x}}_{ijt},\ \check{x}_{ijt} \leq \overline{\check{x}}_{ijt} \\ \forall j \in \mathcal{A}_i, t \in \mathcal{T} \end{array} \right\},$$

with $\boldsymbol{\delta}_i := \mathrm{col}(\delta_{it})_{t\in\mathcal{T}}$, and $\overline{\hat{x}}_{ijt}, \overline{\check{x}}_{ijt} \in \mathbb{R}_{>0}$, for all $i \in \mathcal{P}$. Here, $\overline{\hat{x}}_{ijt}$ and $\overline{\check{x}}_{ijt}$ represent local energy-transmission limits for prosumer i.

Energy Storage Systems

To take advantage of peak-generation periods, it is convenient to equip the grid with ESSs. The task of ESSs is to provide energy reserves during low-generation time windows, e.g., at night when referring to photovoltaic systems. Thus, let us define $\mathcal{S} \subset \mathcal{A}$ as the set of ESSs, with each $i \in \mathcal{S}$ characterized by a first-order dynamics of the form[2]

$$s_{i(t+1)} = \alpha_i s_{it} + \sum_{j\in\mathcal{A}_i} \left(\hat{\eta}_i \hat{x}_{ijt} - \frac{1}{\check{\eta}_i} \check{x}_{ijt} \right), \tag{2.7}$$

where $s_{it} \in \mathbb{R}_{\geq 0}$ is the total stored energy in the i-th ESS at time t, and $\alpha_i, \hat{\eta}_i, \check{\eta}_i \in (0,1)$ are the leakage coefficient, the charging efficiency, and the discharging efficiency, respectively. Equivalently, given an initial stored energy $s_{i0} \in \mathbb{R}_{\geq 0}$, and defining $\hat{x}_{ij0} = \check{x}_{ij0} = 0$, it follows that

$$s_{it}\left(\hat{\mathbf{x}}_i, \check{\mathbf{x}}_i\right) = \alpha_i^t s_{i0} + \sum_{\tau=1}^{t} \alpha_i^{t-\tau} \sum_{j\in\mathcal{A}_i} \left(\hat{\eta}_i \hat{x}_{ij\tau} - \frac{1}{\check{\eta}_i} \check{x}_{ij\tau} \right).$$

In fact, for all times $t \in \mathcal{T}$, it is required that $0 \leq s_{it}\left(\hat{\mathbf{x}}_i, \check{\mathbf{x}}_i\right) \leq \overline{s}_i$, where $\overline{s}_i \in \mathbb{R}_{>0}$ is the maximum storage capacity of the i-th ESS. Therefore, the local constraints set of the i-th ESS is

$$\mathcal{X}_i = \left\{ (\hat{\mathbf{x}}_i, \check{\mathbf{x}}_i) \in \mathbb{R}^{2n_i}_{\geq 0} : \begin{array}{l} 0 \leq s_{it}(\hat{\mathbf{x}}_i, \check{\mathbf{x}}_i) \leq \overline{s}_i \\ \hat{x}_{ijt} \leq \overline{\hat{x}}_{ijt},\ \check{x}_{ijt} \leq \overline{\check{x}}_{ijt} \\ \forall j \in \mathcal{A}_i, t \in \mathcal{T} \end{array} \right\},$$

where $\overline{\hat{x}}_{ijt}$ and $\overline{\check{x}}_{ijt}$ represent local energy-transmission limits for the i-th ESS.

2.4 The Proposed Approach

To state our proposed approach to solve the GNEP in Definition 2.3.1, we reformulate the OPs in (2.3) in an equivalent yet more convenient form. For all $(i,j,t) \in \mathcal{A} \times \mathcal{A}_i \times \mathcal{T}$, let $y_{ijt} \in \mathbb{R}$ be an auxiliary variable to be computed by agent i, and define $\mathbf{y}_{ij}$, $\mathbf{y}_i$, $\mathbf{y}$, and $\mathbf{y}_{-i}$ according to (2.1). By introducing constraint $\check{x}_{ijt} = y_{ijt}$, constraints (2.2b)-(2.2c) can be equivalently stated as the four constraints: $\hat{\mathbf{x}}_i = \mathbf{y}_{-i}$, $\check{\mathbf{x}}_{-i} = \mathbf{y}_{-i}$, $\check{\mathbf{x}}_i = \mathbf{y}_i$, and $\hat{\mathbf{x}}_{-i} = \mathbf{y}_i$. As such, the decision of each agent $i \in \mathcal{A}$ now regards the tuple $(\hat{\mathbf{x}}_i, \check{\mathbf{x}}_i, \mathbf{y}_i, \mathbf{p}_i) \in \tilde{\Omega}_i\left(\mathbf{y}_{-i}\right) \times \Phi_i\left(\check{\mathbf{x}}_i\right) \times \mathbb{R}^{n_i}_{\geq 0}$, with

$$\begin{aligned} \tilde{\Omega}_i\left(\mathbf{y}_{-i}\right) &= \{(\hat{\mathbf{x}}_i, \check{\mathbf{x}}_i) \in \mathcal{X}_i \colon \hat{\mathbf{x}}_i = \mathbf{y}_{-i}\} \\ \Phi_i\left(\check{\mathbf{x}}_i\right) &= \{\mathbf{y}_i \in \mathbb{R}^{n_i} \colon \mathbf{y}_i = \check{\mathbf{x}}_i\}. \end{aligned}$$

On the other hand, the feasible set regarding such augmented decisions for the entire energy community is given by $\Psi \times \mathbb{R}^n_{\geq 0}$, where

$$\Psi = \left\{ (\hat{\mathbf{x}}, \check{\mathbf{x}}, \mathbf{y}) \in \prod_{i\in\mathcal{A}} \mathcal{X}_i \times \mathbb{R}^n : \begin{array}{l} \hat{\mathbf{x}} = \mathbf{B}\mathbf{y} \\ \check{\mathbf{x}} = \mathbf{y} \end{array} \right\},$$

[2]Note that higher-order dynamics for s_{it} might be used, as long as the resulting $\mathcal{X}_i$ is closed and convex.

and by Standing Assumption 2.3.1 it holds that Ψ is a closed convex set with non-empty relative interior.

For every $i \in \mathcal{A}$, the OPs in (2.3) can then be equivalently redefined as

$$\min_{\hat{\mathbf{x}}_i, \check{\mathbf{x}}_i} f_i\left(\hat{\mathbf{x}}_i, \check{\mathbf{x}}_i, \mathbf{p}_i, \mathbf{p}_{-i}\right) \text{ s.t. } \left(\hat{\mathbf{x}}_i, \check{\mathbf{x}}_i\right) \in \tilde{\Omega}_i\left(\mathbf{y}_{-i}\right) \tag{2.8a}$$

$$\min_{\mathbf{y}_i, \mathbf{p}_i} \frac{\rho_i}{2} \left\|\mathbf{p}_i - \mathbf{g}_i\left(\hat{\mathbf{x}}_{-i}\right)\right\|^2 \text{ s.t. } \left(\mathbf{y}_i, \mathbf{p}_i\right) \in \Phi_i\left(\check{\mathbf{x}}_i\right) \times \mathbb{R}^{n_i}. \tag{2.8b}$$

Note that in contrast to the OP in (2.3a), for a given agent i, the OP in (2.8a) is decoupled from the decisions $\hat{\mathbf{x}}_{-i}$ and $\check{\mathbf{x}}_{-i}$ of other agents, i.e., the inter-agent coupling in (2.8a) is only due to variables $\mathbf{p}_{-i}$ and $\mathbf{y}_{-i}$. Therefore, simultaneously solving (2.8a) for all i and under a fixed pair $(\mathbf{y}', \mathbf{p}')$ is equivalent to solving the OP given by

$$\min_{\hat{\mathbf{x}}, \check{\mathbf{x}}} \sum_{i \in \mathcal{A}} f_i\left(\hat{\mathbf{x}}_i, \check{\mathbf{x}}_i, \mathbf{p}'_i, \mathbf{p}'_{-i}\right) \text{ s.t. } \left(\hat{\mathbf{x}}, \check{\mathbf{x}}\right) \in \prod_{i \in \mathcal{A}} \tilde{\Omega}_i\left(\mathbf{y}'_{-i}\right), \tag{2.9}$$

which is separable over $\mathcal{A}$. Similarly, the inter-agent coupling in (2.8b) is only obtained through variable $\hat{\mathbf{x}}_{-i}$. Thus, simultaneously solving (2.8b) for all i and under a fixed pair $\left(\hat{\mathbf{x}}', \check{\mathbf{x}}'\right)$ is equivalent to solving the OP given by

$$\min_{\mathbf{y}, \mathbf{p}} \sum_{i \in \mathcal{A}} \frac{\rho_i}{2} \left\|\mathbf{p}_i - \mathbf{g}_i\left(\hat{\mathbf{x}}'_{-i}\right)\right\|^2 \text{ s.t. } (\mathbf{y}, \mathbf{p}) \in \prod_{i \in \mathcal{A}} \Phi_i\left(\check{\mathbf{x}}'_i\right) \times \mathbb{R}^{n_i}, \tag{2.10}$$

which is separable over $\mathcal{A}$ as well. Based on these observations, we remark that Gauss-Seidel ADMM-type GNEP solving methods [8] can be applied to the OPs in (2.8) following a three-block iterative scheme rather than iterating over the total number of agents. Consequently, in this Chapter, we adapt [8, Algorithm 4.1] to our framework. Note that [8, Algorithm 4.1] enjoys the simple structure of the celebrated ADMM algorithm, and as a Gauss-Seidel-type method it tends to converge faster than its Jacobi-type counterpart [7].

For every agent $i \in \mathcal{A}$, let $\hat{\mathbf{u}}_i \in \mathbb{R}^{n_i}$ and $\check{\mathbf{u}}_i \in \mathbb{R}^{n_i}$ be the Lagrange multipliers associated to the coupling constraints $\hat{\mathbf{x}}_i = \mathbf{y}_{-i}$ and $\check{\mathbf{x}}_i = \mathbf{y}_i$, respectively. Besides, define $\hat{\mathbf{u}}, \check{\mathbf{u}} \in \mathbb{R}^n$ using the ordering in (2.1). Let $k \in \mathbb{Z}_{\geq 0}$ denote the iteration index, and let $\hat{\mathbf{x}}^k$, $\check{\mathbf{x}}^k$, $\mathbf{y}^k$, $\mathbf{p}^k$, $\hat{\mathbf{u}}^k$, and $\check{\mathbf{u}}^k$, denote the values of the corresponding optimization variables at iteration k. Applying [8, Algorithm 4.1] to (2.9)-(2.10) yields the (sequential) updates given by

$$\begin{aligned}\left(\hat{\mathbf{x}}^{k+1}, \check{\mathbf{x}}^{k+1}\right) = \underset{(\hat{\mathbf{x}}, \check{\mathbf{x}}) \in \mathcal{X}}{\operatorname{argmin}} \Bigg\{ \sum_{i \in \mathcal{A}} f_i\left(\hat{\mathbf{x}}_i, \check{\mathbf{x}}_i, \mathbf{p}_i^k, \mathbf{p}_{-i}^k\right) + \\ \begin{bmatrix}\hat{\mathbf{u}}^k \\ \check{\mathbf{u}}^k\end{bmatrix}^\top \begin{bmatrix}\hat{\mathbf{x}} \\ \check{\mathbf{x}}\end{bmatrix} + \frac{\gamma_1}{2} \left\| \begin{bmatrix}\hat{\mathbf{x}} - \hat{\mathbf{x}}^k \\ \check{\mathbf{x}} - \check{\mathbf{x}}^k\end{bmatrix} \right\|^2 + \frac{\beta}{2} \left\| \begin{bmatrix}\hat{\mathbf{x}} - \mathbf{B}\mathbf{y}^k \\ \check{\mathbf{x}} - \mathbf{y}^k\end{bmatrix} \right\|^2 \Bigg\}\end{aligned} \tag{2.11a}$$

$$\begin{aligned}\left(\mathbf{y}^{k+1}, \mathbf{p}^{k+1}\right) = \underset{(\mathbf{y}, \mathbf{p}) \in \mathbb{R}^{2n}}{\operatorname{argmin}} \Bigg\{ \sum_{i \in \mathcal{A}} \frac{\rho_i}{2} \left\|\mathbf{p}_i - \mathbf{g}_i\left(\hat{\mathbf{x}}_{-i}^{k+1}\right)\right\|^2 - \\ \begin{bmatrix}\hat{\mathbf{u}}^k \\ \check{\mathbf{u}}^k\end{bmatrix}^\top \begin{bmatrix}\mathbf{B}\mathbf{y} \\ \mathbf{y}\end{bmatrix} + \frac{\gamma_2}{2} \left\| \begin{bmatrix}\mathbf{y} - \mathbf{y}^k \\ \mathbf{p} - \mathbf{p}^k\end{bmatrix} \right\|^2 + \frac{\beta}{2} \left\| \begin{bmatrix}\hat{\mathbf{x}}^{k+1} - \mathbf{B}\mathbf{y} \\ \check{\mathbf{x}}^{k+1} - \mathbf{y}\end{bmatrix} \right\|^2 \Bigg\}\end{aligned} \tag{2.11b}$$

$$\begin{bmatrix}\hat{\mathbf{u}}^{k+1} \\ \check{\mathbf{u}}^{k+1}\end{bmatrix} = \begin{bmatrix}\hat{\mathbf{u}}^k \\ \check{\mathbf{u}}^k\end{bmatrix} + \beta \begin{bmatrix}\hat{\mathbf{x}}^{k+1} - \mathbf{B}\mathbf{y}^{k+1} \\ \check{\mathbf{x}}^{k+1} - \mathbf{y}^{k+1}\end{bmatrix}, \tag{2.11c}$$

where $\mathcal{X} = \prod_{i\in\mathcal{A}} \mathcal{X}_i$, and $\gamma_1, \gamma_2, \beta \in \mathbb{R}_{>0}$ are constant parameters of the algorithm. Now, note that (2.11b) has the closed-form solution given by

$$\begin{aligned}\mathbf{y}^{k+1} &= \frac{1}{\gamma_2 + 2\beta}\left(\beta\mathbf{B}\hat{\mathbf{x}}^{k+1} + \beta\check{\mathbf{x}}^{k+1} + \gamma_2\mathbf{y}^k + \mathbf{B}\hat{\mathbf{u}}^k + \check{\mathbf{u}}^k\right)\\ \mathbf{p}^{k+1} &= \left(\mathbf{P} + \gamma_2\mathbf{I}_n\right)^{-1}\left(\operatorname{col}\left(\rho_i\mathbf{g}_i\left(\hat{\mathbf{x}}_{-i}^{k+1}\right)\right)_{i\in\mathcal{A}} + \gamma_2\mathbf{p}^k\right),\end{aligned}$$

with $\mathbf{P} = \operatorname{diag}\left(\rho_i\mathbf{I}_{n_i}\right)_{i\in\mathcal{A}} \in \mathbb{R}^{n\times n}_{\geq 0}$. Thus, using the facts that $\mathbf{Bz} = \operatorname{col}\left(\mathbf{z}_{-i}\right)_{i\in\mathcal{A}}$, $\mathbf{B} = \mathbf{B}^\top$, and $\mathbf{B}^\top\mathbf{B} = \mathbf{I}_n$ (c.f., Remark 2.3.1), the updates in (2.11) yield our proposed Algorithm 1, where we have defined $\mathbf{v}_i^k := \left(\hat{\mathbf{x}}_i^k, \check{\mathbf{x}}_i^k, \mathbf{y}_i^k, \mathbf{y}_{-i}^k, \mathbf{p}_i^k, \mathbf{p}_{-i}^k, \hat{\mathbf{u}}_i^k, \check{\mathbf{u}}_i^k\right)$ and

$$\begin{aligned}h_i\left(\hat{\mathbf{x}}_i, \check{\mathbf{x}}_i, \mathbf{v}_i^k\right) = f_i\left(\hat{\mathbf{x}}_i, \check{\mathbf{x}}_i, \mathbf{p}_i^k, \mathbf{p}_{-i}^k\right) + \begin{bmatrix}\hat{\mathbf{u}}_i^k\\ \check{\mathbf{u}}_i^k\end{bmatrix}^\top\begin{bmatrix}\hat{\mathbf{x}}_i\\ \check{\mathbf{x}}_i\end{bmatrix}\\ + \frac{\gamma_1}{2}\left\|\begin{bmatrix}\hat{\mathbf{x}}_i - \hat{\mathbf{x}}_i^k\\ \check{\mathbf{x}}_i - \check{\mathbf{x}}_i^k\end{bmatrix}\right\|^2 + \frac{\beta}{2}\left\|\begin{bmatrix}\hat{\mathbf{x}}_i - \mathbf{y}_{-i}^k\\ \check{\mathbf{x}}_i - \mathbf{y}_i^k\end{bmatrix}\right\|^2. \quad (2.12)\end{aligned}$$

Algorithm 1: ADMM Distributed GNE computation

1 Set parameters $\gamma_1, \gamma_2, \beta \in \mathbb{R}_{>0}$.

2 Initialize $\hat{\mathbf{x}}_i^0, \check{\mathbf{x}}_i^0, \mathbf{y}_i^0, \mathbf{p}_i^0, \hat{\mathbf{u}}_i^0, \check{\mathbf{u}}_i^0 \in \mathbb{R}^{n_i}_{\geq 0}$, $\forall i \in \mathcal{A}$.

3 Every agent $i \in \mathcal{A}$ receives $\mathbf{y}_{-i}^k$, $\mathbf{p}_{-i}^k$, and computes:

$$\left(\hat{\mathbf{x}}_i^{k+1}, \check{\mathbf{x}}_i^{k+1}\right) = \underset{(\hat{\mathbf{x}}_i, \check{\mathbf{x}}_i)\in\mathcal{X}_i}{\operatorname{argmin}}\left\{h_i\left(\hat{\mathbf{x}}_i, \check{\mathbf{x}}_i, \mathbf{v}_i^k\right)\right\}$$

4 Every agent $i \in \mathcal{A}$ receives $\hat{\mathbf{x}}_{-i}^{k+1}$, $\check{\mathbf{x}}_{-i}^{k+1}$, $\hat{\mathbf{u}}_{-i}^k$, $\check{\mathbf{u}}_{-i}^k$, and computes:

$$\begin{aligned}\mathbf{y}_i^{k+1} &= \frac{\beta\hat{\mathbf{x}}_{-i}^{k+1} + \beta\check{\mathbf{x}}_i^{k+1} + \gamma_2\mathbf{y}_i^k + \hat{\mathbf{u}}_{-i}^k + \check{\mathbf{u}}_i^k}{\gamma_2 + 2\beta}\\ \mathbf{p}_i^{k+1} &= \frac{\rho_i\mathbf{g}_i\left(\hat{\mathbf{x}}_{-i}^{k+1}\right) + \gamma_2\mathbf{p}_i^k}{\rho_i + \gamma_2}\\ \hat{\mathbf{u}}_i^{k+1} &= \hat{\mathbf{u}}_i^k + \beta\left(\hat{\mathbf{x}}_i^{k+1} - \boldsymbol{\omega}_i\right)\\ \check{\mathbf{u}}_i^{k+1} &= \check{\mathbf{u}}_i^k + \beta\left(\check{\mathbf{x}}_i^{k+1} - \mathbf{y}_i^{k+1}\right),\end{aligned}$$

with $\boldsymbol{\omega}_i = \frac{\beta\hat{\mathbf{x}}_i^{k+1} + \beta\check{\mathbf{x}}_{-i}^{k+1} + \gamma_2\mathbf{y}_{-i}^k + \hat{\mathbf{u}}_i^k + \check{\mathbf{u}}_{-i}^k}{\gamma_2 + 2\beta}$.

5 If the termination criterion is met, then stop. Otherwise, update $k \leftarrow k+1$ and go back to Step 3.

The effectiveness of Algorithm 1 is certified by Corollary 2.4.1, which provides sufficient conditions to guarantee its asymptotic convergence to a GNE of the energy community.

Corollary 2.4.1

If $\gamma_1, \gamma_2, \beta \in \mathbb{R}_{>0}$ and

$$\gamma_2 > \frac{1}{\mu}\left(4\beta^2 + \sum_{i\in\mathcal{A}}\left(\hat{L}_i^2 + \check{L}_i^2\right)\right),$$

then the iterations of Algorithm 1 converge strongly to the unique vGNE of the GNEP of Definition 2.3.1. That is, as $k \to \infty$, it holds that $\left(\hat{\mathbf{x}}^k, \check{\mathbf{x}}^k, \mathbf{p}^k\right) \to (\hat{\mathbf{x}}^*, \check{\mathbf{x}}^*, \mathbf{p}^*)$,

where $(\hat{\mathbf{x}}^*, \check{\mathbf{x}}^*, \mathbf{p}^*)$ *is a GNE.*

Proof. Note that under Standing Assumption 2.3.1, the augmented pseudo-gradient $\tilde{\mathbf{q}}(\hat{\mathbf{x}}, \check{\mathbf{x}}, \mathbf{y}, \mathbf{p}) = \left[\mathbf{q}(\hat{\mathbf{x}}, \check{\mathbf{x}}, \mathbf{p})^\top, \mathbf{0}_n^\top\right]^\top$ is monotone in all the variables, and μ-strongly monotone in $(\hat{\mathbf{x}}, \check{\mathbf{x}}, \mathbf{p})$. Thus, the result follows from [8, Theorem 4.6]. □

The input of Algorithm 1 regards the (arbitrary) initial values $(\hat{\mathbf{x}}^0, \check{\mathbf{x}}^0, \mathbf{y}^0, \mathbf{p}^0, \hat{\mathbf{u}}^0, \check{\mathbf{u}}^0)$, and its output corresponds to the optimal values $(\hat{\mathbf{x}}^*, \check{\mathbf{x}}^*, \mathbf{y}^*, \mathbf{p}^*, \hat{\mathbf{u}}^*, \check{\mathbf{u}}^*)$, such that $(\hat{\mathbf{x}}^*, \check{\mathbf{x}}^*, \mathbf{p}^*)$ is a GNE for the energy community. Observe that the computational effort of Algorithm 1 lies primarily in Step 3, which requires each agent to solve a local OP. Nonetheless, due to Standing Assumption 2.3.1 such OPs are both smooth and strongly convex, and thus can be readily solved locally by each agent using numerical tools as [14]. Finally, note that Algorithm 1 is indeed distributed, as each agent $i \in \mathcal{A}$ computes its own variables using local information obtained by communicating with its neighbors, and only two rounds of communication are required per each iteration of the algorithm.

2.5 Numerical Results

In this section, we illustrate the proposed framework through a numerical simulation over a 24 hours period, i.e., $T = 24$. As such, consider an energy community comprised of 2 ERs, 9 prosumers, and 3 ESSs, i.e., $N = 14$. Without loss of generality, we set

$$f_i\left(\hat{\mathbf{x}}_i, \check{\mathbf{x}}_i, \mathbf{p}_i, \mathbf{p}_{-i}\right) = \chi_i \left\|\hat{\mathbf{x}}_i + \check{\mathbf{x}}_i\right\|^2 + \mathbf{p}_{-i}^\top \hat{\mathbf{x}}_i - \mathbf{p}_i^\top \check{\mathbf{x}}_i$$

$$\mathbf{g}_i\left(\hat{\mathbf{x}}_{-i}\right) = \frac{\nu_i}{N_i} \mathbf{1}_{N_i} \otimes \operatorname{col}\left(\sum_{j \in \mathcal{A}_i} \hat{x}_{jit}\right)_{t \in \mathcal{T}},$$

for all $i \in \mathcal{A}$. Here, $\chi_i, \nu_i \in \mathbb{R}_{>0}$ are constant parameters. Note that $f_i(\cdot,\cdot,\cdot,\cdot)$ regards quadratic energy-transmission-related costs, weighted by χ_i, while the considered pricing function $\mathbf{g}_i(\cdot)$ corresponds to a linear map on the averaged aggregate energy request of the neighbors of agent i, weighted by ν_i. In fact, such a pricing function can be rewritten as $\mathbf{g}_i(\hat{\mathbf{x}}_{-i}) = \mathbf{Q}_i \hat{\mathbf{x}}_{-i}$, with $\mathbf{Q}_i = (\nu_i/N_i)\left(\mathbf{1}_{N_i}\mathbf{1}_{N_i}^\top\right) \otimes \mathbf{I}_T$. Thus, $\mathbf{Q}_i^\top \mathbf{Q}_i = \nu_i \mathbf{Q}_i$, and $\lambda_{\max}\left(\mathbf{Q}_i^\top \mathbf{Q}_i\right) = \nu_i^2$. Hence, the considered functions fit the setup of Proposition 2.3.1 with $\underline{\theta} = 2\min_{i \in \mathcal{A}} \chi_i$ and $\overline{\lambda} = \max_{i \in \mathcal{A}} \nu_i^2$. For simplicity, for our numerical experiments we set $\rho_i = 1$, and we randomly sample $\chi_i \sim \mathcal{U}[1.5, 2]$ and $\nu_i \sim \mathcal{U}[0.5, 1]$, for all $i \in \mathcal{A}$. Therefore, (2.5) simplifies to $\underline{\theta} \geq \mu + (2/(1-\mu))$. Since $\underline{\theta} \geq 3$, it follows that (2.5) is satisfied with $\mu = 0.26$. Finally, note that for the considered functions it follows that $\hat{L}_i = \check{L}_i = 1$.

Regarding the graph $\mathcal{G}$, we consider a random undirected topology plus a star graph with an ER as the central node. An illustration of the network is reported in Fig. 2.2.

For the agents' parameters, we sample $\overline{\hat{x}}_{ijt}, \overline{\check{x}}_{ijt} \sim \mathcal{U}[4, 6]$ kWh, $\hat{a}_{it}, \check{a}_{it} \sim \mathcal{U}[50, 80]$ kWh, $\delta_{it} = G_{it} - D_{it}$ where $G \sim \mathcal{N}[T/2, \sigma_i]$ kWh represents the energy generation (with $\sigma_i \sim \mathcal{U}[0, 2]$), and $D \sim \mathcal{U}[0, 2]$ kWh represents the demand, $\overline{s}_i \sim \mathcal{U}[20, 30]$ kWh, $s_{ij0} \sim \mathcal{U}[0, \overline{s}_i/N_i]$ kWh, and $\alpha_i, \hat{\eta}_i, \check{\eta}_i \sim \mathcal{U}[0.95, 0.98]$, for all the corresponding $i \in \mathcal{A}$, $j \in \mathcal{A}_i$, and $t \in \mathcal{T}$. Nonetheless, we numerically check that Ω is non-empty so that Standing Assumption 2.3.1 holds. Moreover, although the simulation data is synthetic, G_{it} follows the typical bell-shaped curve of photovoltaic generation so that the obtained results follow plausible trends.

Finally, regarding the parameters of Algorithm 1, we let $\gamma_1 = \beta = 0.5$, and we set $\gamma_2 = 112$. Thus, the sufficient condition of Corollary 2.4.1 is satisfied and the convergence of Algorithm 1 to the unique GNE of the energy community is guaranteed. In fact, Fig.

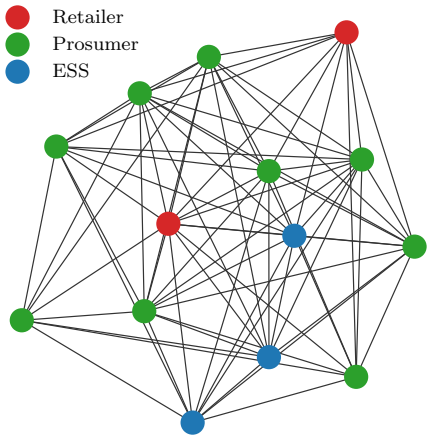

Figure 2.2: The energy trading network considered for the numerical examples (edges enable both communication and trading). The grid is composed by 2 retailers (red), 8 prosumers (green), and 3 ESSs (blue).

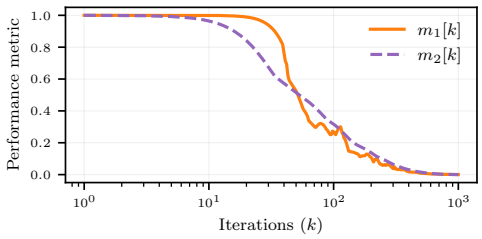

Figure 2.3: Evolution of the selected performance metrics over 10^3 iterations of Algorithm 1. Without loss of generality, the initial condition is taken as $\hat{\mathbf{x}}_i^0, \check{\mathbf{x}}_i^0, \mathbf{y}_i^0, \mathbf{p}_i^0, \hat{\mathbf{u}}_i^0, \check{\mathbf{u}}_i^0 = \mathbf{0}_{n_i}$, for all $i \in \mathcal{A}$.

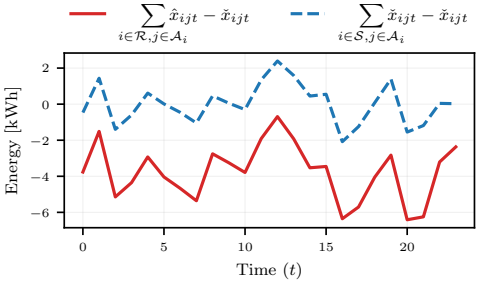

Figure 2.4: Net aggregate energy flow for ERs (red, solid) and ESSs (blue, dashed) during the $T = 24$ hours window.

2.3 depicts the evolution of the performance metrics

$$m_1[k] = \frac{\left\|\hat{\mathbf{x}}^k - \mathbf{B}\check{\mathbf{x}}^k\right\|_\infty}{\left\|\hat{\mathbf{x}}^1 - \mathbf{B}\check{\mathbf{x}}^1\right\|_\infty}, \qquad m_2[k] = \frac{\left\| \begin{bmatrix} \hat{\mathbf{x}}^k - \hat{\mathbf{x}}^* \\ \check{\mathbf{x}}^k - \check{\mathbf{x}}^* \\ \mathbf{p}^k - \mathbf{p}^* \end{bmatrix} \right\|_\infty}{\left\| \begin{bmatrix} \hat{\mathbf{x}}^1 - \hat{\mathbf{x}}^* \\ \check{\mathbf{x}}^1 - \check{\mathbf{x}}^* \\ \mathbf{p}^1 - \mathbf{p}^* \end{bmatrix} \right\|_\infty},$$

where $(\hat{\mathbf{x}}^*, \check{\mathbf{x}}^*, \mathbf{p}^*)$ is the unique GNE of the energy community. Namely, metric $m_1[k]$ measures the satisfaction of the agreement constraints in (2.2b)-(2.2c), for all $i \in \mathcal{A}$, while $m_2[k]$ yields the infinity-norm distance to the GNE (both metrics are normalized over the first iteration's results). That is, if $m_1[k] = 0$, then the computed energy transactions at iteration k are attainable over the energy community and if $m_2[k] = 0$, then the computed solution at iteration k is a GNE for the energy community. As shown, in Fig. 2.3, the selected metrics indeed converge asymptotically to 0, verifying the effectiveness of Algorithm 1.

Figure 2.4 reports the net aggregate energy flow of the ERs and ESSs. These aggregate flows represent the total collective amount of energy sold (bought) to (from) the ERs, and the amount of energy injected (drawn) to (from) the ESSs, respectively. The two curves in Fig. 2.4 have the same shape due to the shared cyclicity of the renewable source, which reaches its peak during the middle of the day.

2.6 Conclusions

In this Chapter, we have formulated an energy transactive framework to model energy communities comprised of (but not limited to) prosumers, energy storage systems, and energy retailers. The underlying control task is formulated as a so-called GNEP, and a distributed Gauss-Seidel-type alternating direction method of multipliers algorithm is devised to solve it. Furthermore, sufficient conditions on the local cost and energy pricing functions are provided, so that the convergence of the algorithm is guaranteed.

References

[1] Akorede, M. F., Hizam, H., and Pouresmaeil, E., "Distributed energy resources and benefits to the environment," *Renewable and Sustainable Energy Reviews*, vol. 14, no. 2, pp. 724–734, 2010.

[2] Jarventausta, P., Repo, S., Rautiainen, A., and Partanen, J., "Smart grid power system control in distributed generation environment," *Annual Reviews in Control*, vol. 34, no. 2, pp. 277–286, 2010.

[3] Osborne, M. J., *An introduction to game theory*. Oxford University Press New York, 2004, vol. 3.

[4] Facchinei, F. and Kanzow, C., "Generalized Nash equilibrium problems," *Annals of Operations Research*, vol. 175, no. 1, pp. 177–211, 2010.

[5] Yi, P. and Pavel, L., "Distributed generalized Nash equilibria computation of monotone games via double-layer preconditioned proximal-point algorithms," *IEEE Transactions on Control of Network Systems*, vol. 6, no. 1, pp. 299–311, 2019. DOI: 10.1109/TCNS.2018.2813928.

[6] Belgioioso, G., Yi, P., Grammatico, S., and Pavel, L., "Distributed generalized Nash equilibrium seeking: An operator-theoretic perspective," *IEEE Control Systems Magazine*, vol. 42, no. 4, pp. 87–102, 2022.

[7] Borgens, E. and Kanzow, C., "A distributed regularized Jacobi-type ADMM-method for generalized Nash equilibrium problems in Hilbert spaces," *Numerical Functional Analysis and Optimization*, vol. 39, no. 12, pp. 1316–1349, 2018.

[8] Borgens, E. and Kanzow, C., "ADMM-type methods for generalized Nash equilibrium problems in Hilbert spaces," *SIAM Journal on Optimization*, vol. 31, no. 1, pp. 377–403, 2021. DOI: 10.1137/19M1284336.

[9] Wang, Z., Liu, F., Ma, Z., *et al.*, "Distributed generalized Nash equilibrium seeking for energy sharing games in prosumers," *IEEE Transactions on Power Systems*, vol. 36, no. 5, pp. 3973–3986, 2021. DOI: 10.1109/TPWRS.2021.3058675.

[10] Mignoni, N., Carli, R., and Dotoli, M., "Distributed noncooperative mpc for energy scheduling of charging and trading electric vehicles in energy communities," *IEEE Transactions on Control Systems Technology*, 2023.

[11] Martinez-Piazuelo, J., Quijano, N., and Ocampo-Martinez, C., "Decentralized charging coordination of electric vehicles under feeder capacity constraints," *IEEE Transactions on Control of Network Systems*, vol. 9, no. 4, pp. 1600–1610, 2021.

[12] Mignoni, N., Scarabaggio, P., Carli, R., and Dotoli, M., "Control frameworks for transactive energy storage services in energy communities," *Control Engineering Practice*, vol. 130, p. 105 364, 2023.

[13] Facchinei, F. and Pang, J.-S., *Finite-dimensional variational inequalities and complementarity problems*. Springer, 2003, vol. 1.

[14] Agrawal, A., Verschueren, R., Diamond, S., and Boyd, S., "A rewriting system for convex optimization problems," *Journal of Control and Decision*, vol. 5, no. 1, pp. 42–60, 2018.

Chapter 3

Control Frameworks for Transactive Energy Storage Services in Energy Communities

III

Abstract

Recently, the decreasing cost of storage technologies and the emergence of economy-driven mechanisms for energy exchange are contributing to the spread of energy communities. In this context, this Chapter aims to define innovative transactive control frameworks for energy communities equipped with independent service-oriented energy storage systems. The addressed control problem consists of optimally scheduling the energy activities of a group of prosumers, characterized by their demand and renewable generation, and a group of energy storage service providers, able to store the prosumers' energy surplus and, subsequently, release it upon a fee payment. We propose two novel resolution algorithms based on a game theoretical control formulation, a coordinated and an uncoordinated one, which can be alternatively used depending on the underlying communication architecture of the grid. The two proposed approaches are validated through numerical simulations of realistic scenarios. Results show that the use of a particular framework does not alter fairness, at least at the community level, i.e., no participant in the groups of prosumers or providers can strongly benefit from changing its strategy while compromising others' welfare. Lastly, the approaches are compared with a centralized control method showing better computational results.

Contents

3.1 Introduction

A powerful solution contributing to the green transformation of modern power systems is represented by the so-called *energy community* [1]. The term denotes a community of users (private, public, or mixed) located in a specific reference area, where all stakeholders – such as end-users (e.g., citizens, companies, etc.), market players (e.g., utilities, service providers), practitioners, planners and policy-makers – actively cooperate to develop a 'smart' energy system. More specifically, these communities promote the optimal exploitation of renewable sources and the widespread use of distributed storage while enabling the application of measures oriented to cost-effectiveness, sustainability, and reliability [1]–[3]. In the last years, community action on the use of renewable energy has increased remarkably, pushed by several energy-efficiency initiatives as well as financial incentives [4], [5].

Fostered by the decreasing cost of storage technologies and emerging mechanisms of energy exchange and sharing, a viable solution to attain self-consumption of on-site

production is represented by the use of *energy storage systems* (ESSs) that are valuable resources of the community at the local level [6]. The use of ESSs allows users to create energy arbitrage by discharging during price peaks and charging during off-peak periods if a variable energy price is considered [7], [8]. In addition, ESSs contribute to the overall resilience of the energy community when facing systematic failures or natural disasters [9]. Moreover, ESSs guarantee stability and power quality when uncertain renewable energy sources, such as wind power and photovoltaic, highly influence the energy community [10], [11]. Nevertheless, the full penetration of ESSs presents various challenges. Due to economic and logistic reasons, the deployment of an individual ESS for each prosumer is not always a viable option. Conversely, sharing ESSs among prosumers or relying on energy storage services innovatively offered by providers is a widespread solution in energy communities [12], [13].

Among the most popular methods, the *transactive control* techniques are especially suitable to address the issues related to energy storage sharing sustainably and reliably [14]. Indeed, transactive energy management methods incorporate powerful economy-driven control mechanisms for effectively coordinating and trading energy flows among the actors of microgrids and energy communities [15]. Differently from peer-to-peer (P2P) energy trading, which suffers from sustainability issues (if a prosumer sells energy to another one, the former gains an economical bonus, but it is not guaranteed that the latter will be able to provide energy to the former when needed: in such a case, the prosumer lacking energy will be forced to resort to the retailer [16]), the deployment of energy storage services continuously guarantee that the amount of stored energy is available for future use, injecting back energy sourced from renewable means.

In this context, this Chapter aims to define innovative transactive control frameworks to optimally manage and share energy within a community with multiple and independent service-oriented energy storage systems. In particular, the considered energy community comprises prosumers, characterized by their own demand and renewable generation, and energy storage service providers, able to store the prosumers' energy surplus and subsequently release it upon a fee payment. The addressed control problem consists of optimally scheduling the energy activities of prosumers and providers, relying on an economy-driven mechanism, to make the prosumers' energy supply more efficient while creating a sustainable and profitable business model for storage providers. In order to guarantee a solution to the problem, an energy retailer, characterized by conventional power generation, allows prosumers to buy/sell energy from/to the main grid. The novel proposed resolution algorithms are based on a game theoretical control formulation of the transactive energy storage management problem. In particular, a coordinated and an uncoordinated control scheme are defined, to be alternatively used depending on the underlying communication architecture of the grid. The two proposed approaches are validated through numerical simulations of realistic scenarios. Lastly, the approaches are compared with a centralized control method showing better computational results.

3.1.1 Related Works

The traditional approach in utilizing energy resources relies on the individual distributed framework, in which an individually-owned resource is installed for each user separately [17]. Due to the logistic and cost inefficiency of such a framework, and the spread of energy community initiatives, recent studies suggest the sharing strategy for the utilization of key components such as ESSs to fully exploit their potentials [18]. However, no unifying framework has been proposed in the face of several access schemes based on the paradigms of physical/financial rights and resource capacity/energy sharing [19]. A comprehensive review of the design and application of shared ESSs is provided in [20]. In such a paper, authors provide an architectural classification of shared ESSs, categorized into *private*, *interconnected*, *common*, and *independent* ESS solutions. Private and interconnected ESSs, which contemplate the presence of one ESS per user, are a highly inefficient solution, due to high infrastructural and maintenance costs as well as the necessity of a dedicated physical space [20]. For these reasons, researchers are focusing on both the alternatives of

common and independent ESSs. The former type of ESS consists of a ESS block that can be simultaneously accessed by multiple users. Control strategies for this architecture include formulations as resource allocation problem [21] and aggregator-based management [22]. Conversely, in the independent ESS architecture, storage devices are independently managed by profit-driven operators. Thus, the necessity of designing an adequate market mechanism for handling the interactions between ESS operators and users is necessary. For instance, authors in [23] propose a market framework considering the ESS operator as a stand-alone agent that evaluates the optimal storage trading strategy. In [24], a Stackelberg game-based energy trading strategy is developed for minimizing the energy cost in a neighborhood area with an independent shared ESS.

Many of the common and independent ESS applications fall in the realm of the *sharing economy* (SE) business model (also known as *access economy*), which has been growing in popularity in the last decade. Companies such as Airbnb and Uber are just two of the numerous examples of this economic paradigm. In [25] the opportunities arising from adopting SE models in energy communities have been explored. In particular, the authors consider a collection of firms that invest in ESS to arbitrage against variable energy prices and share the surplus of their stored energy. Authors in [26] show that applications of SE paradigms in ESS are an economically attractive solution for both ESS operators as well as ESS investors. In [27] the potential of shared ESS for a neighborhood area is demonstrated, in which residents are able to dynamically optimize the energy load of the storage level to minimize their electricity costs. Regarding control schemes of SE applications of ESS, authors in [28] explore different market design options based on cooperative and non-cooperative game-theoretic models, showing that SE reduces the cost volatility for most users while keeping the community operational costs unchanged. Among the different SE-based implementations of shared ESS, two promising concepts are the *Virtual ESS* (VESS) [29], [30] and the *Cloud ESS* (CESS) [31], [32]. The VESS is inspired by the *Virtual Power Plant* (VPP) concept. VPPs work as aggregators of coordinated distributed energy sources, to optimize the energy supply. Similarly, the VESS concept is based on integrating different distributed ESSs, to create a virtual single storage system, able to serve users in the network. In [33], an agent-based ESS management system is proposed for allowing the integration of storage devices into a VESS. Authors in [34] investigate the value of merchant-owned ESS in the day-ahead electricity market, developing an offering strategy for operating and optimizing the virtual storage plant constructed by merging the merchant-owned ESS units. In [35], a two-stage optimization model for VESS sharing is studied, where, in the first phase, the investment and pricing for the storage capacity are determined by the aggregator. In contrast, the purchase of virtual capacity is performed by the users during the second phase. As for the CESS, the originating idea is borrowed from *cloud computing* in computer science, where distributed machines are coordinated to provide data storage and computational power efficiently and readily. CESS adopts the same concept for ESS, differing from VESS in terms of size, since CESS applications are meant to reach grid-scale energy markets. In [31], the authors propose the concept of CESS which is constructed by centralizing ESS resources. The same authors also demonstrate the benefits of CESS by investigating the investment and operating decisions of both the CESS coordinator and the consumers [36]. Regarding the control mechanisms for CESS, peer-to-peer energy sharing and coordination mechanisms are designed in [32] in order to make the penetration of renewable energy sources more effective.

3.1.2 Contributions

From the above literature review, it follows that the majority of studies on multiple ESS sharing focuses on the economy-driven control mechanisms that enable the interaction between the users and ESS operators. Despite the rich state of the art on energy storage services and management, very few research studies pay attention to crucial operational aspects of the adopted transactive mechanism. In fact, to allow the large-scale deployment

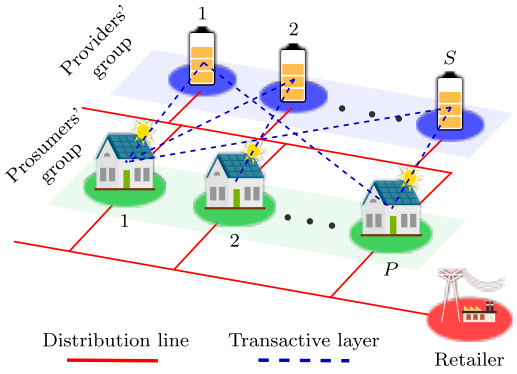

Figure 3.1: Energy community model: an overview of distribution lines and transactive layer. Dashed lines represent the economic transactions allowed between the involved actors. For instance, in the figure, prosumer 1 negotiates with providers 1, 2, and S (i.e., $\mathcal{A}_{11} = 1$, $\mathcal{A}_{12} = 1$, $\mathcal{A}_{1S} = 1$); prosumer 2 negotiates with providers 2 and S (i.e., $\mathcal{A}_{22} = 1$, $\mathcal{A}_{1S} = 1$); prosumer P negotiates with providers 1 and S (i.e., $\mathcal{A}_{P1} = 1$, $\mathcal{A}_{PS} = 1$).

of VESSs or CESSs, challenges such as practical effectiveness, computational efficiency, scalability, and privacy are obviously of primary importance.

Differently from the reviewed works, the contributions of this Chapter can be summarized as follows.

- We define a transactive energy management model, characterized by limited information sharing and a scalable communication architecture, which includes two groups of participants, namely, the energy storage service providers and the energy community prosumers (intended as customers of the energy storage service). Thanks to its scalability, the proposed approach can be implemented more efficiently than contributions [23], [24], where only a single ESS can be handled. Moreover, differently from [32], where the ESS is considered ideal, in our work we employ a realistic model, which accounts for energy losses.
- Differently from most approaches, such as [27], [31], that consider only a central coordinator managing all the different aspects of the energy community, we also propose a non-coordinated and fully distributed control architecture. However, we do not employ cooperative frameworks, such as [32], that cannot fully capture the real market interactions, or non-cooperative ones that are computationally demanding [28]. In fact, we develop uncoordinated and coordinated distributed control frameworks, which reach an overall economic performance close to the optimal centralized global formulation, whose implementation is in turn impractical for service-based solutions and is unfeasible from a computational point of view.
- Moreover, we avoid straightforward investments analysis act to guarantee economic feasibility such as in [25], [26], but we fully analyze the proposed approach from an operational point of view, ensuring the feasibility of the underlying business model arising from the prosumer-provider interactions, by simulating the latter on real-case scenarios.
- Lastly, we compare the results of the optimal centralized global formulation, like in [35], with the ones of our frameworks. We show a considerable saving in the computational effort by our approaches, with minimal loss on the economic performance.

3.2 The Energy Community Model

Let us introduce some basic notation used throughout the rest of the paper. $\mathbb{R}$ and $\mathbb{R}_{\geq 0}$ denote the set of real and positive real numbers, respectively. $\mathbb{N}$ denotes the set of natural numbers. $\mathbf{A}^\top$ denotes the transpose of matrix $\mathbf{A}$. $\|\mathbf{a}\|$ is the 2-norm of vector $\mathbf{a}$. Moreover, for a set $\mathcal{N} := \{1, ..., i, ..., N\} \subset \mathbb{N}$ we have that $\mathbf{x} := (\mathbf{x}_i)_{i \in \mathcal{N}}$ is equal to $\mathbf{x} := (\text{vec}(\mathbf{x}_1)^\top, ..., \text{vec}(\mathbf{x}_n)^\top, ..., \text{vec}(\mathbf{x}_N)^\top)^\top$ where $\text{vec}(\cdot)$ is the vectorization operator.

In this Section, we describe the proposed energy community model, shown in Fig. 3.1, which includes several independent actors. In particular, we formally define the set of

energy community actors (or agents) $\mathcal{C} := \{1, ..., C\} \subset \mathbb{B}$ as the union of the group of *prosumers* $\mathcal{P} := \{1, ..., P\} \subset \mathbb{N}$ and the group of *energy storage providers* –briefly called *providers*– $\mathcal{S} := \{1, ..., S\} \subset \mathbb{N}$. Note that $\mathcal{C} = \mathcal{S} \cup \mathcal{P}$ while $\mathcal{S} \cap \mathcal{P} = \varnothing$ (consequently, $C = P + S$). Let us now define the topology related to the allowed economic transactions between active agents. In particular, we define the matrix $\mathcal{A}$ as a symmetric $P \times S$ binary matrix such that for each prosumer $i \in \mathcal{P}$ and provider $j \in \mathcal{S}$ the element $\mathcal{A}_{ij} = 1$ if the two agents have an agreement for exchanging energy or zero otherwise. Moreover, we indicate the set of the provider neighbors associated to the prosumer $i \in \mathcal{P}$ as $\mathcal{N}_i = \{j \in \mathcal{S} \mid \mathcal{A}_{ij} = 1\}$ with cardinality $N_i = |\mathcal{N}_i|$, and the set of the prosumer neighbors associated to the provider j as $\mathcal{M}_j = \{i \in \mathcal{P} \mid \mathcal{A}_{ij} = 1\}$ with cardinality $M_j = |\mathcal{M}_j|$.

The control frameworks proposed in this Chapter are based on the well-known rolling horizon paradigm, therefore let us define a control horizon composed of T time intervals, with $\mathcal{T} := \{1, ..., T\} \in \mathbb{N}$ [37].

The proposed energy community model relies on the following standing assumptions that are typically employed in the related literature, e.g., [38], [39]

- *Market structure*: the energy transactions between members of the same group cannot occur (e.g., a prosumer cannot exchange energy with another prosumer).
- *Energy retailer (ER)*: the energy community interacts with an external passive actor, required to guarantee the power balance in the community network. In particular, the ER allows prosumers/sell energy from/to the main grid.
- *Perfect competition*: the profile of the energy storage pricing coefficient is equal for all providers.
- *Storage efficiencies*: the ESSs parameters, such as the leakage coefficient and the charging/discharging efficiencies, are constant for all providers.
- *Nonstochasticity*: the energy demand and the renewable energy production profiles are known for the entire time horizon and deterministic.

Having defined the structure of the energy community and the standing assumptions, we now describe in detail the model of the aforementioned independent actors.

3.2.1 Prosumers

These actors are characterized by variable load consumption and renewable energy production. They sell the surplus energy to or buy the deficit energy from the ER following time-variable pricing. As an alternative, they can store/withdraw energy in/from the ESSs owned by the storage providers, upon a renting fee.

For prosumer $i \in \mathcal{P}$, we indicate the energy demand and generation, at the generic time slot $t \in \mathcal{T}$, with D_{it} and G_{it}, respectively. The energy bought from the retailer at the time slot $t \in \mathcal{T}$ is $\hat{p}_{it}$, while the energy sold to it is denoted by $\check{p}_{it}$. Moreover, the energy delivered to the storage provider $h \in \mathcal{N}_i$ at the time slot $t \in \mathcal{T}$ is $\check{d}_{iht}$, while the retrieved amount is $\hat{d}_{iht}$. The portion of the charge level fraction dedicated to prosumer $i \in \mathcal{P}$ by provider $h \in \mathcal{N}_i$ is indicated with s_{iht}. We define vectors $\mathbf{p}_i^{\uparrow} = (\hat{p}_{it})_{t\in\mathcal{T}}$, $\check{\mathbf{p}}_i = (\check{p}_{it})_{t\in\mathcal{T}}$, $\hat{\mathbf{d}}_i = (\hat{\mathbf{d}}_{it})_{t\in\mathcal{T}}$, $\check{\mathbf{d}}_i = (\check{\mathbf{d}}_{it})_{t\in\mathcal{T}}$, $\mathbf{s}_i = (s_{it})_{t\in\mathcal{T}}$ collecting all the aforementioned variables for the entire control horizon $\mathcal{T}$, where $\hat{\mathbf{d}}_{it} = (\hat{d}_{iht})_{h\in\mathcal{N}_i}$, $\check{\mathbf{d}}_{it} = (\check{d}_{iht})_{h\in\mathcal{N}_i}$, $\mathbf{s}_{it} = (s_{iht})_{h\in\mathcal{N}_i}$. Accordingly, we define the control vector $\mathbf{x}_{\mathcal{P},i} = (\mathbf{p}_i^{\uparrow}, \check{\mathbf{p}}_i, \hat{\mathbf{d}}_i, \check{\mathbf{d}}_i, \mathbf{s}_i)$ to collect all the decision variables for prosumer $i \in \mathcal{P}$.

Each prosumer $i \in \mathcal{P}$ aims at determining the optimal value of the control vector that minimizes the energy cost incurred throughout the entire time horizon $\mathcal{T}$, which can be

formally defined as follows

$$J_{\mathcal{P},i}(\mathbf{x}_{\mathcal{P},i}) = \sum_{t\in\mathcal{T}} \Bigg[\underbrace{C_t\hat{p}_{it} - R_t\check{p}_{it} + L_t \sum_{h\in\mathcal{N}_i} s_{iht}}_{\substack{\text{Energy exchange cost/revenue} \\ \text{and storage fee}}} + \underbrace{\frac{1}{2}\xi_i \left(p_{it}^{\uparrow^2} + p_{it}^{\downarrow^2} + \sum_{h\in\mathcal{N}_i} \left(d_{iht}^{\uparrow^2} + d_{iht}^{\downarrow^2} \right) \right)}_{\text{Energy transmission costs}} \Bigg] \tag{3.1}$$

where $C_t \in \mathbb{R}_{\geq 0}$ and $R_t \in \mathbb{R}_{\geq 0}$ are the retailer's energy selling price and buying cost, respectively. Moreover, $L_t \in \mathbb{R}_{\geq 0}$ is the storage fee coefficient, which is equal for all providers, while $\xi_i \in \mathbb{R}_{\geq 0}$ represents the energy transmission cost coefficient for prosumer $i \in \mathcal{P}$. Note that the cost function (3.1) comprises two terms: the first contribution is composed of linear terms representing the cost/revenue due to energy exchanged with the retailer and the storage fee, while the second includes quadratic terms modelling the transmission costs. Each i-th prosumer, $i \in \mathcal{P}$, is forced to respect the following constraints, for all $t \in \mathcal{T}$:

$$D_{it} - G_{it} = \sum_{h\in\mathcal{N}_i} \left(\hat{d}_{iht} - \check{d}_{iht} \right) + \hat{p}_{it} - \check{p}_{it}, \tag{3.2a}$$

$$s_{iht} = \alpha s_{ih,t-1} + \hat{\eta}\check{d}_{iht} - \check{\eta}\hat{d}_{iht}, \qquad \forall h \in \mathcal{N}_i \tag{3.2b}$$

$$s_{ih1} = s_{ihT}, \qquad \forall h \in \mathcal{N}_i \tag{3.2c}$$

$$\hat{d}_{igt},\ \check{d}_{igt} = 0, \qquad \forall g \notin \mathcal{N}_i \tag{3.2d}$$

$$0 \leq\ \check{d}_{iht},\ \hat{d}_{iht} \leq d_i^{\max}, \qquad \forall h \in \mathcal{N}_i \tag{3.2e}$$

$$0 \leq\ \check{p}_{it},\ \hat{p}_{it} \leq p_i^{\max}, \tag{3.2f}$$

$$s_{iht} \geq 0, \qquad \forall h \in \mathcal{N}_i \tag{3.2g}$$

Constraints (3.2a) represent the energy balance equation over the whole control horizon. Constraints (3.2b) include the dynamical state equation for the charge level related to the ESS of each provider $h \in \mathcal{N}_i$, where α, $\hat{\eta}$, and $\check{\eta}$ denote the leakage coefficient, and the charging and discharging efficiencies, respectively. Constraint (3.2c) ensures that the storage fraction held by prosumer $i \in \mathcal{P}$ in the ESS of provider $h \in \mathcal{N}_i$ is equal, at the end of time horizon, to the initial level. Constraints (3.2d) impose that the energy flow between prosumer i and any disconnected provider $g \notin \mathcal{N}_i$ is null. Equations (3.2e) and (3.2f) are technological constraints imposing the energy flows towards the ESS of each provider $h \in \mathcal{N}_i$ and towards the ER to be non-negative and limited by the upper bounding values $d_i^{\max}$ and $p_i^{\max}$, respectively. Lastly, (3.2g) ensures the non-negativity of the i-th prosumer storage fraction. The resulting feasible set $\mathcal{K}_{\mathcal{P},i}$ for each prosumer $i \in \mathcal{P}$ is thus defined as:

$$\mathcal{K}_{\mathcal{P},i} = \left\{ \mathbf{x}_{\mathcal{P},i} \in \mathbb{R}_{\geq 0}^{2T+3TN_i} \mid (3.2a) - (3.2g)\ \text{hold} \right\}. \tag{3.3}$$

3.2.2 Energy Storage Providers

These actors are characterized by an energy storage capacity that can be used to store the prosumers' exceeding energy generation in return for a rental fee. Energy storage is a key feature in energy communities, contributing to different services such as load shifting, frequency regulation, peak shaving, and energy arbitrage. Several energy storage technologies – such as electrochemical (batteries and fuel cells), electromechanical (flywheels and pump hydro), electrostatic (ultra-capacitors), and electromagnetic (superconducting magnetic storage) types – are available. However, electrochemical batteries have recently been recognized as the game-changing technology in energy communities, due to their high applicability and low cost. Hence, in this work, we assume that each provider owns an electrochemical battery, whose model is detailed in the following.

For each provider $j \in \mathcal{S}$, we indicate the energy stored by and released to prosumer $k \in \mathcal{M}_j$ at the generic time slot $t \in \mathcal{T}$ with $\hat{q}_{kjt}$ and $\check{q}_{kjt}$, respectively. The portion of the

charge level reserved to prosumer $k \in \mathcal{M}_j$ by provider $j \in \mathcal{S}$ at time slot $t \in \mathcal{T}$ is indicated with b_{kjt}. We define vectors $\mathbf{q}_j^{\uparrow} = (\mathbf{q}_{jt}^{\uparrow})_{t\in\mathcal{T}}$, $\mathbf{q}_j^{\downarrow} = (\mathbf{q}_{jt}^{\downarrow})_{t\in\mathcal{T}}$, $\mathbf{b}_j = (\mathbf{b}_{jt})_{t\in\mathcal{T}}$ collecting all the aforementioned variables for the entire control horizon $\mathcal{T}$, where $\mathbf{q}_{jt}^{\uparrow} = (\hat{q}_{kjt})_{k\in\mathcal{M}_j}$, $\mathbf{q}_{jt}^{\downarrow} = (\check{q}_{kjt})_{k\in\mathcal{M}_j}$ and $\mathbf{b}_{jt}^{\downarrow} = (b_{kjt}^{\downarrow})_{k\in\mathcal{M}_j}$. Accordingly, we define the control vector $\mathbf{x}_{\mathcal{S},j} = (\mathbf{q}_j^{\uparrow}, \mathbf{q}_j^{\downarrow}, \mathbf{b}_j)$ including all the decision variables for the j-th provider.

Each provider $j \in \mathcal{S}$ aims at determining the optimal value of the control vector that minimizes the energy storage service cost throughout the entire time horizon $\mathcal{T}$, which can be formally defined as:

$$J_{\mathcal{S},j}(\mathbf{x}_{\mathcal{S},j}) = \sum_{t\in\mathcal{T}} \sum_{k\in\mathcal{M}_j} \Bigg[\underbrace{\frac{1}{2}\zeta_j(\hat{q}_{kjt} + \check{q}_{kjt})^2}_{\text{ESS degradation costs}} - \underbrace{L_t b_{kjt}}_{\text{Revenues}} \Bigg] \tag{3.4}$$

where $L_t \in \mathbb{R}_{\geq 0}$ is the storage revenue coefficient that is the same for all providers and $\zeta_j \in \mathbb{R}_{\geq 0}$ is the ESS technological degradation coefficient, modelled as in Eq. (4) of [38]. The cost function (3.4) comprises two terms: the first contribution is a quadratic term accounting for the degradation cost of the ESS (to be minimized), whilst the second represents the revenue obtained from the provided storage service (to be maximized). Each j-th provider, $j \in \mathcal{S}$, is forced to respect the following constraints, for all $t \in \mathcal{T}$:

$$b_{kjt} = \alpha b_{kj,t-1} + \hat{\eta}\hat{q}_{kjt} - \check{\eta}\check{q}_{kjt}, \qquad \forall k \in \mathcal{M}_j \tag{3.5a}$$

$$b_{kj1} = b_{kjT}, \qquad \forall k \in \mathcal{M}_j \tag{3.5b}$$

$$\hat{q}_{gjt},\ \check{q}_{gjt} = 0, \qquad \forall g \notin \mathcal{M}_j \tag{3.5c}$$

$$0 \leq\ \hat{q}_{kjt},\ \check{q}_{kjt} \leq q_j^{\max}, \qquad \forall k \in \mathcal{M}_j \tag{3.5d}$$

$$\sum_{k\in\mathcal{M}_j} b_{kjt} \leq b_j^{\max}, \tag{3.5e}$$

$$b_{kjt} \geq 0, \qquad \forall k \in \mathcal{M}_j. \tag{3.5f}$$

Similarly to the prosumer case, constraints (3.5a) include the dynamical state equation for the portion of charge level reserved to each prosumer $k \in \mathcal{M}_j$. Constraint (3.5b) ensures that the storage fraction held by provider $j \in \mathcal{S}$ for prosumer $k \in \mathcal{M}_j$ at the end of the time horizon is equal to the initial level. Constraints (3.5c) imposes that the energy flow between any provider $j \in \mathcal{S}$ and any disconnected prosumer $g \notin \mathcal{M}_j$ is null. Constraints (3.5d) impose that charging and discharging flows are non-negative and limited by the upper bound $q_j^{\max}$. Lastly, (3.5e) and (3.5f) impose that the cumulative charge level, for all prosumers connected to provider $j \in \mathcal{S}$, is upper bounded by the maximum storage capacity $b_j^{\max}$ and that the charge level fraction reserved to each prosumer $k \in \mathcal{M}_j$ is non-negative. The constraints set $\mathcal{K}_{\mathcal{S},j}$ for each provider $j \in \mathcal{S}$ is thus defined as:

$$\mathcal{K}_{\mathcal{S},j} = \left\{ \mathbf{x}_{\mathcal{S},j} \in \mathbb{R}_{\geq 0}^{3TM_j} \mid (3.5a) - (3.5f) \text{ hold} \right\}. \tag{3.6}$$

Note that, despite the similarity of the two equations, (3.2) and (3.5) do not express in general the same dynamics. They represent the storage dynamics that prosumers and providers are *willing* to follow, respectively, but not necessarily agree upon. However, to work properly, we define a suitable mechanism which ensures that (3.2) and (3.5) converge to a common dynamics, as it will be shown in the following.

3.3 The Transactive Energy Storage Management Problem

The transactive energy management problem involving prosumers and providers in the considered energy community can be formulated in several ways. As a first approach, all the agents in $\mathcal{C}$ (i.e., all prosumers in $\mathcal{P}$ and providers in $\mathcal{S}$), constitute the grand coalition pursuing a common goal, i.e., guarantee the global community welfare. From a game-theoretical point of view, agents behave cooperatively, concurring to the minimization of

a collective cost function, $J_{\mathcal{C}}$, defined as the sum of the individual cost functions:

$$J_{\mathcal{C}}(\mathbf{x}_{\mathcal{C}}) = \sum_{n \in \mathcal{C}} J_{\mathcal{C},n}(\mathbf{x}_{\mathcal{C},n}) \tag{3.7}$$

where, for the sake of compactness, we define $\mathbf{x}_{\mathcal{C}} = (\mathbf{x}_{\mathcal{C},n})_{n \in \mathcal{C}}$ as the concatenation of all the decision variable vectors for all players. Note that $\mathbf{x}_{\mathcal{C},n} = \mathbf{x}_{\mathcal{P},n}$, $\forall n \in \mathcal{P}$ and $\mathbf{x}_{\mathcal{C},n} = \mathbf{x}_{\mathcal{S},n}$, $\forall n \in \mathcal{S}$, while $J_{\mathcal{C},n} = J_{\mathcal{P},n}$, $\forall n \in \mathcal{P}$ and $J_{\mathcal{C},n} = J_{\mathcal{S},n}$, $\forall n \in \mathcal{S}$. As for the constraints sets, we indicate $\mathcal{K}_{\mathcal{C},n} = \mathcal{K}_{\mathcal{P},n}$, $\forall n \in \mathcal{P}$ and $\mathcal{K}_{\mathcal{C},n} = \mathcal{K}_{\mathcal{S},n}$, $\forall n \in \mathcal{S}$.

It is possible to prove that optimizing (3.7) provides a Pareto solution to all players [40], [41]. Function $J_{\mathcal{C}}$ is composed only of exogenous cost sources concerning the coalition $\mathcal{C}$. In other words, the storage fees paid by the prosumers over the time horizon correspond to the total revenues earned by the providers for the storage service.

In addition to the local feasible sets $\mathcal{K}_{\mathcal{C},n}$, the coherence of the energy flow has to be ensured under the following *coupling constraints*:

$$\hat{d}_{ijt} = \check{q}_{ijt}, \quad \forall i \in \mathcal{P}, \forall j \in \mathcal{S} \tag{3.8a}$$

$$\check{d}_{ijt} = \hat{q}_{ijt}, \quad \forall i \in \mathcal{P}, \forall j \in \mathcal{S}. \tag{3.8b}$$

Therefore, we can define the global constraints set as:

$$\mathcal{K}_{\mathcal{C}} = \left\{ \mathbf{x}_{\mathcal{C}} \in \bigcup_{n \in \mathcal{C}} \mathcal{K}_{\mathcal{C},n} \;\middle|\; (3.8a) - (3.8b) \text{ hold} \right\}. \tag{3.9}$$

Summing up, from the global perspective, the optimization problem is compactly written as:

$$\mathbf{x}^*_{\mathcal{C}} = \underset{\mathbf{x}_{\mathcal{C}} \in \mathcal{K}_{\mathcal{C}}}{\arg\min}\, J_{\mathcal{C}}(\mathbf{x}_{\mathcal{C}}). \tag{3.10}$$

The above-formulated problem can be solved in a centralized fashion by a central unit that operates on behalf of all actors while scheduling and assigning resources accordingly. In particular, since (3.10) constitutes a quadratic programming problem, because of the quadratic terms in (3.1) and (3.4), the resolution of the global approach is straightforwardly achieved by using any convex optimization solver [42]. However, the global approach presents several drawbacks. First, such a formulation aims at minimizing the overall community cost, possibly penalizing some actors in the resulting control strategy. Furthermore, in the centralized architecture, privacy issues are not considered. In fact, the model is composed of heterogeneous agents for whom limiting the amount of shared information is highly recommended, if not requested. This is particularly relevant to providers, being independent companies for which data sharing could result in economic and security-related vulnerabilities. Finally, centralized solutions are prone to computational scalability concerns, when the number of agents becomes large, and low fault resiliency issues.

To overcome these drawbacks, let us introduce a reformulation of the transactive energy management problem, employing the non-cooperative game theory, assuming that each player addresses its energy scheduling problem. In this way, each player $n \in \mathcal{C}$ aims at minimizing its own objective function $J_{\mathcal{C},n}(\mathbf{x}_{\mathcal{C},n})$ by modifying its decision variable vector $\mathbf{x}_{\mathcal{C},n}$, given the choices of all the other players $\mathbf{x}_{\mathcal{C},-n}$, where $\mathbf{x}_{C,-n} = (\mathbf{x}_{\mathcal{C},1}, \cdots, \mathbf{x}_{\mathcal{C},n-1}\ \mathbf{x}_{\mathcal{C},n+1}\ \cdots\ \mathbf{x}_{\mathcal{C},C})^\top$. Hence, we have that each player solves an independent optimization problem:

$$\mathbf{x}^*_{C,n} = \underset{\mathbf{x}_{C,n} \in \mathcal{K}_{\mathcal{C}}(\mathbf{x}_{C,-n})}{\arg\min}\ J_{\mathcal{C},n}(\mathbf{x}_{C,n}), \quad \forall n \in \mathcal{C}. \tag{3.11}$$

This formulation can be considered as a GNEP, since the decisions of the players are coupled through not only the cost functions but also a shared feasible set [43]. The solution of the GNEP is the so-called GNE hereafter formally defined.

Definition 3.3.1

A solution $\mathbf{x}^*_{\mathcal{C}} \in \mathcal{K}_{\mathcal{C}}$ *is a GNE if*

$$J_{\mathcal{C},n}(\mathbf{x}^*_{C,n}) \leq J_{\mathcal{C},n}(\mathbf{x}_{C,n}), \quad \forall \mathbf{x}_{C,n} \in \mathcal{K}_{\mathcal{C}}(\mathbf{x}_{C,-n}). \tag{3.12}$$

holds for all $n \in \mathcal{C}$.

In other words, at a GNE no player can benefit from independently changing its strategy, given that all the remaining players don't deviate from their own. In general, the existence of a GNE is not guaranteed; neither the uniqueness nor the convergence to an equilibrium is ensured.

In particular, the solution of a GNEP is a nontrivial problem, mainly due to the variability of the feasible sets. Several approaches to solve this problem are based on its reformulation through a variational inequality (VI). It can be proven that every solution of the VI is a solution for its corresponding GNEP, but the vice versa is, in general, not true [44]. The solutions of the GNEP that are also valid for the VI are called "variational solutions" and are usually referred to as economically fair. These points have a fair behaviour between all the possible GNEs due to the equivalence of the Lagrangian multipliers (acting as penalizing coefficients) for all players' stationarity and primal feasibility conditions [42]. Moreover, variational solutions are preferred in several applications, due to their uniqueness when further assumptions hold [45].

The following section is focused on describing effective methods aimed at reaching the variational solution for the above-defined individual formulation (3.11).

3.4 The Proposed Control Frameworks

In this section, we focus on solving the individual formulation transactive energy management problem, since it grasps the competitiveness of the real-world energy market better than the global formulation. Several alternative algorithms have been proposed to solve the VI formulation of a GNEP [46].

In particular, two approaches are presented, namely the coordinated and the uncoordinated framework. In both cases, we leverage on a modified version of the classical Augmented Lagrangian Method (ALM) [47], where the quadratic penalty term of the Lagrangian $\mathcal{L}$ is substituted by a proximal regularizer, i.e.,

$$\mathcal{L}(\mathbf{x}_{\mathcal{C},n}, \boldsymbol{\pi}) = J_{\mathcal{C},n}(\mathbf{x}_{\mathcal{C},n}) + \boldsymbol{\pi}^\top \mathbf{c}(\mathbf{x}_{\mathcal{C},n}) + \frac{\rho}{2} \left\| \mathbf{x}_{\mathcal{C},n} - \mathbf{x}^{(\tau-1)}_{\mathcal{C},n} \right\|^2 \tag{3.13}$$

with $\mathbf{c}(\mathbf{x}_{\mathcal{C},n})$ and $\boldsymbol{\pi}$ being, respectively, the vectors of the coupling constraints and related Lagrange multipliers vector. Note that in (3.13), and throughout the rest of the Chapter, τ denotes the iteration step. The regularization coefficient $\rho = \kappa a^C$ in (3.13) is based on parameters $\kappa, a \in \mathbb{R}_{\geq 0}$, determined empirically. The update rule for $\boldsymbol{\pi}$ is based on the well-known gradient formula:

$$\boldsymbol{\pi}^{(\tau)} = \boldsymbol{\pi}^{(\tau-1)} + \chi \left(\mathbf{x}^{(\tau-1)}_{\mathcal{C},n} - \mathbf{c}\left(\mathbf{x}^{(\tau-1)}_{\mathcal{C},n} \right) \right) \tag{3.14}$$

where $\chi \in \mathbb{R}_{\geq 0}$ is the convergence step-size. In the following, we characterize each term of (3.13) for, respectively, the uncoordinated and coordinated frameworks.

3.4.1 Uncoordinated Framework

In the uncoordinated framework, agents in $\mathcal{P}$ and $\mathcal{S}$ can interact with each other directly. The communication layer for this framework is shown in Fig. 3.2, where each prosumer communicates with the retailer and is allowed to communicate with all the providers. As regards the technological point of view, distributed ledger technologies have been proven to reliably support distributed communication and control in smart grids, in terms of cost-efficiency and privacy [48].

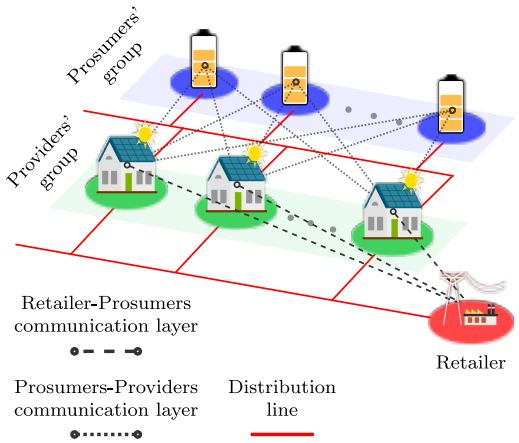

Figure 3.2: Energy community model: an overview of the communication layer in case of the uncoordinated control framework: any prosumer can exchange information with any provider; each prosumer communicates with the retailer.

Algorithm 2: Uncoordinated ALM

$\tau \leftarrow 0$
forall $i \in \mathcal{P}$, $j \in \mathcal{S}$, $t \in \mathcal{T}$ **do**
  $\lambda_{ijt}^{(\tau)} \leftarrow 0, \ \mu_{ijt}^{(\tau)} \leftarrow 0$
  $d_{ijt}^{(\tau)} \leftarrow 0, \ q_{ijt}^{(\tau)} \leftarrow 0$
while *stopping criterion is not reached* **do**
  $\tau \leftarrow \tau + 1$
  do in parallel
    Agents in $\mathcal{C}$ solve (3.18);
    Each prosumers $i \in \mathcal{P}$ communicates $d_{ijt}^{(\tau)}$ and $d_{ijt}^{(\tau)}$ to providers in $\mathcal{N}_i$;
    Each provider $j \in \mathcal{S}$ communicates $q_{ijt}^{(\tau)}$ and $q_{ijt}^{(\tau)}$ to prosumers in $\mathcal{M}_j$;
    Agents in $\mathcal{C}$ update the Lagrange multipliers by (3.15).

We now reformulate the Lagrangian formulation in (3.13) to solve the individual scheduling problem in (3.11) in the case of the uncoordinated architecture. To this aim, we define the Lagrange multipliers vectors $\lambda_{iht}^{(\tau)}$ and $\mu_{kjt}^{(\tau)}$ respectively associated to coupling constraints (3.8a)-(3.8b), whose update equations follow (3.14) for all $t \in \mathcal{T}$, i.e.,

$$\lambda_{iht}^{(\tau)} = \lambda_{iht}^{(\tau-1)} + \chi \left(\hat{d}_{iht}^{(\tau-1)} - \check{q}_{iht}^{(\tau-1)} \right), \quad \forall i \in \mathcal{P}, \forall h \in \mathcal{N}_i, \tag{3.15a}$$

$$\mu_{kjt}^{(\tau)} = \mu_{kjt}^{(\tau-1)} + \chi \left(\check{d}_{kjt}^{(\tau-1)} - \check{q}_{kjt}^{(\tau-1)} \right), \quad \forall j \in \mathcal{S}, \ \forall k \in \mathcal{M}_j. \tag{3.15b}$$

Therefore, each prosumer and provider can calculate its penalty regularizers $\gamma_{\mathcal{P},i}^{(\tau)}$ and $\gamma_{\mathcal{S},j}^{(\tau)}$, defined, for all $i \in \mathcal{P}$ and $j \in \mathcal{S}$, as:

$$\gamma_{\mathcal{P},i}^{(\tau)} = \sum_{t \in \mathcal{T}} \sum_{h \in \mathcal{N}_i} \left(\lambda_{iht}^{(\tau)} \left(\hat{d}_{iht} - \check{q}_{iht} \right) + \mu_{iht}^{(\tau)} \left(\check{d}_{iht} - \hat{q}_{iht} \right) \right), \tag{3.16a}$$

$$\gamma_{\mathcal{S},j}^{(\tau)} = \sum_{t \in \mathcal{T}} \sum_{k \in \mathcal{M}_j} \left(\lambda_{kjt}^{(\tau)} \left(\hat{d}_{kjt} - \check{q}_{kjt} \right) + \mu_{kjt}^{(\tau)} (\check{d}_{kjt} - \hat{q}_{kjt}) \right). \tag{3.16b}$$

To guarantee convergence, proximal regularization terms $\theta_{\mathcal{P},i}^{(\tau)}$ and $\theta_{\mathcal{S},j}^{(\tau)}$ are added to prosumers' and the providers' objective functions respectively, i.e.,

$$\theta_{\mathcal{P},i}^{(\tau)} = \frac{\rho}{2} \left(\left\| \check{\mathbf{d}}_i - \check{\mathbf{d}}_i^{(\tau-1)} \right\|^2 + \left\| \hat{\mathbf{d}}_i - \hat{\mathbf{d}}_i^{(\tau-1)} \right\|^2 \right), \quad \forall i \in \mathcal{P} \tag{3.17a}$$

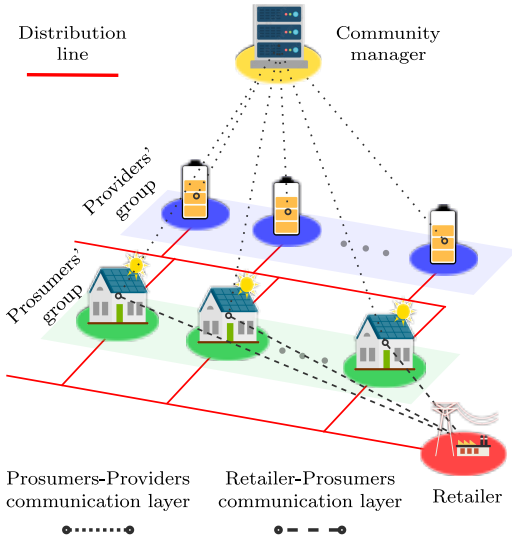

Figure 3.3: Energy community model: an overview of the communication layer in the case of coordinated control framework: the coordinator allows any prosumer to exchange information with providers and each prosumer communicates with the retailer.

$$\theta_{\mathcal{S},j}^{(\tau)} = \frac{\rho}{2}\left(\left\|\check{\mathbf{q}}_j - \check{\mathbf{q}}_j^{(\tau-1)}\right\|^2 + \left\|\hat{\mathbf{q}}_j - \hat{\mathbf{q}}_j^{(\tau-1)}\right\|^2\right), \quad \forall j \in \mathcal{S}. \tag{3.17b}$$

For the sake of compactness, we define $\gamma_{\mathcal{C},n}^{(\tau)} = \gamma_{\mathcal{P},n}^{(\tau)}$, $\forall n \in \mathcal{P}$ and $\gamma_{\mathcal{C},n}^{(\tau)} = \gamma_{\mathcal{S},n}^{(\tau)}$, $\forall n \in \mathcal{S}$, while $\theta_{\mathcal{C},n}^{(\tau)} = \theta_{\mathcal{P},n}^{(\tau)}$, $\forall n \in \mathcal{P}$ and $\theta_{\mathcal{C},n}^{(\tau)} = \theta_{\mathcal{S},n}^{(\tau)}$, $\forall n \in \mathcal{S}$. Therefore, we can write the Lagrangian form of the optimization problem for the uncoordinated framework as:

$$\mathbf{x}_{C,n}^{(\tau+1)} = \underset{\mathbf{x}_{C,n} \in \mathcal{K}_{\mathcal{C}_n}}{\arg\min} \left(J_{\mathcal{C},n}(\mathbf{x}_{C,n}) + \gamma_{\mathcal{C},n}^{(\tau)} + \theta_{\mathcal{C},n}^{(\tau)}\right), \quad \forall n \in \mathcal{C}. \tag{3.18}$$

The corresponding uncoordinated algorithm is summarized in Algorithm 2, and is described in detail in the sequel. First, all agents initialize the penalty factors and flow variables (lines 2-4). The non-cooperative solution is reached in an uncoordinated manner through an iterative process until a termination criterion is not reached (lines 5-6). In detail, at each iteration τ, each agent independently solves its own optimization problem (line 9) and communicates the state of the energy flow variables to the corresponding neighbours (line 10). Lastly, the Lagrange multipliers are updated (line 11).

3.4.2 Coordinated Framework

In the coordinated framework, agents in $\mathcal{P}$ and $\mathcal{S}$ do not directly interact, since a coordinator is present to gather the energy flow variables determined by the prosumers and providers, compute the Lagrange multipliers on behalf of all the agents, and sending back to prosumers and providers the updated Lagrange multipliers vectors. The coordinator is thus a non-profit actor that supports the selfish agents in the community in reaching an optimal solution to the transactive energy management problem while ensuring that the energy balance coupling constraints are satisfied. The communication layer for the coordinated framework is shown in Fig. 3.3, where each prosumer communicates with the retailer and all actors exchange information through the coordinator. This entity monitors and controls the energy activities in the community relying on an appropriate communication network (e.g., wireless radio connection, dial-up lines, Ethernet and IP protocol). Wireless data communications are more convenient in comparison to wired communications since several advantages are available: cost-effective installation, fast placement, and remote applicability increase the attractiveness of these approaches. Particularly, Internet of Things solutions, combined with edge computing, are increasingly gaining attention [49].

We now reformulate the Lagrangian formulation in (3.13) to solve the individual scheduling problem in (3.11) in the case of the coordinated architecture. In such a case,

Algorithm 3: Coordinated ALM

1 $\tau \leftarrow 0$
2 **forall** $i \in \mathcal{P}$, $j \in \mathcal{S}$, $t \in \mathcal{T}$ **do**
3 $\quad \lambda_t^{(\tau)} \leftarrow 0, \ \mu_t^{(\tau)} \leftarrow 0$
4 $\quad d_{ijt}^{(\tau)} \leftarrow 0, \ q_{ijt}^{(\tau)} \leftarrow 0$
5 **while** *stopping criterion is not reached* **do**
6 $\quad \tau \leftarrow \tau + 1$
7 $\quad$ **do in parallel**
8 $\quad\quad$ Agents in $\mathcal{C}$ solve (3.23);
9 $\quad\quad$ Prosumers in $\mathcal{P}$ communicate flow variables $d_{ijt}^{(\tau)}$ and $d_{ijt}^{(\tau)}$ to the coordinator;
10 $\quad\quad$ Providers in $\mathcal{S}$ communicate flow variables $q_{ijt}^{(\tau)}$ and $q_{ijt}^{(\tau)}$ to the coordinator;
11 $\quad$ The coordinator aggregates the energy flow by (3.20), updates the Lagrange multipliers by (3.21), and sends the updated back to all agents.

the Lagrange multipliers are equal for all agents, for each time slot t, since the coordinator is in charge of ensuring the balance of the *aggregate energy flow*, following the following *coupling constraints*:

$$\hat{D}_t = \check{Q}_t, \quad \forall t \in \mathcal{T} \tag{3.19a}$$

$$\check{D}_t = \hat{Q}_t, \quad \forall t \in \mathcal{T} \tag{3.19b}$$

where $\hat{D}_t$, $\check{D}_t$, $\hat{Q}_t$ and $\check{Q}_t$ are introduced to denote the flow variables aggregates:

$$\hat{D}_t = \sum_{i \in \mathcal{P}} \sum_{h \in \mathcal{N}_i} \hat{D}_{iht}, \quad \check{D}_t = \sum_{i \in \mathcal{P}} \sum_{h \in \mathcal{N}_i} \check{D}_{iht}, \tag{3.20a}$$

$$\hat{Q}_t = \sum_{j \in \mathcal{S}} \sum_{k \in \mathcal{M}_j} \hat{Q}_{kjt}, \quad \check{Q}_t = \sum_{j \in \mathcal{S}} \sum_{k \in \mathcal{M}_j} \check{Q}_{kjt}. \tag{3.20b}$$

In particular, the Lagrange multipliers $\lambda_t^{(\tau)}$ and $\mu_t^{(\tau)}$ associated to constraints (3.19) are computed as follows:

$$\lambda_t^{(\tau)} = \lambda_t^{(\tau-1)} + \chi(\hat{D}_t - \check{Q}_t), \quad \forall t \in \mathcal{T} \tag{3.21a}$$

$$\mu_t^{(\tau)} = \mu_t^{(\tau-1)} + \chi(\check{D}_t - \hat{Q}_t), \quad \forall t \in \mathcal{T} \tag{3.21b}$$

so that the penalty regularizers of the coordinated framework, $\varphi_{\mathcal{P},i}^{(\tau)}$ and $\varphi_{\mathcal{S},j}^{(\tau)}$, can be defined, for all $i \in \mathcal{P}$, $j \in \mathcal{S}$, as:

$$\varphi_{\mathcal{P},i}^{(\tau)} = \varphi_{\mathcal{S},j}^{(\tau)} = \sum_{t \in \mathcal{T}} \left(\lambda_t^{(\tau)} (\hat{d}_t - \check{q}_t) + \mu_t^{(\tau)} (\check{d}_t - \hat{q}_t) \right). \tag{3.22}$$

Similarly to the previous case, we define $\varphi_{\mathcal{C},n}^{(\tau)} = \varphi_{\mathcal{P},n}^{(\tau)}, \forall n \in \mathcal{P}$ and $\varphi_{\mathcal{C},n}^{(\tau)} = \varphi_{\mathcal{S},n}^{(\tau)}, \forall n \in \mathcal{S}$, while $\theta_{\mathcal{C},n}^{(\tau)} = \theta_{\mathcal{P},n}^{(\tau)}$, $\forall n \in \mathcal{P}$ and $\theta_{\mathcal{C},n}^{(\tau)} = \theta_{\mathcal{S},n}^{(\tau)}$, $\forall n \in \mathcal{S}$. Therefore, the Lagrangian form of the optimization problem for the coordinated framework is written as follows:

$$\mathbf{x}_{C,n}^{(\tau+1)} = \underset{\mathbf{x}_{C,n} \in \mathcal{K}_{\mathcal{C}_n}}{\arg\min} \ J_{\mathcal{C},n}(\mathbf{x}_{C,n}) + \varphi_{\mathcal{C},n}^{(\tau)} + \theta_{\mathcal{C},n}^{(\tau)}, \quad \forall n \in \mathcal{C}. \tag{3.23}$$

The coordinated algorithm, summarized in Algorithm 3, is hereafter described in detail. Similarly to the uncoordinated algorithm, we initialize the common Lagrange multipliers vectors and the energy flow variables (lines 2-4). The non-cooperative solution is reached in a coordinated fashion through an iterative process until a termination criterion is

Table 3.1: Parameters setup.

	Parameter	Value
Time horizon	T	24 (hours)
Group size	P	10
	S	8
Efficiencies	α	0.98
	$\eta^{\downarrow}$	1.03
	$\eta^{\uparrow}$	0.97
	σ	0.03
	$\overline{\zeta_j}$	0.005
	$\overline{\xi_j}$	0.0003
	ξ_j	$\sim N(\overline{\xi_i}, \sigma^2)$
	ζ_j	$\sim N(\overline{\zeta_i}, \sigma^2)$
Economical coefficients	ϵ	0.7
	β	0.5
Decision variables boundaries	$p^{\max}$	6 (kWh)
	$d^{\max}$	6 (kWh)
	$q^{\max}$	6 (kWh)
	$b^{\max}$	10 (kWh)
	b^{init}	0 (kWh)
	s^{init}	0 (kWh)
Convergence parameters	γ	0.098^{*}; $0.98^{\dagger}$
	a	$1.04^{*,\dagger}$
	χ	0.01^{*}; $0.7^{\dagger}$

* Coordinated
† Uncoordinated

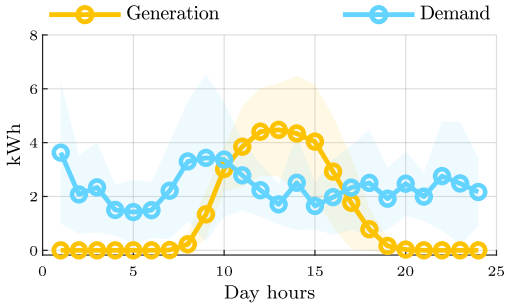

Figure 3.4: Prosumers' energy generation (yellow) and demand (cyan) curves. Lines correspond to the values averaged over the involved agents, while the shaded areas are the bounds of the standard deviation.

reached (lines 5-6). At each iteration τ, every agent computes its optimal energy schedule (line 8) and communicates the updated strategy to the coordinator (lines 9-10). Then, the coordinator calculates the flow variables aggregates $\hat{d}_t$, $\check{d}_t$, $\hat{q}_t$, and $\check{q}_t$, updates the Lagrange multipliers (line 11), and sends the updated Lagrange multipliers back both to prosumers and providers (line 12).

3.5 Numerical Results

In this section, we assess the performance of the two proposed energy community control frameworks through numerical experiments on realistic scenarios. For the sake of providing a comparison with a reference method, the results obtained by the proposed uncoordinated and the coordinated distributed control framework is compared with those achieved by an optimal centralized framework.

All simulations are performed in MATLAB, using the Optimization Toolbox library, installed on a middle-end machine equipped with an Intel i5-7400, 3.00 GHz (4 cores) CPU, and 8 GB of RAM. Source code and dataset are fully available at [50].

Table 3.2: Total costs and revenues for the group of prosumers, the groups of providers, and the retailer for each control framework.

		Cost of bought energy [€]	Revenues of sold energy [€]	Cost of storage service [€]	Cost of inefficiency* [€]	Community costs† [€]	Total costs§ [€]
Centralized	**Prosumers**	21.41	5.00	19.15	7.35	42.93	**7.70**
	Providers	-	-	-19.15	0.34	-18.81	
	Retailer	5.00	21.41	-	-	-16.42	
Coordinated	**Prosumers**	23.62	7.05	3.81	8.91	29.30	**8.93**
	Providers	-	-	-3.81	0.014	-3.80	
	Retailer	7.05	23.62	-	-	-16.57	
Uncoordinated	**Prosumers**	23.83	7.31	1.70	9.51	27.77	**9.51**
	Providers	-	-	-1.70	0.0035	-1.69	
	Retailer	7.31	23.83	-	-	-16.57	

* Value related to the quadratic term in eq. (3.1) and eq. (3.4) for prosumers and providers, respectively.
† Value computed as: (Cost of bought energy) + (Cost of storage service) + (Cost of inefficiency) − (Revenues of sold energy).
§ Sum of the terms in the "Community cost" column.

In particular, we consider a residential energy community equipped with distributed energy generation sources and service-based energy storage. The actors of the energy community include 10 prosumers and 8 providers. The control horizon corresponds to the entire day, equally subdivided into one-hour time slots.

Prosumers' energy generation and demand data are known parameters of the control frameworks, corresponding to the curves reported in Fig. 3.4. In particular, the reported data refer to a yearly report of energy consumption and production of an urban condominium [50]. The renewable source considered in the experiments is a set of 27 PV panels (PEIMAR SG300M), each generating 300 Wp and a three-phase inverter (SolarEdge-SE8K), serving shared devices of the condominium, such as heat generator, water pump, lighting, and elevator.

Energy buying and selling prices are defined over the time horizon and known by all agents in both the prosumers and providers groups. In particular, the considered energy cost is related to the Italian Enel "E-Light Bioraria" tariff [51]. This billing plan divides the day into two zones:

- *Orange*: Monday to Friday, from 8.00 to 19.00. The buying energy cost C_t is € 0.0774.
- *Blue*: Monday to Friday, from 19.00 to 8.00 and the entire day during weekends. The buying energy cost C_t is € 0.0574.

The relationship between the energy buying cost (i.e., C_t) and the energy selling price (i.e., R_t) for prosumers is the following:

$$R_t = \epsilon C_t, \quad \epsilon \in [0, 1] \tag{3.24}$$

where ϵ is the increment due to exogenous factors (e.g., taxes). As for the storage service pricing (i.e., L_t), for the sake of simplicity, a weighted average of the buying and selling price is considered:

$$L_t = \beta C_t + (1 - \beta) R_t \tag{3.25}$$

with $\beta \in [0, 1]$ being an arbitrary weight. By tuning the value of β, a large number of policies can be experimented with, independently from the energy buying and selling price curves.

Finally, in Table 3.1 we report the tuning parameters of the proposed algorithms, as well as the technological parameters of the ESSs. In particular, the technological coefficients are sampled from normal distributions and the charge level of ESSs is set to zero at the beginning of the day.

Since our work is focused on transactive control frameworks for energy communities, for the sake of assessing the performance of the proposed methods comprehensively, we adopt both economic (i.e., energy cost incurred by prosumers, revenue gained by providers, and revenue gained by the retailer), energy (i.e., prosumers' energy demand and generation as well as energy bought from and sold to the retailer, energy-charged

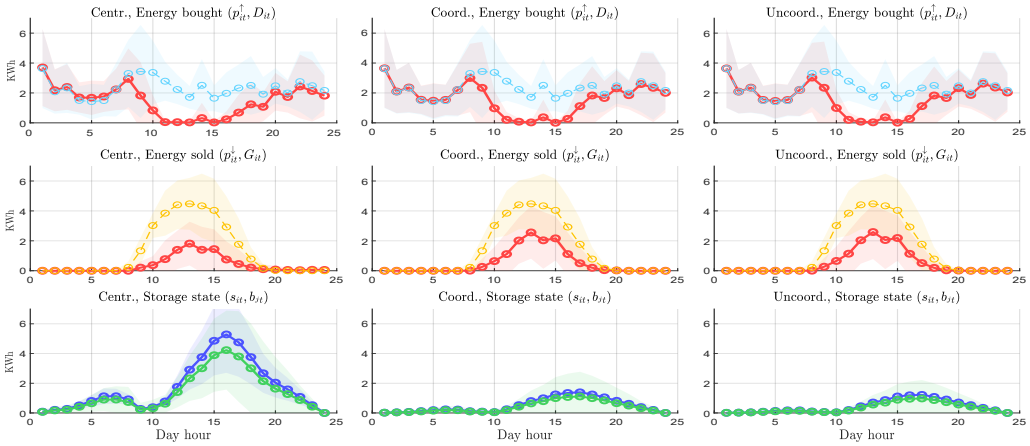

Figure 3.5: Energy transfer dynamics: the first, second, and third subplots column refers to the centralized, coordinated, and uncoordinated framework, respectively. The first subplot row shows the profile of prosumers demand D_{it} (cyan) and the profile of energy bought from the retailer $\hat{p}_{it}$ (red). The second subplot row represents the profile of prosumers generation G_{it} (yellow) and the profile of energy sold to the retailer $\check{p}_{it}$ (red). The third subplot row shows the profile of prosumers stored energy s_{iht} (green) and the profile of providers charge level b_{kjt} (blue). In all subplots Lines correspond to the values averaged over the involved agents, while the corresponding shaded areas are the bounds of the standard deviation.

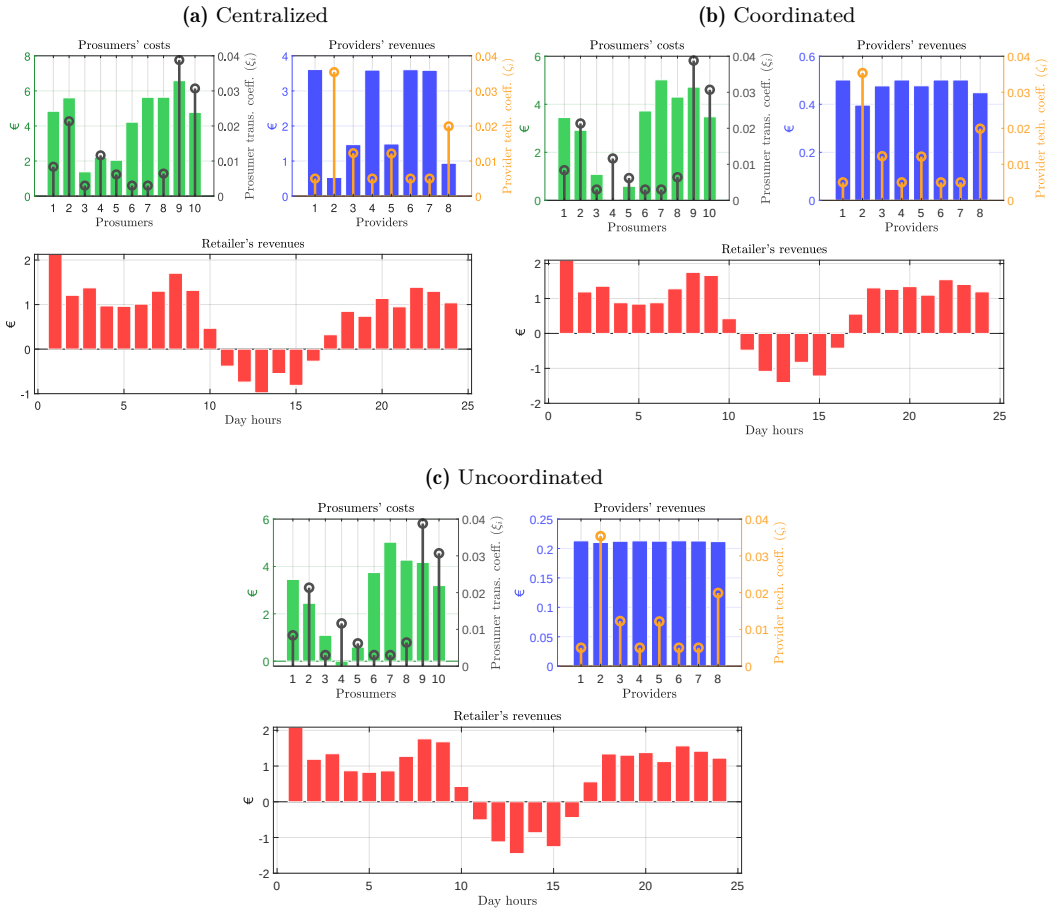

Figure 3.6: Economic results for the centralized (a), coordinated (b), and uncoordinated (c) framework. Total daily prosumers' costs (green bars) and provider revenues (blue bars) are reported on a single-agent basis. Retailer revenues (red bars) are indicated on a time-slot basis. The brown and orange stems denote the values of the technological coefficients ξ_i and ζ_j over prosumers and providers, respectively.

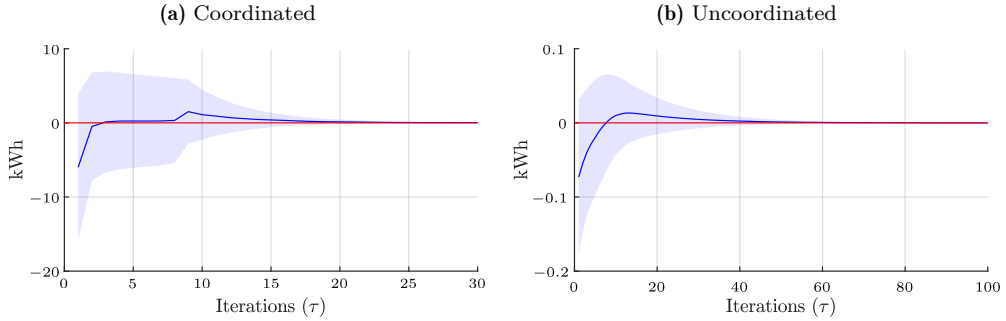

Figure 3.7: Convergence of the coordinated (a) and the uncoordinated (b) algorithm. The blue line indicates the average over the residual of (3.19) and (3.8) for the coordinated and the uncoordinated case, respectively. The shaded area is the bound of the standard deviation.

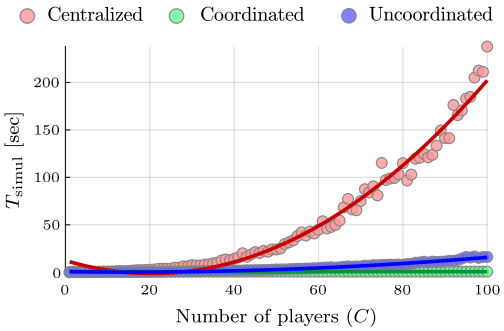

Figure 3.8: Run time versus number of agents (up to 100) for each framework. Curves represent polynomial fitting.

and discharged by the ESSs as well the storage state), and control/computational (i.e., residual of the coupling constraints for convergence and run time for scalability purpose) performance evaluation indicators.

Figure 3.5 reports the evolution of the energy flow variables over the control horizon. It is apparent that prosumers buy most of the energy during the early hours of the day when the autonomous generation is at the lowest level, and sell the surplus during the middle hours of the day. It is worthwhile noting the effects of the storage service at the latest hours: the amount of bought energy is lower than the demand since prosumers start to retrieve the stored energy to compensate for the low autonomous production. As for the sold energy, the main volume is located, as expected, during the middle hours of the day. Furthermore, it can be noticed that the global amount of energy stored in the case of coordinated and uncoordinated frameworks is lower than in the centralized one. Moreover, its variance is narrower in the non-centralized frameworks, indicating that the storage service demand is uniformly distributed among providers.

Figures 3.6a, 3.6b, and 3.6c graphically summarize the costs and revenues sustained by each agent over the control horizon. Providers' revenues are negatively correlated with ζ, since such a coefficient indicates the tendency of ESSs to deteriorate. Some considerations related to the energy flow dynamics directly follow from the above-reported findings: the middle hours of the day are the less profitable ones for the retailer, which buys energy from the prosumer, instead of selling it. The retailer achieves the highest profit in the early morning when the solar generation is at the minimum level. During the latest hours of the day, revenues are still positive, although prosumers start using the stored surplus to satisfy the demand. An important aspect is that, for all the considered frameworks, the distribution of the economic curves follows the same trend. This implies that solving the optimization problem with a particular framework does not alter *fairness*, at least at the community level, i.e., no participant in the groups of prosumers or providers can strongly benefit from changing its strategy while compromising others' welfare. Also, it can be noticed that the distribution of the revenues for the providers becomes more

homogeneous as we move from the centralized solution to the coordinated one, while the largest uniformity is obtained in the uncoordinated case. This is a consequence of the perfect competition hypothesis and the non-cooperative behaviour of agents. Table 3.2 reports the revenues and the costs for the groups of prosumers and providers, as well as for the retailer. In particular, the "Total costs" column indicates the sum of the costs of all participants, including both the groups of prosumers and providers and the retailer. For the centralized case, it corresponds to the optimal value determined as a result of (3.7), whilst in the uncoordinated and coordinated cases it is the sum of the optimal values determined as results of (3.11). It can be noticed that the total cost value increases moving from the centralized to the uncoordinated through the coordinated approach. From the prosumers' perspective, this means that the lowest total cost is achieved in the uncoordinated framework, whereas the lowest profit is made by providers. Retailer revenues are added for completeness's sake in Table 3.2, being itself part of the economic frame, even if we consider it as a passive agent.

Figures 3.7a and 3.7b report the residual value of the coupling constraints over iterations respectively for the coordinated and the uncoordinated algorithm, thus showing that convergence is ensured for both the proposed frameworks.

Finally, Fig. 3.8 reports the run time required by each framework. For the uncoordinated framework, the communication graph (Fig. 3.2) has been considered as *complete*, since it is the worst-case scenario from a computational perspective. For the non-centralized frameworks, simulation time T_{simul} is calculated as

$$T_{\text{simul}} = \max\left(T_{\mathcal{P}}, T_{\mathcal{S}}\right) \cdot N_{\text{iter}} \tag{3.26}$$

with $N_{\text{iter}} \approx 150$ being the number of iterations and $T_{\mathcal{P}}$ and $T_{\mathcal{S}}$ being the average simulation time for prosumers and providers, respectively. From Fig. 3.8 it is evident that T_{simul} approaches a sublinear trend $o(C)$ for the coordinated case and the uncoordinated case, while the centralized case shows the polynomial trend $\mathcal{O}(C^2)$. As a result, the inevitable economic performance loss occurring in the coordinated and uncoordinated frameworks comes with operational advantages from a computational point of view.

3.6 Conclusions

In the last decade, distributed energy generation and storage have significantly contributed to the spread of energy communities. This increasing trend makes it necessary to develop suitable control strategies, to efficiently exploit the generation and storage capabilities of the energy community. For the sake of satisfying such a need, in this Chapter, we propose two novel transactive control schemes for energy communities – namely, the coordinated and the uncoordinated frameworks – with the following objectives:

- formulating a scalable energy management architecture for communities equipped with multiple prosumers and independent ESS service providers;
- assessing the feasibility of the underlying client-service business model by simulating the frameworks on real-case scenarios;
- improving the computational effort concerning the optimal centralized approach while keeping the degree of information sharing at the minimum level and with minimal loss in the economic performance.

An additional merit of the presented approaches lies in their generalizability to address different service provisioning in energy communities, for instance, in the case of optimally trading local energy exchanges at the peer-to-peer level and sharing common energy resources among the involved actors.

Nonetheless, this study is not without limitations, that need to be addressed in future developments. In particular, the energy generation and demand curves, as well as energy pricing profiles, are assumed to be deterministic, whilst the control frameworks are assumed to be not affected by modelling errors and non-idealities (e.g., latency, faults,

etc.). Moreover, the individual objectives of involved actors could be enhanced to include wider sustainability payoffs beyond economic benefits. Lastly, the energy distribution network ignores the constraints flow constraints regarding active and reactive power. Therefore, future works will focus on these points, by effectively dealing with the presence of the uncertainty that affects the decision parameters, and integrating additional terms in the objective functions and realistic grid in the proposed frameworks.

References

[1] Gjorgievski, V. Z., Cundeva, S., and Georghiou, G. E., "Social arrangements, technical designs and impacts of energy communities: A review," *Renewable Energy*, 2021.

[2] Kim, B.-Y., Oh, K.-K., and Ahn, H.-S., "Coordination and control for energy distribution in distributed grid networks: Theory and application to power dispatch problem," *Control Engineering Practice*, vol. 43, pp. 21–38, 2015.

[3] Weaver, W. W., Robinett III, R. D., Parker, G. G., and Wilson, D. G., "Distributed control and energy storage requirements of networked dc microgrids," *Control Engineering Practice*, vol. 44, pp. 10–19, 2015.

[4] Soeiro, S. and Dias, M. F., "Community renewable energy: Benefits and drivers," *Energy Reports*, vol. 6, pp. 134–140, 2020.

[5] Hosseini, S. M., Carli, R., and Dotoli, M., "Robust optimal energy management of a residential microgrid under uncertainties on demand and renewable power generation," *IEEE Transactions on Automation Science and Engineering*, vol. 18, no. 2, pp. 618–637, 2020.

[6] Bartolini, A., Carducci, F., Munoz, C. B., and Comodi, G., "Energy storage and multi energy systems in local energy communities with high renewable energy penetration," *Renewable Energy*, vol. 159, pp. 595–609, 2020.

[7] Bradbury, K., Pratson, L., and Patiño-Echeverri, D., "Economic viability of energy storage systems based on price arbitrage potential in real-time us electricity markets," *Applied Energy*, vol. 114, pp. 512–519, 2014.

[8] Kolodziejczyk, W., Zoltowska, I., and Cichosz, P., "Real-time energy purchase optimization for a storage-integrated photovoltaic system by deep reinforcement learning," *Control Engineering Practice*, vol. 106, p. 104 598, 2021.

[9] Nguyen, H. T., Muhs, J. W., and Parvania, M., "Assessing impacts of energy storage on resilience of distribution systems against hurricanes," *Journal of Modern Power Systems and Clean Energy*, vol. 7, no. 4, pp. 731–740, 2019.

[10] Toledo, O. M., Oliveira Filho, D., and Diniz, A. S. A. C., "Distributed photovoltaic generation and energy storage systems: A review," *Renewable and Sustainable Energy Reviews*, vol. 14, no. 1, pp. 506–511, 2010.

[11] Iovine, A., Rigaut, T., Damm, G., De Santis, E., and Di Benedetto, M. D., "Power management for a dc microgrid integrating renewables and storages," *Control Engineering Practice*, vol. 85, pp. 59–79, 2019.

[12] Carli, R., Dotoli, M., Jantzen, J., Kristensen, M., and Othman, S. B., "Energy scheduling of a smart microgrid with shared photovoltaic panels and storage: The case of the ballen marina in samso," *Energy*, vol. 198, p. 117 188, 2020.

[13] Scarabaggio, P., Carli, R., Jantzen, J., and Dotoli, M., "Stochastic model predictive control of community energy storage under high renewable penetration," in *2021 29th Mediterranean Conference on Control and Automation (MED)*, IEEE, 2021, pp. 973–978.

[14] Abrishambaf, O., Lezama, F., Faria, P., and Vale, Z., "Towards transactive energy systems: An analysis on current trends," *Energy Strategy Reviews*, vol. 26, p. 100 418, 2019.

[15] Akter, M. N., Mahmud, M. A., Haque, M. E., and Oo, A. M., "An optimal distributed energy management scheme for solving transactive energy sharing problems in residential microgrids," *Applied Energy*, vol. 270, p. 115 133, 2020.

[16] Soto, E. A., Bosman, L. B., Wollega, E., and Leon-Salas, W. D., "Peer-to-peer energy trading: A review of the literature," *Applied Energy*, vol. 283, p. 116 268, 2021.

[17] Sen, S. and Kumar, V., "Microgrid control: A comprehensive survey," *Annual Reviews in control*, vol. 45, pp. 118–151, 2018.

[18] Tucker, N. and Alizadeh, M., "An online scheduling algorithm for a community energy storage system," *arXiv preprint arXiv:2110.02396*, 2021.

[19] Parra, D., Swierczynski, M., Stroe, D. I., *et al.*, "An interdisciplinary review of energy storage for communities: Challenges and perspectives," *Renewable and Sustainable Energy Reviews*, vol. 79, pp. 730–749, 2017.

[20] Dai, R., Esmaeilbeigi, R., and Charkhgard, H., "The utilization of shared energy storage in energy systems: A comprehensive review," *IEEE Transactions on Smart Grid*, 2021.

[21] Wang, Z., Gu, C., Li, F., Bale, P., and Sun, H., "Active demand response using shared energy storage for household energy management," *IEEE Transactions on Smart Grid*, vol. 4, no. 4, pp. 1888–1897, 2013.

[22] Terlouw, T., AlSkaif, T., Bauer, C., and Van Sark, W., "Multi-objective optimization of energy arbitrage in community energy storage systems using different battery technologies," *Applied energy*, vol. 239, pp. 356–372, 2019.

[23] Szabó, D. Z., Duck, P., and Johnson, P., "Optimal trading of imbalance options for power systems using an energy storage device," *European Journal of Operational Research*, vol. 285, no. 1, pp. 3–22, 2020.

[24] Mediwaththe, C. P., Shaw, M., Halgamuge, S., Smith, D. B., and Scott, P., "An incentive-compatible energy trading framework for neighborhood area networks with shared energy storage," *IEEE Transactions on Sustainable Energy*, vol. 11, no. 1, pp. 467–476, 2019.

[25] Kalathil, D., Wu, C., Poolla, K., and Varaiya, P., "The sharing economy for the electricity storage," *IEEE Transactions on Smart Grid*, vol. 10, no. 1, pp. 556–567, 2017.

[26] Lombardi, P. and Schwabe, F., "Sharing economy as a new business model for energy storage systems," *Applied energy*, vol. 188, pp. 485–496, 2017.

[27] Le Cadre, H. and Mercier, D., "Is energy storage an economic opportunity for the eco-neighborhood?" *NETNOMICS: Economic Research and Electronic Networking*, vol. 13, no. 3, pp. 191–216, 2012.

[28] Vespermann, N., Hamacher, T., and Kazempour, J., "Access economy for storage in energy communities," *IEEE Transactions on Power Systems*, pp. 1–1, 2020. DOI: 10.1109/TPWRS.2020.3033999.

[29] Nikonowicz, L. B. and Milewski, J., "Virtual power plants-general review: Structure, application and optimization," *Journal of power technologies*, vol. 92, no. 3, p. 135, 2012.

[30] Ghavidel, S., Li, L., Aghaei, J., Yu, T., and Zhu, J., "A review on the virtual power plant: Components and operation systems," in *2016 IEEE International Conference on Power System Technology (POWERCON)*, IEEE, 2016, pp. 1–6.

[31] Liu, J., Zhang, N., Kang, C., Kirschen, D., and Xia, Q., "Cloud energy storage for residential and small commercial consumers: A business case study," *Applied energy*, vol. 188, pp. 226–236, 2017.

[32] Zhou, Y., Ci, S., Lin, N., Li, H., and Yang, Y., "Distributed energy management of p2p energy sharing in energy internet based on cloud energy storage," in *Proceedings of the Ninth International Conference on Future Energy Systems*, 2018, pp. 173–177.

[33] Unger, D. and Myrzik, J. M., "Agent based management of energy storage devices within a virtual energy storage," in *2013 IEEE Energytech*, IEEE, 2013, pp. 1–6.

[34] Pandžić, K., Pandžić, H., and Kuzle, I., "Virtual storage plant offering strategy in the day-ahead electricity market," *International Journal of Electrical Power & Energy Systems*, vol. 104, pp. 401–413, 2019.

[35] Zhao, D., Wang, H., Huang, J., and Lin, X., "Virtual energy storage sharing and capacity allocation," *IEEE transactions on smart grid*, vol. 11, no. 2, pp. 1112–1123, 2019.

[36] Liu, J., Zhang, N., Kang, C., Kirschen, D. S., and Xia, Q., "Decision-making models for the participants in cloud energy storage," *IEEE Transactions on Smart Grid*, vol. 9, no. 6, pp. 5512–5521, 2017.

[37] Koike, M., Ishizaki, T., Ramdani, N., and Imura, J.-i., "Optimal scheduling of battery storage systems and thermal power plants for supply–demand balance," *Control Engineering Practice*, vol. 77, pp. 213–224, 2018.

[38] Scarabaggio, P., Carli, R., and Dotoli, M., "A game-theoretic control approach for the optimal energy storage under power flow constraints in distribution networks," in *2020 IEEE 16th International Conference on Automation Science and Engineering (CASE)*, 2020, pp. 1281–1286.

[39] Atzeni, I., Ordóñez, L. G., Scutari, G., Palomar, D. P., and Fonollosa, J. R., "Demand-side management via distributed energy generation and storage optimization," *IEEE Trans. Smart Grid*, vol. 4, no. 2, pp. 866–876, 2012.

[40] Zadeh, L., "Optimality and non-scalar-valued performance criteria," *IEEE transactions on Automatic Control*, vol. 8, no. 1, pp. 59–60, 1963.

[41] French, S., "Multi-objective decision analysis with engineering and business applications," *Journal of the Operational Research Society*, vol. 34, no. 5, pp. 449–450, 1983.

[42] Boyd, S., Boyd, S. P., and Vandenberghe, L., *Convex optimization*. Cambridge university press, 2004.

[43] Scarabaggio, P., Grammatico, S., Carli, R., and Dotoli, M., "Distributed demand side management with stochastic wind power forecasting," *IEEE Trans. Control Syst. Technol.*, pp. 1–16, 2021, 10.1109/TCST.2021.3056751.

[44] Facchinei, F., Fischer, A., and Piccialli, V., "On generalized nash games and variational inequalities," *Operations Research Letters*, vol. 35, no. 2, pp. 159–164, 2007.

[45] Facchinei, F. and Kanzow, C., "Generalized nash equilibrium problems," *4or*, vol. 5, no. 3, pp. 173–210, 2007.

[46] Pang, J.-S., Scutari, G., Palomar, D. P., and Facchinei, F., "Design of cognitive radio systems under temperature-interference constraints: A variational inequality approach," *IEEE Transactions on Signal Processing*, vol. 58, no. 6, pp. 3251–3271, 2010.

[47] Chatzipanagiotis, N., Dentcheva, D., and Zavlanos, M. M., "An augmented lagrangian method for distributed optimization," *Mathematical Programming*, vol. 152, no. 1, pp. 405–434, 2015.

[48] Lombardi, F., Aniello, L., De Angelis, S., Margheri, A., and Sassone, V., "A blockchain-based infrastructure for reliable and cost-effective iot-aided smart grids," 2018.

[49] Chen, S., Wen, H., Wu, J., *et al.*, "Internet of things based smart grids supported by intelligent edge computing," *IEEE Access*, vol. 7, pp. 74 089–74 102, 2019.

[50] Mignoni, N., Scarabaggio, P., Carli, R., and Dotoli, M., *Multiple storage systems in smart grids*, Accessed: 2021-16-08. [Online]. Available: https://github.com/nicomignoni/Multiple-storage-systems-in-smart-grids.

[51] Enel, *E-light bioraria*, Accessed: 2021-23-05. [Online]. Available: https://www.enel.it/it/luce-e-gas/luce/offerte/e-light-bioraria.

Part II: Non-cooperative Plug-in Electric Vehicles for V1G and V2B

Chapter 4

Distributed Non-cooperative MPC for Energy Scheduling of Charging and Trading Electric Vehicles in Energy Communities

Abstract

In this Chapter, we propose a novel control strategy for the optimal scheduling of an energy community constituted by prosumers and equipped with unidirectional vehicle-to-grid (V1G) and vehicle-to-building (V2B) capabilities. In particular, V2B services are provided by long-term parked plug-in electric vehicles (PEVs), used as temporary storage systems by prosumers, who in turn offer the V1G service to PEVs provisionally plugged into charging stations. To tackle the stochastic nature of the framework, we assume that PEVs communicate their parking and recharging time distribution to prosumers, allowing them to improve the energy allocation process. Acting as selfish agents, prosumers and PEVs interact in a rolling horizon control framework with the aim of achieving an agreement on their operating strategies. The resulting control problem is formulated as a GNEP, addressed through the variational inequality theory, and solved in a distributed fashion leveraging on the accelerated distributed augmented Lagrangian method, showing sufficient conditions for guaranteeing convergence. The proposed model predictive control approach is validated through numerical simulations under realistic scenarios.

Contents

4.1 Introduction

In the book *The high cost of free parking*, Donald Shoup states that "the average car spends about 95 percent of its life parked" [1]. Following the author's analysis, the main consequences of free parking – whose principal objective would be to alleviate traffic congestion – are increased automobile dependency, rapid urban sprawl, and debasing of urban design. Economic damages and environmental degradation follow naturally [2]. However, in an era of proliferation of PEVs and smart design of energy communities (ECs), this deleterious phenomenon could be turned into an opportunity.

The penetration of renewable energy sources (RESs) [3] is transforming the structure of the current energy sector, traditionally based on thermal means of production and large-scale transmission systems [4]. The current panorama comprises users with semi-autonomous generation capabilities and access to energy storage systems (ESSs), which are shifting the network topology towards a decentralized infrastructure [5]. EVs can,

as well, interact with the grid, by using it for unidirectional battery recharge and bidirectional injection, respectively, through the one-way vehicle-to-grid (V1G) and bidirectional vehicle-to-grid (V2G) technology, or for trading energy with buildings and houses, respectively, through the vehicle-to-building (V2B) and the vehicle-to-home (V2H) strategy. Furthermore, the technology which allows PEVs to transfer energy with any of these actors is called vehicle-to-everything (V2X) [6]. In this scenario, the arising research question is: how can ECs take advantage of PEVs' inactivity periods? A possible solution is the adoption of the *sharing economy* paradigm, which has been long proved to be effective in the energy realm [7].

Based on these premises, and leveraging on the large amount of data that modern PEVs collect, we propose a novel scalable stochastic model predictive control (MPC) approach, which allows prosumers to exploit the presence of long-parked PEVs, acting as energy buffers, while at the same time providing recharging capabilities to active PEVs. The resulting control problem is formulated as a GNEP, addressed through the variational inequality theory, and solved in a distributed fashion leveraging on the ADALM, showing sufficient conditions for guaranteeing convergence. The proposed MPC approach is validated through numerical simulations under realistic scenarios [8], [9].

The rest of the Chapter is organized as follows. Section 4.2 analyzes the recent literature on the available control techniques for V1G/V2B-equipped grids. Section 4.3 presents the system architecture, while the proposed control strategy is formalized in Section 4.4. The results obtained from numerical experiments on the case study are illustrated, analyzed, and compared in Section 4.5. Lastly, conclusions and remarks for future work are presented in Section 4.6.

4.2 Literature Review and Contributions

4.2.1 Related Works

V2G allows PEVs to bi-directionally exchange energy with the main electric grid. Since its invention in 1995 and further developments [10], several implementations succeeded, up to modern technologies such as V1G, V2B, V2H, and V2X. A thorough review of the rich literature regarding PEVs energy management with integrated RESs is provided in [11] and [12]: the focus is directed on the state-of-the-art standards, energy resources, charging topologies and infrastructures, energy management systems classification, power conditional units, and electric load management. It is evident that allowing PEVs to participate in the energy market share brings several positive effects. For instance, authors in [13] simulate the energy sharing process for a 50-households microgrid, equipped with V1G, and bidirectional V2H and V2G chargers, showing that peer-to-peer (P2P) trading strategies, such as V1G and V2H, can improve micro-grid self-supply and household bills. Moreover, the effectiveness of the charging process for long-term parked PEVs is studied in [14]. In order to implement this technology, several control approaches can be employed: a taxonomy of the most popular frameworks discussed in the literature (e.g., game theory and MPC) is summarized in Table 4.1.

Numerous studies analyzed the problem under the lenses of game theory: a non-cooperative two-phase game is proposed in [15] for coordinating a microgrid with residential loads, RESs, ESSs, and PEVs. During the first phase, agents try to predict the day-ahead energy demand, while in the second phase, they mitigate the deviation between the instantaneous real-time consumption and the day-ahead predictions. Authors in [16] propose a game-theoretic approach, using non-cooperative or cooperative games, to stimulate PEVs to provide frequency regulation services for the grid. The non-cooperative formulation is a Stackelberg game, while the cooperative one is a potential game. A charge scheduling problem is studied in [17], where the uncertainty resides in the price determination. The authors adopt a data-driven paradigm, where the demand-response aggregator is included as a player in the arising game. Instead, in [18], where the underlying approach is a Stackelberg model, stochasticity regards the behavior of PEVs users. A Stackelberg equilibrium results from a coalitional setup in [19], where multiple

Table 4.1: Taxonomy of control approaches for EV-integrated ECs

Authors and references	Game theory	MPC
Tushar *et al.* [15]	✓	
Chen and Leung [16]	✓	
Mendoza *et al.* [19]	✓	
Fele *et al.* [17]	✓	
Fijani *et al.* [18]	✓	
Shi *et al.* [21]		✓
Iacobucci *et al.* [22]		✓
Hu *et al.* [23]		✓
Zhao *et al.* [26]	✓	✓
Stephens *et al.* [25]	✓	✓

retailers compete to satisfy the EG energy demand. Other game-theoretic approaches rely on mean-field games: an example is provided by [20], which is used for dynamic demand management of electrical appliances.

Another line of work on control strategies for PEVs-integrated smart grids focuses on MPC. Authors in [21] propose an MPC-based solution for the PEVs' recharge scheduling problem, keeping households' energy demand under consideration. In [22] an MPC scheme is developed for optimizing fleet charging and minimizing V2G services cost over a long timescale. The presence of PEVs in the network not only allows for storage capacity, but also acts as a means for voltage regulation. A distributed MPC (DMPC) strategy is proposed in [23], aiming at real-time voltage regulation by exploiting the presence of aggregated reactive power provided by PEV chargers. Game-theoretical strategies and MPC are usually considered separate techniques, since they stem from different backgrounds. However, several attempts to merge the MPC capabilities with game-theoretical optimization have been proposed. Authors in [24] propose the use of DMPC for controlling a group of islanded microgrids, which behaves non-cooperatively. The control loop ensures stability while needing a limited amount of communication between microgrids. A more general game-theoretic MPC framework for demand side management is discussed in [25].

4.2.2 Contribution

In this Chapter, we propose a novel stochastic distributed MPC-based control strategy for ECs with RES and V1G/V2B capabilities, able to provide energy to PEVs in need of recharge CEVs, while taking advantage of the presence of long-term parked PEVs. The latter, referred to as trading PEVs (TEVs), can provide quasi-continuous buffer capacity, allowing prosumers to store energy that will be discharged during peak load periods. So far, the existing literature has not focused on the simultaneous availability of V1G and V2B, under the assumption of EV's stochastic parking and recharging time, which is essential for a robust design of ancillary service-based ECs. Differently from [14], we consider the possibility of bidirectional exchange with the prosumer households, in addition to the charging process. We employ a non-cooperative game-theoretical formulation for resolving the agreement problem among PEVs and prosumers, which consists of both parties reaching a consensus over prices and exchanging energy amounts. Particularly, differently from [27], where authors propose a robust control strategy under price and energy uncertainty, we limit the uncertainty to the energy-related data. Moreover, differently from [15], [18], [28], [29], we devise a leaderless, single-phase game, showing that the optimization problem formulation guarantees convergence to a Nash Equilibrium solution. The latter is formalized as a variational problem and computed using ADALM.

(a) Power line architecture.

(b) Communication layer.

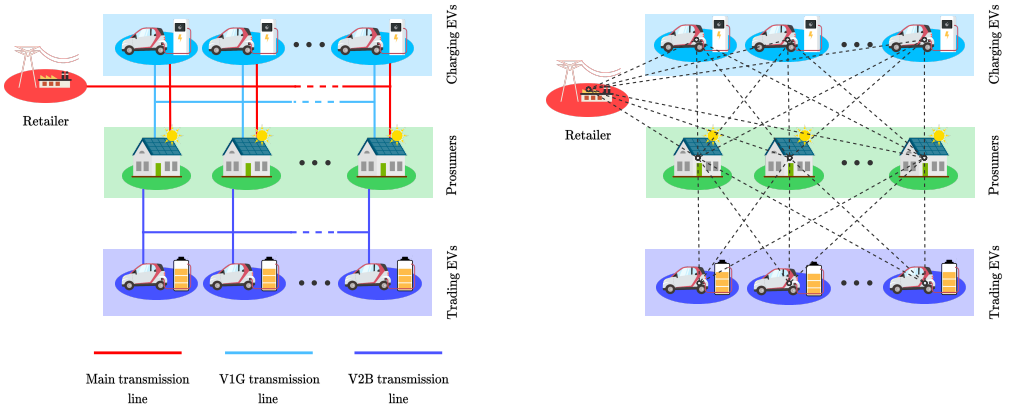

(c) Characterization of the energy flow variables among a generic prosumer-tEV-cEV triplet (note that the same energy flow is labeled differently with respect to the considered agent, except for the ones related to the retailer).

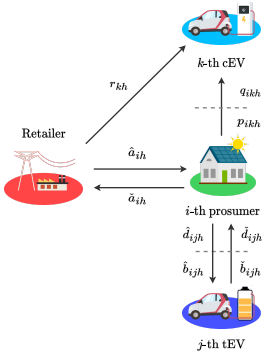

Figure 4.1: Model of the EC of prosumers with CEVs and TEVs.

4.3 System Model

Notation: $\mathbb{R}$, $\mathbb{R}_{\geq 0}$, $\mathbb{N}$, $\mathbb{N}_{\geq 0}$, and $\mathbb{B}$ indicate the sets of real, positive real, integer, positive integer, and binary (i.e., $\{0,1\}$) numbers, respectively; given a set $\mathcal{A}$, $|\mathcal{A}|$ denotes the cardinality of $\mathcal{A}$; $\mathbb{S}^n$ indicates the set of symmetric matrices of size $n \times n$; for $a, b \in \mathbb{N}, a \leq b$, $[a,b]_{\mathbb{N}} := [a,b] \cap \mathbb{N}$; given $n, m \in \mathbb{N}$, $\mathbf{I}_n$ is the identity matrix of size $n \times n$, while $\mathbf{0}_{n,m}$ and $\mathbf{1}_{n,m}$ are the null and all-ones matrices of sizes $n \times m$, respectively; given $x_1, \ldots, x_N \in \mathbb{R}$, $(x_i)_{i \in [1,N]_{\mathbb{N}}}$ indicates the column vector $\mathbf{x} = (x_1, \ldots, x_N)$; $\mathbf{x}^\top$ indicates the transpose of vector $\mathbf{x}$; given $\mathbf{x}_1, \ldots, \mathbf{x}_N \in \mathbb{R}^n$, the notations $[\mathbf{x}_1; \ldots; \mathbf{x}_N]$ and $(\mathbf{x}_i)_{i \in [1,N]_{\mathbb{N}}}$ denote the column vector $\mathbf{x} := (\mathbf{x}_1^\top, \ldots, \mathbf{x}_N^\top)^\top$ collecting all the column vectors $\mathbf{x}_1, \ldots, \mathbf{x}_N$; $\mathrm{diag}(\mathbf{x}, i)$ is the null matrix having $\mathbf{x}$ as i-th diagonal, with $\mathrm{diag}(\mathbf{x}) = \mathrm{diag}(\mathbf{x}, 0)$; given two matrices A, B, $A \otimes B$ denotes their Kronecker product; given matrix $A = [A_{ij}]$, we indicate the number of non-zero elements of the i-th row as $\omega_i(A) := |\{j \mid A_{ij} \neq 0\}|$, and the *maximum degree* of A as $\omega(A) := \max_i \omega_i(A)$. Given the stochastic variable Ψ, $\mathbb{E}[\Psi]$ denotes the expectation of Ψ. The generic energy flow variable x decorated as $\hat{x}$ indicates inward flow or charged energy, while $\check{x}$ indicates outward flow or discharged energy. Being $t \in \mathbb{N}_{\geq 0}$ the current time step, $\mathcal{H}_t = \{t, \ldots, t+H-1\}$ denotes the H-step control horizon, starting from t.

4.3.1 Energy Community Architecture

The EC model comprises the following agents:

• *Charging PEVs* (CEVs) - These are non-resident PEVs that are temporarily plugged into charging stations of the EC and connected to the grid with the only aim of recharging their own batteries.

• *Trading PEVs* (TEVs) - These are PEVs that are parked long-term in the parking spots of the EC and connected to the grid with the aim of renting their free battery capacity to prosumers as temporary ESS.

• *Prosumers* - These are the community members equipped with autonomous generation systems (e.g., photovoltaic, eolic sources), and characterized by local energy demand. Their energy surplus can be either stored using the temporary ESS capacity of TEVs, sold to CEVs for their recharging purpose, or sold to the retailer.

• *Retailer* - This is a passive agent, responsible for selling energy both to prosumers and CEVs, as well as buying energy from prosumers, at any moment in time, with fixed pricing curves. Its presence is needed in order to guarantee the energy balance in the EC.

We indicate the sets of prosumers, CEVs, and TEVs respectively by $\mathcal{P}$ (with $|\mathcal{P}| = P$), $\mathcal{C}_t$ (with $|\mathcal{C}_t| = C_t$), and $\mathcal{S}_t$ (with $|\mathcal{S}_t| = S_t$), while the set of all PEVs is denoted as $\mathcal{V}_t = \mathcal{C}_t \cup \mathcal{S}_t$ (with $|\mathcal{V}_t| = V_t$). We highlight that the sets of CEVs and TEVs depend on time t and we remark that $\mathcal{P} \cap \mathcal{C}_t = \mathcal{P} \cap \mathcal{S}_t = \mathcal{S}_t \cap \mathcal{C}_t = \emptyset$. Figure 4.1a represents the grid topology of the EC. All agents are allowed to communicate and exchange energy in accordance with the tripartite graph shown in Fig. 4.1b: the communication network is assumed to be ideal since assessing the impacts of delay and latency is out of the scope of this Chapter. Moreover, Fig. 4.1c illustrates the energy flows of a generic triplet of agents, indicating the choice of variables described in the sequel.

4.3.2 Stochastic Characterization of Electric Vehicles Parking and Recharging Durations

EVs have a stochastic behavior, since owners may move their vehicles from the parking spots, in the case of TEVs, or from the recharging stations before the charging process is finished, in the case of CEVs. Nevertheless, each PEV has local knowledge of its parking and charging time patterns, in terms of probability distribution parameters, based on the data acquisition features of on-board pervasive electronic devices [30]. These parameters are anonymously shared with prosumers when an PEV arrives at the parking spot or recharging station. Throughout the Chapter, we assume the agents' *fairness* in communicating information. However, to circumvent such an assumption, frameworks for secure data exchange are available [31]. We indicate the arrival time of the v-th PEV with $t_v^{(a)}$, and its departure time with $t_v^{(d)} \sim \mathcal{D}_v(\boldsymbol{\mu}_v)$, being a random variable following a known distribution $\mathcal{D}_v$ with parameters $\boldsymbol{\mu}_v$. When the PEV departs, we have that $v \notin \mathcal{V}_t$, $\forall t \geq t_v^{(d)}$. Let $\delta_{vh} \in \mathbb{B}$ be an indicator variable signaling whether the v-th PEV is in the parking/charging spot at $h \in \mathcal{H}_t$, or not, i.e.,

$$\delta_{vh} = \begin{cases} 1, & \text{if } h < t_v^{(d)} \\ 0, & \text{otherwise} \end{cases} \tag{4.1}$$

Clearly, δ_{vh} is a stochastic function of $t_v^{(d)}$. We assume that if an PEV leaves the parking/charging spot, it does not return.

4.3.3 Charging Electric Vehicles

Each k-th cEV has a physical battery capacity equal to $\overline{S}_k$ and arrives at the charging station with an initial battery level $\underline{S}_k$. For each time step h in the control horizon $\mathcal{H}_t$, each k-th cEV can buy the energy amount r_{kh} (at time-varying price $\hat{K}_h$) from the retailer, or the amount q_{ikh} (at time-varying price ψ_{ikh}) from the i-th prosumer. These

energy variables are bounded as follows:

$$\forall h \in \mathcal{H}_t,\ \forall i \in \mathcal{P} : \begin{cases} 0 \leq r_{kh} \leq M_{\mathcal{RC}}, & \text{(4.2a)} \\ 0 \leq q_{ikh} \leq M_{\mathcal{PC}} & \text{(4.2b)} \end{cases}$$

with $M_{\mathcal{RC}}$ and $M_{\mathcal{PC}}$ being the maximum amount of exchangeable energy with the retailer and each prosumer, respectively. Therefore, the battery charge level of the k-th cEV, s_{kh}, is modeled over the control horizon $\mathcal{H}_t$ as follows:

$$\forall h \in \mathcal{H}_t : \begin{cases} s_{kh} = \alpha s_{k,h-1} + \hat{\eta} \left(r_{kh} + \sum_{i \in \mathcal{P}} q_{ikh} \right), & \text{(4.3a)} \\ s_{k,t_k^{(a)}} = \underline{S}_k & \text{(4.3b)} \end{cases}$$

where (4.3b) represents the battery level at arrival, while $\alpha \in (0, 1]$ and $\hat{\eta} \in (0, 1]$ are the leakage coefficient and the charging efficiency, respectively, both assumed constant and equal for all PEVs. Furthermore, we assume that the CEVs' batteries have an optimal charging profile [32], s_{kh}^{op}, given by the following exponential curve:

$$s_{kt}^{\text{op}} = \overline{S}_k + (s_{k,t-1} - \overline{S}_k) e^{-\gamma_k (h-t+1)} \tag{4.4}$$

where $\gamma_k \in \mathbb{R}_{\geq 0}$ represents the nominal recharging rate. Hence, replacing (4.4) in (4.3a), the optimal charge dynamics s_{kh}^{op} turns into:

$$s_{kh}^{\text{op}} = \alpha s_{k,h-1}^{\text{op}} + \hat{\eta} \mathrm{I}_{kh}^{\text{op}} \tag{4.5}$$

where $\mathrm{I}_{kh}^{\text{op}}$ is the optimal energy intake thus being equal to:

$$\mathrm{I}_{kh}^{\text{op}} = \min \left(\frac{1}{\hat{\eta}} \left(s_{kh}^{\text{op}} - \alpha s_{k,h-1}^{\text{op}} \right), M_{\mathcal{RC}} + P M_{\mathcal{PC}} \right) \tag{4.6}$$

Note that $\mathrm{I}_{kh}^{\text{op}}$ is upper-bounded by the maximum exchangeable energy. Finally, recalling constraints (4.2), the total optimal energy intake is:

$$r_{kh} + \sum_{i \in \mathcal{P}} q_{ikh} = \delta_{kh} \mathrm{I}_{kh}^{\text{op}} \tag{4.7}$$

which drops to zero when the cEV is not plugged into the recharging station any longer. The k-th cEV tries to obtain the needed energy intake in (4.7) by optimally determining the profiles of energy flow to be bought from the retailer and the prosumers over the control horizon $\mathcal{H}_t$, denoted as $\mathbf{r}_k = (r_{kh})_{h \in \mathcal{H}_t}$ and $\mathbf{q}_k = (\mathbf{q}_{ik})_{i \in \mathcal{P}}$, respectively. Note that the vector $\mathbf{q}_{ik} = (q_{ikh})_{h \in \mathcal{H}_t}$ is the profile of energy intake from the i-th prosumer. Hence, vectors $\mathbf{r}_k$ and $\mathbf{q}_k$ are thus collected in the decision variables' vector $\mathbf{x}_k^{\mathcal{C}} \in \mathbb{R}^{H(1+P)}$ defined as:

$$\mathbf{x}_k^{\mathcal{C}} = \text{col}(\mathbf{r}_k, \mathbf{q}_k). \tag{4.8}$$

We collect the feasible decision vectors, satisfying the inequalities independent from δ_{kh}, in the set $\mathcal{U}_{\mathcal{C}} := \{\mathbf{x}_k^{\mathcal{C}} \mid (4.2) \text{ holds}\}$, and re-write (4.7) as $\mathbf{A}_k^{\mathcal{C}} \mathbf{x}_k^{\mathcal{C}} + \mathbf{b}_k^{\mathcal{C}} = \mathbf{0}$, where

$$\mathbf{A}_k^{\mathcal{C}} = \begin{bmatrix} \mathbf{I}_H & \mathbf{1}_P \otimes \mathbf{I}_H \end{bmatrix}, \quad \mathbf{b}_k^{\mathcal{C}} = -\boldsymbol{\delta}_k \mathbf{I}_k^{\text{op}} \tag{4.9}$$

and $\boldsymbol{\delta}_k = (\delta_{kh})_{h \in \mathcal{H}_t}$ and $\mathbf{I}_k^{\text{op}} = (\mathrm{I}_{kh}^{\text{op}})_{h \in \mathcal{H}_t}$. Lastly, the total cost sustained for the recharging process by the k-th cEV, $J_{\mathcal{C}}\left(\mathbf{x}_k^{\mathcal{C}}\right)$, is defined as:

$$J_{\mathcal{C}}\left(\mathbf{x}_k^{\mathcal{C}}\right) = \sum_{h \in \mathcal{H}_t} \delta_{kh} \left(\underbrace{\hat{K}_h r_{kh}}_{\substack{\text{Retailer's} \\ \text{energy cost}}} + \sum_{i \in \mathcal{P}} \underbrace{\psi_{ikh} q_{ikh}}_{\substack{\text{Prosumers'} \\ \text{energy cost}}} \right) \tag{4.10}$$

comprising the costs for the energy bought by the CEVs both from the retailer and all prosumers (corresponding to the first and second term in (4.10), respectively).

4.3.4 Trading Electric Vehicles

Differently from CEVs, the generic j-th TEV is characterized by a free amount of storage that can be used by prosumers. We indicate the battery level at the time of the j-th TEV arrival as $\underline{Z}_j$ and the maximum battery capacity as $\overline{Z}_j$. Hence, the following inequality must be satisfied:

$$\sum_{i \in \mathcal{P}} w_{ijh} \leq \overline{Z}_j - \underline{Z}_j, \quad h \in \mathcal{H}_t \tag{4.11}$$

where w_{ijh} is the amount of storage that the j-th PEV holds for the i-th prosumer, modeled as follows:

$$\begin{matrix} \forall h \in \mathcal{H}_t, \\ \forall i \in \mathcal{P} \end{matrix} : \begin{cases} w_{ijh} = \delta_{jh} \left(\alpha w_{ij,h-1} + \hat{\eta} \hat{b}_{ijh} - \check{\eta} \check{b}_{ijh} \right), & \text{(4.12a)} \\ w_{ijh} \geq 0, & \text{(4.12b)} \\ w_{ij t_j^{(a)}} = 0 & \text{(4.12c)} \end{cases}$$

where (4.12a) is the storage update equation, while (4.12c) imposes that the fraction of storage held for the i-th prosumer when the j-th TEVs arrives at the parking spot is null. Coefficients α and $\hat{\eta}$ are characterized as in (4.3a), while $\check{\eta} \in (0, 1]$ is the constant discharging efficiency, equal for all TEVs. Quantities $\hat{b}_{ijh}$ and $\check{b}_{ijh}$ are respectively the charged and discharged energy, bounded as follows:

$$\forall h \in \mathcal{H}_t, \ \forall i \in \mathcal{P} : \begin{cases} \hat{b}_{ijh} \geq 0, & \text{(4.13a)} \\ \check{b}_{ijh} \geq 0, & \text{(4.13b)} \\ \hat{b}_{ijh} + \check{b}_{ijh} \leq M_{\mathcal{PS}} & \text{(4.13c)} \end{cases}$$

with $M_{\mathcal{PS}}$ being the maximum amount of exchangeable energy for storage charging and discharging, respectively. Constraint (4.13c) adopts the complementarity constraint approximation proposed in [33], since introducing binary variables for modeling the switching dynamics of storage charging and discharging will make the problem computationally infeasible. The profile of the energy stored on behalf of the i-th prosumer in the battery of the j-th tEV, over the control horizon, is indicated as $\mathbf{w}_{ij} = (w_{ijh})_{h \in \mathcal{H}_t}$.

The j-th TEV aims at optimally determining the profiles of energy charged from and discharged towards prosumers, over the control horizon $\mathcal{H}_t$, denoted as $\hat{\mathbf{b}}_{ij} = (\hat{b}_{ijh})_{h \in \mathcal{H}_t}$ and $\check{\mathbf{b}}_{ij} = (\check{b}_{ijh})_{h \in \mathcal{H}_t}$, respectively. Vectors $\hat{\mathbf{b}}_j = (\hat{\mathbf{b}}_{ij})_{i \in \mathcal{P}}$, $\check{\mathbf{b}}_j = (\check{\mathbf{b}}_{ij})_{i \in \mathcal{P}}$, and $\mathbf{w}_j = (\mathbf{w}_{ij})_{i \in \mathcal{P}}$ are thus collected in the decision variables' vector $\mathbf{x}_j^{\mathcal{S}} \in \mathbb{R}^{3PH}$, defined as:

$$\mathbf{x}_j^{\mathcal{S}} = \text{col} \left(\hat{\mathbf{b}}_j, \check{\mathbf{b}}_j, \mathbf{w}_j \right). \tag{4.14}$$

We collect the feasible decision vectors, satisfying the equalities and inequalities independent of δ_{jh}, in the set $\mathcal{U}_{\mathcal{S}} := \{\mathbf{x}_j^{\mathcal{S}} \mid (4.12\text{b}), \ (4.12\text{c}), \ (4.13) \text{ hold}\}$. The dynamic for w_{ijh} in (4.12a) can be written as $\mathbf{A}_j^{\mathcal{S}} \mathbf{x}_j^{\mathcal{S}} = \mathbf{0}$, where

$$\mathbf{A}_j^{\mathcal{S}} = \begin{bmatrix} \mathbf{I}_P \otimes \hat{\eta} \, \text{diag} \left(\boldsymbol{\delta}_j \right) \\ -\mathbf{I}_P \otimes \check{\eta} \, \text{diag} \left(\boldsymbol{\delta}_j \right) \\ \alpha \, \text{diag} \left(\mathbf{1}_{PH-1}, 1 \right) - \mathbf{I}_{PH} \end{bmatrix}^\top \tag{4.15}$$

with $\boldsymbol{\delta}_j = (\delta_{jh})_{h \in \mathcal{H}_t}$. We indicate the time-varying unitary costs that the i-th prosumer pays to the j-th TEV for the storage charging and discharging services with $\hat{\varphi}_{ijh}$ and $\check{\varphi}_{ijh}$, respectively. However, from the prosumers' point of view, the drawback of the TEVs' storage usage is that the latter may leave the parking spot with part of the energy put aside for prosumers. Hence, we introduce the time-varying *leaving fee* θ_{ijh}, representing the "refund" the j-th TEV is willing to repay to the i-th prosumer for every unit of lost storage. In addition, TEVs have to account for costs related to the battery's physical degradation (i.e., the cost of having the battery life shortened due to recharging/discharging cycles), which are expressed through function $Q(\check{b}_{ijh}, \hat{b}_{ijh})$. Details of battery degradation models for control applications can be found in [34], [35]. However, we keep $Q(\check{b}_{ijh}, \hat{b}_{ijh})$ generical, provided that the following assumption is satisfied.

Assumption 4.3.1

The degradation cost function $Q(\check{b}_{ijh}, \hat{b}_{ijh})$ is a non-negative, monotonically increasing, continuously differentiable convex function.

As an example, $Q(\check{b}_{ijh}, \hat{b}_{ijh})$ can be modeled through a quadratic term depending on the battery technological coefficient ζ, as in [36], i.e., $Q(\check{b}_{ijh}, \hat{b}_{ijh}) := \zeta(\check{b}_{ijh} + \hat{b}_{ijh})^2$.

Summing up, the total cost sustained by the j-th tEV, $J_{\mathcal{S}}\left(\mathbf{x}_j^{\mathcal{S}}\right)$, is defined as follows

$$J_{\mathcal{S}}\left(\mathbf{x}_j^{\mathcal{S}}\right) = \sum_{h\in\mathcal{H}_t}\sum_{i\in\mathcal{P}}\Bigg(\delta_{jh}\underbrace{Q(\check{b}_{ijh},\hat{b}_{ijh})}_{\text{Degradation costs}} - \delta_{jh}\underbrace{\left[(\hat{\varphi}_{ijh}\hat{b}_{ijh} + \check{\varphi}_{ijh}\check{b}_{ijh})\right]}_{\substack{\text{Storage revenues}\\ \text{from prosumers}}} + (1-\delta_{jh})\underbrace{\left[(\theta_{ijh} - \hat{K}_h)w_{ij,h-1}\right]}_{\text{Leaving fee}}\Bigg) \tag{4.16}$$

Note that in the case $\theta_{ijh} < \hat{K}_h$, the TEV would still save money by leaving the parking spot with part of the energy stored by the i-th prosumer, since the leaving fee is lower than the recharging cost the TEV would pay if supplied by the retailer.

4.3.5 Prosumers

At each time step $h \in \mathcal{H}_t$, the i-th prosumer is characterized by a known autonomous generation, G_{ih}, and by an energy demand, D_{ih}. On the one hand, in the case $D_{ih} > G_{ih}$, the i-th prosumer can buy the energy amount $\hat{a}_{ih}$ supplied by the retailer (at time-varying price $\hat{K}_h$) and/or retrieve the energy amount $\check{d}_{ijh}$, discharged by the j-th tEV, (at time-varying price $\check{\varphi}_{ijh}$). On the other hand, in case $G_{ih} > D_{ih}$, the i-th prosumer can sell the energy amount $\check{a}_{ih}$ to the retailer (at time-varying price $\check{K}_h$), sell the energy amount p_{ikh} to the k-th cEV (at time-varying price ψ_{ikh}) as charging service, and/or store the energy amount $\hat{d}_{ijh}$ in the j-th TEV (at time-varying price $\hat{\varphi}_{ijh}$). At each time step, the following energy balance equation must be satisfied for the i-th prosumer:

$$G_{ih} - D_{ih} + \hat{a}_{ih} - \check{a}_{ih} + \sum_{j\in\mathcal{S}_t}\delta_{jh}\left(\hat{d}_{ijh} - \check{d}_{ijh}\right) - \sum_{k\in\mathcal{C}_t}\delta_{kh}p_{ikh} = 0, \quad h \in \mathcal{H}_t. \tag{4.17}$$

Moreover, all energy flows $\hat{a}_{ih}$, $\check{a}_{ih}$, $\hat{d}_{ijh}$, $\check{d}_{ijh}$, and p_{ikh} are bounded as follows:

$$\forall h \in \mathcal{H}_t : \begin{cases} 0 \le \hat{a}_{ih} \le M_{\mathcal{RP}}, & & (4.18a)\\ 0 \le \check{a}_{ih} \le M_{\mathcal{RP}}, & & (4.18b)\\ \hat{d}_{ijh} \ge 0, & \forall j \in \mathcal{S}_t & (4.18c)\\ \check{d}_{ijh} \ge 0, & \forall j \in \mathcal{S}_t & (4.18d)\\ \hat{d}_{ijh} + \check{d}_{ijh} \le M_{\mathcal{PS}}, & \forall j \in \mathcal{S}_t & (4.18e)\\ 0 \le p_{ikh} \le M_{\mathcal{PC}} & \forall k \in \mathcal{C}_t. & (4.18f) \end{cases}$$

where $M_{\mathcal{RP}}$ is the maximum amount of energy exchangeable with the retailer, while $M_{\mathcal{PC}}$ and $M_{\mathcal{PS}}$ are defined as for (4.2) and (4.13), respectively. Constraint (4.18e) corresponds to the same complementarity constraint relaxation in (4.13c). The amount of energy the j-th TEV stores for the i-th prosumer is indicated with u_{ijh}, whilst its profile over the control horizon is denoted as $\mathbf{u}_{ij} = (u_{ijh})_{h\in\mathcal{H}_t}$. Hence, similarly to (4.12), we have:

$$\begin{matrix}\forall h \in \mathcal{H}_t,\\ \forall j \in \mathcal{S}_t\end{matrix} : \begin{cases} u_{ijh} = \delta_{jh}\left(\alpha u_{ij,h-1} + \hat{\eta}\hat{d}_{ijh} - \check{\eta}\check{d}_{ijh}\right) & (4.19a)\\ u_{ijh} \ge 0 & (4.19b)\\ u_{ijt_j^{(a)}} = 0 & (4.19c) \end{cases}$$

where (4.19a), similarly to (4.12a), is the storage update equation, while (4.19c) imposes that the fraction of storage held by the j-th TEVs, when it arrives at the parking spot, is null.

Remark 4.3.1

Couples (w_{ijh}, u_{ijh}), $(\hat{d}_{ijh}, \hat{b}_{ijh})$, $(\check{d}_{ijh}, \check{b}_{ijh})$ and $(\check{p}_{ikh}, \check{q}_{ikh})$ represent the same quantity from the prosumers and PEVs perspective. Using different variables will allow us to formulate the equilibrium problem, as it will be shown in Section 4.4.

The i-th prosumer aims at optimally determining the profiles of energy to be bought from and sold to the retailer ($\hat{\mathbf{a}}_i = (\hat{a}_{ih})_{h\in\mathcal{H}_t}$ and $\check{\mathbf{a}}_i = (\check{a}_{ih})_{h\in\mathcal{H}_t}$), of energy sold to each cEV ($\mathbf{p}_{ik} = (p_{ikh})_{h\in\mathcal{H}_t}$, $\forall k \in \mathcal{C}_t$), and energy to be charged in and discharged from each TEV ($\hat{\mathbf{d}}_{ij} = (\hat{d}_{ijh})_{h\in\mathcal{H}_t}$ and $\check{\mathbf{d}}_{ij} = (\check{d}_{ijh})_{h\in\mathcal{H}_t}$, $\forall j \in \mathcal{S}_t$), over the control horizon $\mathcal{H}_t$. Vectors $\hat{\mathbf{a}}_i$, $\check{\mathbf{a}}_i$, $\mathbf{p}_i = (\mathbf{p}_{ik})_{k\in\mathcal{C}_t}$, $\hat{\mathbf{d}}_i = (\hat{\mathbf{d}}_{ij})_{j\in\mathcal{S}_t}$, $\check{\mathbf{d}}_i = (\check{\mathbf{d}}_{ij})_{j\in\mathcal{S}_t}$, and $\mathbf{u}_i = (\mathbf{u}_{ij})_{j\in\mathcal{S}_t}$ are thus collected in the decision variables' vector $\mathbf{x}_i^{\mathcal{P}} \in \mathbb{R}^{H(2+C_t+3S_t)}$ defined as:

$$\mathbf{x}_i^{\mathcal{P}} = \operatorname{col}\left(\hat{\boldsymbol{a}}_i, \check{\boldsymbol{a}}_i, \mathbf{p}_i, \hat{\mathbf{d}}_i, \check{\mathbf{d}}_i, \mathbf{u}_i\right). \tag{4.20}$$

We collect the feasible decision vectors, satisfying the equalities and inequalities independent from δ_{kh} and δ_{jh}, in the set $\mathcal{U}_{\mathcal{P}} := \{\mathbf{x}_i^{\mathcal{P}} \mid (4.18),\ (4.19b),\ (4.19c) \text{ hold}\}$. Equations (4.19a) and (4.17) can be expressed as $\mathbf{A}_i^{\mathcal{P}}\mathbf{x}_i^{\mathcal{P}} + \mathbf{b}_i^{\mathcal{P}} = \mathbf{0}$, where

$$\mathbf{A}_i^{\mathcal{P}} = \begin{bmatrix} \mathbf{I}_H & \mathbf{0}_{S_t,S_tH} \\ -\mathbf{I}_H & \mathbf{0}_{S_t,S_tH} \\ \mathbf{1}_{S_t} \otimes \operatorname{diag}(\boldsymbol{\delta}_j) & \mathbf{I}_{S_t} \otimes \hat{\eta} \operatorname{diag}(\boldsymbol{\delta}_j) \\ -\mathbf{1}_{S_t} \otimes \operatorname{diag}(\boldsymbol{\delta}_j) & -\mathbf{I}_{S_t} \otimes \check{\eta} \operatorname{diag}(\boldsymbol{\delta}_j) \\ -\mathbf{1}_{C_t} \otimes \operatorname{diag}(\boldsymbol{\delta}_k) & \alpha \operatorname{diag}(\mathbf{1}_{S_tH-1},1) - \mathbf{I}_{S_tH} \end{bmatrix}^\top \tag{4.21a}$$

$$\mathbf{b}_i^{\mathcal{P}} = \begin{bmatrix} \mathbf{d}_i - \boldsymbol{G}_i \\ \mathbf{0}_{S_tH} \end{bmatrix} \tag{4.21b}$$

Finally, the total cost sustained by the i-th prosumer, $J_{\mathcal{P}}\left(\mathbf{x}_i^{\mathcal{P}}\right)$, can be expressed as follows:

$$J_{\mathcal{P}}\left(\mathbf{x}_i^{\mathcal{P}}\right) = \sum_{h\in\mathcal{H}_t} \Bigg(\underbrace{\hat{K}_h \hat{a}_{ih} - \check{K}_h \check{a}_{ih}}_{\substack{\text{Cost and revenues} \\ \text{from the retailer}}} - \sum_{k\in\mathcal{C}} \delta_{kh} \underbrace{\psi_{ikh} p_{ikh}}_{\substack{\text{Revenues} \\ \text{from CEVs}}} + \sum_{j\in\mathcal{S}_t} \Big[\delta_{jh} \underbrace{(\hat{\varphi}_{ijh} \hat{d}_{ijh} + \check{\varphi}_{ijh} \check{d}_{ijh})}_{\text{Storage cost}} - (1-\delta_{jh}) \underbrace{\theta_{ijh} u_{ij,h-1}}_{\substack{\text{Refund from} \\ \text{leaving TEVs}}} \Big] \Bigg) \tag{4.22}$$

consisting of the costs and revenues resulting from the energy trading with the retailer, revenues from the energy sold to CEVs, and costs of TEVs' storage usage.

4.4 The Proposed Control Strategy

The proposed control strategy relies on a non-cooperative stochastic MPC approach, which allows all agents in the EC (i.e., prosumers, CEVs, and TEVs) to agree on an energy exchange equilibrium. First, we formally describe the non-cooperative formulation of the game and the employed resolution algorithm; then, we illustrate its integration into the MPC scheme.

4.4.1 Non-cooperative Game Model

Consider a given $t \in \mathbb{N}_{\geq 0}$. For each time step $h \in \mathcal{H}_t$, each agent $n \in \mathcal{N} := \mathcal{C}_t \cup \mathcal{S}_t \cup \mathcal{P}$ acts selfishly, determining the best strategy which ensures that its cost function is minimized

and local constraints are satisfied. Following [37], we tackle the stochastic nature of parameter δ_{vh}, which indicates the PEV presence in the charging slot at time h, by considering the expectation related to the cost function and local constraints of each agent. To this aim, we first define the local constraints sets $\mathcal{K}_n$

$$\mathcal{K}_n := \left\{ \begin{array}{lll} \mathbf{x}_n^{\mathcal{C}} \in \mathcal{U}_{\mathcal{C}} : & \mathbb{E}_\delta[A_n^{\mathcal{C}} \mathbf{x}_n^{\mathcal{C}} + \mathbf{b}_n^{\mathcal{C}}] = \mathbf{0} & \text{if } n \in \mathcal{C}_t \\ \mathbf{x}_n^{\mathcal{S}} \in \mathcal{U}_{\mathcal{S}} : & \mathbb{E}_\delta[A_n^{\mathcal{S}} \mathbf{x}_n^{\mathcal{S}}] = \mathbf{0} & \text{if } n \in \mathcal{S}_t \\ \mathbf{x}_n^{\mathcal{P}} \in \mathcal{U}_{\mathcal{P}} : & \mathbb{E}_\delta[A_n^{\mathcal{P}} \mathbf{x}_n^{\mathcal{P}} + \mathbf{b}_n^{\mathcal{P}}] = \mathbf{0} & \text{if } n \in \mathcal{P} \end{array} \right\} \tag{4.23}$$

However, the energy amount that each agent eventually buys from or sells to one of its neighbors must be equal to the quantity the latter decides to release or acquire. We indicate the vectors collecting the residuals of the energy flows between prosumers and CEVs, as well as prosumers and TEVs with $\mathbf{c}_{ik}^{\mathcal{PC}}$ and $\mathbf{c}_{ij}^{\mathcal{PS}}$, respectively:

$$\forall i \in \mathcal{P} : \left\{ \begin{array}{ll} \mathbf{c}_{ik}^{\mathcal{PC}} := \left[\mathbf{q}_{ik} - \mathbf{p}_{ik}\right] = \mathbf{0}_H, & \forall k \in \mathcal{C}_t \quad (4.24a) \\ \mathbf{c}_{ij}^{\mathcal{PS}} := \begin{bmatrix} \hat{\mathbf{d}}_{ij} - \hat{\mathbf{b}}_{ij} \\ \check{\mathbf{d}}_{ij} - \check{\mathbf{b}}_{ij} \\ \mathbf{u}_{ij} - \mathbf{w}_{ij} \end{bmatrix} = \mathbf{0}_{3H}, & \forall j \in \mathcal{S}_t \quad (4.24b) \end{array} \right.$$

Constraints (4.24) constitute the so-called *coupling constraints*. They can be interpreted as the result of the "agreement" on the energy amounts to be exchanged among agents, which is also known as "market-clearing" process. Formally, this agreement means finding the NE of the non-cooperative game $\mathfrak{G}(\mathcal{N}, \mathcal{X}, \mathcal{J})$, defined as follows:

- $\mathcal{N}$ is the set of agents, with $|\mathcal{N}| = N$;
- $\mathcal{X} = \prod_{n \in \mathcal{N}} \mathcal{X}_n(\mathbf{x}_{-n})$ is the set of strategies, where $\mathcal{X}_n(\mathbf{x}_{-n})$ is the strategy set of the n-th agent:

$$\mathcal{X}_n(\mathbf{x}_{-n}) = \left\{ \mathbf{x}_n \in \mathcal{K}_n : \begin{array}{ll} (4.24a) \text{ hold}, & \text{if } n \in \mathcal{C}_t \\ (4.24b) \text{ hold}, & \text{if } n \in \mathcal{S}_t \\ (4.24) \text{ hold}, & \text{if } n \in \mathcal{P} \end{array} \right\} \tag{4.25}$$

with $\mathbf{x}_n$ and $\mathbf{x}_{-n} := (\mathbf{x}_m)_{m \in \mathcal{N} \setminus \{n\}}$ being the strategy of the n-th agent and of all the remaining agents in $\mathcal{N} \setminus \{n\}$, respectively;

- $\mathcal{J} = \{J_n(\mathbf{x}_n),\ n \in \mathcal{N}\}$ is the set of objective functions:

$$J_n(\mathbf{x}_n) = \left\{ \begin{array}{ll} \mathbb{E}_\delta[J_{\mathcal{C}}(\mathbf{x}_n^{\mathcal{C}})], & \text{if } n \in \mathcal{C}_t \\ \mathbb{E}_\delta[J_{\mathcal{S}}(\mathbf{x}_n^{\mathcal{S}})], & \text{if } n \in \mathcal{S}_t \\ \mathbb{E}_\delta[J_{\mathcal{P}}(\mathbf{x}_n^{\mathcal{P}})] & \text{if } n \in \mathcal{P}. \end{array} \right. \tag{4.26}$$

being the expected value, with respect to either δ_{kh} or δ_{jh} of the total costs defined in Section 4.3. The optimal strategy $\mathbf{x}_n^*$ of the n-th agent results from the following inter-dependent optimization problems:

$$\mathbf{x}_n^* = \underset{\mathbf{x}_n \in \mathcal{X}_n(\mathbf{x}^*_{-n})}{\operatorname{argmin}} \ J_n(\mathbf{x}_n), \quad \forall n \in \mathcal{N}. \tag{4.27}$$

Definition 4.4.1

A NE is a collective strategy $(\mathbf{x}_n^*)_{n \in \mathcal{N}}$ such that no agent can benefit from a unilateral deviation if all the other agents act according to the NE, i.e.:

$$J_n(\mathbf{x}_n^*) \leq \inf \{J_n(\mathbf{x}_n) :\ \mathbf{x}_n \in \mathcal{X}(\mathbf{x}^*_{-n})\},\ \forall n \in \mathcal{N}. \tag{4.28}$$

Note that, due to the presence of the coupling constraints in (4.24), the above-defined problem is a GNEP [38] and a corresponding solution is denoted as a GNE. It is well-known that a GNEP is a hard problem, for which there are no general solutions. However,

there exists a class of GNEPs that can be treated as a variational inequality (VI) problem [39]. Given a convex closed set $\mathcal{K} \subseteq \mathbb{R}^n$ and a continuous function $\mathbf{F} : \mathcal{K} \to \mathbb{R}^n$, solving the variational problem $VI(\mathcal{K}, \mathbf{F})$ means finding a vector $\mathbf{x} \in \mathcal{K}$ such that:

$$\mathbf{F}(x)^\top (\mathbf{x} - \mathbf{y}) \geq 0, \quad \forall \mathbf{y} \in \mathcal{K}. \tag{4.29}$$

In particular, if $\mathbf{F} = (\nabla_{\mathbf{x}_1} J_1(\mathbf{x}_1); \ldots; \nabla_{\mathbf{x}_N} J_N(\mathbf{x}_N))$, then $VI(\mathbf{F}, \mathcal{X})$ is the associated VI problem to $\mathfrak{G}(\mathcal{N}, \mathcal{X}, \mathcal{J})$.

Proposition 4.4.1

Every solution of the $VI(\mathcal{X}, \mathbf{F})$ formulation of $\mathfrak{G}(\mathcal{N}, \mathcal{X}, \mathcal{J})$ is also a solution of the GNEP.

Proof. The proof consists in verifying that the following sufficient conditions provided in [39] (by which every solution of the VI formulation of a GNEP problem is a GNE) hold in the case of problem (4.27):

(1.1) $J_n \in \mathcal{J}$ is continuously differentiable, for all $n \in \mathcal{N}$;

(1.2) $J_n(\mathbf{x}_n)$ is pseudo-convex in $\mathbf{x}_n \in \mathcal{K}_n$, for all $n \in \mathcal{N}$;

(1.3) The set $\mathcal{X}_n(\mathbf{x}_{-n})$ is closed and convex, for all $n \in \mathcal{N}$.

Condition (1.1) is readily verified by definitions in (4.10), (4.16), and (4.22). In addition, differentiability of (4.16) is verified from Assumption 4.3.1. Condition (1.2) is verified for (4.10) and (4.22) since these are affine, while in the case of (4.16), for $Q(\check{b}_{ijh}, \hat{b}_{ijh})$ quadratic, it follows from the positive semi-definiteness of the Hessian matrix $\mathbf{H}_j \in \mathbb{S}^{3PH}$ of $J_{\mathcal{S}}(\mathbf{x}_j^{\mathcal{S}})$, i.e.,

$$\mathbf{H}_j = \begin{bmatrix} \mathbf{H}_j^{\text{nw}} & \mathbf{0}_{2PH,PH} \\ \mathbf{0}_{PH,2PH} & \mathbf{0}_{PH,PH} \end{bmatrix} \succeq 0, \quad \forall j \in \mathcal{S}_t \tag{4.30}$$

where $\mathrm{H}_j^{\text{nw}} \in \mathbb{S}^{2PH}$ is the north-west minor of matrix H_j, defined as:

$$\mathbf{H}_j^{\text{nw}} := \zeta \mathbf{1}_{2,2} \otimes (\mathbf{I}_P \otimes \operatorname{diag}(\boldsymbol{\delta}_j)) \succeq 0, \quad \forall j \in \mathcal{S}_t. \tag{4.31}$$

Note that eq. (4.31) holds from Theorem 4.2.12 in [40]. As for condition (1.3), convexity is guaranteed since (4.25) results from the intersection of affine sets (4.23) and (4.24); closure and boundedness are both verified since all decision variables are non-negative and bounded from above with non-strict inequalities; consequently, the set $\mathcal{X}_n(\mathbf{x}_{-n})$ defined in (4.25) is a convex polytope [41] for all $n \in \mathcal{N}$. □

4.4.2 Equilibrium Computation

A well-known class of algorithms for solving a distributed VI with coupling equality constraints (as in (4.24)) is the augmented Lagrangian method (ALM). In particular, following [42], we employ the so-called ADALM. The basic idea consists of iteratively minimizing the Lagrangian of the cost function $J_n(\mathbf{x}_n)$ for each agent $n \in \mathcal{N}$, whose general form is:

$$\mathcal{L}_n(\mathbf{x}_n, \boldsymbol{\lambda}_n) = J_n(\mathbf{x}_n) + \boldsymbol{\lambda}_n^\top \mathbf{c}_n + \frac{\rho}{2} \|\mathbf{c}_n\|^2 \tag{4.32}$$

where $\mathbf{c}_n$ represents the equality constraints in (4.24), $\boldsymbol{\lambda}_n$ is the associated vector of Lagrange multipliers, and $\rho \in \mathbb{R}_{\geq 0}$ is the regularization strength. Recalling (4.8), (4.14) and (4.20), $\mathbf{c}_n$ is defined as:

$$\mathbf{c}_n := \begin{cases} \operatorname{col}(\mathbf{c}_{in}^{\mathcal{PC}})_{i \in \mathcal{P}} & \text{if } n \in \mathcal{C}_t \\ \operatorname{col}(\mathbf{c}_{in}^{\mathcal{PS}})_{i \in \mathcal{P}} & \text{if } n \in \mathcal{S}_t \\ \left[\operatorname{row}(\mathbf{c}_{nj}^{\mathcal{PS}})_{j \in \mathcal{S}_t} \;\; \operatorname{row}(\mathbf{c}_{nk}^{\mathcal{PC}})_{k \in \mathcal{C}_t} \right]^\top & \text{if } n \in \mathcal{P}. \end{cases} \tag{4.33}$$

Algorithm 4: ADALM

Input: ρ_t, χ, $\mathbf{x}_n^{(0)}$, $\boldsymbol{\lambda}_n^{(0)}$, $\quad \forall n \in \mathcal{N}$

1 $\tau \leftarrow 0$

Output: $\mathbf{x}_n^*, \quad \forall n \in \mathcal{N}$

2 **while** *stopping criterion is not reached* **do**

3 $\quad \tau \leftarrow \tau + 1$

4 $\quad$ **do in parallel**

5 $\quad\quad$ Each agent $n \in \mathcal{N}$ locally minimizes their Lagrangian, i.e.:

$$\tilde{\mathbf{x}}_n^{(\tau)} = \underset{\mathbf{x}_n \in \mathcal{K}_n}{\operatorname{argmin}} \mathcal{L}_n \left(\mathbf{x}_n, \boldsymbol{\lambda}_n^{(\tau-1)} \right) \tag{4.34}$$

6 $\quad\quad$

$$\mathbf{x}_n^{(\tau)} = \mathbf{x}_n^{(\tau-1)} + \chi \left(\tilde{\mathbf{x}}_n^{(\tau)} - \mathbf{x}_n^{(\tau-1)} \right) \tag{4.35}$$

7 $\quad\quad$ Each prosumer $n \in \mathcal{P}$ broadcasts $\hat{\mathbf{d}}_n^{(\tau)}, \check{\mathbf{d}}_n^{(\tau)}$, $\mathbf{u}_n^{(\tau)}$ to TEVs and $\mathbf{p}_n^{(\tau)}$ to CEVs.

8 $\quad\quad$ Each cEV $n \in \mathcal{C}_t$ broadcasts $\mathbf{q}_n^{(\tau)}$ to prosumers.

9 $\quad\quad$ Each TEV $n \in \mathcal{S}_t$ broadcasts $\hat{\mathbf{b}}_n^{(\tau)}, \check{\mathbf{b}}_n^{(\tau)}$, $\mathbf{w}_n^{(\tau)}$ to prosumers.

10 $\quad\quad$ Each agent $n \in \mathcal{N}$ locally updates the Lagrangian multipliers, i.e.:

$$\boldsymbol{\lambda}_n^{(\tau)} = \boldsymbol{\lambda}_n^{(\tau-1)} + \rho_t \chi \mathbf{c}_n^{(\tau)}, \quad \forall n \in \mathcal{N} \tag{4.36}$$

The ADALM-based iterative process is summarized in Algorithm 4, where τ in the variables' superscript denotes the iteration count. Given an initial solution $\mathbf{x}_n^{(0)}$ and multipliers vector $\boldsymbol{\lambda}_n^{(0)}$, for all $n \in \mathcal{N}$, at each iteration τ, each agent in the EC solves its own local optimization problem, using the previous Lagrange multipliers' vector, as in (4.34). Each agent's strategy is thus updated through the preconditioning step in (31), with $\chi \in \mathbb{R}_{\geq 0}$ being the constant step size. Subsequently, each agent broadcasts the updated energy flow variables to its neighbors (line 7). Having received the updated strategies of neighbors, each agent finally updates its own local vector of Lagrange multipliers as in (4.36).

Remark 4.4.1

Due to the tripartite communication topology of the EC (see Fig. 4.1b), the update step in (4.36) can be evaluated by agents locally, without the need for a coordinator. In fact, the tripartite topology of the communication layer makes the EC suitable for a distributed control approach, since convergence is reached by simple broadcasting [43].

Remark 4.4.2

A natural of choice of the Lagrange multipliers are the storage and energy prices $\hat{\varphi}_{ijh}$, $\check{\varphi}_{ijh}$, ψ_{ikh} and θ_{ijh}, since they represent the shadow prices for the usage of the flow variables in (4.24). Therefore, given $\hat{\boldsymbol{\varphi}}_{ij} = (\hat{\varphi}_{ijh})_{h \in \mathcal{H}_t}$, $\check{\boldsymbol{\varphi}}_{ij} = (\check{\varphi}_{ijh})_{h \in \mathcal{H}_t}$, $\boldsymbol{\psi}_{ik} = (\psi_{ikh})_{h \in \mathcal{H}_t}$ and $\boldsymbol{\theta}_{ij} = (\theta_{ijh})_{h \in \mathcal{H}_t}$, we define $\boldsymbol{\lambda}_n^{(\tau)}$ as:

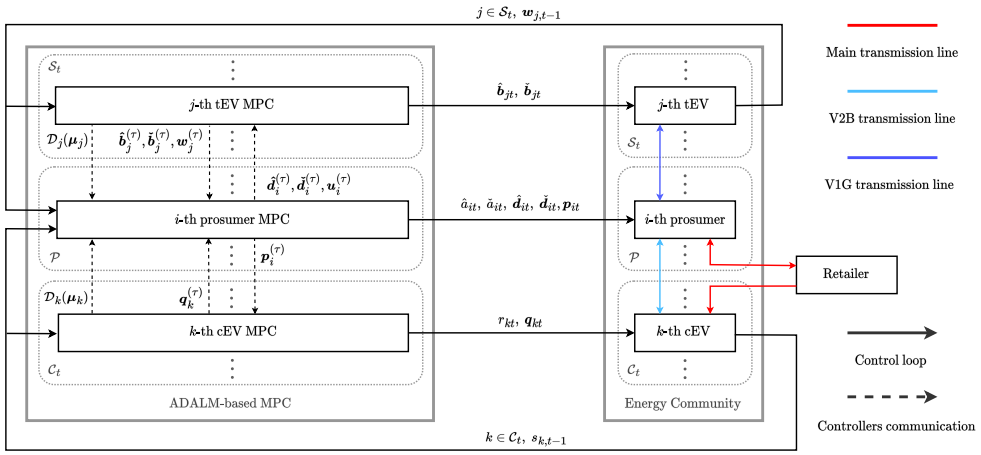

Figure 4.2: Scheme of the non-cooperative MPC controlling the EC of prosumers with CEVs and TEVs.

$$\boldsymbol{\lambda}_n^{(\tau)} := \begin{cases} \operatorname{col}\left(\boldsymbol{\psi}_{in}^{(\tau)}\right)_{i\in\mathcal{P}}, & \text{if } n \in \mathcal{C}_t \\ \begin{bmatrix} \operatorname{col}\left(\hat{\boldsymbol{\varphi}}_{in}^{(\tau)}\right)_{i\in\mathcal{P}} \\ \operatorname{col}\left(\check{\boldsymbol{\varphi}}_{in}^{(\tau)}\right)_{i\in\mathcal{P}} \\ \operatorname{col}\left(\boldsymbol{\theta}_{in}^{(\tau)}\right)_{i\in\mathcal{P}} \end{bmatrix}, & \text{if } n \in \mathcal{S}_t \\ \begin{bmatrix} \operatorname{col}\left(\hat{\boldsymbol{\varphi}}_{nj}^{(\tau)}\right)_{j\in\mathcal{S}_t} \\ \operatorname{col}\left(\check{\boldsymbol{\varphi}}_{nj}^{(\tau)}\right)_{j\in\mathcal{S}_t} \\ \operatorname{col}\left(\boldsymbol{\theta}_{nj}^{(\tau)}\right)_{j\in\mathcal{S}_t} \\ \operatorname{col}\left(\boldsymbol{\psi}_{nk}^{(\tau)}\right)_{k\in\mathcal{C}_t} \end{bmatrix}, & \text{if } n \in \mathcal{P}. \end{cases} \tag{4.37}$$

The economic interpretation of (4.37) is straightforward: each agent iteratively updates the price related to the exchanged energy, the amount of which must be agreed upon with the neighboring agents' amount. Equation (4.37) implies that part of the term $\boldsymbol{\lambda}_n^\top \mathbf{c}_n$ is contained in $J_n(\mathbf{x}_n)$, given (4.10), (4.16) and (4.22), from which we have

$$\nabla_{\mathbf{x}_n} \mathcal{L}(\mathbf{x}_n, \boldsymbol{\lambda}_n) = \nabla_{\mathbf{x}_n} J_n(\mathbf{x}_n) + \rho \nabla_{\mathbf{x}_n} \|\mathbf{c}_n\| \tag{4.38}$$

The value of $\boldsymbol{\lambda}_n^{(0)}$ depends on the service prices $\hat{\boldsymbol{\varphi}}_{ij}^{(0)}$, $\check{\boldsymbol{\varphi}}_{ij}^{(0)}$, $\boldsymbol{\theta}_{ij}^{(0)}$, $\boldsymbol{\psi}_{ik}^{(0)}$, which are used when evaluating the initial solution. A possible choice for $\boldsymbol{\lambda}_n^{(0)}$ is the following

$$\boldsymbol{\psi}_{ik}^{(0)} = \boldsymbol{\theta}_{ij}^{(0)} = \hat{\boldsymbol{\varphi}}_{ij}^{(0)} = \check{\boldsymbol{\varphi}}_{ij}^{(0)} = \mathbf{0} \tag{4.39}$$

which can be seen as an incentive for all agents to exploit the storage and recharging services. Differently, one may consider $\boldsymbol{\psi}_{ik}^{(0)} = \check{\boldsymbol{K}}$ corresponding to the price such that it is indifferent to prosumers whether to sell to CEVs or to the retailer. Similarly, setting $\boldsymbol{\theta}_{ij}^{(0)} = \check{\boldsymbol{K}}$ corresponds to the opportunity cost of losing the energy stored using TEVs capacity. Note that different choices of $\boldsymbol{\lambda}_n^{(0)}$ affect the finally reached GNE; in fact, it can be easily seen that $J_n(\mathbf{x}_n)$ is non-strictly convex, for all $n \in \mathcal{N}$, including $n \in \mathcal{S}_t$, since the Hessian of (4.16) is diagonally non-dominant. Therefore, the GNE in (4.28) is not unique (see Proposition 4.9 in [38]).

The convergence properties of Algorithm 1 are formally addressed by the following propositions.

Proposition 4.4.2

For any $\chi \in (0, 1/2)$, the sequence $\mathbf{x}_n^{(\tau)}$ converges as $\mathcal{O}(1/\epsilon)$ to an ϵ-optimal and ϵ-feasible solution $\mathbf{x}_n^*$ for all $n \in \mathcal{N}$ and $\epsilon \in \mathbb{R}_{\geq 0}$.

Proof. Coupling constraints in (4.24) can be written in the canonical form $\mathbf{A}\mathbf{x} = \mathbf{0}$, where $\mathbf{x}$ is the collective strategy vector, defined as

$$\mathbf{x} := \operatorname{col}(\mathbf{x}_n)_{n\in\mathcal{N}} = \left[\operatorname{col}(\mathbf{x}_k)_{k\in\mathcal{C}_t},\ \operatorname{col}(\mathbf{x}_j)_{j\in\mathcal{S}_t},\ \operatorname{col}(\mathbf{x}_i)_{i\in\mathcal{P}}\right] \tag{4.40}$$

and $\mathbf{A}$ is the coupling constraints matrix, defined as

$$\mathbf{A} = \begin{bmatrix} \mathbf{I}_{C_t} \otimes \mathbf{A}_{\mathcal{C}} & & \mathbf{I}_P \otimes \mathbf{A}_{\mathcal{PC}} \\ & \mathbf{I}_{S_t} \otimes \mathbf{A}_{\mathcal{S}} & \mathbf{I}_P \otimes \mathbf{A}_{\mathcal{PS}} \end{bmatrix} \tag{4.41}$$

where matrices $\mathbf{A}_{\mathcal{C}}$, $\mathbf{A}_{\mathcal{S}}$, $\mathbf{A}_{\mathcal{PC}}$, and $\mathbf{A}_{\mathcal{PS}}$ are defined as

$$\mathbf{A}_{\mathcal{S}} = -\mathbf{I}_{3PH} \tag{4.42a}$$
$$\mathbf{A}_{\mathcal{C}} = \begin{bmatrix} \mathbf{0}_{PH,H} & \mathbf{I}_{PH} \end{bmatrix} \tag{4.42b}$$
$$\mathbf{A}_{\mathcal{PC}} = \begin{bmatrix} \mathbf{0}_{C_t,2H} & -\mathbf{I}_{C_tH} & \mathbf{0}_{C_tH,3H} \end{bmatrix} \tag{4.42c}$$
$$\mathbf{A}_{\mathcal{PS}} = \begin{bmatrix} \mathbf{0}_{3S_tH,H(2+C_t)} & \mathbf{I}_{3S_tH} \end{bmatrix} \tag{4.42d}$$

The proof follows [42], and consists in proving that the ADALM scheme is convergent for $\chi \in (0, 1/\omega(\mathbf{A}))$, under the following assumptions:

(2.1) $J_n \in \mathcal{J}$ is convex and $\mathcal{X}_n(\mathbf{x}_{-n})$ is non-empty closed convex for all $n \in \mathcal{N}$;

(2.2) The duality gap associated with $\mathbf{x}_n^*$ is 0;

(2.3) All sub-problems in (4.34) are solvable at any iteration $\tau \in \mathbb{N}_{\geq 0}$.

Rows of matrix $\mathbf{A}$ are either null or with 1 and -1 as unique non-null elements. Therefore, $\omega(\mathbf{A}) = 2$. Condition (2.1) is verified following the same arguments of conditions (1.1) and (1.3) in the proof of Proposition 4.4.1. Condition (2.2) is verified since (4.10), (4.16), and (4.22) are convex and continuous. As specified in [42], condition (2.3) is satisfied if, for all $n \in \mathcal{N}$, $\mathcal{X}_n(\mathbf{x}_{-n})$ is compact, which is proved for Proposition 4.4.1. □

Apart from χ, a further term that requires to be determined is ρ. To the best of the authors' knowledge, choosing a $\boldsymbol{\lambda}_n^{(0)} \neq \mathbf{0}$ does not allow us to optimally determine ρ, as it will be shown in the following.

Proposition 4.4.3

Let $\boldsymbol{\lambda}_n^{(0)} = \mathbf{0}$, for all $n \in \mathcal{N}$. The optimal choice of regularization strength at time $t \in \mathbb{N}_{\geq 0}$, ρ^*, is evaluated as

$$\rho^* = \frac{1}{|\max(\mathbf{x})|\sqrt{2HN(PC_t + 3PS_t)}} \tag{4.43}$$

The proof is reported in Appendix A.2. Given an upper bound on the agents' sets cardinalities and parameters over time, we can set ρ^* independently of t. This is usually practically feasible, given that charging stations and parking lots have a finite capacity, the maximum transmissible power is a characterizing parameter of the grid, and battery capacity can be bounded over the commercially available PEVs. Alternatively, the regularization coefficient can be re-evaluated in a distributed fashion, when changes in the number of agents occur, by means of linear consensus mechanisms, which usually converge after a few iteration rounds.

Algorithm 5: MPC

1 **forall** $t = 1 \dots T$ **do**
2 Update PEVs' sets $\mathcal{C}_t$ and $\mathcal{S}_t$.
3 **do in parallel**
4 Each PEV $v \in \mathcal{V}_t$ broadcasts $\mathcal{D}_v(\mu_v)$ to prosumer $i \in \mathcal{P}$
5 Each agent $n \in \mathcal{N}$ initializes $\boldsymbol{\lambda}_n^{(0)}$ as in (4.39)
6 Each agent $n \in \mathcal{N}$ calculates $\mathbf{x}_n^{(0)}$ as

$$\mathbf{x}_n^{(0)} = \underset{\mathbf{x}_n \in \mathcal{K}_n}{\operatorname{argmin}} J_n(\mathbf{x}_n). \tag{4.44}$$

7 Each agent $n \in \mathcal{N}$ solves ADALM in accordance with Algorithm 1.

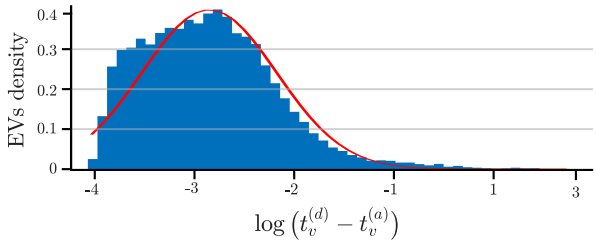

Figure 4.3: Trucated normal distribution fitting of the car parking durations on a logarithmic time scale (Southbank Boulevard - Riverside Quay crossroad) in the *On-street Car Parking Sensor Data - 2017* database

4.4.3 The MPC Algorithm

The MPC control approach is summarized in Algorithm 5, while Fig. 4.2 provides an overview of the MPC control scheme. On the one hand, the plant is constituted by the $P+S_t+C_t$ agents trading energy in the EC, i.e., the TEVs, CEVs, and prosumers belonging to $\mathcal{S}_t$, $\mathcal{C}_t$ (whose cardinality may change at each time t), and $\mathcal{P}$, respectively. On the other hand, the core of the MPC is represented by the distributed mechanism (i.e., the ADALM algorithm) solving the online optimization problem (4.27), which in turn minimizes the cost functions (4.10), (4.16), and (4.22), incorporates the individual dynamics of agents (4.23) and their coupled interactions (4.24), and aims at determining the control variables (4.8), (4.14), and (4.20). Given the large number of definitions available in the literature regarding non-centralized control systems, we refer to distributed MPC architectures following the definition reported in [44]. In particular, as highlighted in Fig. 4.2, the proposed scheme is composed of $P + S_t + C_t$ controllers, each controlling an agent in the EC and all exchanging information in accordance with the underlying communication layer (Fig. 4.1b), with the aim of achieving an agreement on the operational strategies. At each time t, the state of the PEVs' set is updated (line 2) and prosumers acquire the parking time distributions, $\mathcal{D}_v(\boldsymbol{\mu}_v)$ from the respective PEVs (line 4). Then, all agents evaluate the initial solution $\mathbf{x}_n^{(0)}$ as in (4.44), which corresponds to the optimal solution each agent could reach if constraints in (4.24) were not in place (line 8). Finally, all agents participate in the game-based energy market through ADALM, which at each time t yields the control strategies over the whole control horizon (line 9). Results are applied to all agents for a one-time step (i.e., $h = t + 1$) in a closed-loop control fashion.

4.5 Numerical Results

Numerical simulations of the proposed control framework have been carried out in Python 3.9.0. The optimization problems have been compiled through the CVXPY [45] library

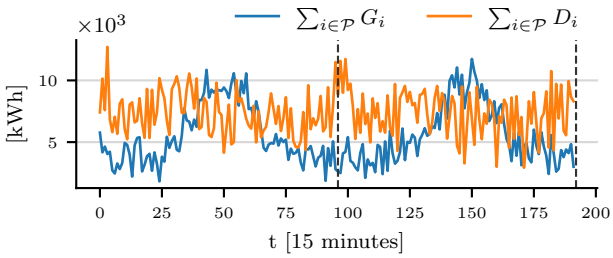

Figure 4.4: Aggregate energy demand and renewable generation for prosumers.

and computed using the numerical solver ECOS [46]. All tests have been performed on a single machine equipped with an Intel Core i5-7400 3.00 GHz (4 cores) CPU and 8 GB of memory. Data and source code are fully available [47].

4.5.1 Parameters

We consider an EC with a time-invariant number of prosumers $P = 5$ and an initial number of PEVs $C_0 = S_0 = 5$. The retailer's energy selling price, $\hat{K}_h$, corresponds to one of the billing plans offered by the Italian distribution system operator [48], which is characterized by peak and off-peak periods, i.e., $\hat{K}_h = 0.322$ € from 08:00 to 19:00 and $\hat{K}_h = 0.267$ € from 00:00 to 8:00 and from 19:00 to 23:00. Prosumers' energy demand and generation, in the considered EC, are summarized in Fig. 4.4, where lines represent the aggregate over all prosumers. Data were sampled from the yearly consumption and solar generation of an urban condominium. Each prosumer is characterized by its own energy curves, uniformly drawn from the aforementioned dataset. Moreover, its buying price corresponds to a fraction $\xi \in (0, 1]$ of the latter, i.e., $\check{K}_h = \xi \hat{K}_h$, as to exclude the taxation increment. $\hat{K}_h$ and $\check{K}_h$ are both expressed in €/kWh. The conducted experiments refer to a 2-day simulation, using a time step of 15 minutes, i.e. $t \in [1, 192]_{\mathbb{N}}$, and a control horizon of 3 hours, i.e., $H = 12$. Data regarding PEVs' battery and charging information are compliant with the specifications detailed by the *Electric Vehicle Database*, which collects 189 PEV models [9]. Particularly, the availability of technical information regarding battery capacity and charging times allows to uniformly sample $\overline{S}_k$, $\underline{S}_k$, $\overline{Z}_j$, $\underline{Z}_j$, and γ_k. For the generic v-th EV, we assume, without loss of generality, that $\mathcal{D}_v(\mu_v)$ is a truncated normal (TN) distribution [49]. Specifically, let $l_v \sim \mathcal{TN}(\mu_v, \sigma_v, 0, +\infty)$ being the parking/charging duration of the v-th EV, following a TN distribution with average μ_v, standard deviation σ_v and bounded between 0 and $+\infty$. Clearly, $l_v = t_v^{(d)} - t_v^{(a)}$, therefore $\mathbb{P}(t_v^{(d)} \geq h) = \mathbb{P}(l_v \geq h - t_v^{(a)})$, from which we have

$$\mathbb{P}(t_v^{(d)} \geq h) = \begin{cases} \dfrac{1 - \Phi\left(\frac{h - t_v^{(a)} - \mu_v}{\sigma_v}\right)}{1 - \Phi\left(\frac{\mu_v}{\sigma_v}\right)}, & \text{if } h > t \\ 1, & \text{if } h = t \end{cases} \tag{4.45}$$

where $\Phi(\cdot)$ is the normal cumulative distribution. The formulation in (4.45) is supported by the existing literature. For instance, by analyzing the parking time in [50] (office-type car park data), [18] (resulting data of a National Household Travel survey), and [51] (data from Electric Power Research Institute [52]), the best-fitting curve results to be a normal curve. In particular, Fig. 4.3 provides the results of the curve fitting for parking data in [8]. Regarding the charging and parking duration distributions, each PEV $v \in \mathcal{V}_t$ is characterized by its own parameters μ_v and σ_v, which are uniformly sampled as follows

$$\mu_k \sim U(0, \overline{\mu}_{\mathcal{C}}), \ \sigma_k \sim U(1, \overline{\sigma}_{\mathcal{C}}), \quad k \in \mathcal{C}_t \tag{4.46a}$$
$$\mu_j \sim U(0, \overline{\mu}_{\mathcal{S}}), \ \sigma_j \sim U(1, \overline{\sigma}_{\mathcal{S}}), \quad j \in \mathcal{S}_t \tag{4.46b}$$

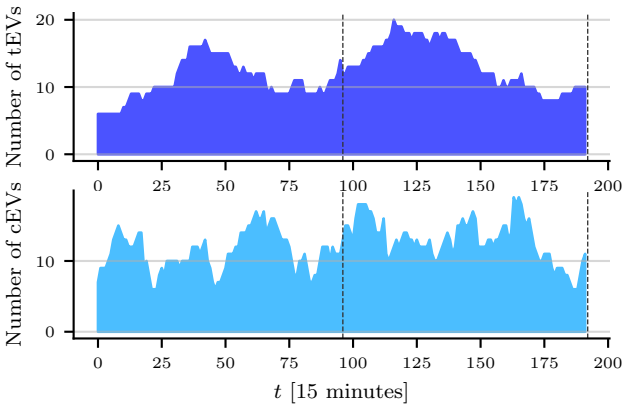

Figure 4.5: Total number of TEVs and CEVs present in the EC over time steps.

where $\overline{\mu}_{\mathcal{C}}$ and $\overline{\mu}_{\mathcal{S}}$ are the maximum average charging and parking duration, respectively, while $\overline{\sigma}_{\mathcal{C}}$ and $\overline{\sigma}_{\mathcal{S}}$ are the maximum standard deviations for charging and parking duration, respectively. Note that the minimum value for $\overline{\sigma}_{\mathcal{C}}$ and $\overline{\sigma}_{\mathcal{S}}$ is 1, in order to prevent numerical instabilities, although a zero value is virtually possible.

For simulations purposes, without loss of generality, the PEVs' arrival is modeled as a Poisson distribution, with $\beta_{\mathcal{C}}$ and $\beta_{\mathcal{S}}$ being the constant average number of newly arrived TEVs and CEVs, respectively. Without loss of generality, we consider $\beta_{\mathcal{C}} = 0.8$ and $\beta_{\mathcal{S}} = 0.4$ as constants, although one may experiment with time-dependent distribution in order to more accurately simulate the systems with respect to the local PEVs parking and charging patterns. We stress that both the arrival distribution and the charging and parking time distributions are independent of the model formulation.

4.5.2 Simulation Results and Discussion

In the following, we discuss the results yielded by MPC approach for the proposed framework, which is compared against the common EC setup, where no energy storage is provided by TEVs. The dynamics of PEVs' arrival and departure are summarized in Figs. 4.5, which represents the total number of PEVs present in the EC over time. The maximum number of PEVs simultaneously present in the EC reaches 39 on the second day. We illustrate both the energy flow dynamics and the sustained costs and revenues. We focus on the prosumers' dynamic, since they are the only agents whose numerosity remains constant throughout the simulations and they are related to both TEVs and CEVs.

Figure 4.6a collects the energy flow variables. Thicker lines represent the aggregate value of the indicated variable over all prosumers at time t, while dashed lines correspond to the future projections over the receding control horizon $\mathcal{H}_t \setminus \{t\}$. The intensity of the shade of dashed lines is proportional to its distance with respect to t, i.e., the lighter, the further away. The first plot illustrates the dynamics of the aggregate energy bought from the retailer. It can be noticed that its amount is consistent throughout the day, even during off-peak periods. This suggests that there is a strong arbitrage component in the dynamics. Contrarily, the aggregate surplus sold to the retailer, summarized in the second plot, is almost zero for the entirety of the simulations. In fact, the surplus is almost totally stored, using the capacity provided by TEVs, or sold to CEVs for recharging. The third plot represents the aggregate energy stored in the batteries of TEVs. At the beginning of the simulation, the initial storage is null for all prosumers. After the initial buildup, the trend seems to synchronize with the peak/off-peak period, so that the charging amount corresponds to a combination of the prosumers' autonomous generation surplus and energy bought from the retailer as a result of arbitrage. Lastly, the fourth plot represents the aggregate amount of energy prosumers sold to CEVs, which are the preferred buyers,

(a) Aggregate energy flow dynamics of the EC with TEVs' buffering service.

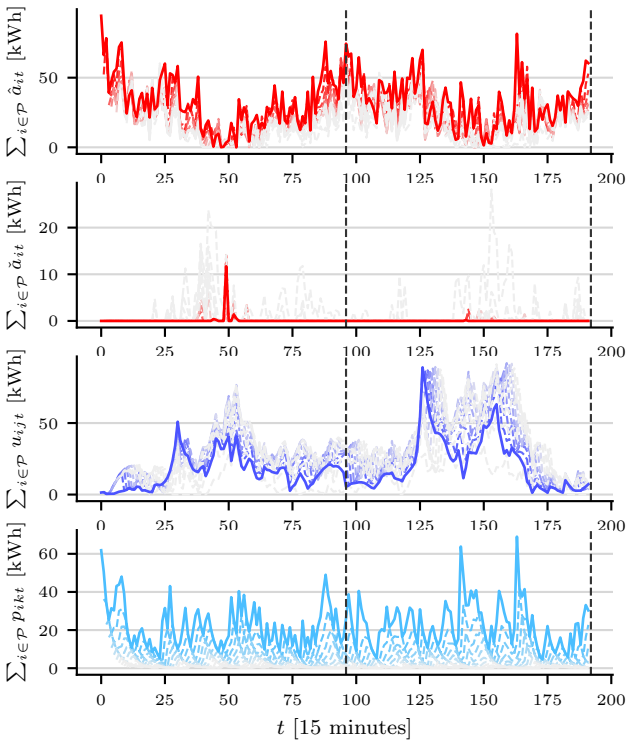

(b) Aggregate energy flow dynamics of the EC with no TEVs' buffering service.

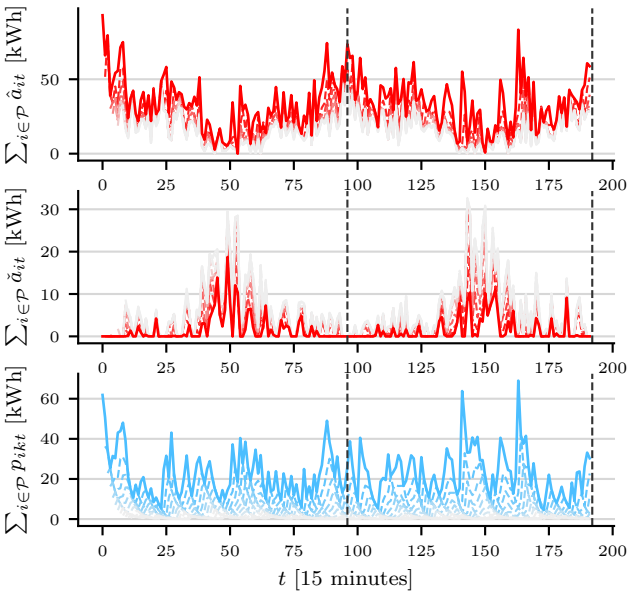

Figure 4.6: MPC results in terms of prosumers' aggregate energy profiles. Thicker lines represent the actual aggregate energy flow at time t, while dotted lines indicate the future projections over $\mathcal{H}_t \setminus \{t\}$.

with respect to the retailer. Figure 4.7b illustrates the energy flow dynamics of the EC – including energy generation, demand, arrival time, and departing probabilities – but without the availability of TEVs. Clearly, the graph plotting $\check{a}_{it}$ reports a more

(a) Aggregate prosumers' costs and revenues with TEVs' buffering service usage.

(b) Aggregate prosumers' costs and revenues with no TEVs' buffering service usage.

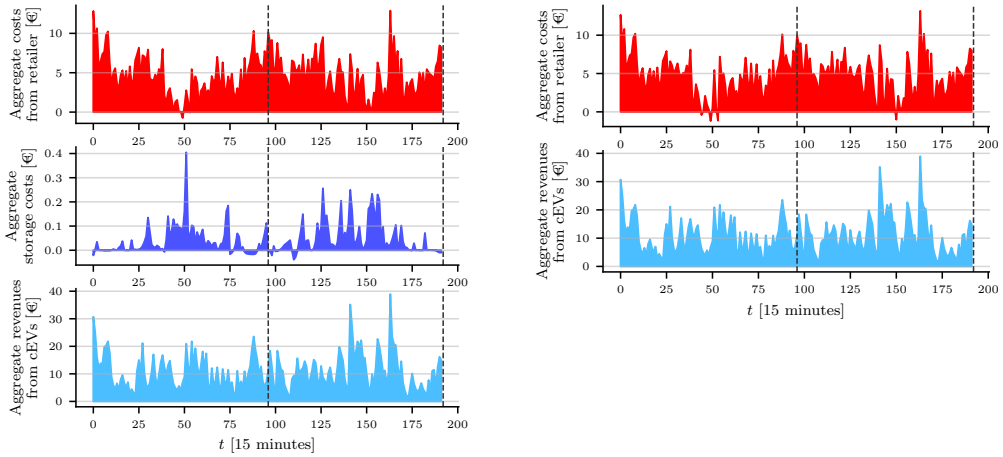

Figure 4.7: Prosumers' aggregate economic performance: each curve represents a cost/revenue component at t, i.e., the difference between costs and revenues from energy exchanges.

intensive energy buying from the retailer, due to the absence of storage where energy could be stored during off-peak periods. Arbitrage is still strong since energy output from prosumers towards CEVs is still consistent.

Figure 4.7a reports the aggregate economic dynamics of the prosumers, where the first graph represents the net difference between the costs and revenues coming from energy bought from and sold to the retailer. Its trend is a direct consequence of the arbitrage discussed for the related graphs in Fig. 4.6a. The second plot represents the aggregate storage costs. It can be noticed that, for some t, the cost becomes negative, i.e., it becomes revenue. This corresponds to the refund obtained from a TEV which left the parking lot with part of the prosumer stored energy. Lastly, the third graph illustrates the revenues resulting from selling energy to CEVs. Similarly to Fig. 4.6b, Fig. 4.7b reports the aggregate costs and revenues sustained by prosumers when no buffering service is provided by TEVs. Since the impact of storage costs is limited with respect to the revenues from CEVs and retailers' net costs, the overall economic dynamic looks equivalent to the one in Fig. 4.7a. This suggests that the absence of TEVs in the community is not disruptive with respect to the overall economic performance: their addition results in a win-win scenario where prosumers gain a further energy trading option and TEVs become able to gain a, albeit low, passive income. Given a prosumer $i \in \mathcal{P}$, its self-supply (SS_i) measures how much of the generated energy is used for self-consumption, while its energy-independence (EI_i) measures how well it can independently satisfy its own demand. They are calculated as follows:

$$\forall i \in \mathcal{P} : \begin{cases} \mathrm{SS}_i = 1 - \dfrac{\sum_{t\in[1,T]} \check{a}_{it}}{\sum_{t\in[1,T]} G_{it}} \\ \mathrm{EI}_i = 1 - \dfrac{\sum_{t\in[1,T]} \hat{a}_{it}}{\sum_{t\in[1,T]} D_{it}} \end{cases} \tag{4.47}$$

Table 4.2 reports the aforementioned indices for the community of prosumers with and without buffering service provided by TEVs: it can be noticed how integrating the latter improves both the self-sufficiency and energy-independence of the EC.

Finally, Fig. 4.8 reports the residuals of the coupling constraints in (4.24). In particular, the reported results regard the simulation time as having the highest number of PEVs participating in the market. In order to avoid prolonged loops, the maximum number of ADALM iterations has been capped at 30. However, despite the limited number of iterations, ADALM yields a good performance with the final residual values standing

Table 4.2: Comparison of prosumers performance in the proposed framework with and without TEVs

With TEVs energy buffer					
i	1	2	3	4	5
EI_i	17.50%	15.90%	17.60%	17.60%	4.60%
SS_i	99.10%	100.0%	100.0%	99.60%	100.0%
Without TEVs energy buffer					
i	1	2	3	4	5
EI_i	11.90%	13.50%	17.00%	12.10%	2.20%
SS_i	91.50%	95.60%	98.10%	91.90%	95.50%

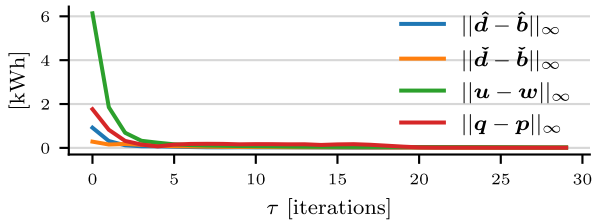

Figure 4.8: Convergence of Algorithm 1 in terms of residuals of the coupling constraints in (4.24) for the ADALM instance having the highest number of PEVs.

less than 1e-3. Moreover, the computational runtime on the aforementioned hardware for solving the MPC online optimization at each iteration $t \in \mathbb{N}_{\geq 0}$ ranges from 1 to 2 seconds.

4.6 Conclusions

In this work, we have presented a non-cooperative distributed control framework, where an energy community provides recharging services to PEVs, while exploiting the energy storage capabilities of long-term parked non-resident PEVs. We have defined a rolling horizon control strategy based on a quadratic optimization model, that is solved in a distributed fashion leveraging on the accelerated distributed augmented Lagrangian method. We have proved the convergence properties of such a method in the considered setting. The effectiveness of the proposed control strategy has been shown through numerical experiments based on real datasets.

Future work will focus on extending the architecture to different communication and energy-sharing settings, as well as ensuring the correct operation of the control framework in case of untrustworthy PEVs, which may communicate biased parking distribution parameters in order to increase their own profit. Finally, extending the framework to coalitional games will be explored, in order to assess the feasibility and utility of enforcing the cooperative behavior of involved agents.

References

[1] Shoup, D. C., *The high cost of free parking*. Routledge, 2021.

[2] Gallagher, J. and Lago, C., "How parked cars affect pollutant dispersion at street level in an urban street canyon? a cfd modelling exercise assessing geometrical detailing and pollutant decay rates," *Science of the Total Environment*, vol. 651, pp. 2410–2418, 2019.

[3] Kåberger, T., "Progress of renewable electricity replacing fossil fuels," *Global Energy Interconnection*, vol. 1, no. 1, pp. 48–52, 2018.

[4] Østergaard, P. A., Duic, N., Noorollahi, Y., and Kalogirou, S. A., *Recent advances in renewable energy technology for the energy transition*, 2021.

[5] Lo, C.-H. and Ansari, N., "Decentralized controls and communications for autonomous distribution networks in smart grid," *IEEE transactions on smart grid*, vol. 4, no. 1, pp. 66–77, 2012.

[6] Chen, S., Hu, J., Shi, Y., *et al.*, "Vehicle-to-everything (v2x) services supported by lte-based systems and 5g," *IEEE Communications Standards Magazine*, vol. 1, no. 2, pp. 70–76, 2017.

[7] Kalathil, D., Wu, C., Poolla, K., and Varaiya, P., "The sharing economy for the smart grid," *arXiv preprint arXiv:1608.06990*, 2016.

[8] Melbourne - Open Data Portal, C. of. "On-street car parking sensor data - 2017." (), [Online]. Available: https://data.melbourne.vic.gov.au/Transport/On-street-Car-Parking-Sensor-Data-2017/u9sa-j86i. (accessed: 22.01.2022).

[9] "Electric vehicles database." ((Accessed: 21.01.2022)), [Online]. Available: https://ev-database.org/.

[10] Ma, Y., Zhang, B., Zhou, X., *et al.*, "An overview on v2g strategies to impacts from ev integration into power system," in *2016 Chinese Control and Decision Conference (CCDC)*, IEEE, 2016, pp. 2895–2900.

[11] Alsharif, A., Tan, C. W., Ayop, R., Dobi, A., and Lau, K. Y., "A comprehensive review of energy management strategy in vehicle-to-grid technology integrated with renewable energy sources," *Sustainable Energy Technologies and Assessments*, vol. 47, p. 101 439, 2021.

[12] Khalid, M. R., Khan, I. A., Hameed, S., Asghar, M. J., and Ro, J.-S., "A comprehensive review on structural topologies, power levels, energy storage systems, and standards for electric vehicle charging stations and their impacts on grid," *IEEE Access*, 2021.

[13] Hutty, T. D., Pena-Bello, A., Dong, S., Parra, D., Rothman, R., and Brown, S., "Peer-to-peer electricity trading as an enabler of increased pv and ev ownership," *Energy Conversion and Management*, vol. 245, p. 114 634, 2021.

[14] Ghotge, R., Wijk, A. van, and Lukszo, Z., "Off-grid solar charging of electric vehicles at long-term parking locations," *Energy*, vol. 227, p. 120 356, 2021.

[15] Tushar, M. H. K., Zeineddine, A. W., and Assi, C., "Demand-side management by regulating charging and discharging of the ev, ess, and utilizing renewable energy," *IEEE Transactions on Industrial Informatics*, vol. 14, no. 1, pp. 117–126, 2017.

[16] Chen, X. and Leung, K.-C., "Non-cooperative and cooperative optimization of scheduling with vehicle-to-grid regulation services," *IEEE Transactions on Vehicular Technology*, vol. 69, no. 1, pp. 114–130, 2019.

[17] Fele, F. and Margellos, K., "Scenario-based robust scheduling for electric vehicle charging games," in *2019 IEEE International Conference on Environment and Electrical Engineering and 2019 IEEE Industrial and Commercial Power Systems Europe (EEEIC/I&CPS Europe)*, IEEE, 2019, pp. 1–6.

[18] Fijani, R. F., Azimian, B., Ghotbi, E., and Wang, X., "Game theory approach on modeling of residential electricity market by considering the uncertainty due to the battery electric vehicles (bevs)," *arXiv preprint arXiv:1902.05028*, 2019.

[19] Mendoza, F. G., Baldivieso-Monasterios, P. R., Bauso, D., and Konstantopoulos, G., "Demand-side management in a micro-grid with multiple retailers: A coalitional game approach," in *2021 European Control Conference (ECC)*, IEEE, 2021, pp. 347–352.

[20] Bagagiolo, F. and Bauso, D., "Mean-field games and dynamic demand management in power grids," *Dynamic Games and Applications*, vol. 4, pp. 155–176, 2014.

[21] Shi, Y., Tuan, H. D., Savkin, A. V., Duong, T. Q., and Poor, H. V., "Model predictive control for smart grids with multiple electric-vehicle charging stations," *IEEE Transactions on Smart Grid*, vol. 10, no. 2, pp. 2127–2136, 2018.

[22] Iacobucci, R. and Bruno, R., "Cascaded model predictive control for shared autonomous electric vehicles systems with v2g capabilities," in *2019 IEEE International Conference on Communications, Control, and Computing Technologies for Smart Grids (SmartGridComm)*, IEEE, 2019, pp. 1–7.

[23] Hu, J., Ye, C., Ding, Y., Tang, J., and Liu, S., "A distributed mpc to exploit reactive power v2g for real-time voltage regulation in distribution networks," *IEEE Transactions on Smart Grid*, vol. 13, no. 1, pp. 576–588, 2021.

[24] Zhao, Z., Guo, J., Lai, C. S., Xiao, H., Zhou, K., and Lai, L. L., "Distributed model predictive control strategy for islands multimicrogrids based on noncooperative game," *IEEE Transactions on Industrial Informatics*, vol. 17, no. 6, pp. 3803–3814, 2020.

[25] Stephens, E. R., Smith, D. B., and Mahanti, A., "Game theoretic model predictive control for distributed energy demand-side management," *IEEE Transactions on Smart Grid*, vol. 6, no. 3, pp. 1394–1402, 2014.

[26] Karimi, A. and Haeri, M., "Game theory meets distributed model predictive control in vehicle-to-grid systems," in *2019 11th International Conference on Electrical and Electronics Engineering (ELECO)*, IEEE, 2019, pp. 764–768.

[27] Hosseini, S. M., Carli, R., Parisio, A., and Dotoli, M., "Robust decentralized charge control of electric vehicles under uncertainty on inelastic demand and energy pricing," in *2020 IEEE International Conference on Systems, Man, and Cybernetics (SMC)*, IEEE, 2020, pp. 1834–1839.

[28] Dominguez-Navarro, J., Dufo-Lopez, R., Yusta-Loyo, J., Artal-Sevil, J., and Bernal-Agustin, J., "Design of an electric vehicle fast-charging station with integration of renewable energy and storage systems," *International Journal of Electrical Power & Energy Systems*, vol. 105, pp. 46–58, 2019.

[29] Zhang, J., Che, L., Wang, L., and K Madawala, U., "Game-theory based v2g coordination strategy for providing ramping flexibility in power systems," *Energies*, vol. 13, no. 19, p. 5008, 2020.

[30] Chung, Y.-W., Khaki, B., Chu, C., and Gadh, R., "Electric vehicle user behavior prediction using hybrid kernel density estimator," in *2018 IEEE International Conference on Probabilistic Methods Applied to Power Systems (PMAPS)*, IEEE, 2018, pp. 1–6.

[31] Sikeridis, D., Bidram, A., Devetsikiotis, M., and Reno, M. J., "A blockchain-based mechanism for secure data exchange in smart grid protection systems," in *2020 IEEE 17th Annual Consumer Communications & Networking Conference (CCNC)*, IEEE, 2020, pp. 1–6.

[32] Methekar, R., Ramadesigan, V., Braatz, R. D., and Subramanian, V. R., "Optimum charging profile for lithium-ion batteries to maximize energy storage and utilization," *ECS Transactions*, vol. 25, no. 35, p. 139, 2010.

[33] Shen, Z., Wei, W., Wu, D., Ding, T., and Mei, S., "Modeling arbitrage of an energy storage unit without binary variables," *CSEE Journal of Power and Energy Systems*, vol. 7, no. 1, pp. 156–161, 2020.

[34] Romero, A., Goldar, A., Couto, L. D., Garone, E., and Maestre, J. M., "Fast charge of li-ion batteries using a two-layer distributed mpc with electro-chemical and thermal constraints," in *2019 18th European Control Conference (ECC)*, IEEE, 2019, pp. 1796–1803.

[35] Fortenbacher, P., Mathieu, J. L., and Andersson, G., "Modeling, identification, and optimal control of batteries for power system applications," in *2014 Power Systems Computation Conference*, IEEE, 2014, pp. 1–7.

[36] Scarabaggio, P., Carli, R., and Dotoli, M., "A game-theoretic control approach for the optimal energy storage under power flow constraints in distribution networks," in *2020 IEEE 16th International Conference on Automation Science and Engineering (CASE)*, IEEE, 2020, pp. 1281–1286.

[37] Heirung, T. A. N., Paulson, J. A., O'Leary, J., and Mesbah, A., "Stochastic model predictive control—how does it work?" *Computers & Chemical Engineering*, vol. 114, pp. 158–170, 2018.

[38] Facchinei, F. and Kanzow, C., "Generalized Nash equilibrium problems," *Annals of Operations Research*, vol. 175, no. 1, pp. 177–211, 2010.

[39] Facchinei, F., Fischer, A., and Piccialli, V., "On generalized nash games and variational inequalities," *Operations Research Letters*, vol. 35, no. 2, pp. 159–164, 2007.

[40] Horn, R., Horn, R., and Johnson, C., *Topics in Matrix Analysis*. Cambridge University Press, 1994. [Online]. Available: https://books.google.it/books?id=LeuNXB2bl5EC.

[41] Grünbaum, B., Klee, V., Perles, M. A., and Shephard, G. C., *Convex polytopes*. Springer, 1967, vol. 16.

[42] Chatzipanagiotis, N., Dentcheva, D., and Zavlanos, M. M., "An augmented lagrangian method for distributed optimization," *Mathematical Programming*, vol. 152, no. 1, pp. 405–434, 2015.

[43] Hu, J. and Zheng, W. X., "Bipartite consensus for multi-agent systems on directed signed networks," in *52nd IEEE Conference on Decision and Control*, IEEE, 2013, pp. 3451–3456.

[44] Scattolini, R., "Architectures for distributed and hierarchical model predictive control–a review," *Journal of process control*, vol. 19, no. 5, pp. 723–731, 2009.

[45] Diamond, S. and Boyd, S., "CVXPY: A Python-embedded modeling language for convex optimization," *Journal of Machine Learning Research*, vol. 17, no. 83, pp. 1–5, 2016.

[46] Domahidi, A., Chu, E., and Boyd, S., "ECOS: An SOCP solver for embedded systems," in *European Control Conference (ECC)*, 2013, pp. 3071–3076.

[47] Mignoni, N. "Data and source code." GitHub repository, accessed 30/03/2022. (2022).

[48] Enel, *E-light bioraria*, Accessed: 2021-23-05. [Online]. Available: https://www.enel.it/it/luce-e-gas/luce/offerte/e-light-bioraria.

[49] Burkardt, J., "The truncated normal distribution," *Department of Scientific Computing Website, Florida State University*, pp. 1–35, 2014.

[50] He, T., Zhu, J., Zhang, J., and Zheng, L., "An optimal charging/discharging strategy for smart electrical car parks," *Chinese Journal of Electrical Engineering*, vol. 4, no. 2, pp. 28–35, 2018.

[51] Cao, Y. and Wang, Y., "Robust charging schedule for autonomous electric vehicles with uncertain covariates," *IEEE Access*, vol. 9, pp. 161 565–161 575, 2021.

[52] EPRI. "Transportation electrication: A technology overview." (), [Online]. Available: https://www.epri.com/research/products/000000000001021334. (accessed: 22.01.2022).

Chapter 5

Real-Time Power Allocation for Plug-in Electric Vehicles via Event-Triggered Evolutionary Dynamics

V

Abstract

Motivated by evolutionary game theory and evolutionary dynamics models (EDMs), in this paper, we devise an event-triggered EDM-based control strategy for real-time power allocation in the charging coordination of a fleet of plug-in electric vehicles (PEVs). Based on the hybrid Lyapunov stability theory, we deduce sufficient conditions to guarantee the asymptotic stability of the closed-loop system comprised of our proposed controller and the (unknown and nonlinear) dynamics of the PEVs' batteries. Furthermore, the dynamical power allocation is guaranteed to satisfy the operational constraints of the system at all times, which include the limited power availability of the ER that feeds the fleet of PEVs. The event-triggered configuration of the controller allows us to model triggering events such as PEVs' arrivals, departures, and charging completion, while the EDM-based setup guarantees that the allocation process achieves a Nash equilibrium among the PEVs, i.e., a self-enforceable agreement where no PEV can benefit by unilaterally deviating from it. The effectiveness of the proposed approach is illustrated through a numerical case study considering multiple PEVs under random arrivals, departures, and power requirements.

Contents

5.1 Introduction

Approximately 20% of the world carbon emissions can be attributed to automobiles powered by internal combustion engines [1]. Specifically, 75% of the total amount of transportation emissions are generated by road vehicles. Although their impact is not as severe as the energy production sector, which accounts for 73% [2] of the global greenhouse gas emission, they constitute a non-negligible environmental concern, especially for densely populated urban areas [3]. A non-disruptive solution is provided by plug-in electric vehicles (PEVs), whose employment reduces the overall footprint left by the transport sector, without compromising road mobility. The increasing number of PEVs populating roads calls for effective procedures to guarantee efficient charging coordination. Being electric devices, in fact, PEVs actively participate in the energy market, constituting non-fixed loads that need to be handled accordingly by the distribution system operators. The task of smoothly merging PEVs' charging activities with the preexisting power grid's operations is, however, far from trivial [4]. Distributed and intermittent loads tend to disrupt the nominal working scheduling of the grid, although their unpredictability can be mitigated

when the degree of PEVs' adoption stabilizes the periodicity of peak periods [5]. Efforts have been made in this direction, with the aim of forecasting the PEVs' charging windows by, e.g., predicting PEVs' departure [6], or users' demographic [7], possibly through the use of machine-learning-based methods [8]. Apart from the infrastructural perspective, coordinating the recharging process of a fleet of PEVs should keep into consideration the agents' selfish behavior, arising from the need to share a limited resource, i.e., the grid output [9]. Indeed, the energy market is well-modeled by frameworks that keep into consideration antagonistic and/or coalitional behaviors of agents. Namely, given that the electrical energy supply is a limited resource, together with the fact that the demand signal is hardly constant, including non-cooperative and cooperative actions turns out to be a convenient feature in the design of control approaches for smart grids [10], [11]. The core idea of game theory revolves around the concept of equilibrium, where the most common is the one formulated by Nash [12], i.e., a state where no agent has incentives to unilaterally deviate from their selected strategy.

Within the branches of game theory, a particularly relevant one for energy systems is evolutionary game theory (EGT) [13], [14]. The EGT framework models large populations of decision-making agents with bounded rationality levels, and the resulting evolutionary dynamics models (EDMs) [15] have certain invariance and stability properties that render them attractive for dynamical resource allocation applications [16], including the power allocation for PEVs [17], [18].

5.1.1 Related Works

EGT has been recently used to model the interactions between competing companies and policymakers in the realm of traditional energy production systems [19], [20], including the design of incentives to reduce greenhouse gas generation [21], [22]. The penetration of PEVs in the transportation sector is, in fact, often incentivized with the aim of reducing the environmental impact of fuel-based vehicles. Regarding PEVs penetration, the authors in [23] use EGT to model the partnerships among investors, hydrogen-powered vehicle users, and solar power plants. A similar tripartite structure is analyzed in [24], where authors focus on influential factors of PEV development resulting from the interplay of enterprises, users, and governments. Proper integration of PEVs in the urban environment also requires the deployment of necessary infrastructure, such as charging stations (CSs). Authors in [25] analyze this aspect under the lens of EGT by balancing subsidy and tax policies while considering the consumers' mobility preferences.

While the aforementioned works apply evolutionary game theoretical frameworks to tackle managerial and organizational problems, EGT has also been employed to address issues at the operational level. Specifically, in the context of PEVs charging coordination, EGT has been used in [26] for navigating PEVs to CSs, with the aim of better integrating the power grid with the electric transport network. After arriving at a CS, the plugged PEV constitutes a temporary load for the network grid. In fact, the problem of power allocation for PEVs has been recently studied from various perspectives, even beyond evolutionary game theoretical ones. A popular approach employs a receding-horizon high-level optimization perspective, where the time horizon is split into multiple time slots, and optimization-based methods are used to compute the power to be charged by each PEV during each time slot. Some recent examples of such a perspective are [27]–[29], where the authors formulate multi-stage optimization schemes to compute the power profiles of the PEVs while satisfying the operational constraints of the system. One caveat of such a framework, however, is that the computed power profile is applied in open loop during each time slot, and it is only recomputed at the beginning of the next time slot. Thus, the system cannot deal with real-time disturbances regarding random arrivals or departures of PEVs as well as unmodeled dynamics on the PEVs' batteries. To cope with such an issue, the authors in [17] formulate some continuous-time EGT-based dynamics for the real-time charging coordination of PEVs under feeder capacity constraints, which allows the system to operate in real-time while still guaranteeing the satisfaction of the operational constraints. Nonetheless, the closed-loop feedback interconnection between

the PEVs and the CSs is not considered in the analysis. In contrast, the authors in [30] devise a charging coordination algorithm based on mean-field games, which indeed includes the battery dynamics of the PEVs, yet they are assumed to be linear and fully modeled, without considering system-level operational constraints. In contrast to the aforementioned previous works, the control method formulated in this Chapter i) can respond in real-time to disturbances regarding arrivals and departures of PEVs; ii) satisfies the operational constraints of the system at all times (including the coupled constraint on the limited power availability of the retailer); and iii) is model-free as regards unmodeled nonlinear dynamics for the PEVs' batteries. Different from the receding-horizon methods in [27]–[29], our proposed approach only computes the power allocation for the current time instant. Nonetheless, the proposed framework offers a potential low-level control strategy that could be integrated into the aforementioned multi-stage methods, exploiting the advantages of both perspectives.

5.1.2 Contributions

Motivated by the EGT framework and the invariance and stability properties of EDMs, in this Chapter we devise a novel hybrid (event-triggered) control system [31], based on population dynamics [13], for the dynamic power allocation in a fleet of PEVs fed by a single ER with limited power availability. As the main technical contribution, we show that, under realistic assumptions, the proposed controller satisfies the system's operational constraints at all times, and the closed-loop interconnection between the controller and the (unknown and nonlinear) dynamics of the PEVs' batteries reaches a stable equilibrium point where all connected PEVs are fully charged. As such, the proposed method comprises a model-free real-time control strategy for the dynamic power allocation in the charging coordination of PEVs. Moreover, the power allocation is based on so-called precedence functions, which allow for expressing economic and performance indicators of the PEVs, e.g., state of charge, battery degradation and power-related costs, and the devised strategy seeks to achieve a NE for the power allocation among the PEVs, i.e., a power allocation where no PEV can benefit by unilaterally deviating from it. In fact, the proposed methodology allows PEVs to maintain non-transactive relationships, i.e., they communicate with each other in order to increase (reduce) their power demands, with the aim of speeding up (slowing down) their charging processes, on the basis of the designed incentives. This fact allows the ER to allocate power by exploiting local PEV information, avoiding the infrastructural cost and the resulting high complexity of a full-fledged vehicle-to-vehicle setup. Furthermore, the presented hybrid system configuration allows us to model triggering events, e.g., PEVs' arrivals, departures, and charging completion, which increases the practical expressiveness of the proposed method. As such, the effectiveness of the designed controller is illustrated through a numerical case study considering a fleet of PEVs under random arrivals, departures, and power requirements.

The remainder of this Chapter, is organized as follows. Section 5.2 provides some preliminaries on hybrid systems and EDMs. Section 5.3 describes the considered setup and formally defines the problem to be faced. Section 5.4 presents our proposed solution. Section 5.5 depicts a numerical case study that illustrates the effectiveness of the proposed method. Finally, Section 5.6 concludes the Chapter. The technical results are proven in the Appendix.

5.1.3 Literature Review

EGT has found several applications in the context of energy systems at large, as it emerges from the review work in [14]. The subset of works preserving the conceptual baseline of EGT is the one where the latter is used to model the interactions between stakeholders and policymakers in the realm of traditional energy production systems. This extends to capturing the often discordant relationships between competing energy companies [19], and coal enterprises with regulatory authorities, either at the governmental [32] or private

[20] level. Perhaps the most studied cause of idiosyncratic behavior among energy market participants regards the limitations imposed by carbon emission policies, aimed at toning down the effect of climate change [33]. Examples of works addressing this issue have been considering incentive mechanisms for containing greenhouse gas generation [21], and enterprise and supervision organizations relationships [22]. The penetration of PEV in the transportation sector is, in fact, often incentivized to reduce the environmental impact of fuel-based vehicles. However, this introduces the need to balance the prerogatives of several grid actors. EGT provides a possible conceptual road: in [23] authors use them to model partnerships among investors, hydrogen-powered vehicle users, and solar power plants. A similar tripartite structure is analyzed in [24], where authors focus on influential factors of PEV development resulting from the interplay of enterprises, users, and governments. Proper integration of PEVs in the urban environment also requires the deployment of necessary infrastructure, such as charging stations (CSs). Authors in [25] analyze this aspect under the lens of EGT by balancing subsidy and tax policies while considering the consumers' mobility preferences.

The aforementioned works use evolutionary game frameworks to tackle managerial and organizational problems, although they have also been employed to address issues on the operational level. Specifically, in the context of PEVs charging coordination, EGT has been used in [26] for navigating PEVs to CSs, with the aim of better integrating the power grid with the electric transport network. After arriving at a CS, the plugged PEV constitutes a temporary load for the network grid. Coordinating the simultaneous charging of a fleet of PEVs can be performed by employing EGT as proposed in [17], where continuous-time primal-dual gradient dynamics achieve real-time control of the charging of multiple PEVs under feeder capacity constraints. Differently from [17], we extend the system model in order to consider the PEVs' (unknown) battery dynamics, as well as operational conditions, e.g., the arrival and departure of a vehicle.

5.1.4 Chapter Contributions

In this Chapter, we study an EGT-based approach for the real-time CSs' power scheduling of a PEVs charging lot, which is served by an ER with fixed power availability. Differently from [17], we extend the system model in order to consider the PEVs' (unknown) battery dynamics, as well as operational conditions, e.g., the arrival and departure of a vehicle. As such, we employ the framework of hybrid dynamical systems [31] to devise event-triggered EGT-based dynamics for the charging coordination of a fleet of PEVs. In fact, the flow dynamic of the proposed hybrid system expresses the strategic revision protocol that PEVs use to update their charging power, while the jump dynamic allows for capturing event-based triggers, which increases the practical expressiveness of the proposed method. Moreover, the proposed coordination mechanism is based on so-called precedence functions, which allow for expressing arbitrary economic and performance indicators of the PEVs, e.g., battery degradation and aggregate power costs. In fact, the proposed methodology lets PEVs maintain non-transactive relationships, i.e., they communicate with each other in order to lower (increase) their power absorption, with the aim of speeding up (slowing down) others' charging process, on the basis of the designed incentives. This allows the ER to allocate power by exploiting local PEV information, avoiding the infrastructural cost and resulting complexity of a full-fledged vehicle-to-vehicle setup. Finally, the proposed approach is well-suited for distributed coalitional architectures, due to the locality of the required computations and limited data sharing.

5.2 Preliminaries

Notation: $\mathbb{R}$, $\mathbb{R}_{\geq 0}$, and $\mathbb{R}_{>0}$ are the sets of real, non-negative real, and positive real numbers, respectively. $\mathbb{B} := \{0, 1\}$ and when used in logical expressions, $\mathbb{B}$ overloads boolean values. We use a standard font for scalars, a bold font for vectors and matrices, and a calligraphic font for sets. All vectors are taken as columns by default and the operator

$\text{col}(\cdot)$ creates a column vector of its arguments. Given a vector $\mathbf{z} \in \mathbb{R}^m$, we let z_i denote its i-th element, and $\text{supp}(\mathbf{z}) = \{i \in \{1, 2, \ldots, m\} : z_i > 0\}$ denote its support. Also, let $\text{avg}\{\mathbf{z}\} := \mathbf{1}^\top \mathbf{z}/m$ be the average for the elements of $\mathbf{z}$ and let $\text{std}\{\mathbf{z}\} := \|\mathbf{z} - \text{avg}\{\mathbf{z}\}\|$ be their standard deviation. We let $t \in \mathbb{R}_{\geq 0}$ indicate the continuous-time index and, given a time-varying variable $z_i(t)$, we drop the time index when time is irrelevant, i.e., z_i. Given any $z \in \mathbb{R}$, we let $[z]_+ := \max\{0, z\}$. Given a logical proposition P, $\mathbb{1}(\cdot) \mapsto \mathbb{B}$ is an indicator function such that $\mathbb{1}(P) = 1$ if P is true and $\mathbb{1}(P) = 0$ otherwise.

5.2.1 Hybrid dynamical systems

A hybrid dynamical system (HDS) [31] is comprised both of continuous-time and discrete-time dynamics that rule the temporal evolution of its state. Namely, let $\mathbf{x}(t) \in \mathcal{X} \subseteq \mathbb{R}^n$, $\mathbf{u}(t) \in \mathcal{U} \subseteq \mathbb{R}^m$, and $\mathbf{y}(t) \in \mathcal{Y} \subseteq \mathbb{R}^o$, denote the state, input, and output vectors of the system at time $t \geq 0$, respectively. Here, $\mathcal{X}$, $\mathcal{U}$, and $\mathcal{Y}$ denote the state, input, and output spaces of the system, respectively. For the purposes of this paper, an HDS is characterized by a flow set $\mathcal{F} \subseteq \mathcal{X} \times \mathcal{U}$, a (single-valued) flow map $\mathbf{F} : \mathcal{X} \times \mathcal{U} \to \mathbb{R}^n$, a jump set $\mathcal{J} \subset \mathcal{F}$, and a (set-valued) jump map $\mathbf{J} : \mathcal{X} \times \mathcal{U} \rightrightarrows \mathcal{X}$. The temporal evolution of a hybrid system is as follows. If the state and input pair are in the flow set at time t, i.e., $(\mathbf{x}(t), \mathbf{u}(t)) \in \mathcal{F}$, then the system is allowed to *flow* (evolve) following the continuous-time dynamics given by $\dot{\mathbf{x}}(t) = \mathbf{F}(\mathbf{x}(t), \mathbf{u}(t))$. On the other hand, if the state and input pair are within the jump set at time t, i.e., $(\mathbf{x}(t), \mathbf{u}(t)) \in \mathcal{J}$, then an instantaneous *jump* (update) of the state is produced at time t. Such an instantaneous update is denoted by $\mathbf{x}^+(t) \in \mathbf{J}(\mathbf{x}(t), \mathbf{u}(t))$. Thus, HDSs might exhibit discontinuous trajectories of the state. A particularly important application of HDSs is in the context of event-triggered control [34], where the state/control variables of the system are updated only at the occurrence of a given event. As such, the formalism of HDSs is useful to consider logical constraints to rule the evolution of the state.

Definition 5.2.1 (*Well-posed HDS*)

In this paper, a HDS is said to be well-posed if it satisfies the following conditions:

i) *$\mathcal{F}$ and $\mathcal{J} \subset \mathcal{F}$ are compact subsets of $\mathcal{X} \times \mathcal{U}$.*

ii) *The single-valued map $\mathbf{F}(\cdot, \cdot)$ is Lipschitz continuous.*

iii) *The set-valued map $\mathbf{J}(\cdot, \cdot)$ is outer semicontinuous and locally bounded relative to $\mathcal{J}$.*

iv) *The flow set $\mathcal{F}$ is positively invariant under the dynamics of the HDS, i.e., the input space $\mathcal{U}$ and the flow and jump maps $\mathbf{F}(\cdot, \cdot)$ and $\mathbf{J}(\cdot, \cdot)$ guarantee that $(\mathbf{x}(t), \mathbf{u}(t)) \in \mathcal{F}$, for all $t \geq 0$.*

v) *The total number of jumps that occur over any finite window of time is finite, i.e., the HDS is free from Zeno behavior.*

Based on [35, Proposition 2.3.4], if the HDS is well-posed, then given a constant input $\mathbf{u}(t) = \mathbf{u}^*$, there exists a (complete) solution $\mathbf{x}(t)$, for all $t \geq 0$ and for every initial condition $(\mathbf{x}(0), \mathbf{u}^*) \in \mathcal{F}$. Furthermore, following the Hybrid Lyapunov Theorem [35, Theorem 3.19], if there exists a non-negative continuously differentiable function $V : \mathcal{F} \to \mathbb{R}_{\geq 0}$ such that

$$\begin{aligned} \nabla_{\mathbf{x}} V(\mathbf{x}, \mathbf{u}^*)^\top \mathbf{F}(\mathbf{x}, \mathbf{u}^*) < 0, \quad \forall \mathbf{x} \in \mathcal{F} \setminus \mathcal{E} \\ \max_{\mathbf{z} \in \mathbf{J}(\mathbf{x}, \mathbf{u}^*)} V(\mathbf{z}, \mathbf{u}^*) - V(\mathbf{x}, \mathbf{u}^*) < 0, \quad \forall \mathbf{x} \in \mathcal{J}, \end{aligned}$$

where $\mathcal{E} \subset \mathcal{F}$ is a nonempty and compact set of equilibrium points satisfying that

$$\begin{aligned} \mathcal{J} \cap \mathcal{E} &= \emptyset \\ V(\mathbf{x}^*, \mathbf{u}^*) = 0 \quad &\Leftrightarrow \quad (\mathbf{x}^*, \mathbf{u}^*) \in \mathcal{E} \\ \mathbf{F}(\mathbf{x}^*, \mathbf{u}^*) = 0 \quad &\Leftrightarrow \quad (\mathbf{x}^*, \mathbf{u}^*) \in \mathcal{E}, \end{aligned}$$

then it holds that $\mathcal{E}$ is asymptotically stable under the HDS.

5.2.2 Population games and evolutionary dynamics

Population games [13] provide an evolutionary game theoretical framework to model the decision-making process of large populations of strategic agents. In this paper, we are interested in the properties of the evolutionary dynamics models (EDMs) that describe the aggregate expected strategic behavior of the agents. Following [13, Section 4.2], such a strategic behavior is modeled by the (mean) dynamics given by

$$\begin{aligned} \dot{x}_i(t) &= \sum_{j\in\mathcal{S}} x_j(t)\varrho_{ji}(t) - x_i(t)\varrho_{ij}(t), \quad \forall i \in \mathcal{S} \\ x_i(0) &\in \mathbb{R}_{\geq 0}, \qquad\qquad\qquad\qquad\quad \forall i \in \mathcal{S}, \end{aligned} \tag{5.1}$$

where $\mathcal{S} = \{1, 2, \ldots, n\}$ is the set of strategies available to the agents; $x_i(t) \in \mathbb{R}_{\geq 0}$ represents the portion of agents choosing strategy $i \in \mathcal{S}$ at time $t \geq 0$; $\varrho_{ij}(t) \in \mathbb{R}_{\geq 0}$ corresponds to the so-called revision protocol which characterizes the conditional switch rate of agents switching from strategy i to strategy $j \in \mathcal{S}$ at time t. Different EDMs may arise depending on the form of $\varrho_{ij}(t)$. In this paper, we focus on the revision protocol of the form

$$\varrho_{ij}(t) := [\bar{x}_j - x_j(t)]_+ [\pi_j(t) - \pi_i(t)]_+, \quad \forall i, j \in \mathcal{S}, \tag{5.2}$$

where $\bar{x}_j \in \mathbb{R}_{>0}$ is a constant parameter representing the carrying capacity of strategy j, and $\pi_i(t)$ represents the *fitness* or *payoff* of strategy i at time t.

Based on [36] and [37], it follows that the EDM given by (5.1)-(5.2) satisfies the following subsequent properties. First, by [36, Prop. 1],

$$\begin{aligned} \sum_{i\in\mathcal{S}} x_i(t) &= \sum_{i\in\mathcal{S}} x_i(0), \quad \forall t \geq 0 \\ 0 \leq x_i(0) \leq \bar{x}_i &\Rightarrow 0 \leq x_i(t) \leq \bar{x}_i, \quad \forall t \geq 0, \quad \forall i \in \mathcal{S}. \end{aligned}$$

That is, the set $\left\{\mathbf{x} \in \prod_{i\in\mathcal{S}}[0, \bar{x}_i] \,:\, \mathbf{1}_n^\top \mathbf{x} = \mathbf{1}_n^\top \mathbf{x}(0)\right\}$ is positively invariant over time under the dynamics in (5.1)-(5.2). Here, $\mathbf{x} = \operatorname{col}\left((x_i)_{i\in\mathcal{S}}\right) \in \mathbb{R}^n$. Second, by [37, Theorem 1],

$$\dot{\mathbf{x}}(t) = \mathbf{0}_n \Leftrightarrow \left[x_i(t) > 0 \Rightarrow \pi_i(t) \geq \pi_j(t), \forall i, j \in \mathcal{S}\right], \forall t \geq 0.$$

More precisely, every equilibrium point of the EDM given by (5.1)-(5.2) satisfies that the used strategies (i.e., those with $x_i > 0$) are only the ones yielding the maximum fitness value. As such, the set of equilibria of the EDM coincides with the set of Nash equilibria of the underlying population game. Namely, a Nash equilibrium is a population state $\mathbf{x}^*$ where no agent can increase their perceived fitness by unilaterally changing their strategy. Finally, by [36, Theorem 2], if the fitness signals satisfy certain monotonicity conditions, then the set of Nash equilibria of the population game is asymptotically stable under the EDM given by (5.1)-(5.2).

5.3 Model Description

Consider a set of CSs for PEVs, all powered by a single energy retailer. The set of CSs is indexed by $\mathcal{C} = \{1, 2, \ldots, N\}$, where $N \in \mathbb{Z}_{\geq 1}$ is the total number of CSs, and the retailer is represented by the index ℓ. For each CS $i \in \mathcal{C}$, let $p_i(t) \in \mathbb{R}_{\geq 0}$ be the power (in kW) provided by the retailer to the i-th CS at time $t \in \mathbb{R}_{>0}$. In contrast, let $p_\ell(t) \in \mathbb{R}_{\geq 0}$ be the remaining available power of the retailer at time t. As such, it is required that:

$$p_\ell(t) + \sum_{i\in\mathcal{C}} p_i(t) = A, \quad \forall t \geq 0, \tag{5.3}$$

where $A \in \mathbb{R}_{>0}$ represents the limited power capacity of the retailer. The power balance constraint in (5.3) ensures that the power drained by the CSs at time t does not surpass

the capacity of the retailer, i.e., that $\sum_{i\in\mathcal{C}} p_i(t) \leq A$ for all t. Throughout, we let $\mathbf{p}(t) = \operatorname{col}\left(p_i(t)\right)_{i\in\mathcal{C}\cup\{\ell\}} \in \mathbb{R}^{N+1}_{\geq 0}$, and so the constraint in (5.3) is equivalent to the requirement that $\mathbf{p}(t) \in \Delta := \{\mathbf{z} \in \mathbb{R}^{N+1}_{\geq 0} : \mathbf{1}^\top_{N+1}\mathbf{z} = A\}$, for all t.

We now proceed to describe in detail the models for the PEVs and the CSs (along with the retailer), respectively.

5.3.1 The PEV's model

Let $\mathcal{C}_c(t) \subseteq \mathcal{C}$ denote the subset of CSs that have a PEV connected to them at time t. Without the risk of confusion, we use $\mathcal{C}_c(t)$ to identify the set of PEVs that are connected to the system at time t. As such, for each PEV $i \in \mathcal{C}_c(t)$ we let $b_i(t) \in \mathbb{R}_{\geq 0}$, $B_i \in \mathbb{R}_{>0}$, and $C_i \in \mathbb{R}_{>0}$ be the battery charge (in kWh), the battery capacity (in kWh), and the maximum charging power intake (in kW) of the PEV connected to the i-th CS at time t, respectively. Thus, it is required that

$$0 \leq b_i(t) \leq B_i, \quad \forall i \in \mathcal{C}_c(t), \quad \forall t \geq 0 \tag{5.4a}$$

$$0 \leq p_i(t) \leq C_i, \quad \forall i \in \mathcal{C}_c(t), \quad \forall t \geq 0. \tag{5.4b}$$

Throughout, each connected PEV $i \in \mathcal{C}_c(t)$ is modeled as a continuous-time dynamical system, with state $b_i(t)$ and input $p_i(t)$, whose dynamics are given by

$$\dot{b}_i(t) = f_i\left(b_i(t), p_i(t)\right), \quad b_i(0) \in [0, B_i), \quad \forall i \in \mathcal{C}_c(t), \tag{5.5}$$

where $f_i : [0, B_i] \times [0, C_i] \to \mathbb{R}$ is unknown yet it is locally Lipschitz continuous. Moreover, it is assumed that the battery of a PEV does not discharge while connected to a CS, it does not have any charging dead zones, and it will only charge under a non-zero input power. Such conditions are formally stated in Assumption 5.3.1.

Assumption 5.3.1

The function $f_i(\cdot,\cdot)$ satisfies $f_i(b_i, p_i) \geq 0$, for all $(b_i, p_i) \in [0, B_i] \times [0, C_i]$, and $f_i(b_i, p_i) = 0$ if and only if $p_i = 0$, for all $i \in \mathcal{C}_c(t)$.

On the other hand, each PEV $i \in \mathcal{C}_c(t)$ has an associated precedence (fitness) function $g_i : [0, B_i] \times \mathbb{R}^{N+1}_{\geq 0} \to \mathbb{R}$ of the form

$$g_i(b_i, \mathbf{p}) = \alpha \frac{B_i - b_i}{B_i} - (1 - \alpha) h_i(\mathbf{p}),$$

where $\alpha \in (0, 1)$ is a constant weight, and $h_i : \mathbb{R}^{N+1}_{\geq 0} \to \mathbb{R}$ is continuously differentiable and satisfies Assumption 5.3.2.

Assumption 5.3.2

For all $i \in \mathcal{C}_c(t)$, $h_i(\cdot)$ satisfies

$$\frac{\partial h_i(\mathbf{p})}{\partial p_\ell} = 0 \tag{5.6a}$$

$$p_i = 0 \Rightarrow h_i(\mathbf{p}) \leq 0 \tag{5.6b}$$

$$\left(h_i(\mathbf{p}) - h_i(\tilde{\mathbf{p}})\right)\left(p_i - \tilde{p}_i\right) \geq \mu, \quad \forall \mathbf{p}, \tilde{\mathbf{p}} \in \Delta, \tag{5.6c}$$

for some $\mu \in \mathbb{R}_{>0}$.

Namely, the precedence function of each PEV $i \in \mathcal{C}_c(t)$ regards the state of charge of its battery, i.e., a lower battery charge yields higher precedence, as well as power-related costs captured by the function $h_i(\cdot)$ (e.g., costs regarding the deviation from a desired charging power, costs associated to the price of energy, or battery degradation costs, among others). In fact, note that the costs captured by $h_i(\cdot)$ might even be coupled to the charging power of other PEVs in the system, thus allowing the consideration

of aggregated-demand-dependent energy prices [30]. The technical condition in (5.6a) implies that the function $h_i(\cdot)$ is independent of the retailer's remaining power p_ℓ, and (5.6b) implies that the power-related costs for the i-th PEV must be non-positive if no power is injected into the battery of the i-th PEV. In contrast, (5.6c) is a μ-strong monotonicity condition often considered in the context of non-cooperative game theory [38], and it implies that the power-related cost of the i-th PEV is an increasing function of its individual charging power, with such an increment lower-bounded by μ. Thus, the precedence of the i-th PEV is a decreasing function of its own charging power.

Remark 5.3.1

Given that $h_i(\cdot)$ is continuously differentiable, for all $i \in \mathcal{C}_c(t)$, condition (5.6c) in Assumption 5.3.2 implies that $\boldsymbol{\chi}^\top \mathrm{D}\,\mathbf{h}(\mathbf{p})\boldsymbol{\chi} \geq \mu \boldsymbol{\chi}^\top \boldsymbol{\chi}$, for all $\mathbf{p} \in \Delta$ and all $\boldsymbol{\chi} \in \mathrm{T}\,\Delta$, where $\mathrm{D}\,\mathbf{h}(\mathbf{p})$ is the Jacobian matrix of $\mathbf{h}(\cdot) = \operatorname{col}\left(h_i(\cdot)\right)_{i \in \mathcal{C}_c(t)}$ evaluated at $\mathbf{p}$, and $\mathrm{T}\,\Delta$ is the tangent space of Δ.

Throughout, it is assumed that the battery dynamics and the precedence functions satisfy Assumption 5.3.3.

Assumption 5.3.3

For all $i \in \mathcal{C}_c(t)$, there exist a continuously differentiable function $S_i : [0, B_i] \times [0, C_i] \to \mathbb{R}_{\geq 0}$ and a non-negative function $\zeta_i : [0, B_i] \times \Delta \times \mathbb{R} \to \mathbb{R}_{\geq 0}$ such that $S_i(b_i, p_i) = 0 \Leftrightarrow f_i(b_i, p_i) = 0$, and

$$\begin{aligned} \frac{\partial S_i(b_i, p_i)}{\partial b_i} f_i(b_i, p_i) + \frac{\partial S_i(b_i, p_i)}{\partial p_i} u \leq \frac{\alpha}{B_i} f_i(b_i, p_i) u \\ + (1 - \alpha)\mu u^2 \\ - \zeta_i(b_i, p_i, u), \end{aligned} \tag{5.7}$$

for all $(b_i, p_i, u) \in [0, B_i] \times [0, C_i] \times \mathbb{R}$. Here, $\mu \in \mathbb{R}_{>0}$ satisfies (5.6c), for all $i \in \mathcal{C}_c(t)$.

Assumption 5.3.3 is an energy dissipation property related to the notion of δ-dissipative continuous-time dynamical systems [39]. For the sake of illustration, in Lemma 5.3.1 we provide sufficient conditions on the functions $f_i(\cdot, \cdot)$ and $h_i(\cdot)$ that guarantee the satisfaction of Assumptions 5.3.1 and 5.3.3.

Lemma 5.3.1

For all $i \in \mathcal{C}_c(t)$, let $f_i(b_i, p_i) = \eta_i(b_i, p_i) p_i$, where $\eta_i : [0, B_i] \times [0, C_i] \to \mathbb{R}$ is continuously differentiable, and let (5.6c) hold. Moreover, suppose that, for all $(b_i, p_i) \in [0, B_i] \times [0, C_i]$, the next conditions hold for every $i \in \mathcal{C}_c(t)$:

$$\kappa_1 \leq \eta_i(b_i, p_i) \tag{5.8a}$$

$$\frac{\partial \eta_i(b_i, p_i)}{\partial b_i} \leq -\kappa_2 \tag{5.8b}$$

$$\left| \frac{\partial \eta_i(b_i, p_i)}{\partial p_i} \right| \leq \kappa_3 \tag{5.8c}$$

$$\alpha p_i^4 \kappa_3^2 \leq 8(1 - \alpha)\mu B_i p_i^3 \kappa_1 \kappa_2, \tag{5.8d}$$

for some $\kappa_1, \kappa_2 \in \mathbb{R}_{>0}$ and $\kappa_3 \in \mathbb{R}_{\geq 0}$. Then, Assumptions 5.3.1 and 5.3.3 are satisfied.

The proof is reported in Appendix A.3.

Remark 5.3.2

Observe that if the codomain of the function $\eta_i(\cdot, \cdot)$ in Lemma 5.3.1 is restricted to $(0, 1]$, then such a function can be interpreted as the charging efficiency of the i-th PEV. Consequently, the conditions (5.8) can be checked in practice by inspecting the charging-efficiency curves that characterize the PEVs. Moreover, (5.8d) provides a technical criterion to design the power-related costs $h_i(\cdot)$ and the weight α that

characterize the precedence functions.

5.3.2 The CS's and retailer's models

To each CS $i \in \mathcal{C}$, we associate a binary variable $s_i(t) \in \mathbb{B}$, which represents the state of the i-th CS at time t. Namely, $s_i(t)$ takes the value 1 if there is a non-fully charged PEV connected to the i-th CS at time t, or takes the value 0 otherwise (i.e., $s_i(t) = 0$ if there is not a PEV connected to the i-th CS or if the connected PEV is fully charged). As such, we let $\mathbf{s}(t) = \operatorname{col}\big((s_i(t))_{i\in\mathcal{C}}\big) \in \mathbb{B}^N$ summarize the state of all CSs, and we define the set of active stations at time t as $\mathcal{C}_a(t) = \operatorname{supp}(\mathbf{s}(t))$. Clearly, $\mathcal{C}_a(t) \subseteq \mathcal{C}_c(t) \subseteq \mathcal{C}$ for every time t, and it is required that

$$p_i(t) = 0, \quad \forall i \in \mathcal{C} \setminus \mathcal{C}_a(t), \quad \forall t \geq 0. \tag{5.9}$$

Namely, the constraint in (5.9) implies that inactive CSs must not drain power from the retailer.

We highlight that the state vector $\mathbf{s}(t)$ is only partially controllable. More precisely, while we might induce a switch from $s_i(t) = 1$ to $s_i(t) = 0$ by fully charging the PEV connected to the CS $i \in \mathcal{C}_a(t)$, we cannot control the arrivals or departures of PEVs. That is, a PEV might randomly arrive at a vacant CS or depart from an occupied CS, resulting in an uncontrollable switch in the corresponding state variable. In Section 5.4, we formally define the switching logic and dynamics for the state variable $s_i(t)$, for all $i \in \mathcal{C}$. However, throughout this Chapter, we assume that such state variables are properly initialized at $t = 0$ as stated in Assumption 5.3.4.

Assumption 5.3.4

For all $i \in \mathcal{C}$, the state variable $s_i(t)$ is properly initialized at time $t = 0$ in the sense that: $s_i(0) = 1$ if there is a non-fully charged PEV connected to the i-th CS at $t = 0$, and $s_i(0) = 0$ if at $t = 0$ there is not a PEV connected to the i-th CS or if the connected PEV is fully charged.

In contrast to the PEVs, the retailer and CSs are modeled as (hybrid) dynamical systems. Namely, based on the considered framework, the retailer is modeled as an unforced system with state $p_\ell(t)$, whilst each CS $i \in \mathcal{C}$ is modeled as a system with state $(p_i(t), s_i(t))$ and input $(b_i(t), \bar{b}_i(t), \bar{c}_i(t))$, where $b_i(t) = 0$ for all vacant CSs by default, and $\bar{b}_i(t), \bar{c}_i(t) \in \mathbb{R}_{\geq 0}$ are (uncontrollable) exogenous signals defined as

$$\bar{b}_i(t) = \begin{cases} B_i, & \text{if a PEV is connected to CS } i \in \mathcal{C} \\ 0, & \text{otherwise} \end{cases} \tag{5.10a}$$

$$\bar{c}_i(t) = \begin{cases} C_i, & \text{if a PEV is connected to CS } i \in \mathcal{C} \\ 0, & \text{otherwise.} \end{cases} \tag{5.10b}$$

Also, we let $\mathbf{b}(t) = \operatorname{col}\big((b_i(t))_{i\in\mathcal{C}}\big)$, $\bar{\mathbf{b}}(t) = \operatorname{col}\big(\big(\bar{b}_i(t)\big)_{i\in\mathcal{C}}\big)$, and $\bar{\mathbf{c}}(t) = \operatorname{col}\big((\bar{c}_i(t))_{i\in\mathcal{C}}\big)$. As such, observe that the input $\bar{b}_i(t)$ can be used to unambiguously identify whether there is a PEV connected to the CS $i \in \mathcal{C}$ or not (recall that $B_i > 0$ by definition). That is, $\mathcal{C}_c(t) = \operatorname{supp}\big(\bar{\mathbf{b}}(t)\big)$. Furthermore, with a slight abuse of notation, we let $\dot{\bar{b}}_i(t) \in \{-\infty, 0, +\infty\}$ denote the instantaneous change of $\bar{b}_i(t)$ at time t. Therefore, the event of a PEV arriving to the vacant CS $i \in \mathcal{C}$ at time t is identified by the unitary impulse-like signal $\delta_{a,i}(t) = \mathbb{1}\big(\dot{\bar{b}}_i(t) > 0\big) \in \mathbb{B}$, while the event of a PEV departing from the occupied CS $i \in \mathcal{C}$ at time t is identified by the unitary impulse-like signal $\delta_{d,i}(t) = \mathbb{1}\big(\dot{\bar{b}}_i(t) < 0\big) \in \mathbb{B}$.

Similar to the PEVs', each CS $i \in \mathcal{C}$ is characterized by a maximum output power $O_i \in \mathbb{R}_{>0}$ (in kW), such that

$$p_i(t) \leq O_i, \quad \forall i \in \mathcal{C}, \quad \forall t \geq 0. \tag{5.11}$$

Therefore, by (5.10b) and (5.11), the maximum output power that a CS can provide at time t is $\bar{p}_i(t) = \min\{\bar{c}_i(t), O_i\}$, for all $i \in \mathcal{C}$. Consequently, the (time-varying) set of admissible power profiles that satisfy the charging constraints (5.3), (5.9), (5.4), and (5.11), for all $i \in \mathcal{C}$, is given by

$$\mathcal{P}(t) = \left\{ \mathbf{p} \in \Delta : \begin{array}{ll} p_i \leq \bar{p}_i(t), & \forall i \in \mathcal{C} \\ p_i = 0, & \forall i \in \mathcal{C} \setminus \mathcal{C}_a(t) \end{array} \right\}.$$

Here, we recall that $\mathcal{C}_a(t)$ denotes the set of CSs with a non-fully charged PEV connected to them. Thus, if $\mathbf{p}(t) \in \mathcal{P}(t)$ and the PEV connected to the CS $j \in \mathcal{C}$ is fully charged, then $j \notin \mathcal{C}_a(t)$ and $p_j(t) = 0$ by the definition of $\mathcal{P}(t)$. Hence, $\mathbf{p}(t) \in \mathcal{P}(t)$ satisfies (5.4a) by means of Assumption 5.3.1.

Based on the considered framework, we now formally introduce the notion of a NE for the power allocation, and define the problem to be solved by the CSs and the retailer.

Definition 5.3.1 (*Nash equilibrium*)

Given a vector of battery charges $\mathbf{b}(t)$, the corresponding set of Nash equilibria for the power allocation at time $t \geq 0$ is defined as

$$\mathrm{NE}\left(\mathbf{b}(t), t\right) = \left\{ \mathbf{p} : \ \mathbf{p} \in \arg\max_{\tilde{\mathbf{p}} \in \mathcal{P}(t)} \sum_{i \in \mathcal{C}_a(t)} \tilde{p}_i g_i\left(b_i(t), \mathbf{p}\right) \right\}.$$

Thus, $\mathbf{p}(t)$ is an NE at time t if and only if $\mathbf{p}(t) \in \mathrm{NE}\left(\mathbf{b}(t), t\right)$.

Definition 5.3.2 (*Problem statement*)

Under Assumptions 5.3.1-5.3.4 and for every time $t \geq 0$, each node $i \in \mathcal{N} = \mathcal{C} \cup \{\ell\}$ should compute its corresponding $p_i(t)$ such that the following statements hold:

i) *The power allocation is admissible, i.e., $\mathbf{p}(t) \in \mathcal{P}(t)$.*

ii) *All connected PEVs get fully charged asymptotically over time, i.e., $\lim_{t\to\infty} b_i(t) = B_i$, $\forall i \in \mathcal{C}_c(t)$.*

iii) *The power allocation is updated towards $\mathrm{NE}\left(\mathbf{b}(t), t\right)$.*

Remark 5.3.3

From Definition 5.3.1, it follows that an NE is a power allocation where no PEV can increase its precedence function by unilaterally deviating from the NE. As a result, we can think of an NE as a self-enforceable agreement among the PEVs. Therefore, seeking an NE as the desired power allocation is a suitable solution concept when multiple (non-cooperative) PEVs share the limited power capacity A.

To solve the problem in Definition 5.3.2, we should design appropriate dynamics for the CSs and the retailer. In particular, note that such dynamics must not only guarantee the asymptotic stability of the fully charged state of the connected PEVs (under the unknown and nonlinear dynamics of the PEVs' batteries) but also ensure the forward-time invariance of the set $\mathcal{P}(t)$ while steering the power allocation towards a NE. We now proceed to formulate our proposed dynamics to solve the considered power allocation problem.

5.4 The Proposed CS's and Retailer's Dynamics

The dynamics for the CSs and the retailer must be designed to correctly update $\mathbf{p}(t)$ and $\mathbf{s}(t)$ for all times $t \geq 0$. The power profile should satisfy $\mathbf{p}(t) \in \mathcal{P}(t)$, for all t, whilst the state variables should remain meaningful as intended, i.e., $s_i(t) := \mathbb{1}\left(b_i(t) \in \left(0, \bar{b}_i(t)\right)\right)$,

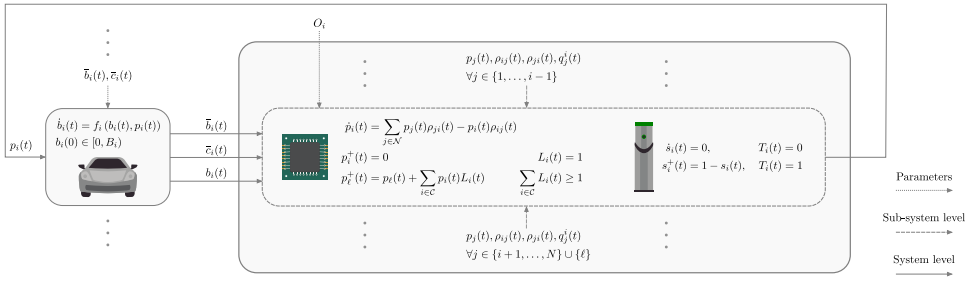

Figure 5.1: Schematic view of the proposed control system and its main components. PEVs, characterized by the battery dynamics, constitute the system input. The charging lot comprises the CS and controller subsystem, where the former interfaces with the PEV, while the latter provides the power allocation strategy, closing the system loop.

for all $i \in \mathcal{C}$. Therefore, we propose an event-triggered scheme to update $\mathbf{p}(t)$ and $\mathbf{s}(t)$ over time. Throughout the Chapter, we consider the triggering signals given by

$$T_i(t) = \begin{cases} \delta_{a,i}(t), & \forall i \in \mathcal{C} \setminus \mathcal{C}_c(t) \\ \max\{\delta_{d,i}(t),\, \theta_i(t)\}, & \forall i \in \mathcal{C}_c(t), \end{cases}$$

with $\theta_i(t) := s_i(t)\mathbb{1}\left(b_i(t) = B_i\right)$. In particular, $T_i(t) = 1$ occurs under three possible events: i) if a PEV arrives to the (previously vacant) CS $i \in \mathcal{C}$ at time t (i.e., $\delta_{a,i}(t) = 1$); ii) if the connected PEV departs from the (previously occupied) CS $i \in \mathcal{C}$ at time t (i.e., $\delta_{d,i}(t) = 1$); or iii) if the PEV connected to the i-th CS reaches a full charge at time t (i.e., $\theta_i(t) = 1$).

Based on the proposed triggering signals, if an event occurs at the CS $i \in \mathcal{C}$ at time t, i.e., $T_i(t) = 1$, then $\mathbf{p}(t)$ and $\mathbf{s}(t)$ are (instantaneously) updated according to

$$p_i^+(t) = 0 \tag{5.12a}$$
$$p_j^+(t) = p_j(t) + q_j^i(t), \qquad \forall j \in \mathcal{N} \setminus \{i\} \tag{5.12b}$$
$$s_i^+(t) = 1 - s_i(t) \tag{5.12c}$$
$$s_k^+(t) = s_k(t), \qquad \forall k \in \mathcal{C} \setminus \{i\}, \tag{5.12d}$$

where $q_j^i(t)$ is the j-th element of the vector $\mathbf{q}^i(t)$ given by

$$\mathbf{q}^i(t) = \arg \max_{\mathbf{q} \in \mathcal{Q}_i(t)} \sum_{z \in \mathcal{C}_c(t)} q_z g_z\left(b_z(t), \mathbf{p}(t)\right) - \nu\left(\bar{q} - q_z\right)^2 \tag{5.13}$$

with $\nu \in \mathbb{R}_{>0}$, $\bar{q} = \sum_{a \in \mathcal{C}_c(t)} q_a / \left|\mathcal{C}_c(t)\right|$, and

$$\mathcal{Q}_i(t) := \left\{ \mathbf{q} \in \mathbb{R}_{\geq 0}^{N+1} : \begin{array}{ll} p_j(t) + q_j \leq \bar{p}_j(t), & \forall j \in \mathcal{C} \\ (1 - s_j(t))q_j = 0, & \forall j \in \mathcal{C} \\ \sum_{k \in \mathcal{N}} q_k = p_i(t) & \\ q_i = 0 & \end{array} \right\}.$$

Here, we follow the convention that all the updates in (5.12) are applied simultaneously at the same time, meaning that the right-hand side of (5.12) and the optimization problem in (5.13) consider the values of $\mathbf{p}(t)$ and $\mathbf{s}(t)$ before the event-triggered updates. Moreover, in the case that an event occurs simultaneously for more than one CS, i.e., $\sum_{i \in \mathcal{C}} T_i(t) > 1$ (which is unlikely to happen in practice), then (5.12) is executed sequentially for every triggered CS. Note that the dynamics in (5.12a)-(5.12b) provide an instantaneous reallocation for the power $p_i(t)$ of the CS $i \in \mathcal{C}$ where an event occurs. Namely, the term $q_j^i(t)$ represents the power reallocated from i to $j \in \mathcal{N}$ at the triggering time t. Furthermore, we remark that (5.13) is a quadratic programming problem, whose

unique solution corresponds to the (regularized) best-response reallocations of the power $p_i(t)$ based on the precedence functions. The parameter ν is an arbitrarily small (yet positive) regularization weight to ensure the uniqueness of solutions. On the other hand, the dynamics in (5.12c)-(5.12d) maintain $s_i(t)$ meaningful as intended, for all $i \in \mathcal{C}$, granted that Assumption 5.3.4 holds.

In contrast, for all times in between events, i.e., all t such that $\sum_{i\in\mathcal{C}} T_i(t) = 0$, the state variables are updated continuously over time as follows

$$\dot{p}_i(t) = \sum_{j\in\mathcal{N}} p_j(t)\rho_{ji}(t) - p_i(t)\rho_{ij}(t), \quad \forall i \in \mathcal{N} \tag{5.14a}$$

$$\dot{s}_i(t) = 0, \quad \forall i \in \mathcal{C}, \tag{5.14b}$$

where, for all $i, j \in \mathcal{N}$,

$$\rho_{ij}(t) = s_i(t)s_j(t)\left[\hat{p}_j(t)\right]_+ \left[g_j(t) - g_i(t)\right]_+$$
$$\hat{p}_j(t) = \bar{p}_j(t) - p_j(t),$$

and for consistency we define $s_\ell(t) := 1$, $\bar{p}_\ell(t) := A$, $g_k(t) := g_k\big(b_k(t), \mathbf{p}(t)\big)$, and $g_z(t) := 0$, for all $k \in \mathcal{C}_c(t)$ and all $z \in \{\ell\} \cup \big(\mathcal{C} \setminus \mathcal{C}_c(t)\big)$. The dynamics in (5.14a) are inspired by the EDM introduced in Section 5.2.2, and they provide a power exchange scheme between the CSs and retailer based on the precedence functions of the connected PEVs. In particular, the term $p_j(t)\rho_{ji}(t)$ represents the power that node j yields to node i at time t. As such, a node $j \in \mathcal{N}$ with $s_j(t)p_j(t) > 0$ will yield power to a CS $i \in \mathcal{C}$ granted that $p_i(t) < \bar{p}_i(t)$, $g_i(t) > g_j(t)$, and $s_i(t) = 1$. That is, CSs with lower precedence reduce their power consumption so that CSs with higher precedence can increase it. Finally, the dynamics in (5.14b) simply maintain the state variables constant in between events.

Overall, the dynamics in (5.12)-(5.14) comprise an HDS as stated in Definition 5.4.1.

Definition 5.4.1 (*Proposed Hybrid Dynamical System*)

The proposed dynamics in (5.12)-(5.14) *characterize an HDS with state, input, and output vectors given by*

$$\mathbf{x}(t) = \operatorname{col}\left(\mathbf{p}(t), \mathbf{s}(t)\right) \in \mathcal{X} \subseteq \mathbb{R}^{N+1} \times \mathbb{B}^N$$
$$\mathbf{u}(t) = \operatorname{col}\left(\mathbf{b}(t), \bar{\mathbf{b}}(t), \bar{\mathbf{c}}(t)\right) \in \mathcal{U} \subseteq \mathbb{R}^N \times \mathbb{R}^N \times \mathbb{R}^N$$
$$\mathbf{y}(t) = \mathbf{p}(t).$$

Here, $\mathcal{X}$ and $\mathcal{U}$ denote the state and input spaces, respectively. In addition, the hybrid system is characterized by the flow set ($\mathcal{F}$), flow map ($\mathbf{F}$), jump set ($\mathcal{J}$), and jump map ($\mathbf{J}$) given by

$$\mathcal{F} = \left\{ (\mathbf{x}, \mathbf{u}) \in \mathcal{X} \times \mathcal{U} \,:\, \begin{array}{l} \mathbf{p} \in \Delta \\ \mathbf{s} \in \mathbb{B}^N \\ \mathbf{b} \in \prod_{i\in\mathcal{C}}[0, B_i] \\ \bar{\mathbf{b}} \in \prod_{i\in\mathcal{C}}\{0, B_i\} \\ \bar{\mathbf{c}} \in \prod_{i\in\mathcal{C}}\{0, C_i\} \end{array} \right\} \tag{5.15a}$$

$$\mathbf{F}(\mathbf{x}, \mathbf{u}) = \begin{bmatrix} \operatorname{col}\left(\left(\sum_{j\in\mathcal{N}} p_j\rho_{ji} - p_i\rho_{ij}\right)_{i\in\mathcal{N}}\right) \\ \mathbf{0}_N \end{bmatrix} \tag{5.15b}$$

$$\mathcal{J} = \cup_{i\in\mathcal{C}} \mathcal{J}_i \tag{5.15c}$$

$$\mathbf{J}(\mathbf{x}, \mathbf{u}) \in \left\{ \mathbf{J}_i(\mathbf{x}, \mathbf{u}) \,:\, (\mathbf{x}, \mathbf{u}) \in \mathcal{J}_i,\, i \in \mathcal{C} \right\}, \tag{5.15d}$$

where, for all $i \in \mathcal{C}$,

$$\mathcal{J}_i = \{(\mathbf{x}, \mathbf{u}) \in \mathcal{F} \,:\, T_i = 1\}$$
$$\mathbf{J}_i(\mathbf{x}, \mathbf{u}) = \begin{bmatrix} \operatorname{col}\big(p_1 + q_1^i, \ldots, p_{i-1} + q_{i-1}^i, 0, \\ \qquad p_{i+1} + q_{i+1}^i, \ldots, p_{N+1} + q_{N+1}^i\big) \\ \operatorname{col}\left(s_1, \ldots, s_{i-1}, 1 - s_i, s_{i+1}, \ldots, s_N\right) \end{bmatrix}.$$

Namely, while $(\mathbf{x}(t), \mathbf{u}(t)) \in \mathcal{F}$ *the state evolves in continuous time by* $\dot{\mathbf{x}}(t) = \mathbf{F}(\mathbf{x}(t), \mathbf{u}(t))$. *On the other hand, if an event occurs at the CS* $i \in \mathcal{C}$ *at time* t, *i.e.,* $T_i(t) = 1$, *then the state is updated instantaneously by* $\mathbf{x}^+(t) = \mathbf{J}_i(\mathbf{x}(t), \mathbf{u}(t))$.

The HDS of Definition 5.4.1 is to be interconnected in closed loop with the battery dynamics in (5.5) of the connected PEVs. For the sake of illustration, the schematic of the closed-loop system is depicted in Fig. 5.1. We now state our main technical result on such a system.

Theorem 5.4.1

Consider the HDS in Definition 5.4.1 in closed loop with the battery dynamics in (5.5). Let Assumptions 5.3.1-5.3.4 be satisfied, and suppose that $\mathbf{p}(0) \in \mathcal{P}(0)$. *Then, the following properties hold:*

i) *The power profile satisfies that* $\mathbf{p}(t) \in \mathcal{P}(t)$, *for all* $t \geq 0$.

ii) *The state where* $p_\ell^* = A$, $b_i^* = B_i$, $p_i^* = 0$, *and* $s_j^* = 0$, *for all* $i \in \mathcal{C}_c(t)$ *and all* $j \in \mathcal{C}$, *is asymptotically stable under the considered closed-loop system.*

iii) *For every time* $t \geq 0$ *where the HDS flows, the power profile* $\mathbf{p}(t)$ *is updated towards the set* $\mathrm{NE}(\mathbf{b}(t), t)$.

The proof is reported in Appendix A.4.

According to Theorem 5.4.1, the proposed dynamics indeed solve the problem in Definition 5.3.2. In particular, Claim iii) together with the best response reallocation (5.13) imply that the proposed dynamics are always seeking a NE for the power allocation among the PEVs.

Remark 5.4.1

As shown in Fig. 5.1, we highlight that the proposed dynamics in (5.12a)-(5.12b) *and* (5.14a) *require for all the nodes in* $\mathcal{N}$ *to communicate between them. In practice, when the number of CSs is large, such a communication requirement can be leveraged by partitioning the system into multiple non-overlapping (disjoint) coalitions, each to be characterized by a complete communication graph and to operate under a fraction of the overall available power A. Moreover, Theorem 5.4.1 can be easily extended to cover such a setup by relying on the multi-population game model of [13]. In this Chapter, we do not focus on the partitioning problem, yet some relevant partitioning methods have been reported in [40], [41], and the fractions of the available power A for each partition could be potentially computed with the aid of high-level methods as the ones in [27]–[29].*

5.5 Numerical Results

In this Section, we provide a numerical illustration of our proposed power allocation method in a case study scenario. We consider a PEVs charging lot with $|\mathcal{C}| = 40$ CSs, serviced by a retailer with availability $A = 300$ kW. Without loss of generality, for all $i \in \mathcal{C}_c(t)$ we let $f_i(b_i, p_i) = \eta_i(b_i)p_i$, with $\eta_i(b_i) = \gamma_i \tanh(\sigma_i B_i - \epsilon_i b_i) + \bar{\eta}_i - \gamma_i$, where $\bar{\eta}_i \in (0, 1]$, $\gamma_i \in [0, 0.5\bar{\eta}_i)$, and $\sigma_i, \epsilon_i \in \mathbb{R}_{>0}$, are parameters of the i-th PEV. As such, $f_i(\cdot, \cdot)$ satisfies Assumptions 5.3.1 and 5.3.3 (see Remark 5.3.2). On the other hand, for all $i \in \mathcal{C}_c(t)$ we let $h_i(\mathbf{p}) = p_i\left(\mu_i + \lambda \sum_{j \in \mathcal{C}} p_j\right)$, where $\mu_i, \lambda \in \mathbb{R}_{>0}$ represent the battery degradation and energy price coefficients, respectively. Clearly, $g_i(\cdot, \cdot)$ satisfies Assumption 5.3.2, for all $i \in \mathcal{C}_c(t)$. Throughout, we randomly draw $\bar{\eta}_i \sim \mathbb{U}[0.8, 0.9]$, $\gamma_i \sim \mathbb{U}[0.05, 0.15]$, $\sigma_i \sim \mathbb{U}[0.1, 0.9]$, and $\epsilon_i \sim \mathbb{U}[0.1, 0.2]$, $\mu_i \sim \mathbb{U}[1, 5]$, and $\lambda_i \sim \mathbb{U}[1, 10]$, for all $i \in \mathcal{C}_c(t)$. The maximum CS output power has been sampled as $O_i \sim \mathbb{U}\{7, 22, 44, 100\}$ [kW], whose sampling values correspond to slow, medium, fast, and ultrafast charging

speeds, respectively. Data related to PEVs' technical specification, i.e., battery capacity B_i and maximum input power C_i have been retrieved from [42].

For the sake of comparison, we also simulate the system under the so-called uniform power allocation given by

$$p_i(t) = \begin{cases} \min\left\{\frac{A}{|\mathcal{C}_a(t)|}, \bar{p}_i(t)\right\}, & \text{if } i \in \mathcal{C}_a(t) \\ A - \sum_{j\in\mathcal{C}} p_j(t), & \text{if } i = \ell \\ 0, & \text{otherwise.} \end{cases} \tag{5.16}$$

Namely, the uniform power allocation equally distributes the retailer's available power to all active CSs, taking into account their maximum power intake $\bar{p}_i(t)$. Note that, both our proposed approach and the uniform power allocation share the same parameters and initial conditions. The state vector $\mathbf{s}(t)$ and the set $\mathcal{C}_a(t)$ are updated according to our proposed event-triggered method. The initial state-of-charge of each PEV $i \in \mathcal{C}_c(t)$ is randomly sampled as $b_i(0) \sim \mathbb{U}[0, 0.5B_i]$, while the initial power allocation $\mathbf{p}(0)$ is set as

$$p_i(0) = \begin{cases} \min\left\{\frac{A}{|\mathcal{C}_a(0)|}, \bar{p}_i(0)\right\}, & \forall i \in \mathcal{C}_a(0) \\ 0, & \forall i \in \mathcal{C} \setminus \mathcal{C}_a(0) \end{cases}$$
$$p_\ell(0) = A - \sum_{j\in\mathcal{C}} p_j(0).$$

To differentiate between the two approaches of power allocation, the variables associated with the uniform power allocation are marked with the symbol †.

Figure 5.2a depicts the selected performance metric $\phi(t) := \left\|\bar{\mathbf{b}}(t) - \mathbf{b}(t)\right\|^2 / \left\|\bar{\mathbf{b}}(0) - \mathbf{b}(0)\right\|^2$, under both power allocation methods. The considered metric characterizes the speed of the aggregate charging process. Notice that the proposed approach reaches a higher charging speed throughout the process than the uniform power allocation, both in terms of average values and dispersion. This behavior is a consequence of the setup of the proposed system, where its participants modulate their power absorption based on their precedence functions. In contrast, the uniform power allocation does not consider the state of charge of the PEVs or the economic costs that PEVs might sustain. On the other hand, Fig. 5.2b reports the dispersion of the collective precedence cost, expressed as the standard deviation (SD) of $\mathbf{g}(t)$. We remark that the proposed method keeps a lower precedence SD with respect to the uniform power allocation, except for the transient state, where the trajectories overlap due to the identical initial points. Such a fact implies that the costs each PEV is incurring are not much greater than the others. Finally, Fig. 5.2c shows that the proposed method indeed satisfies the constraint on the limited power capacity of the retailer at all times. The results shown correspond to one of the 100 executed simulation runs. The aggregate results are collected in Fig.5.2d and 5.2e.

5.6 Conclusions

In this Chapter, we have formulated an event-triggered control strategy, based on population evolutionary dynamics models, for the real-time power allocation in the charging process of a fleet of PEVs that are fed by a single ER with limited power capacity. We have formally proven the feasibility (in terms of constraint satisfaction) and asymptotic stability of the method under mild assumptions. Moreover, we have shown that the proposed controller seeks a Nash equilibrium (characterized by the so-called precedence functions of the PEVs) as the solution concept for the allocation of the limited power capacity of the system. The effectiveness of the proposed approach has been illustrated through a numerical case study, highlighting the advantages of the proposed method.

Future work will focus on extending the results to include leaking battery dynamics, as well as generalizing the hybrid dynamics framework to describe other smart grid actors.

(a) Transient behavior of the aggregate state-of-charge of the fleet of PEVs.

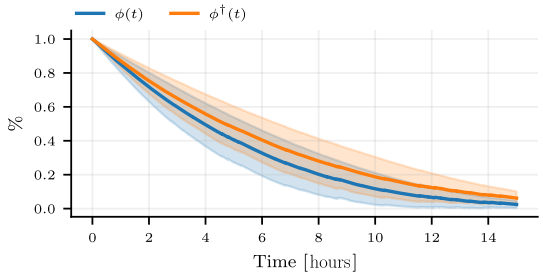

(b) Transient behavior of the precedence standard deviation.

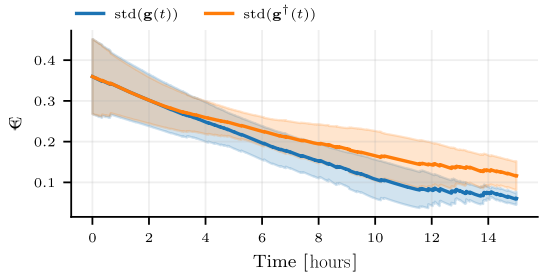

(c) Transient behavior of the retailer's power availability and constraint (5.3).

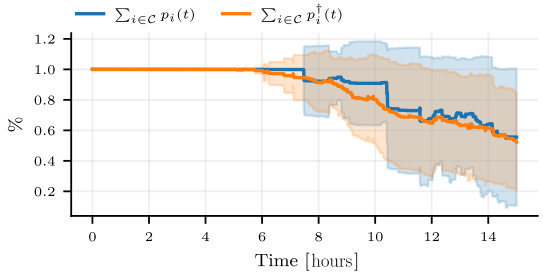

(d) Total $\phi(t)$ and $\phi^\dagger(t)$

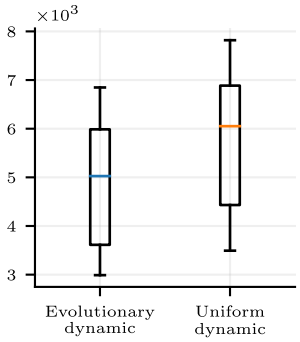

(e) Total std($\mathbf{g}(t)$) and std($\mathbf{g}^\dagger(t)$)

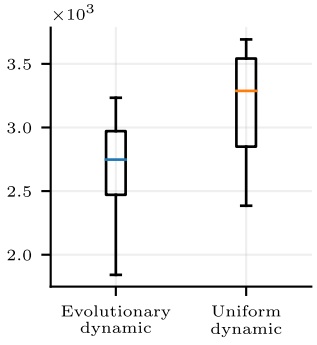

Figure 5.2: Simulation results from a sample run: blue lines refer to the proposed dynamics in (5.15), while the ones in orange refer to the uniform power allocation in (5.16); solid lines represent average values, while the shaded areas are the bounds of the standard deviation.

References

[1] Wang, C., Wood, J., Wang, Y., Geng, X., and Long, X., "CO2 emission in transportation sector across 51 countries along the belt and road from 2000 to 2014," *Journal of Cleaner Production*, vol. 266, p. 122 000, 2020.

[2] Ritchie, H., Roser, M., and Rosado, P., "CO2 and greenhouse gas emissions," *Our World in Data*, 2020, https://ourworldindata.org/co2-and-greenhouse-gas-emissions.

[3] Ercan, T., Onat, N. C., Keya, N., Tatari, O., Eluru, N., and Kucukvar, M., "Autonomous electric vehicles can reduce carbon emissions and air pollution in cities," *Transportation Research Part D: Transport and Environment*, vol. 112, p. 103 472, 2022.

[4] Sulaiman, N., Hannan, M., Mohamed, A., Ker, P. J., Majlan, E., and Daud, W. W., "Optimization of energy management system for fuel-cell hybrid electric vehicles: Issues and recommendations," *Applied energy*, vol. 228, pp. 2061–2079, 2018.

[5] Gnann, T., Klingler, A.-L., and Kühnbach, M., "The load shift potential of plug-in electric vehicles with different amounts of charging infrastructure," *Journal of Power Sources*, vol. 390, pp. 20–29, 2018.

[6] Frendo, O., Gaertner, N., and Stuckenschmidt, H., "Improving smart charging prioritization by predicting electric vehicle departure time," *IEEE Transactions on Intelligent Transportation Systems*, vol. 22, no. 10, pp. 6646–6653, 2020.

[7] Zhang, J., Yan, J., Liu, Y., Zhang, H., and Lv, G., "Daily electric vehicle charging load profiles considering demographics of vehicle users," *Applied Energy*, vol. 274, p. 115 063, 2020.

[8] Dabbaghjamanesh, M., Moeini, A., and Kavousi-Fard, A., "Reinforcement learning-based load forecasting of electric vehicle charging station using q-learning technique," *IEEE Transactions on Industrial Informatics*, vol. 17, no. 6, pp. 4229–4237, 2020.

[9] Navon, A., Ben Yosef, G., Machlev, R., *et al.*, "Applications of game theory to design and operation of modern power systems: A comprehensive review," *Energies*, vol. 13, no. 15, p. 3982, 2020.

[10] Liu, F., Dong, X., Yu, J., Hua, Y., Li, Q., and Ren, Z., "Distributed nash equilibrium seeking of N-coalition noncooperative games with application to uav swarms," *IEEE Transactions on Network Science and Engineering*, vol. 9, no. 4, pp. 2392–2405, 2022.

[11] Nie, Q., Zhang, L., and Li, S., "How can personal carbon trading be applied in electric vehicle subsidies? a stackelberg game method in private vehicles," *Applied Energy*, vol. 313, p. 118 855, 2022.

[12] Nash Jr, J. F., "Equilibrium points in n-person games," *Proceedings of the national academy of sciences*, vol. 36, no. 1, pp. 48–49, 1950.

[13] Sandholm, W. H., *Population games and evolutionary dynamics*. MIT Press, 2010.

[14] Wang, G., Chao, Y., Cao, Y., Jiang, T., Han, W., and Chen, Z., "A comprehensive review of research works based on evolutionary game theory for sustainable energy development," *Energy Reports*, vol. 8, pp. 114–136, 2022.

[15] Park, S., Martins, N. C., and Shamma, J. S., "From population games to payoff dynamics models: A passivity-based approac," in *Proceedings of the 58th IEEE Conference on Decision and Control (CDC)*, 2019, pp. 6584–6601. DOI: 10.1109/CDC40024.2019.9029756.

[16] Quijano, N., Ocampo-Martinez, C., Barreiro-Gomez, J., Obando, G., Pantoja, A., and Mojica-Nava, E., "The role of population games and evolutionary dynamics in distributed control systems: The advantages of evolutionary game theory," *IEEE Control Systems Magazine*, vol. 37, no. 1, pp. 70–97, 2017. DOI: 10.1109/MCS.2016.2621479.

[17] Martinez-Piazuelo, J., Quijano, N., and Ocampo-Martinez, C., "Decentralized charging coordination of electric vehicles under feeder capacity constraints," *IEEE Transactions on Control of Network Systems*, vol. 9, no. 4, pp. 1600–1610, 2021.

[18] Mojica-Nava, E., Macana, C. A., and Quijano, N., "Dynamic population games for optimal dispatch on hierarchical microgrid control," *IEEE Transactions on Systems, Man, and Cybernetics: Systems*, vol. 44, no. 3, pp. 306–317, 2013.

[19] Yang, Y., Yang, W., Chen, H., and Li, Y., "China's energy whistleblowing and energy supervision policy: An evolutionary game perspective," *Energy*, vol. 213, p. 118 774, 2020.

[20] Ma, L., Liu, Q., Qiu, Z., and Peng, Y., "Evolutionary game analysis of state inspection behaviour for coal enterprise safety based on system dynamics," *Sustainable Computing: Informatics and Systems*, vol. 28, p. 100 430, 2020.

[21] Chong, D. and Sun, N., "Explore emission reduction strategy and evolutionary mechanism under central environmental protection inspection system for multi-agent based on evolutionary game theory," *Computer Communications*, vol. 156, pp. 77–90, 2020.

[22] Wang, W., You, X., Liu, K., Wu, Y. J., and You, D., "Implementation of a multi-agent carbon emission reduction strategy under the chinese dual governance system: An evolutionary game theoretical approach," *International Journal of Environmental Research and Public Health*, vol. 17, no. 22, p. 8463, 2020.

[23] Tang, S., Zhou, W., Li, X., Chen, Y., Zhang, Q., and Zhang, X., "Subsidy strategy for distributed photovoltaics: A combined view of cost change and economic development," *Energy Economics*, vol. 97, p. 105 087, 2021.

[24] Encarnação, S., Santos, F. P., Santos, F. C., Blass, V., Pacheco, J. M., and Portugali, J., "Paths to the adoption of electric vehicles: An evolutionary game theoretical approach," *Transportation Research Part B: Methodological*, vol. 113, pp. 24–33, 2018.

[25] Fang, Y., Wei, W., Mei, S., Chen, L., Zhang, X., and Huang, S., "Promoting electric vehicle charging infrastructure considering policy incentives and user preferences: An evolutionary game model in a small-world network," *Journal of Cleaner Production*, vol. 258, p. 120 753, 2020.

[26] Tan, J. and Wang, L., "Real-time charging navigation of electric vehicles to fast charging stations: A hierarchical game approach," *IEEE Transactions on Smart Grid*, vol. 8, no. 2, pp. 846–856, 2015.

[27] Qiu, D., Wang, Y., Sun, M., and Strbac, G., "Multi-service provision for electric vehicles in power-transportation networks towards a low-carbon transition: A hierarchical and hybrid multi-agent reinforcement learning approach," *Applied Energy*, vol. 313, p. 118 790, 2022.

[28] Yan, D., Ma, C., and Chen, Y., "Distributed coordination of charging stations considering aggregate EV power flexibility," *IEEE Transactions on Sustainable Energy*, vol. 14, no. 1, pp. 356–370, 2023. DOI: 10.1109/TSTE.2022.3213173.

[29] Mignoni, N., Carli, R., and Dotoli, M., "Distributed noncooperative mpc for energy scheduling of charging and trading electric vehicles in energy communities," *IEEE Transactions on Control Systems Technology*, 2023.

[30] Kebriaei, H., Sadati-Savadkoohi, S. J., Shokri, M., and Grammatico, S., "Multipopulation aggregative games: Equilibrium seeking via mean-field control and consensus," *IEEE Transactions on Automatic Control*, vol. 66, no. 12, pp. 6011–6016, 2021.

[31] Goebel, R., Sanfelice, R. G., and Teel, A. R., *Hybrid Dynamical Systems: Modeling, Stability, and Robustness*. Princeton University Press, 2012.

[32] Liu, D., Xiao, X., Li, H., and Wang, W., "Historical evolution and benefit–cost explanation of periodical fluctuation in coal mine safety supervision: An evolutionary game analysis framework," *European Journal of Operational Research*, vol. 243, no. 3, pp. 974–984, 2015.

[33] Fetting, C., "The european green deal," *ESDN report*, vol. 53, 2020.

[34] Postoyan, R., Tabuada, P., Nešić, D., and Anta, A., "A framework for the event-triggered stabilization of nonlinear systems," *IEEE Transactions on Automatic Control*, vol. 60, no. 4, pp. 982–996, 2015. DOI: 10.1109/TAC.2014.2363603.

[35] Sanfelice, R. G., *Hybrid feedback control*. Princeton University Press, 2021.

[36] Barreiro-Gomez, J. and Tembine, H., "Constrained evolutionary games by using a mixture of imitation dynamics," *Automatica*, vol. 97, pp. 254–262, 2018. DOI: https://doi.org/10.1016/j.automatica.2018.08.014.

[37] Martinez-Piazuelo, J., Quijano, N., and Ocampo-Martinez, C., "Nash equilibrium seeking in full-potential population games under capacity and migration constraints," *Automatica*, vol. 141, p. 110 285, 2022. DOI: 10.1016/j.automatica.2022.110285.

[38] Scutari, G., Facchinei, F., Pang, J.-S., and Palomar, D. P., "Real and complex monotone communication games," *IEEE Transactions on Information Theory*, vol. 60, no. 7, pp. 4197–4231, 2014.

[39] Schweidel, K. S. and Arcak, M., "Compositional analysis of interconnected systems using delta dissipativity," *IEEE Control Systems Letters*, vol. 6, pp. 662–667, 2022. DOI: 10.1109/LCSYS.2021.3084974.

[40] Barreiro-Gomez, J., Ocampo-Martinez, C., and Quijano, N., "Time-varying partitioning for predictive control design: Density-games approach," *Journal of Process Control*, vol. 75, pp. 1–14, 2019.

[41] Ananduta, W. and Ocampo-Martinez, C., "Event-triggered partitioning for non-centralized predictive-control-based economic dispatch of interconnected microgrids," *Automatica*, vol. 132, p. 109 829, 2021.

[42] Hadasik, B. and Kubiczek, J. "Dataset of electric passenger cars with their specifications." (2021), [Online]. Available: https://data.mendeley.com/datasets/tb9yrptydn/1.

Part III: Towards Behavioural Equilibrium Seeking in Energy Communities

Chapter 6

Equilibrium Seeking in Learning-Based Non-cooperative Nash Games

Abstract

Traditionally, based on convexity, multi-agent decision-making models can hardly handle scenarios where agents' cost functions defy this assumption, which is specifically required to ensure the existence of several equilibrium concepts. More recently, the advent of machine learning (ML), with its inherent non-convexity, has changed the conventional approach of pursuing convexity at all costs. This paper explores and integrates the robustness of game theoretic frameworks in managing conflicts among agents with the capacity of ML approaches, such as deep neural networks (DNNs), to capture complex agent behaviors. Specifically, we employ feed-forward DNNs to characterize agents' best response actions rather than modeling their goals with convex functions. We introduce a technical assumption on the weight of the DNN to establish the existence and uniqueness of Nash equilibria and present two distributed algorithms based on fixed-point iterations for their computation. Finally, we demonstrate the practical application of our framework to a non-cooperative community of smart energy users under a dynamic time-of-use energy pricing scheme.

Contents

6.1 Introduction

Convexity (or concavity) is the cornerstone of equilibrium theory. From the first works by Von Neumann to the fundamental contributions by Nash [1], mathematical elegance and theoretical tractability have steered multi-agent decision-making models in the safe harbor of convexity. Indeed, modern game theory began with Von Neumann's result [2] establishing equilibrium existence in two-player zero-sum games, under the assumption that each player's payoff is concave with respect to their strategy – equivalently, that their cost is convex with respect to their strategy.

Under this assumption, computing equilibria is, in fact, equivalent to convex programming, making the powerful tools of convex optimization readily applicable [3]. Actually, thanks to convexity, the convergence of several classes of multi-agent dynamics (centralized, decentralized, and distributed) to equilibrium can be guaranteed [4]–[8]. While (quasi) convexity is crucial in facilitating the existence of various equilibria, this assumption proves to be overly restrictive. Likewise, non-cooperative games involving non-convex cost functions have garnered some attention in recent works [9], [10]. Among the works, let us mention the equilibrium notions of weak NE [11], local NE [12], generalized equilibrium [13], and critical NE [14]. However, progress in these areas has been restrained,

not due to a lack of interest in non-convex settings, but rather because proving the existence and convergence to equilibria is challenging, thus diminishing their value.

The search for convexity at all costs has recently gone against the advent of machine learning (ML) with its inherent and pervasive non-convexity [15]. Indeed, ML's attitude of embracing non-convexity has led to groundbreaking advances in significant challenges, such as speech and image recognition, text generation, and many more [16], [17].

In recent years, ML has been rapidly expanding its scope to the domain of game theory, emphasizing the importance of studying non-convex games. Many outstanding challenges in this field, such as training deep neural networks (DNN) that are robust to adversarial attacks, training Generative Adversarial Networks (GANs) [18], and Multi-Agent Reinforcement Learning [19] have been defined as multi-player games with utility functions that are non-convex in agents' strategies. Among these, DNNs have proven to be successful in many prediction tasks, particularly in predicting decisions [20]. Thus, they are the perfect candidates for approximating the behavior of agents in a strategic interaction framework such as a game. Nevertheless, despite their poor representation capability, agents are still identified and controlled in most papers based on simple linear models.

The increasing complexity of agents' behavior and the practical necessity of representing them with convex cost functions are the starting points of our work. We aim at harmonizing the effectiveness of game theoretic frameworks in managing conflicting scenarios, where resources are shared among a group of agents, with the capacity of ML, specifically DNNs, to approximate the complex behaviors of agents. Unlike the state-of-the-art, we do not model the agents' behaviors as it is traditionally done, with cost functions representing their ultimate goals. Instead, we approximate these behaviors using a DNN to characterize their response actions. By introducing a technical assumption on the weight of the DNN, we demonstrate the existence of an equilibrium and its uniqueness, under additional assumptions. To compute these equilibria, we define two algorithms based on fixed-point iterations and demonstrate their convergence. Finally, we apply our theoretical results to a non-cooperative community of smart energy users under a dynamic time-of-use energy pricing scheme.

The rest of the Chapter is organized as follows. In Section 6.2 we recall some preliminaries. In Section 6.3 we introduce the novel game theoretic framework with the integration of ML. Section 6.4 discusses the existence and uniqueness of equilibria, while Section 6.5 shows two distributed algorithms for reaching such equilibria. In Section 6.6 we show the illustrative application of our framework. Section 6.7 concludes the work.

6.2 Preliminaries

Notation: $\mathbb{R}^n$ denotes the set of real n-dimensional vectors while $\mathbb{N}$ denotes the set of natural numbers. $\mathbf{A}^\top$ denotes the transpose of matrix $\mathbf{A}$. The norm induced by matrix $\mathbf{A} \succeq 0$ is denoted with $\|\mathbf{x}\|_{\mathbf{A}}$, for any $\mathbf{x} \in \mathbb{R}^n$. The square norm is simply $\|\mathbf{x}\|$. The identity matrix and all-ones vector are denoted as $\mathbf{I}$ and $\mathbf{1}$, respectively. Positive (negative) semidefinite matrices are denoted with $\mathbf{A} \succeq 0$ ($\mathbf{A} \preceq 0$). For a generic set $\mathcal{X}$, its cardinality is defined by $|\mathcal{X}|$. Moreover, $\mathbf{x} := \text{col}(\mathbf{x}_1, ..., \mathbf{x}_n)$ is equal to $\mathbf{x} := (\mathbf{x}_1^\top, ..., \mathbf{x}_n^\top)^\top$. A set-value mapping $\mathcal{M} : \mathcal{A} \rightrightarrows \mathcal{B}$ is such that $\mathcal{A} \mapsto 2^{\mathcal{B}}$, for some sets $\mathcal{A}, \mathcal{B}$, where $2^{\mathcal{B}}$ is the power set of $\mathcal{B}$. We define the mapping $\text{proj}_{\mathcal{X}} : \mathbb{R}^n \to \mathcal{X}$ as the projection into the generic closed non-empty set $\mathcal{X} \subseteq \mathbb{R}^n$, i.e., $\text{proj}_{\mathcal{X}}(\mathbf{y}) = \text{argmin}_{\mathbf{x} \in \mathcal{X}} \|\mathbf{x} - \mathbf{y}\|$. A possibly (nonlinear) mapping $F : \mathbb{R}^n \to \mathbb{R}^n$ is said to be Lipschitz continuous with a constant $\ell \in \mathbb{R}_{>0}$ if $\|F(\mathbf{x}) - F(\mathbf{y})\| \leq \ell \|\mathbf{x} - \mathbf{y}\|$, $\forall \mathbf{x}, \mathbf{y} \in \mathbb{R}^n$. Given two mappings $F : \mathcal{X} \to \mathcal{Y}$ and : $\mathcal{Y} \to \mathcal{Z}$, their composition $H : \mathcal{X} \to \mathcal{Z}$ such that $H(\cdot) = F(G(\cdot))$ is denoted as $H(\cdot) = F \circ G(\cdot)$.

6.2.1 Preliminaries on Game Theory

Let us consider the standard mathematical setting of non-cooperative games [21]. Thus, let us consider a set of N agents $\mathcal{N}$, indexed by $i \in \mathcal{N} := \{1, ..., N\} \subseteq \mathbb{N}$ each with decision

variables $\mathbf{x}_i \in \mathbb{R}^{n_i}$, for some $n_i \in \mathbb{N}$. Moreover, let $n := \sum_{i \in \mathcal{N}} n_i$. We define vector $\mathbf{x}_{-i} := \text{col}(\mathbf{x}_1, \dots, \mathbf{x}_{i-1}, \mathbf{x}_{i+1}, \dots, \mathbf{x}_N) \in \mathbb{R}^{n-i}$, where $n_{-i} := n - n_i$, which collects the strategies of all agents but i, as well as vector $\mathbf{x} := \text{col}(\mathbf{x}_1, \dots, \mathbf{x}_i, \dots, \mathbf{x}_N) \in \mathbb{R}^n$, collecting the strategy of all agents. Each agent $i \in \mathcal{N}$ tries to minimize a (possibly non-convex) cost function $f_i(\mathbf{x}_i, \mathbf{x}_{-i}) : \mathbb{R}^n \times \mathbb{R}^{n-n_i} \to \mathbb{R}$ by choosing a strategy in a (possibly non-convex) feasible set $\mathbf{x}_i \in \Omega_i \subseteq \mathbb{R}^n$. Moreover, let $\mathbf{x} \in \Omega = \prod_{i \in \mathcal{N}} \Omega_i$. One can thus define the so-called NEP as the following N interdependent optimization problem:

$$\forall i \in \mathcal{N} : \quad \underset{\mathbf{x}_i \in \Omega_i}{\text{minimize}} \; f_i(\mathbf{x}_i, \mathbf{x}_{-i}). \tag{6.1}$$

A solution for (6.1) is a NE, formally defined as follows.

Definition 6.2.1 (*Nash equilibrium*)

A NE is a collective strategy $\mathbf{x}^\bullet \in \mathcal{X}$ such that:

$$\forall i \in \mathcal{N} : \quad f_i(\mathbf{x}_i^\bullet, \mathbf{x}_{-i}^\bullet) \leq \inf \left\{ f_i(\mathbf{x}_i, \mathbf{x}_{-i}^\bullet) \,|\, \mathbf{x}_i \in \Omega_i \right\}. \tag{6.2}$$

In other words, a NE is a collective strategy profile that satisfies the property that no single agent in the game can improve its objective function by unilaterally changing its strategy to another feasible one.

A standard requirement, often introduced in related works, is that cost functions are convex, or at least quasi-convex, with respect to their own strategy. Therefore, we lay out the following Assumption.

Assumption 6.2.1

For each $i \in \mathcal{N}$ and for every $\mathbf{x}_{-i}$, the function $f_i(\cdot, \mathbf{x}_{-i})$ is convex and continuously differentiable.

Assumption 6.2.2

The set Ω is convex and compact.

For instance, Assumptions 6.2.1 and 6.2.2 are necessary for setting up many fixed-point formulations used to demonstrate the existence and convergence of Nash equilibria [22]. Notably, equilibrium existence may break without (quasi-)convexity, even for very simple games [23].

6.2.2 Preliminaries on Neural Networks

We consider a feed-forward DNN, thus a network where information moves in only one direction with no cycles or loops [24]. Each layer $l \in \mathcal{L} := \{1, ..., L\} \subseteq \mathbb{N}$ is a processing ensemble comprising a set of neurons $\mathcal{P}_l$. The output of each layer $\mathbf{x}_l \in \mathbb{R}^{|\mathcal{P}_l|}$ can be computed as:

$$\mathbf{x}_l = \Phi_l \left(\mathbf{W}_l \mathbf{x}_{l-1} + \mathbf{b}_l \right), \quad \forall l \in \mathcal{L} \tag{6.3}$$

where $\mathbf{W}_l \in \mathbb{R}^{|\mathcal{P}_l| \times |\mathcal{P}_{l-1}|}$ is the weight matrix, $\mathbf{b}_l \in \mathbb{R}^{|\mathcal{P}_l|}$ the bias vector and $\Phi_l : \mathbb{R}^{|\mathcal{P}_l|} \to \mathbb{R}^{|\mathcal{P}_l|}$ the activation function of the layer. The weights and biases are the parameters that define the function approximator, and their values are identified through a data-driven optimization process known as training [25]. During training, weights and biases are modified to minimize a loss function, typically representing the discrepancy between the predicted outputs and the actual targets in a given dataset.

By setting $\mathbf{x}_0 \in \mathbb{R}^{|\mathcal{P}_0|}$ as the input and $\mathbf{x}_L \in \mathbb{R}^{|\mathcal{P}_L|}$ as the output of the DNN, we can define the overall input-output relationship of the network $\Phi : \mathbb{R}^{|\mathcal{P}_0|} \to \mathbb{R}^{|\mathcal{P}_L|}$ in the following form:

$$\mathbf{x}_L = \Phi \left(\mathbf{x}_0 \right) \tag{6.4}$$

where $\Phi(\cdot) = \Phi_L \circ \Phi_{L-1} \circ \cdots \circ \Phi_1(\cdot)$.

Let us restrict our attention to a specific class of layers and activation functions.

Assumption 6.2.3

Assume that the following properties hold:

i) *Given* $\mathbf{y}_l, \mathbf{z}_l \in \mathbb{R}^{|\mathcal{P}_l|}$, *there exists a* $\gamma_l \in \mathbb{R}_{\geq 0}$ *such that:*

$$\| \left(\mathbf{W}_l \mathbf{y}_{l-1} + \mathbf{b}_l\right) - \left(\mathbf{W}_l \mathbf{z}_{l-1} + \mathbf{b}_l\right) \| \leq \gamma_l \|\mathbf{y}_{l-1} - \mathbf{z}_{l-1}\|, \quad \forall l \in \mathcal{L}. \tag{6.5}$$

ii) *Given* $\mathbf{y}_l, \mathbf{z}_l \in \mathbb{R}^{|\mathcal{P}_l|}$:

$$\|\Phi_l\left(\mathbf{y}_{l-1}\right) - \Phi_l\left(\mathbf{z}_{l-1}\right)\| \leq \|\mathbf{y}_{l-1} - \mathbf{z}_{l-1}\|, \quad \forall l \in \mathcal{L}. \tag{6.6}$$

It follows from Assumption i) that

$$\begin{aligned} \| \left(\mathbf{W}_l \mathbf{y}_{l-1} + \mathbf{b}_l\right) - \left(\mathbf{W}_l \mathbf{z}_{l-1} + \mathbf{b}_l\right) \| &= \|\mathbf{W}_l(\mathbf{y}_{l-1} - \mathbf{z}_{l-1})\| \\ &= \|\mathbf{y}_{l-1} - \mathbf{z}_{l-1}\|_{\mathbf{H}_l} \\ &\leq \gamma_l \|\mathbf{y}_{l-1} - \mathbf{z}_{l-1}\| \end{aligned}$$

where $\mathbf{H}_l := \mathbf{W}_l^\top \mathbf{W}_l \succeq 0$. By rearranging the terms in the last inequality, we obtain

$$\begin{aligned} \gamma_l \|\mathbf{y}_{l-1} - \mathbf{z}_{l-1}\| - \|\mathbf{y}_{l-1} - \mathbf{z}_{l-1}\|_{\mathbf{H}_l} &= \|\mathbf{y}_{l-1} - \mathbf{z}_{l-1}\|_{\gamma_l \mathbf{I} - \mathbf{H}_l} \\ &\geq 0 \end{aligned}$$

which holds iff $\gamma_l \mathbf{I} - \mathbf{H}_l \succeq 0$. Albeit no requirements are needed for the biases, the last inequality forces the training process into a semidefinite optimization problem, with the non-convex constraint $\mathbf{W}_l^\top \mathbf{W}_l \preceq \gamma_l \mathbf{I}$. A naive idea to overcome such issue is to evaluate $\tilde{\mathbf{H}}_l = \mathbf{H}_l - \mathbf{H}_l \mathbf{1} - \gamma_l \mathbf{I} \preceq 0$, where the latter holds from Gershgorin circle theorem, and then recovering $\tilde{\mathbf{W}}_l^\top \tilde{\mathbf{W}}_l = \tilde{\mathbf{H}}_l$ through Cholesky decomposition. An in-depth discussion on the properties of Lipschitz neural network is provided in [26].

Additionally, it is trivial to show that the most commonly used activation functions, such as sigmoid, hyperbolic tangent, and rectified linear unit (ReLU), satisfy Assumption ii). In contrast, the Gaussian activation function does not satisfy it.

Lemma 6.2.1

A feed-forward DNN (6.4) *respecting Assumption 6.2.3 is a Lipschitz continuous map with constant* $\gamma = \prod_{l \in \mathcal{L}} \gamma_l$.

Proof 6.2.1

A feed-forward DNN is essentially a stack of layers, where each layer transforms the previous layer's output and feeds its output to the next ones. By the composition property of Lipschitz functions the map $\Phi(\cdot) = \Phi_L \circ \Phi_{L-1} \circ \cdots \circ \Phi_1$ *is Lipschitz continuous with a constant* $\gamma = \prod_{l \in \mathcal{L}} \gamma_l$, *being* γ_l *the Lipschitz constant of the layer* $l \in \mathcal{L}$. ■

6.3 Learning-Based Games

Games are typically formulated, as in (6.1), by approximating agents' preferences using cost functions which ultimately drive the agent's behavior. Thus, the applicability of such multi-agent models is limited by (i) the possibility of finding suitable functions that realistically model agents' preferences and (ii) constraining their formulation to be convex, as per Assumption 6.2.1. As a result, these limitations do not allow for modeling scenarios where agents' behaviors are extremely complex.

Despite the challenging task of defining a function that realistically approximates agents' preferences, several applications allow for measuring agents' behavior in the sense of evaluating their response to a given environment whose state depends on given parameters and other agents' decisions.

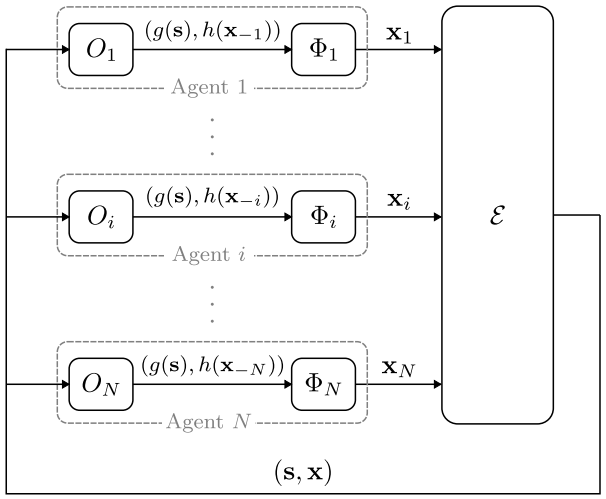

Figure 6.1: Scheme of the proposed learning-based non-cooperative game framework.

Let $\mathcal{E} := \mathcal{S} \times \Omega$ abstract an environment whose state is (uniquely) determined by a certain scenario $\mathbf{s} \in \mathcal{S} \subset \mathbb{R}^m$, for some $m \in \mathbb{N}$, and the collective actions taken by the agents $\mathbf{x} \in \Omega$. From the perspective of agent $i \in \mathcal{N}$, however, only set $\mathcal{E}_i := \mathcal{S}_i \times \Omega_{-i}$ is accessible, where $\mathcal{S}_i \subset \mathbb{R}^{q_i}$, with $q_i \leq m$ (possibly strictly), acting as the co-domain of some $g_i : \mathcal{S} \to \mathcal{S}_i$, represents the information agent $i \in \mathcal{N}$ acquires regarding scenario $\mathbf{s} \in \mathcal{S}$. Moreover, let $\Omega_{-i} := \Omega_1 \cap \cdots \cap \Omega_{i-1} \cap \Omega_{i+1} \cap \cdots \cap \Omega_N$ constitute the set of all strategies but the one of player $i \in \mathcal{N}$. Formally, we can introduce an observer $O_i : \mathcal{E} \to \mathcal{E}_i$ which maps $(\mathbf{s}, \mathbf{x}) \mapsto \mathrm{col}(g_i(\mathbf{s}), h_i(\mathbf{x}_{-i}))$ for some $h_i : \Omega_{-i} \to \mathbb{R}^{p_i}$, with $p_i \leq n - n_i$ (possibly strictly). The latter represents the information quota that agent i receives regarding other agents strategies. A scheme of this framework is shown in Fig. 6.1. Therefore, each agent has a possibly limited view of the environment, albeit a full knowledge of some function of the other's decisions. In full-information games, one has $h(\mathbf{x}_{-i}) = \mathbf{x}_{-i}$. Similarly, popular equilibrium-seeking algorithms follow such a setup, e.g., in the class of aggregative games, we have $h_i(\mathbf{x}_{-i}) = \sum_{j \in \mathcal{N} \setminus \{i\}} x_j$.

Such a formulation allows us to define the training set and target vector against which each agent $i \in \mathcal{N}$ can develop its response strategy. Specifically, we assume that each agent $i \in \mathcal{N}$ can access a training set $\mathcal{T}_i \subset \mathcal{E}_i \times \Omega_i$, so that a tuple $(O_i(\mathbf{s}, \mathbf{x}), \mathbf{x}_i) \in \mathcal{T}_i$ is such that each the environmental input $O_i(\mathbf{s}, \mathbf{x})$ determines a response action $\mathbf{x}_i \in \Omega_i$. A note of caution should be used in defining the nature of the response $\mathbf{x}_i$: due to the lack of an index capable of introducing a preference relation on Ω_i, the action taken by each agent, as a response to environmental stimuli does not necessarily classify as "optimal". Therefore, such a setup bears weaker assumptions on the nature of $\mathbf{x}_i$, with respect to the most commonly used best-response formulations, where each agent reacts to others' actions by iteratively solving (6.1). This allows for modeling agents with limited rationality and subject to environmental conditioning. Equipped with a dataset $\mathcal{T}_i$, we can define a feed-forward DNN as in (6.4), and train it to approximate the behavior of agent $i \in \mathcal{N}$ as:

$$\forall i \in \mathcal{N} : \quad \tilde{\mathbf{x}}_i = \Phi_i \left(\begin{bmatrix} g_i(\mathbf{s}) \\ h_i(\mathbf{x}_{-i}) \end{bmatrix} \right) = \Phi_i(O_i(\mathbf{s}, \mathbf{x})) \tag{6.7}$$

where $\tilde{\mathbf{x}}_i$ is the response of agent $i \in \mathcal{N}$ yielded by the feed-forward DNN when the actions of other agents are $\mathbf{x}_{-i} \in \mathbb{R}^{n-n_i}$ under scenario $\mathbf{s} \in \mathcal{S}$. Note that, as the strategy returned by (6.7) may yield infeasible as is provided by a feed-forward DNN, i.e., $\tilde{\mathbf{x}}_i \notin \Omega_i$. Thus, let us project into the feasible set Ω_i the DNN output as:

$$\forall i \in \mathcal{N} : \quad \mathbf{x}_i = \mathrm{proj}_{\Omega_i} \left\{ \Phi_i(O_i(\mathbf{s}, \mathbf{x})) \right\}. \tag{6.8}$$

Remark 6.3.1

Once trained, (6.8) *becomes an alternative approach to evaluating* $\mathbf{x}_i = \text{argmin}_{\mathbf{x}_i \in \Omega_i} f_i(\mathbf{x}_i, \mathbf{x}_{-i})$*, as in* (6.1)*, when deriving suitable convex objectives is inconvenient.*

6.4 Existence and Uniqueness of Equilibria

Having redefined agents' behavior, the standard setting for Nash equilibria does not hold here. Thus, let us search for different equilibrium conditions and introduce a notion of *Learning-Based Equilibrium* (LBE), defined as follows.

Definition 6.4.1 (*Learning-Based Equilibrium*)

A LBE is a strategy profile $\mathbf{x}^* \in \Omega$ *such that, for any* $\mathbf{s} \in \mathcal{S}$*:*

$$\forall i \in \mathcal{N}: \quad \mathbf{x}_i^* = \text{proj}_{\Omega_i}\left\{\Phi_i(O_i(\mathbf{s}, \mathbf{x}^*))\right\}. \tag{6.9}$$

Intuitively, a LBE comprises strategies satisfying no specific optimality condition, as agents essentially make their moves in response to their opponents' strategies based on the results of a data-based approach, which can lead to suboptimal solutions when compared with the results yielded by an ideal $f_i(\cdot, \cdot)$.

Next, we argue that an LBE equilibrium exists under the following assumptions.

Assumption 6.4.1

For each $i \in \mathcal{N}$ *the feed-forward DNN* $\Phi_i(\cdot)$*, approximating the agent response, is Lipschitz continuous with constant* γ_i*, while* $h_i : \Omega_{-i} \to \mathbb{R}^{p_i}$ *is 1-Lipschitz continuous.*

Note that requiring the feed-forward DNN $\Phi_i(\cdot)$ to be Lipschitz continuous with constant γ_i is equivalent to requiring that it is composed of a set of layers $\mathcal{L}_i$, such that for each layer $l_i \in \mathcal{L}_i$, Assumption 6.2.3 holds with a constant $\gamma_{l,i}$. This requirement ensures that $\gamma_i := \prod_{l \in \mathcal{L}_i} \gamma_{l,i}$, as specified in Lemma 6.2.1.

Proposition 6.4.1 (*Existence*)

Every game satisfying Assumptions 6.2.2 and 6.4.1, has at least one LBE.

The proof is reported in Appendix A.5

Proposition 6.4.2 (*Uniqueness*)

Every game satisfying Assumptions 6.2.2 and 6.4.1 with $\left(\sum_{i \in \mathcal{N}} \gamma_i^2\right)^{1/2} < 1$ *has only one LBE.*

Proof 6.4.1

If $\left(\sum_{i \in \mathcal{N}} \gamma_i^2\right)^{1/2} < 1$*, the mapping* (A.5) *is a contraction that has a unique fixed point [27], which is a LBE due to Proposition 6.4.1.* ■

6.5 Convergence to an Equilibria

In this Section, let us present two distributed LBE-seeking approaches. Intuitively, the mapping $M(\cdot)$ characterizes what would happen if all agents were to synchronously compute and update their strategies based on other agents' decisions. We are thus interested in characterizing the asymptotic properties of the response evolution when this step is repeated indefinitely, as described in Algorithm 6, given an initial state $\mathbf{x}_i^0 \in \Omega_i$ for all agents.

Algorithm 6: Picard-Banach Distributed Scheme

Set $\mathbf{x}_i^0 \in \Omega_i, \forall i \in \mathcal{N}$
forall $k = 0, \ldots, \infty$ **do**
  forall $i \in \mathcal{N}$ **do**
    $\mathbf{x}_i^{k+1} \leftarrow \text{proj}_{\Omega_i}(\Phi_i(O_i(\mathbf{s}, \mathbf{x}^k))$.

Algorithm 7: Krasnoselskij Distributed Scheme

Set $\mathbf{x}_i^0 \in \Omega_i, \forall i \in \mathcal{N}$
forall $k = 0, \ldots, \infty$ **do**
  forall $i \in \mathcal{N}$ **do**
    $\mathbf{x}_i^{k+1} \leftarrow (1-\alpha)\mathbf{x}_i^k + \alpha\, \text{proj}_{\Omega_i}(\Phi_i(O_i(\mathbf{s}, \mathbf{x}^k))$.

Proposition 6.5.1

Suppose that Assumptions 6.2.2 and 7.3.1 hold with $\left(\sum_{i\in\mathcal{N}} \gamma_i^2\right)^{1/2} < 1$. *Then, for an initial state* $\mathbf{x}_i^0 \in \Omega_i$ *for all agents* $i \in \mathcal{N}$ *the sequence* $(\mathbf{x}^k)_{k=0}^{\infty}$ *converges to the unique fixed point of* (A.5). *Thus, by Propositions 6.4.1 and 6.4.2 the sequence* $(\mathbf{x}_i^k)_{k=0}^{\infty}$ *converges to the unique LBE* (6.9).

Proof 6.5.1

Since $\left(\sum_{i\in\mathcal{N}} \gamma_i^2\right)^{1/2} < 1$, *the mapping* $M(\cdot)$ *is a contraction and thus converges, for any initial condition* $\mathbf{x}^{(0)} \in \mathbb{R}^n$, *to its unique fixed point [28], [29], which is a LBE due to Proposition 6.4.1.* ■

The conditions under which Algorithm 1 converges may be too restrictive in some cases, such as the contractiveness of the mapping $M(\cdot)$. Indeed, relaxing this latter assumption and requiring the mapping $M(\cdot)$ to be nonexpansive only is insufficient for the Picard–Banach iteration to converge to a fixed point. Thus, let us assume here that agents compute their response with a convex combination between the current other agents' strategies and the response used at the previous iteration, that is, the well-known Krasnoselskij iteration, described in Algorithm 7.

Proposition 6.5.2

Suppose that Assumptions 6.2.2 and 7.3.1 hold with $\left(\sum_{i\in\mathcal{N}} \gamma_i^2\right)^{1/2} = 1$. *Then for an initial state* $\mathbf{x}_i^0 \in \Omega_i$ *for all agents* $i \in \mathcal{N}$ *the sequence* $(\mathbf{x}^k)_{k=0}^{\infty}$ *converges to a fixed point of* (A.5). *Thus, by Proposition 6.4.1 the sequence* $(\mathbf{x}_i^k)_{k=0}^{\infty}$ *converges for to a LBE* (6.9).

Proof 6.5.2

Since $\left(\sum_{i\in\mathcal{N}} \gamma_i^2\right)^{1/2} = 1$, *the mapping* $M(\cdot)$ *is a nonexpansive mapping thus converges, for any initial condition* $x^{(0)} \in \mathbb{R}^n$, *to a unique fixed point [28], [29], which is a LBE due to Proposition 6.4.1.* ■

6.6 Illustrative Example

As an illustrative example, let us consider an energy community model comprising smart energy users. Each agent $i \in \mathcal{N}$ behaves selfishly, choosing its energy consumption strategy $\mathbf{x}_i$ from a convex and compact feasible set Ω_i, i.e., $\mathbf{x}_i \in \Omega_i$.

For ease of presentation, let us assume that the energy cost in the community follows a dynamic pricing scheme, where the cost incurred by agent $i \in \mathcal{N}$ depends on the strategies

of other agents $\mathbf{x}_{-i}$ [30]. This setting allows us to present our results in an aggregative fashion. Nevertheless, note that the results presented in this section hold for generally coupled games respecting Assumption 6.4.1. This allows us to present our results in an aggregative fashion. However, it's important to note that the results presented in this section are applicable to generally coupled games that adhere to Assumption 6.4.1.

Specifically, we assume that the energy cost for each consumer is an aggregation of other agents' strategies and thus can be computed as:

$$h_i(\mathbf{x}_{-i}) := \sum_{j \in \mathcal{N} \setminus \{i\}} P_{ij} \mathbf{x}_j \tag{6.10}$$

where $P_{i,j}$ indicates the strength of the influence of agent $j \in \mathcal{N}$ on agent $i \in \mathcal{N}$, with 0 denoting no influence. Specifically, we assume $P := \frac{1}{N-1}(\mathbf{1}_N \mathbf{1}_N^\top - I_N)$, which is doubly stochastic satisfying condition $\|P\| \leq 1$. Note that since $\|P\| \leq 1$ Assumption 6.4.1 hold for $h_i(i)$ [31].

To train the DNNs approximating agents' behavior, we utilize data from the *Low Carbon London* project [32]. This dataset comprises energy consumption readings for 5,567 households in London, collected between November 2011 and February 2014 at half-hourly intervals. The households were selected to represent a balanced sample of the Greater London population.

The dataset includes energy consumption in kWh per half hour, unique household identifiers, dates, and times for approximately 1,100 customers subjected to dynamic energy prices. Tariff prices were provided a day in advance through Smart Meter IHDs or text messages to mobile phones. Both the date/time information and the price signal schedule are available in the dataset. Some analysis of this dataset is available here [33].

For the training process, we select 100 customers from the dataset. We train a different DNN for each customer using timestamp information and the corresponding energy price as input features. The target value for each DNN is the respective customer's energy consumption. Thus, each DNN aims to approximate a customer's behavior in deciding how much energy to use in a specific time slot based on the energy price.

The DNNs are trained using the DEEPLip library, which is specifically designed to train Lipschitz layers [34]. In particular, we employ DNNs composed of 5 linear layers with 64 neurons each and fullsort activation functions.

In Fig. 6.2, we show the convergence of strategies to an LBE using Algorithm 6, while in Fig. 6.3, the results of Algorithm 7 with a parameter $\alpha = 0.3$. Please note that the equilibrium reached by both algorithms is the same, as all the DNNs are Lipschitz continuous with $\gamma_i < 1$, ensuring the uniqueness of the LB. From the comparison of the two algorithms, it emerges that the average number of iterations required by Algorithm 6 is lower.

6.7 Conclusion

This Chapter challenges the conventional reliance on convexity in game theory, recognizing the limitations it imposes when agents' utility functions cannot be adequately represented preserving this assumption. Unlike conventional approaches that model agents' behaviors with convex cost functions, we propose using deep neural networks (DNNs) to compute the agents' response actions. Introducing a technical assumption on parameters of the DNN, we establish the existence and uniqueness of equilibria. Two distributed algorithms based on fixed-point iterations are presented for their computation, showing the practicality of our approach.

As a future work, it would be interesting to extend the proposed framework to games with coupling constraints.

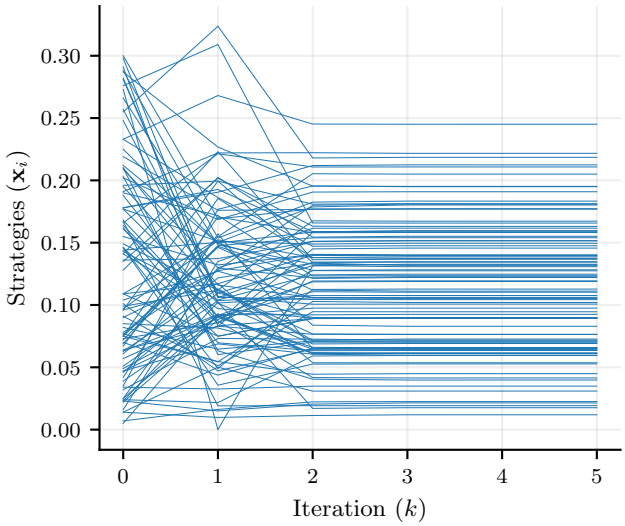

Figure 6.2: Strategy convergence of agents using Algorithm 1.

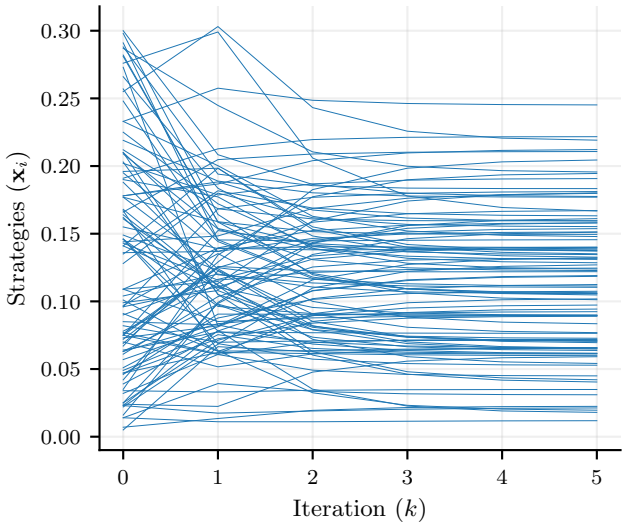

Figure 6.3: Strategy convergence of agents using Algorithm 2.

References

[1] Myerson, R. B., "Nash equilibrium and the history of economic theory," *Journal of Economic Literature*, vol. 37, no. 3, pp. 1067–1082, 1999.

[2] Von Neumann, J., *Zur theorie der gesellschaftsspiele, in «mathematische annalen», 100*, 1928.

[3] Brooks, B. and Reny, P. J., "A canonical game–nearly 75 years in the making–showing the equivalence of matrix games and linear programming," *Available at SSRN 3851583*, 2021.

[4] Mignoni, N., Scarabaggio, P., Carli, R., and Dotoli, M., "Control frameworks for transactive energy storage services in energy communities," *Control Engineering Practice*, vol. 130, p. 105 364, 2023.

[5] Bakolas, E. and Lee, Y., "Decentralized game-theoretic control for dynamic task allocation problems for multi-agent systems," in *2021 American Control Conference (ACC)*, IEEE, 2021, pp. 3228–3233.

[6] Aditya, P. and Werner, H., "A distributed linear-quadratic discrete-time game approach to multi-agent consensus," in *2022 IEEE 61st Conference on Decision and Control (CDC)*, IEEE, 2022, pp. 6169–6174.

[7] Oliveira, T. R., Rodrigues, V. H. P., Krstić, M., and Başar, T., "Nash equilibrium seeking in heterogeneous noncooperative games with players acting through heat pde dynamics and delays," in *2021 60th IEEE Conference on Decision and Control (CDC)*, IEEE, 2021, pp. 1167–1173.

[8] Scarabaggio, P., Grammatico, S., Carli, R., and Dotoli, M., "Distributed demand side management with stochastic wind power forecasting," *IEEE Transactions on Control Systems Technology*, vol. 30, no. 1, pp. 97–112, 2021.

[9] Huang, X., Beferull-Lozano, B., and Botella, C., "Quasi-nash equilibria for non-convex distributed power allocation games in cognitive radios," *IEEE Transactions on Wireless Communications*, vol. 12, no. 7, pp. 3326–3337, 2013.

[10] Scarabaggio, P., Carli, R., and Dotoli, M., "Noncooperative equilibrium seeking in distributed energy systems under ac power flow nonlinear constraints," *IEEE Transactions on Control of Network Systems*, 2022.

[11] Biasi, C., Monis, T. F. M., *et al.*, "Weak local Nash equilibrium," *Topological Methods in Nonlinear Analysis*, vol. 41, no. 2, pp. 409–419, 2013.

[12] Alós-Ferrer, C. and Ania, A. B., "Local equilibria in economic games," *Economics Letters*, vol. 70, no. 2, pp. 165–173, 2001.

[13] Cornet, B. and Czarnecki, M.-O., "Existence of generalized equilibria," *Nonlinear Analysis: Theory, Methods & Applications*, vol. 44, no. 5, pp. 555–574, 2001.

[14] Baye, M. R., Tian, G., and Zhou, J., "Characterizations of the existence of equilibria in games with discontinuous and non-quasiconcave payoffs," *The Review of Economic Studies*, vol. 60, no. 4, pp. 935–948, 1993.

[15] Jin, C., Netrapalli, P., Ge, R., Kakade, S. M., and Jordan, M. I., "On nonconvex optimization for machine learning: Gradients, stochasticity, and saddle points," *Journal of the ACM (JACM)*, vol. 68, no. 2, pp. 1–29, 2021.

[16] Deng, L. and Li, X., "Machine learning paradigms for speech recognition: An overview," *IEEE Transactions on Audio, Speech, and Language Processing*, vol. 21, no. 5, pp. 1060–1089, 2013.

[17] Maier, A., Syben, C., Lasser, T., and Riess, C., "A gentle introduction to deep learning in medical image processing," *Zeitschrift für Medizinische Physik*, vol. 29, no. 2, pp. 86–101, 2019.

[18] Pan, Z., Yu, W., Yi, X., Khan, A., Yuan, F., and Zheng, Y., "Recent progress on generative adversarial networks (gans): A survey," *IEEE access*, vol. 7, pp. 36 322–36 333, 2019.

[19] Zhang, K., Yang, Z., and Başar, T., "Multi-agent reinforcement learning: A selective overview of theories and algorithms," *Handbook of reinforcement learning and control*, pp. 321–384, 2021.

[20] Rosenfeld, A. and Kraus, S., "Predicting human decision-making," in *Predicting Human Decision-Making: From Prediction to Action*, Springer, 2018, pp. 21–59.

[21] De Persis, C. and Grammatico, S., "Distributed averaging integral nash equilibrium seeking on networks," *Automatica*, vol. 110, p. 108 548, 2019.

[22] Nash Jr, J. F., "Equilibrium points in n-person games," *Proceedings of the national academy of sciences*, vol. 36, no. 1, pp. 48–49, 1950.

[23] Daskalakis, C., Golowich, N., Skoulakis, S., and Zampetakis, E., "Stay-on-the-ridge: Guaranteed convergence to local minimax equilibrium in nonconvex-nonconcave games," in *The Thirty Sixth Annual Conference on Learning Theory*, PMLR, 2023, pp. 5146–5198.

[24] Seo, J., Lee, J., and Kim, K., "Decoding of polar code by using deep feed-forward neural networks," in *2018 international conference on computing, networking and communications (ICNC)*, IEEE, 2018, pp. 238–242.

[25] Solarte, B., Wu, C.-H., Liu, Y.-C., Tsai, Y.-H., and Sun, M., "360-mlc: Multi-view layout consistency for self-training and hyper-parameter tuning," *Advances in Neural Information Processing Systems*, vol. 35, pp. 6133–6146, 2022.

[26] Virmaux, A. and Scaman, K., "Lipschitz regularity of deep neural networks: Analysis and efficient estimation," *Advances in Neural Information Processing Systems*, vol. 31, 2018.

[27] Berinde, V. and Pacurar, M., "Fixed points and continuity of almost contractions," *Fixed Point Theory*, vol. 9, no. 1, pp. 23–34, 2008.

[28] Bauschke, H. and Combettes, P., *Convex analysis and monotone operator theory in hilbert spaces, corrected printing*, 2019.

[29] Rockafellar, R. T. and Wets, R. J.-B., *Variational analysis*. Springer Science & Business Media, 2009, vol. 317.

[30] Paccagnan, D., Gentile, B., Parise, F., Kamgarpour, M., and Lygeros, J., "Distributed computation of generalized nash equilibria in quadratic aggregative games with affine coupling constraints," in *2016 IEEE 55th conference on decision and control (CDC)*, IEEE, 2016, pp. 6123–6128.

[31] Eriksson, K., Johnson, C., Estep, D., Eriksson, K., Johnson, C., and Estep, D., "Vector-valued functions of several real variables," *Applied Mathematics: Body and Soul: Calculus in Several Dimensions*, pp. 789–814, 2004.

[32] *Low Carbon London - UKPN Innovation*, [Online; accessed 21. Mar. 2024], Oct. 2023. [Online]. Available: https://innovation.ukpowernetworks.co.uk/projects/low-carbon-london.

[33] *Electricity Consumption in a Sample of London Households – London Datastore*, [Online; accessed 21. Mar. 2024], Mar. 2024. [Online]. Available: https://data.london.gov.uk/blog/electricity-consumption-in-a-sample-of-london-households.

[34] Serrurier, M., Mamalet, F., González-Sanz, A., Boissin, T., Loubes, J.-M., and Del Barrio, E., "Achieving robustness in classification using optimal transport with hinge regularization," in *Proceedings of the IEEE/CVF Conference on Computer Vision and Pattern Recognition*, 2021, pp. 505–514.

Chapter 7

Model Predictive Control with Recursive Multi-step Input Convex Lipschitz Neural Networks: an Application to Smart Buildings

VII

Abstract

Model Predictive Control (MPC) is an optimal control technique that employs a dynamic model of the controlled process and an optimization algorithm to determine the control strategy. Nevertheless, the cost and effort required to create and maintain dynamical models are often high, and solving the resulting optimal control problem can be computationally complex. In recent years, data-driven modeling has become an attractive alternative to approximate the behavior of dynamical systems, with the aim of alleviating these issues. However, using such models for model-based control can be challenging due to their typically nonlinear and nonconvex nature. To address these issues, we propose a recursive multi-step learning-based dynamical modeling framework to capture the temporal behavior of dynamic systems. We take advantage of Input Convex Lipschitz Neural Networks, which are explicitly designed to be convex and continuous with respect to their inputs. We further show that these mathematical proprieties hold in a multi-step dynamical modeling framework. The proposed approach is evaluated in a real-life MPC experiment conducted in a smart building in the Samso Marina, Denmark. We show that the proposed approach keeps the internal temperature within comfort constraints while minimizing heating/cooling energy consumption.

Contents

7.1 Introduction

Model Predictive Control (MPC) is an advanced control technique that uses a dynamical model of the controlled process to make real-time predictions and an optimization algorithm to determine an optimal control strategy [1]. This approach is widely used in various industrial applications, including chemical reactors, wastewater treatment plants, hydroelectric power plants, autonomous driving systems, unmanned vehicles, and aerial vehicles [2]–[6].

The development of effective control strategies for complex dynamical systems has traditionally relied on using conventional dynamical models to make real-time predictions. Still, the cost and complexity of creating and maintaining such an *apparatus* have led to a growing interest in alternative solutions, such as data-driven and learning-based modeling approaches [7], [8]. Specifically, neural networks (NNs) are powerful machine learning models that can learn complex nonlinear relationships between inputs and outputs from

data. They are well-suited for modeling dynamical systems, as they can capture temporal dependencies and approximate the nonlinear dynamics of a system [9], [10]. However, a significant downside is that a NN generally does not lead to convex input-output mappings, making the application of MPC schemes challenging [11]. Indeed, one major drawback of this approach is that the optimization problem in MPC may be multi-modal, nonconvex, and discontinuous, which can result in finding only local minima rather than the global solution [12]. Using such models to approximate systems' dynamics can also lead to longer calculation times, which can be problematic in fast embedded systems [13].

Although not all real-world models are convex, many relevant ones can be approximated by a convex counterpart. Therefore, constructing convex learning-based models from available data is essential, especially when such a property can be advantageous. Recent research has proposed various methods to construct convex learning-based models using NNs to address this issue. One such method is the NN-based cost parametrization proposed in [14]. This approach enables learning-based MPC with generic cost functions that preserve convexity and nominal stability. Furthermore, in [15], the authors show that a one-layer feed-forward NN with exponential activation functions in the inner layer and logarithmic activation in the output neuron is a universal approximator of convex functions. Building Input Convex NNs (ICNNs), where the model output is convex with respect to a subset of the model inputs [16], presents restrictions on the structure and weights of feed-forward NNs. Such networks exhibit high prediction accuracy in many domains, such as multi-label prediction, image completion, and reinforcement learning problems. In [17], the authors extend these formulations to a recurrent network structure for one-shot multi-step ahead predictions. This means a sequence of outputs is predicted with a sequence of inputs in a single prediction step. The authors apply the approach to an MPC scheme for MuJoCo locomotion tasks [18] and to control the Heating, Ventilation, and Air Conditioning (HVAC) system of a simulated building. Lastly, the study in [19] demonstrates that adapting ICNNs for use in building MPC, with additional constraints to achieve a convex input-output relationship for multi-step predictions, can effectively minimize heating/cooling energy consumption while maintaining comfortable room temperatures in real-life experiments.

The literature review emphasizes NNs' potential for constructing convex and continuous learning-based models, which can be highly beneficial in MPC applications. To this aim, we employ a recursive multi-step learning-based dynamical modeling framework for controlling dynamic systems based on the work in [20]. We demonstrate that the resulting learning-based model remains convex and continuous when additional constraints are imposed on the NN structure and weights and can, therefore, be used to define convex and continuous MPC problems.

Unlike the approaches in [17] and [19], which employ multi-shot multi-step predictions, the presented solution has two significant advantages. Firstly, the MPC optimization problem is convex using input convex networks, eliminating issues with multiple suboptimal local minima. Secondly, due to the recursive multi-step architecture, the model identification phase is more straightforward, allowing for less time-consuming and faster identification of the network parameters, as recurrent model training is much more computationally demanding and time-consuming than obtaining the simple one-step-ahead predictor.

To evaluate the accuracy of the proposed networks, we compare their performance with a real-world case study in a warehouse located in the Ballen Marina, Samso, Denmark and equipped with a smart HVAC system. Our experiments demonstrate that the proposed approach can keep room temperatures within comfort constraints while minimizing heating/cooling energy consumption.

The rest of the paper is organized as follows. In Section 7.2 we introduce the MPC architecture and show the beneficial aspect of convexity. Section 7.3 reviews previous NN structures for MPC applications and their limitations in keeping convexity, leading to the introduction of the proposed multi-step learning-based dynamical modeling framework. In Section 7.4 we introduce the experimental case study and discuss the results. Conclusions are drawn in Section 7.5, highlighting possible future research directions.

7.2 Problem Statement

We are interested in controlling a generic discrete-time dynamic system of the form:

$$\mathbf{x}(h+1) = f(\mathbf{x}(h), \mathbf{u}(h), \mathbf{d}(h)), \tag{7.1}$$

through an MPC approach, where $h \in \mathbb{N}$ denotes a generic time step, $\mathbf{x}(h) \in \mathbb{R}^n$ denotes the state vector, $\mathbf{u}(h) \in \mathbb{R}^m$ denotes the input vector, and $\mathbf{d}(h) \in \mathbb{R}^q$ is a vector representing disturbances, for some $n, m, q \in \mathbb{N}$. The (possibly nonconvex) dynamics of the system are defined by the mappings $f : \mathbb{R}^n \times \mathbb{R}^m \times \mathbb{R}^q \to \mathbb{R}^n$.

We define $\mathcal{H}_k := \{k, ..., h, ..., k+H-1\}$ as H-steps prediction horizon for the MPC scheme, starting at time step k, with a fixed and constant step-size. We further assume that the control horizon equals the prediction horizon[1].

Given the system in (7.1), the objective of MPC is to solve a constrained optimal control problem over the control horizon $\mathcal{H}_k$, to select a sequence of control inputs $\mathbf{u}_k = \text{col}(\mathbf{u}(h|k))_{h\in\mathcal{H}_k} \in \mathbb{R}^{mH}$ that minimizes (maximize) a given cost (payoff) function. At the same time, the dynamics of the system $\mathbf{x}_k = \text{col}(\mathbf{x}(h|k))_{h\in\mathcal{H}_k} \in \mathbb{R}^{nH}$, using the current state $\mathbf{x}(k|k)$ as the initial state for the horizon $\mathcal{H}_k$.

In the so-called *economic formulation* of MPC [23], the control problem at the generic time step k can be formally written as follows:

$$\underset{\mathbf{u}_k}{\text{minimize}} \sum_{h\in\mathcal{H}_k} C(\mathbf{x}(h|k), \mathbf{u}(h|k)) + M(\mathbf{x}(k+H|k)) \tag{7.2a}$$

$$\text{subject to } \mathbf{x}(h|k) = f(\mathbf{x}(h|k), \mathbf{u}(h|k), \mathbf{d}(h|k)), \quad \forall h \in \mathcal{H}_k \tag{7.2b}$$

$$\mathbf{x}_k \in \mathcal{X}, \quad \mathbf{u}_k \in \mathcal{U}, \tag{7.2c}$$

where $C : \mathbb{R}^n \times \mathbb{R}^m \to \mathbb{R}$ and $M : \mathbb{R}^n \to \mathbb{R}$ are the so-called stage and terminal costs while sets $\mathcal{X} \subset \mathbb{R}^n$ and $\mathcal{U} \subset \mathbb{R}^m$ collect all feasible states and feasible control inputs, respectively.

At every time instant k, the state of the system $\mathbf{x}(k|k)$ is measured, and (7.2) is solved, i.e., an optimal input sequence $\mathbf{u}_k^*$ is obtained. The controller then applies the first element $\mathbf{u}^*(k+1|k)$ to the system, and the process is repeated. It should be noted that, in the general form of an MPC problem, the cost functions $C(\cdot)$ and $M(\cdot)$, the feasible sets $\mathcal{X}$ and $\mathcal{U}$, and the function representing the dynamics of the system $f(\cdot)$ can also be dependent on the time step k.

The optimization problem (7.2) is generally a nonconvex programming problem. However, in many practical scenarios, it is often approximated or assumed to be convex for computational tractability [24]. A common way to formulate convex MPC schemes is assuming the system dynamics $f(\cdot)$ to be convex and using linear or quadratic cost functions $C(\cdot)$ and $M(\cdot)$ and convex feasible sets $\mathcal{X}$ and $\mathcal{U}$, usually defined by affine functions. This formulation leads to a problem that may be rewritten in the following form:

$$\underset{\mathbf{u}_k}{\text{minimize}} \sum_{h\in\mathcal{H}_k} C\left(\mathbf{x}(h|k), \mathbf{u}(h|k)\right) + M(\mathbf{x}(k+H|k)) \tag{7.3a}$$

$$\text{subject to } \mathbf{x}(h|k) = f(\mathbf{x}(h|k), \mathbf{u}(h|k), \mathbf{d}(h|k)), \quad \forall h \in \mathcal{H}_k \tag{7.3b}$$

$$\mathbf{x}_{\min} \leq \mathbf{x}(h|k) \leq \mathbf{x}_{\max}, \quad \forall h \in \mathcal{H}_k \tag{7.3c}$$

$$\mathbf{u}_{\min} \leq \mathbf{u}(h|k) \leq \mathbf{u}_{\max}, \quad \forall h \in \mathcal{H}_k \tag{7.3d}$$

where $\mathbf{u}_{\min}, \mathbf{u}_{\max} \in \mathcal{U}$ are lower and upper input constraints, respectively, while $\mathbf{x}_{\min}, \mathbf{x}_{\max} \in \mathcal{X}$ are lower and upper state constraints, respectively.

[1] In MPC, the prediction horizon defines how far into the future the system looks ahead from its current state, while the control horizon, typically shorter, is the time period over which the control strategy is computed. Selecting a longer prediction horizon results in weaker control inputs, leading to a long-term transition of the system toward the desired condition. On the other hand, a shorter prediction horizon leads to more aggressive control inputs. Hence, the lengths of these two horizons are crucial in ensuring the stability and effectiveness of the overall MPC scheme (See [21] and [22]).

7.3 Input Convex Lipschitz NNs for Multi-step MPC

Many real-world systems are nonlinear and nonconvex, making it challenging to solve the optimization problem (7.2) using off-the-shelf techniques. In such cases, it is common to identify a simple linear or linearized model that can be used for control despite its lower representation capability. Learning-based models, such as NNs, can bridge the gap between model accuracy and control tractability. Indeed, in NN-based modeling, the system dynamics is approximated by a network that takes the system state, control signal, and disturbances as input and predicts the future states.

More in detail, a NN able to describe the dynamics of a discrete-time system at time step k, and therefore predict the state of the system in the next time instant $\hat{\mathbf{x}}(k+1)$, can be represented by the following general relation:

$$\hat{\mathbf{x}}(k+1) = \hat{f}(\mathbf{x}(k), \mathbf{u}(k), \mathbf{d}(k)) \tag{7.4}$$

where $\hat{\mathbf{x}}(k+1)$ is the predicted state of the system in the subsequent time step and $\hat{f}(\cdot)$ is the NN.

The NN $\hat{f}(\cdot)$ may still be nonconvex. One way to address this issue is to employ a NN such that the scalar output of the network is convex with respect to all input features. Thus, let us consider a feed-forward NN, a network where information moves in only one direction with no cycles or loops [25]. Let $\mathcal{L}$ be the set of NNs' layers, and let $P_l \in \mathbb{N}$ be the number of neurons associated to layer $l \in \mathcal{L}$. The output of each layer $\mathbf{x}_l \in \mathbb{R}^{P_l}$ can be computed as:

$$\mathbf{x}_l = \Phi_l \left(\mathbf{W}_l \mathbf{x}_{l-1} + \mathbf{b}_l \right), \quad \forall l \in \mathcal{L} \tag{7.5}$$

where $\mathbf{W}_l \in \mathbb{R}^{P_l \times P_{l-1}}$ is the weight matrix, $\mathbf{b}_l \in \mathbb{R}^{P_l}$ the bias vector and $\Phi_l : \mathbb{R}^{P_l} \to \mathbb{R}^{P_l}$ the activation function of the layer. Weights and biases are the parameters that define the function approximator, and their values are identified through a data-driven optimization process known as training [26]. During training, weights and biases are modified to minimize a loss function, typically representing the discrepancy between the predicted outputs and targets in a given dataset.

By setting $\mathbf{x}_0 \in \mathbb{R}^{P_0}$ as the input and $\mathbf{x}_L \in \mathbb{R}^{\mathcal{P}_L}$ as the output of the NN, we can define the overall input-output relationship of the network $\Phi : \mathbb{R}^{P_0} \to \mathbb{R}^{\mathcal{P}_L}$ in the following form:

$$\mathbf{x}_L = \Phi \left(\mathbf{x}_0 \right) \tag{7.6}$$

where $\Phi(\cdot) = \Phi_L \circ \Phi_{L-1} \circ \cdots \circ \Phi_1(\cdot)$.

Let us focus on a specific class of layers and activation functions.

Assumption 7.3.1

Assume that the following properties in Assumption 6.2.3 hold for each layer of the network $l \in \mathcal{L}$. Moreover, we add the follwing ones:

i) *Given $\mathbf{x}_l, \mathbf{z}_l \in \mathbb{R}^{P_l}$:*

$$\| \Phi_l \left(\mathbf{x}_{l-1} \right) - \Phi_l \left(\mathbf{z}_{l-1} \right) \| \leq \| \mathbf{x}_{l-1} - \mathbf{z}_{l-1} \|. \tag{7.7}$$

ii) *Given $\mathbf{x}_l, \mathbf{z}_l \in \mathbb{R}^{P_l}$ and $\forall\ \lambda \in (0,1)$:*

$$\Phi_l \left(\lambda \mathbf{x}_{l-1} + (1-\lambda) \mathbf{z}_{l-1} \right) \leq \lambda \Phi_l(\mathbf{x}_{l-1}) + (1-\lambda) \Phi_l(\mathbf{z}_{l-1}). \tag{7.8}$$

Note that Assumption ii) holds with equality, being the feed-forward step at $l \in \mathcal{L}$ affine with respect to the output at the previous later $l-1$. Assumption ii) asserts, in other words, that the activation function employed in each layer must be a non-expansive mapping.

A feed-forward NN respecting Assumption 6.2.3 is said to be an Input Convex Lipschitz NN (ICLNN).

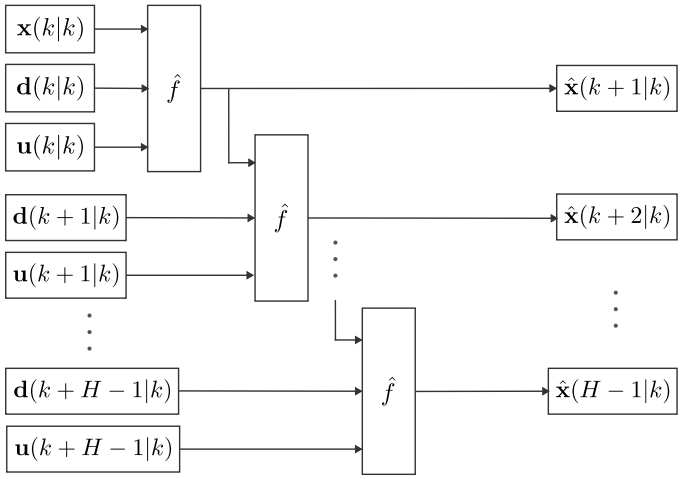

Figure 7.1: Multi-step input convex Lipschitz neural network.

Lemma 7.3.1

A feed-forward NN (7.6) *respecting Assumption 7.3.1 is convex and Lipschitz continuous map with constant* $\gamma = \prod_{l \in \mathcal{L}} \gamma_l$.

Proof 7.3.1

By the composition property of convex and Lipschitz functions the map $\Phi(\cdot) = \Phi_L \circ \Phi_{L-1} \circ \cdots \circ \Phi_1(\cdot)$ *is convex and Lipschitz continuous with a constant* $\gamma = \prod_{l \in \mathcal{L}} \gamma_l$, *being* γ_l *the Lipschitz constant of the layer* $l \in \mathcal{L}$. ■

Informally speaking, the output of a NN is a convex and Lipschitz continuous function with respect to the input if (i) all $\mathbf{W}_l$ are non-negative matrices with their spectrum bounded by 1 and (ii) all $\Phi_l(\cdot)$ are constrained to be convex, non-decreasing, and Lipschitz continuous functions. These constraints can be enforced by performing weight clipping during the training of the network and using activation functions that are both convex and non-decreasing, such as the Rectified Linear Unit (ReLU), LeakyReLU, Exponential Linear Unit (ELU) LogSumExp, and Softplus.

Remark 7.3.1

We remark that the term convex refers to the convexity of the network map. Indeed, training a convex NN is still a (possibly) nonconvex problem.

Convexity in NNs provides a useful tool for approximating the model dynamics, leading to faster and more reliable MPC control, while Lipschitz continuity implies their resilience against input perturbations.

When a ICLNN is used to predict the state of a system in the subsequent time step convexity is guaranteed, however, for subsequent steps are not guaranteed to be so. For example, the generic state at time step $k+1$ can be written as:

$$\hat{\mathbf{x}}(k+1) = \hat{f}(\hat{f}(\mathbf{x}(k-1), \mathbf{u}(k-1), \mathbf{d}(k-1)), \mathbf{u}(k), \mathbf{d}(k))$$

that is thus not guaranteed to be convex both with respect to $\mathbf{u}(k)$ and $\mathbf{u}(k-1)$.

To address this issue, we propose a feed-forward recursive multi-step NN architecture. This type of NN utilizes a recursive architecture to predict multiple future time steps of a time series. Specifically, the output of a feed-forward NN at each time step is used as input for the next time step prediction. Moreover, predictions also rely on some manipulated variable values that were calculated and applied to the process at previous sampling instants.

More precisely, the prediction of the output variable $\mathbf{x}(k)$ is a one-step-ahead prediction that recursively depends on the previous predictions of $\mathbf{x}(k-1)$, $\mathbf{x}(k-2)$, and so on. The idea behind this approach is illustrated in Figure 7.1 and can be expressed formally as follows:

$$\hat{\mathbf{x}}(h) = \hat{F}\left(\mathbf{x}(h), \mathbf{u}(h), \mathbf{d}(h)\right) \tag{7.9}$$

where $\hat{F}$ is the multi-step recursive NN.

The question at hand is whether the convexity of the network is preserved not only for the input at time k, but also for the input at the previous time instant. The results are presented as follows:

Proposition 7.3.1

Each element of the vector output $\hat{\mathbf{x}}(h)$ of the function $\hat{F}$ is convex and Lipschitz continuous in $\mathbf{u}(h)$ provided that each NN used for the single step prediction is convex and Lipschitz continuous.

The proof follows from the vector composition of convex Lipschitz functions [24]. As a result, the predictions of the controlled variables are convex functions of all arguments of the model. This approach allows us to identify the network parameters in a less time-consuming and straightforward manner, as recurrent model training is much more computationally demanding and time-consuming than obtaining the simple one-step-ahead predictor. Nevertheless, the resulting models are susceptible to noise and improper selection of the model order of dynamics; prediction errors are propagated. These factors may lead to inaccurate predictions and low control quality of MPC.

7.4 Numerical Results

In this section, we explore the effectiveness of the proposed approach against a traditional first-order dynamical model and a standard NN. Specifically, the case study aims to investigate the application of the proposed recursive multi-step ICLNN for temperature control in a warehouse in the Ballen Marina, Samso, Denmark. The building is not continuously occupied; however, sailors and locals often use it as a common meeting place. The internal temperature of the warehouse is not kept constant throughout the year. Instead, it is lowered at night and raised in the morning to save energy. The temperature is kept relatively low, and individuals manually adjust the set point using a hand terminal when necessary. However, a schedule ensures that it automatically falls back to the previously set temperature. The temperature is allowed to drop to 10 degrees Celsius to prevent mold. The warehouse is heated/cooled by a heat pump powered mainly by electricity from a photovoltaic (PV) panel on the roof and an ESS. Two thermometers inside the warehouse provide temperature and humidity every fifteen minutes, while the data related to the hourly energy consumption of the heat pump are available from the device. The data related to the external weather conditions have been retrieved from [27]. The average monthly outdoor temperature was in the range 3.5 - 16.9 degrees Celsius (38 - 62 degrees Fahrenheit) in 2023.

Data have been preprocessed, empty data has been removed, and the time series of the different sources has been aligned. The resulting dataset consists of various features for each time step h, such as:

- Internal temperature $T_i(h)$
- External temperature $T_e(h)$
- Internal humidity $U_i(h)$
- External humidity $U_e(h)$
- Energy used for heating/cooling $e(h)$
- Wind speed $S(h)$.

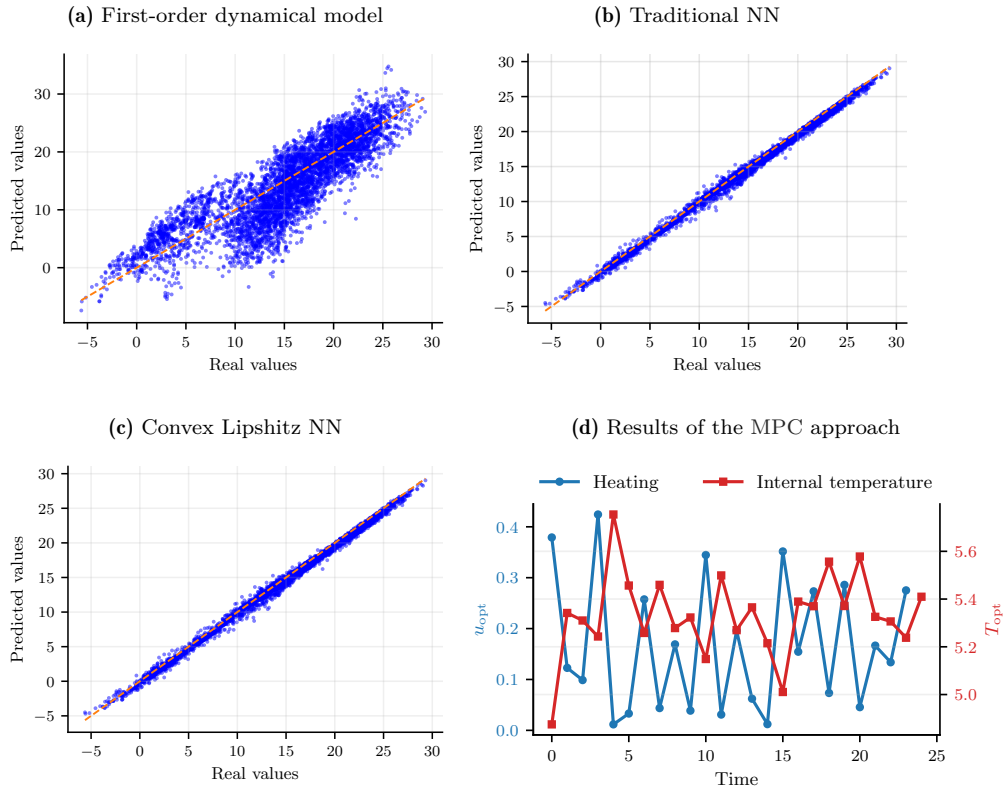

Figure 7.2: Results of the different models and the MPC contoller.

Thus, the feature tuple is defined as $X_a(h) = (T_e(h), T_e(h), U_i(h), U_e(h), S(h), e(h))$. To ensure the model's effectiveness, we augment the feature matrix by appending its negation, resulting in $X(h) = (X_a(h), -X_a(h))$, a technique commonly used to preserve representation capabilities, specifically in our case, as we impose non-negative weights. The internal temperature at the subsequent time slot $T_i(h+1)$ has been selected as the target value.

The dataset is randomly divided into training and test sets with a ratio of $20\% - 80\%$. Training is carried out using the ADAM algorithm for 100 epochs [28]. We compare a traditional NN and the proposed ICLNN consisting of three hidden layers with 120 neurons each. While the first two layers of the traditional NN employ ReLU activation functions, the third layer uses a sigmoid function. Conversely, the convex NN exclusively uses ReLU activation functions to preserve convexity.

For result comparison, we fit the data with a first-order dynamical linear model, where the state represents the internal temperature, and the input corresponds to the heating/cooling energy while considering external temperature disturbances.

The results of the training are depicted in Fig 7.2. Notably, NNs exhibit superiority over the standard model. While the ICLNN yields slightly worse results than the standard one, the overall performance remains satisfactory.

Subsequently, employing the Lipschitz convex NN, we apply the MPC approach considering environmental disturbances and dynamic energy prices. We set the control horizon length to $H = 24$, defining the energy cost as $c(h)$. The total cost for the horizon is denoted as $\mathbf{c}_k = \text{col}(c(h))_{h \in \mathcal{H}_k}$. The resulting problem is defined as:

$$\underset{\mathbf{u}_k}{\text{minimize}} \sum_{h \in \mathcal{H}_k} c(h|k)u(h|k) \tag{7.10a}$$

$$\text{subject to } T(h+1|k) = \hat{f}(T(h|k), \mathbf{u}(h|k)), \qquad \forall h \in \mathcal{H}_k \tag{7.10b}$$

$$T_{\min} \leq T(h|k) \leq T_{\max}, \qquad \forall h \in \mathcal{H}_k \tag{7.10c}$$
$$\mathbf{u}_{\min} \leq \mathbf{u}(h|k) \leq \mathbf{u}_{\max}, \qquad \forall h \in \mathcal{H}_k \tag{7.10d}$$

where $T_{\min} = 5$, $T_{\max} = 15$, $\mathbf{u}_{\min} = \mathbf{0}$ and $\mathbf{u}_{\max} = \mathbf{1}$. The results of the proposed MPC approach are shown in Fig. 4.2 where the internal temperature of the building in one simulation day is plotted with respect to the heating. The results show that the proposed approach is able to keep the temperature within the given bounds while minimizing the total cost of the energy.

7.5 Conclusion

In this work, we proposed a novel approach for controlling dynamical systems with MPC using a convex learning-based modeling framework based on Input Convex Lipschitz Neural Networks. The proposed approach offers advantages in terms of reduced computational complexity and straightforward model identification. The experimental results conducted in a smart building demonstrate the effectiveness of the proposed approach in achieving optimal control while maintaining comfort constraints and minimizing energy consumption.

Ongoing research will focus on more general formulations of the proposed framework including uncertainty.

References

[1] Rawlings, J. B. and Amrit, R., "Optimizing process economic performance using model predictive control," *Nonlinear Model Predictive Control: Towards New Challenging Applications*, pp. 119–138, 2009.

[2] Hermansson, A. W. and Syafiie, S., "Model predictive control of ph neutralization processes: A review," *Control Engineering Practice*, vol. 45, pp. 98–109, 2015.

[3] Liu, C., Lee, S., Varnhagen, S., and Tseng, H. E., "Path planning for autonomous vehicles using model predictive control," in *2017 IEEE Intelligent Vehicles Symposium (IV)*, IEEE, 2017, pp. 174–179.

[4] Vajedi, M. and Azad, N. L., "Ecological adaptive cruise controller for plug-in hybrid electric vehicles using nonlinear model predictive control," *IEEE Transactions on Intelligent Transportation Systems*, vol. 17, no. 1, pp. 113–122, 2015.

[5] Bersani, C., Fossa, M., Priarone, A., Sacile, R., and Zero, E., "Model predictive control versus traditional relay control in a high energy efficiency greenhouse," *Energies*, vol. 14, no. 11, p. 3353, 2021.

[6] Yao, Y. and Shekhar, D. K., "State of the art review on model predictive control (MPC) in heating ventilation and air-conditioning (hvac) field," *Building and Environment*, vol. 200, p. 107 952, 2021.

[7] Bünning, F., Huber, B., Heer, P., Aboudonia, A., and Lygeros, J., "Experimental demonstration of data predictive control for energy optimization and thermal comfort in buildings," *Energy and Buildings*, vol. 211, p. 109 792, 2020. DOI: 10.1016/j.enbuild.2020.109792.

[8] Cheng, L., Liu, W., Hou, Z.-G., Yu, J., and Tan, M., "Neural-network-based nonlinear model predictive control for piezoelectric actuators," *IEEE Transactions on Industrial Electronics*, vol. 62, no. 12, pp. 7717–7727, 2015.

[9] Pimenidis, E. and Jayne, C., *Special issue on engineering applications of neural networks*, 2020. DOI: 10.1007/s00521-020-05028-w.

[10] Silver, D., Schrittwieser, J., Simonyan, K., *et al.*, "Mastering the game of Go without human knowledge," *Nature*, vol. 550, no. 7676, pp. 354–359, 2017. DOI: 10.1038/nature24270. arXiv: 1610.00633.

[11] Benattia, S. E., Tebbani, S., and Dumur, D., "Linearized min-max robust model predictive control: Application to the control of a bioprocess," *International Journal of Robust and Nonlinear Control*, vol. 30, no. 1, pp. 100–120, 2020.

[12] Adajania, V. K., Sharma, A., Gupta, A., Masnavi, H., Krishna, K. M., and Singh, A. K., "Multi-modal model predictive control through batch non-holonomic trajectory optimization: Application to highway driving," *IEEE Robotics and Automation Letters*, vol. 7, no. 2, pp. 4220–4227, 2022.

[13] Lucia, S., Navarro, D., Lucia, O., Zometa, P., and Findeisen, R., "Optimized fpga implementation of model predictive control for embedded systems using high-level synthesis tool," *IEEE transactions on industrial informatics*, vol. 14, no. 1, pp. 137–145, 2017.

[14] Seel, K., Kordabad, A. B., Gros, S., and Gravdahl, J. T., "Convex neural network-based cost modifications for learning model predictive control," *IEEE Open Journal of Control Systems*, vol. 1, pp. 366–379, 2022.

[15] Calafiore, G. C., Gaubert, S., and Possieri, C., "Log-sum-exp neural networks and posynomial models for convex and log-log-convex data," *IEEE transactions on neural networks and learning systems*, vol. 31, no. 3, pp. 827–838, 2019.

[16] Amos, B., Xu, L., and Kolter, J. Z., "Input Convex Neural Networks," in *34th International Conference on Machine Learning, ICML 2017*, vol. 1, PMLR, 2017, pp. 192–206.

[17] Chen, Y., Shi, Y., and Zhang, B., "Optimal control via neural networks: A convex approach," in *7th International Conference on Learning Representations, ICLR 2019*, 2019.

[18] Todorov, E., Erez, T., and Tassa, Y., "MuJoCo: A physics engine for model-based control," in *IEEE International Conference on Intelligent Robots and Systems*, 2012, pp. 5026–5033. DOI: 10.1109/IROS.2012.6386109.

[19] Bünning, F., Schalbetter, A., Aboudonia, A., Badyn, M. H. de, Heer, P., and Lygeros, J., "Input convex neural networks for building MPC," in *Learning for Dynamics and Control*, PMLR, 2021, pp. 251–262.

[20] Wang, Z., Pravin, P., and Wu, Z., "Input convex lipschitz RNN: A fast and robust approach for engineering tasks," *arXiv preprint arXiv:2401.07494*, 2024.

[21] Müller, M. A. and Worthmann, K., "Quadratic costs do not always work in MPC," *Automatica*, vol. 82, pp. 269–277, 2017.

[22] Li, P., Kang, Y., Zhao, Y.-B., and Wang, T., "Networked dual-mode adaptive horizon MPC for constrained nonlinear systems," *IEEE Transactions on Systems, Man, and Cybernetics: Systems*, vol. 51, no. 12, pp. 7435–7449, 2020.

[23] Zwickel, P., Engelmann, A., Gröll, L., Hagenmeyer, V., Sauer, D., and Faulwasser, T., "A comparison of economic MPC formulations for thermal building control," in *2019 IEEE PES Innovative Smart Grid Technologies Europe (ISGT-Europe)*, IEEE, 2019, pp. 1–5.

[24] Boyd, S., Boyd, S. P., and Vandenberghe, L., *Convex optimization*. Cambridge university press, 2004.

[25] Seo, J., Lee, J., and Kim, K., "Decoding of polar code by using deep feed-forward neural networks," in *2018 international conference on computing, networking and communications (ICNC)*, IEEE, 2018, pp. 238–242.

[26] Solarte, B., Wu, C.-H., Liu, Y.-C., Tsai, Y.-H., and Sun, M., "360-mlc: Multi-view layout consistency for self-training and hyper-parameter tuning," *Advances in Neural Information Processing Systems*, vol. 35, pp. 6133–6146, 2022.

[27] *Free Open-Source Weather API | Open-Meteo.com*, [Online; accessed 31. Mar. 2024], Mar. 2024. [Online]. Available: https://open-meteo.com.

[28] Jais, I. K. M., Ismail, A. R., and Nisa, S. Q., "Adam optimization algorithm for wide and deep neural network.," *Knowl. Eng. Data Sci.*, vol. 2, no. 1, pp. 41–46, 2019.

Chapter 8

Conclusions

The modern energy community is comprised by deeply interconnected agents and devices, each characterized by its own prerogatives and needs. In such an environment, considering each actor as an independent and selfish entity guarantees robust design choices for the overall grid. However, under such premises, finding the *working point* of such systems is not an easy task. Scalability, reliability, and latency, which are the requirements for ensuring quality-of-service of the contemporary energy infrastructure. In such a context, non-cooperative game theoretical methods have proven to be effective in the modelling and analysis of grids.

This Thesis tried to contribute to the field by exploring three main research directions. Specifically, the first research direction, discussed in Part I, provided a perspective on the energy community as a transactive environment, where the focus is put on devising appropriate strategies to seek Nash Equilibria for the exchange of energy. In particular:

- Chapter 2 provided a transactive framework where community members have private cost functions coupled through their aggregate demands. To solve the arising Generalized Nash Equilibrium Problem (GNEP) in a distributed fashion, alternating direction method of multipliers (ADMM) algorithm was formulated using Gauss-Seidel-type iterate, reformulating the GNEP into two parallel blocks: energy transactions computation and prices update to overcome scalability issues. Sufficient conditions on cost and pricing functions were provided to ensure strong monotonicity of the pseudo-gradient mapping, guaranteeing convergence of the ADMM algorithm;
- Chapter 3 proposed innovative transactive control frameworks to optimize energy sharing and management in a community with multiple prosumers (energy producers/consumers) and independent storage providers. The goal was to create an efficient and profitable business model for the storage providers while ensuring a sustainable energy supply for the prosumers. Two game-theoretical algorithms were proposed, one coordinated and one uncoordinated, which were validated through numerical simulations and compared favorably with a centralized control method.

The second research direction, whose results have been collected in Part II, explores the integration of plug-in electric vehicles (PEVs) in the modern energy community as selfish agents characterized, on the one hand, by the need to periodically recharge their batteries, and on the other hand, by the possibility of being used as temporary energy storage systems. Specifically:

- Chapter 4 proposed an innovative Model Predictive Control (MPC) approach that leverages the vast amounts of data collected by modern PEVs. This approach enables prosumers to utilize long-parked EVs as energy buffers, while also providing recharging capabilities for active PEVs. The resulting control problem was formulated as a generalized Nash equilibrium, addressed using variational inequality theory and the accelerated distributed augmented Lagrangian method, ensuring sufficient conditions for convergence;
- Chapter 5 devised a novel hybrid control system for dynamic power allocation in a fleet of PEVs fed by a single energy retailer with limited power availability. The controller, based on population dynamics and event-triggered principles, ensures that the PEVs' batteries reach a stable equilibrium where all connected vehicles are fully charged while satisfying operational constraints. Precedence functions are used to express economic and performance indicators of the PEVs, aiming for a NE

in power allocation among them. This enables local information exchange without requiring vehicle-to-vehicle infrastructure.

In order to better model the grid's actors that are not (generally) driven by rational stances, e.g., people, Part III introduces a learning-based equilibrium concept that relies on modelling the agents through machine learning tools, e.g., neural networks, in order to capture their behavior in a more expressive form than the one provided by the traditional optimization-based methods.

- The goal of Chapter 6 was to combine game theory with machine learning techniques to approximate complex agent behaviors. Unlike traditional approaches, this method does not model agents' ultimate goals as cost functions, but instead uses a NN to characterize their response actions. By introducing certain assumptions on the used neural network weights, an equilibrium was proved to be reachable and unique. Two algorithms based on fixed-point iterations are defined to compute these equilibria, with convergence proven. The theoretical results are applied to an energy community under dynamic time-of-use pricing.
- A recursive multi-step learning-based dynamical modeling framework is employed in Chapter 7 for controlling dynamic systems. When certain constraints are imposed on the NN structure, it can be used to define convex MPC problems. Differently from existing literature, it uses input-convex networks, which eliminate issues with multiple suboptimal local minima, and a recursive multi-step architecture that simplifies model identification and reduces computational demands. The proposed method is evaluated through a case study at a warehouse in Denmark equipped with a smart HVAC system, demonstrating its ability to maintain comfortable room temperatures while minimizing energy consumption.

The results collected in this Thesis scratch the surface of the many challenges that incorporating non-cooperative game-theoretical approaches in the energy community brings. All the seeking algorithms employed so far suffer from the common issue of reaching a feasible solution – other than an equilibrium – asymptotically, so that operative tolerances need to be defined *a priori* to sure the correct functioning of the grid. Part II dealt with the stochasticity of arrival and departure time of PEVs, under the assumption of known distributions *with good confidence*. Alternative more robust approaches will be explored in future works, e.g., employing tools from distributionally robust optimization. Being Part III a work-in-progress itself, future effort will focus on extending the learning-based approach to the GNE seeking case.

Appendices

Appendix A

Proofs

A.1 Proposition 2.3.1

Under the considered setup

$$\mathbf{q}\left(\hat{\mathbf{x}},\check{\mathbf{x}},\mathbf{p}\right)=\begin{bmatrix}\tilde{\nabla}_{\hat{\mathbf{x}}}\boldsymbol{\psi}+\mathbf{B}\mathbf{p}\\ \tilde{\nabla}_{\check{\mathbf{x}}}\boldsymbol{\psi}-\mathbf{p}\\ \rho\mathbf{p}-\rho\mathbf{Q}\mathbf{B}\hat{\mathbf{x}}\end{bmatrix},$$

where we have used $\mathbf{p}_{-i}=\mathbf{B}_i\mathbf{p}$, $\hat{\mathbf{x}}_{-i}=\mathbf{B}_i\hat{\mathbf{x}}$, and we have defined $\mathbf{Q}=\operatorname{diag}\left(\mathbf{Q}_i\right)_{i\in\mathcal{A}}\in\mathbb{R}^{n\times n}_{\geq 0}$ and

$$\begin{aligned}\tilde{\nabla}_{\hat{\mathbf{x}}}\boldsymbol{\psi}&:=\operatorname{col}\left(\nabla_{\hat{\mathbf{x}}_i}\psi_i\left(\hat{\mathbf{x}}_i,\check{\mathbf{x}}_i\right)\right)_{i\in\mathcal{A}}\\ \tilde{\nabla}_{\check{\mathbf{x}}}\boldsymbol{\psi}&:=\operatorname{col}\left(\nabla_{\check{\mathbf{x}}_i}\psi_i\left(\hat{\mathbf{x}}_i,\check{\mathbf{x}}_i\right)\right)_{i\in\mathcal{A}}.\end{aligned}$$

Since every $\psi_i(\cdot,\cdot)$ is twice continuously differentiable, it follows that $\mathbf{q}(\cdot,\cdot,\cdot)$ is μ-strongly monotone if it holds that

$$\mathrm{D}\,\mathbf{q}\left(\hat{\mathbf{x}},\check{\mathbf{x}},\mathbf{p}\right)+\mathrm{D}\,\mathbf{q}\left(\hat{\mathbf{x}},\check{\mathbf{x}},\mathbf{p}\right)^{\top}-2\mu\mathbf{I}_{3n}\succeq 0, \tag{A.1}$$

for all $\hat{\mathbf{x}},\check{\mathbf{x}},\mathbf{p}\in\mathbb{R}^n_{\geq 0}$. Here,

$$\mathrm{D}\,\mathbf{q}\left(\hat{\mathbf{x}},\check{\mathbf{x}},\mathbf{p}\right)=\begin{bmatrix}\mathrm{D}_{\hat{\mathbf{x}}}\tilde{\nabla}_{\hat{\mathbf{x}}}\boldsymbol{\psi} & \mathrm{D}_{\check{\mathbf{x}}}\tilde{\nabla}_{\hat{\mathbf{x}}}\boldsymbol{\psi} & \mathbf{B}\\ \mathrm{D}_{\hat{\mathbf{x}}}\tilde{\nabla}_{\check{\mathbf{x}}}\boldsymbol{\psi} & \mathrm{D}_{\check{\mathbf{x}}}\tilde{\nabla}_{\check{\mathbf{x}}}\boldsymbol{\psi} & -\mathbf{I}_n\\ -\rho\mathbf{Q}\mathbf{B} & \mathbf{0}_{n\times n} & \rho\mathbf{I}_n\end{bmatrix}\in\mathbb{R}^{3n\times 3n}.$$

Denote the top left $2n\times 2n$ block of $\mathrm{D}\,\mathbf{q}\left(\hat{\mathbf{x}},\check{\mathbf{x}},\mathbf{p}\right)$ as $\mathbf{J}\left(\hat{\mathbf{x}},\check{\mathbf{x}}\right)$. It follows that $\mathbf{J}\left(\hat{\mathbf{x}},\check{\mathbf{x}}\right)$ is the Hessian matrix of the function $\varphi(\hat{\mathbf{x}},\check{\mathbf{x}})=\sum_{i\in\mathcal{A}}\psi_i\left(\hat{\mathbf{x}}_i,\check{\mathbf{x}}_i\right)$. Therefore, $\mathbf{J}\left(\hat{\mathbf{x}},\check{\mathbf{x}}\right)=\mathbf{J}\left(\hat{\mathbf{x}},\check{\mathbf{x}}\right)^{\top}$ and $\boldsymbol{\zeta}^{\top}\mathbf{J}\left(\hat{\mathbf{x}},\check{\mathbf{x}}\right)\boldsymbol{\zeta}\geq\underline{\theta}\boldsymbol{\zeta}^{\top}\boldsymbol{\zeta}$, for all $\hat{\mathbf{x}},\check{\mathbf{x}}\in\mathbb{R}^n_{\geq 0}$, and all $\boldsymbol{\zeta}\in\mathbb{R}^{2n}$. Moreover, let

$$\begin{aligned}\mathbf{M}_1\left(\hat{\mathbf{x}},\check{\mathbf{x}}\right)&=\begin{bmatrix}\mathbf{J}\left(\hat{\mathbf{x}},\check{\mathbf{x}}\right)-\mu\mathbf{I}_{2n} & \begin{bmatrix}\mathbf{B}\\ -\mathbf{I}_n\end{bmatrix}\\ \begin{bmatrix}\mathbf{B}^{\top} & -\mathbf{I}_n\end{bmatrix} & (\rho-\mu)\mathbf{I}_n\end{bmatrix}\\ \mathbf{M}_2\left(\hat{\mathbf{x}},\check{\mathbf{x}}\right)&=\begin{bmatrix}\mathbf{J}\left(\hat{\mathbf{x}},\check{\mathbf{x}}\right)-\mu\mathbf{I}_{2n} & \begin{bmatrix}-\rho\mathbf{B}^{\top}\mathbf{Q}^{\top}\\ \mathbf{0}_{n\times n}\end{bmatrix}\\ \begin{bmatrix}-\rho\mathbf{Q}\mathbf{B} & \mathbf{0}_{n\times n}\end{bmatrix} & (\rho-\mu)\mathbf{I}_n\end{bmatrix}.\end{aligned}$$

As such, the condition in (A.1) can be equivalently rewritten as $\mathbf{M}_1\left(\hat{\mathbf{x}},\check{\mathbf{x}}\right)+\mathbf{M}_2\left(\hat{\mathbf{x}},\check{\mathbf{x}}\right)\succeq 0$. Hence, if $\mathbf{M}_1\left(\hat{\mathbf{x}},\check{\mathbf{x}}\right)$ and $\mathbf{M}_2\left(\hat{\mathbf{x}},\check{\mathbf{x}}\right)$ are both shown to be positive semi-definite matrices, for all $\hat{\mathbf{x}},\check{\mathbf{x}}\in\mathbb{R}^n_{\geq 0}$, then we can conclude that $\mathbf{q}(\cdot,\cdot,\cdot)$ is μ-strongly monotone.

Consider first $\mathbf{M}_1\left(\hat{\mathbf{x}},\check{\mathbf{x}}\right)$. By the Schur complement, we have that $\mathbf{M}_1\left(\hat{\mathbf{x}},\check{\mathbf{x}}\right)\succeq 0$ if and only if $\rho>\mu$ and

$$\mathbf{J}\left(\hat{\mathbf{x}},\check{\mathbf{x}}\right)-\mu\mathbf{I}_{2n}\succeq\frac{1}{\rho-\mu}\begin{bmatrix}\mathbf{B}\mathbf{B}^{\top} & -\mathbf{B}\\ -\mathbf{B}^{\top} & \mathbf{I}_n\end{bmatrix}.$$

Note that $\mathbf{J}\left(\hat{\mathbf{x}},\check{\mathbf{x}}\right)-\mu\mathbf{I}_{2n}\succeq\left(\underline{\theta}-\mu\right)\mathbf{I}_{2n}$, and

$$\frac{1}{\rho-\mu}\begin{bmatrix}\mathbf{B}\mathbf{B}^{\top} & -\mathbf{B}\\ -\mathbf{B}^{\top} & \mathbf{I}_n\end{bmatrix}\preceq\frac{2}{\rho-\mu}\mathbf{I}_{2n}.$$

Here, the second claim follows from Remark 2.3.1 and the Gershgorin Circle Theorem [1, Fact 4.10.16]. Therefore, if $\rho > \mu$ and $\underline{\theta} - \mu \geq 2/(\rho - \mu)$, then $\mathbf{M}_1(\hat{\mathbf{x}}, \check{\mathbf{x}})$ is positive semi-definite, for all $\hat{\mathbf{x}}, \check{\mathbf{x}} \in \mathbb{R}^n_{\geq 0}$.

Similarly, consider $\mathbf{M}_2(\hat{\mathbf{x}}, \check{\mathbf{x}})$. By the Schur complement, we have that $\mathbf{M}_2(\hat{\mathbf{x}}, \check{\mathbf{x}}) \succeq 0$ if and only if $\rho > \mu$ and

$$\mathbf{J}(\hat{\mathbf{x}}, \check{\mathbf{x}}) - \mu \mathbf{I}_{2n} \succeq \frac{\rho^2}{\rho - \mu} \begin{bmatrix} \mathbf{B}^\top \mathbf{Q}^\top \mathbf{Q} \mathbf{B} & \mathbf{0}_{n \times n} \\ \mathbf{0}_{n \times n} & \mathbf{0}_{n \times n} \end{bmatrix}.$$

By Remark 2.3.1, it follows that $\mathbf{B}^\top \mathbf{Q}^\top \mathbf{Q} \mathbf{B}$ is similar to $\mathbf{Q}^\top \mathbf{Q}$ and so they have the same eigenvalues. Consequently,

$$\frac{\rho^2}{\rho - \mu} \begin{bmatrix} \mathbf{B}^\top \mathbf{Q}^\top \mathbf{Q} \mathbf{B} & \mathbf{0}_{n \times n} \\ \mathbf{0}_{n \times n} & \mathbf{0}_{n \times n} \end{bmatrix} \preceq \frac{\rho^2}{\rho - \mu} \bar{\lambda} \mathbf{I}_{2n}.$$

Thus, if $\rho > \mu$ and $\underline{\theta} - \mu \geq \rho^2 \bar{\lambda}/(\rho - \mu)$, then $\mathbf{M}_2(\hat{\mathbf{x}}, \check{\mathbf{x}})$ is positive semi-definite, for all $\hat{\mathbf{x}}, \check{\mathbf{x}} \in \mathbb{R}^n_{\geq 0}$.

Hence, if $\rho > \mu$ and $\underline{\theta} - \mu \geq \max\left\{2, \rho^2 \bar{\lambda}\right\} / (\rho - \mu)$, then the conditions for the positive semi-definiteness of $\mathbf{M}_1(\cdot, \cdot)$ and $\mathbf{M}_2(\cdot, \cdot)$ are satisfied, and the proof is completed. ■

A.2 Proposition 4.4.3

First, let us recall that the coupling constraints in (4.24) can be written as $\mathbf{A}\mathbf{x} = \sum_{n \in \mathcal{N}} \mathbf{A}_n \mathbf{x}_n = \mathbf{0}$, with $\mathbf{A} = \begin{bmatrix} \mathbf{A}_1 & \cdots & \mathbf{A}_N \end{bmatrix}$, corresponding to (4.41) and partitioned in vertical blocks. Theorem 1 in [2] yields the following bound:

$$\sum_{n \in \mathcal{N}} \rho \|\mathbf{A}_n(\mathbf{x}_n^{(0)} - \mathbf{x}_n^*)\|^2 \leq \rho N \sigma_{\max}^2(\mathbf{A}) \phi^2(\mathcal{X}) + \frac{1}{\rho} \tag{A.2}$$

where $\sigma_{\max}(\mathbf{A})$ is the largest single value of $\mathbf{A}$ and $\phi(\mathcal{X})$ is the diameter of $\mathcal{X}$, evaluated as

$$\phi(\mathcal{X}) = \underset{\mathbf{x}_1, \mathbf{x}_1 \in \mathcal{X}}{\operatorname{argmax}} \|\mathbf{x}_1 - \mathbf{x}_2\| \tag{A.3}$$

Note that the previous is a non-convex problem. Inequality (A.2) can be further bounded from above as follows

$$\rho N \sigma_{\max}^2(\mathbf{A}) \phi^2(\mathcal{X}) + \frac{1}{\rho} \leq \rho N \|\mathbf{A}\|_F^2 \phi(\operatorname{box}(\mathcal{X})) + \frac{1}{\rho} \tag{A.4}$$

where $\|\mathbf{A}\|_F$ is the Frobenius norm of matrix $\mathbf{A}$, while $\operatorname{box}(\mathcal{X})$ is any finite-volume hypercube containing $\mathcal{X}$. The previous inequality holds since $\sigma_{\max}(\mathbf{A}) \leq \|\mathbf{A}\|_F$, from Definition 5.6.0.2 in [3], and $\phi(\mathcal{X}) \leq \phi(\operatorname{box}(\mathcal{X}))$. The last inequality holds since $\mathcal{X} \subseteq \operatorname{box}(\mathcal{X})$. From (4.41), $\|\mathbf{A}\|_F = \sqrt{2H(PC_t + 3PS_t)}$, corresponing to the number of nonzero elements of $\mathbf{A}$. Moreover, since $\mathbf{x}$ is non-negative, one of the hypercube's vertices corresponds to the origin, thus we have that $\phi(\operatorname{box}(\mathcal{X})) = |\max(\mathbf{x})|$. The right-hand side of (A.4) is convex with respect to ρ, so that its minimizer ρ^* is trivially calculated. After substituting $\|\mathbf{A}\|_F$ and $\phi(\operatorname{box}(\mathcal{X}))$, (4.43) is obtained.

A.3 Lemma 5.3.1

Assumption 5.3.1 readily holds with the considered $f_i(\cdot, \cdot)$ and by (5.8a). On the other hand, to show that Assumption 5.3.3 holds it suffices to take $S_i(b_i, p_i) = \alpha \eta_i(b_i, p_i) p_i^2/(2B_i)$ and

$$\begin{aligned} \zeta_i(b_i, p_i, u) = (1 - \alpha)\mu u^2 - \frac{\alpha p_i^2}{2B_i} \frac{\partial \eta_i(b_i, p_i)}{\partial p_i} u \\ - \frac{\alpha p_i^3 \eta_i(b_i, p_i)}{2B_i} \frac{\partial \eta_i(b_i, p_i)}{\partial b_i}. \end{aligned}$$

By (5.8a) it follows that $S_i(b_i,p_i)=0 \Leftrightarrow f_i(b_i,p_i)=0$. Also, since $\zeta_i(\cdot,\cdot,\cdot)$ is a convex quadratic polynomial with respect to u, a sufficient condition to ensure its non-negativity is

$$\left(\frac{\alpha p_i^2}{2B_i}\frac{\partial \eta_i(b_i,p_i)}{\partial p_i}\right)^2 \leq -4(1-\alpha)\mu\frac{\alpha p_i^3\eta_i(b_i,p_i)}{2B_i}\frac{\partial \eta_i(b_i,p_i)}{\partial b_i}.$$

Clearly, such a condition holds by (5.8) and thus we conclude that $\zeta_i(b_i,p_i,u)\geq 0$, for all $(b_i,p_i,u)\in[0,B_i]\times[0,C_i]\times\mathbb{R}$. On the other hand, it follows that

$$\begin{aligned}\frac{\partial S_i(b_i,p_i)}{\partial b_i} &= \frac{\alpha p_i^2}{2B_i}\frac{\partial \eta_i(b_i,p_i)}{\partial b_i}\\ \frac{\partial S_i(b_i,p_i)}{\partial p_i} &= \frac{\alpha p_i^2}{2B_i}\frac{\partial \eta_i(b_i,p_i)}{\partial p_i}+\frac{\alpha}{B_i}\eta_i(b_i,p_i)p_i.\end{aligned}$$

Therefore, using the fact that $f_i(b_i,p_i)=\eta_i(b_i,p_i)p_i$, we conclude that (5.7) holds (in this case with equality). ■

A.4 Theorem 5.4.1

Let us consider Claim i) first. From the jump dynamics in (5.12a)-(5.12b), for all times t where the HDS jumps it holds that if $\mathbf{p}(t)\in\mathcal{P}(t)$, then $\mathbf{p}^+(t)\in\mathcal{P}(t)$. On the other hand, for all times in between jumps, it holds that the signals $s_i(t)$ and $\hat{p}_i(t)$ are constant, for all $i\in\mathcal{C}$. Thus, for all times in between jumps the flow dynamics in (5.14a) become precisely the so-called Smith-Replicator dynamics in [4]. Therefore, by [4, Proposition 1], it follows that $\mathbf{p}(t)\in\mathcal{P}(t)$ for all times where the HDS flows. As such, Claim i) holds.

Without loss of generality, to prove Claims ii) and iii) we restrict the analyses to the times in between arrivals or departures of PEVs, which are uncontrollable and uncertain events. Hence, through the rest of this proof, we assume that $\mathcal{C}_c(t)=\mathcal{C}$, for all times $t\geq 0$. As such, the signals $\bar{b}_i(t)$, $\bar{c}_i(t)$, and $\bar{p}_i(t)$, are constant for all $i\in\mathcal{C}$. Consequently, the closed-loop system does not have any time-varying inputs. Furthermore, it can be shown that the considered closed-loop system comprises a well-posed HDS according to Definition 5.2.1, implying that a complete solution exists for all times $t\geq 0$ and all admissible initial conditions (see Section 5.2.1).

To prove Claim ii) we apply the Hybrid Lyapunov Theorem [5, Theorem 3.19] as adapted in Section 5.2.1. As such, consider the Lyapunov function candidate given by

$$\begin{aligned}V(\mathbf{b},\mathbf{p},\mathbf{s}) = W(\mathbf{b},\mathbf{p},\mathbf{s}) &+ \sum_{i\in\mathcal{C}}\left(S_i(b_i,p_i)+\frac{1}{2}(B_i-b_i)^2\right)\\ &+\beta\bar{W}\sum_{i\in\mathcal{C}}s_i,\end{aligned}$$

where $S_i(\cdot,\cdot)$ is a storage function satisfying Assumption 5.3.3, for all $i\in\mathcal{C}$, $\beta\in\mathbb{R}$ is a constant satisfying $\beta>1$, and $W(\mathbf{b},\mathbf{p},\mathbf{s})=(1/2)\sum_{i\in\mathcal{N}}\sum_{j\in\mathcal{N}}p_i s_i s_j\hat{p}_j\left[g_j-g_i\right]_+^2$, with $g_\ell=0$ and $g_i:=g_i(b_i,\mathbf{p})$, for all $i\in\mathcal{C}$. Besides, $\bar{W}=\max_{(\mathbf{x},\mathbf{u})\in\mathcal{F}}W(\mathbf{b},\mathbf{p},\mathbf{s})$ is an upper-bound of $W(\cdot,\cdot,\cdot)$ over the flow set $\mathcal{F}$ (note that such an upper-bound always exists because $W(\cdot,\cdot,\cdot)$ is continuous and $\mathcal{F}$ is compact). Moreover, from Claim i) it follows that $\mathbf{p}(t)\in\mathcal{P}(t)$, which implies that $W\left(\mathbf{b}(t),\mathbf{p}(t),\mathbf{s}(t)\right)\geq 0$, for all times $t\geq 0$. Hence, $V\left(\mathbf{b}(t),\mathbf{p}(t),\mathbf{s}(t)\right)\geq 0$, for all times $t\geq 0$, and $V\left(\mathbf{b},\mathbf{p},\mathbf{s}\right)=0$ if and only if $S_i(b_i,B_i)=0$, $b_i=B_i$, and $s_i=0$, for all $i\in\mathcal{C}$. By Assumption 5.3.3, $S_i(b_i,B_i)=0\Leftrightarrow f_i(b_i,p_i)=0$, and by Assumption 5.3.1, $f_i(b_i,p_i)=0\Leftrightarrow p_i=0$, for all $i\in\mathcal{C}$. Therefore, we conclude that $V\left(\mathbf{b}^*,\mathbf{p}^*,\mathbf{s}^*\right)=0$ if and only if $p_\ell^*=A$, $b_i^*=B_i$, $p_i^*=0$, and $s_i^*=0$, for all $i\in\mathcal{C}$. That is, $V(\cdot,\cdot,\cdot)$ is a valid Lyapunov function candidate to analyze the stability properties of the considered point $(\mathbf{b}^*,\mathbf{p}^*,\mathbf{s}^*)$, which by [6, Theorem 1] is also the unique equilibrium point of the considered dynamics.

We now proceed to analyze the time derivative of $V(\cdot,\cdot,\cdot)$ along the flow trajectories of the system. To simplify the notation, let $V:=V(\mathbf{b},\mathbf{p},\mathbf{s})$, $W:=W(\mathbf{b},\mathbf{p},\mathbf{s})$ and $\xi_{ij}:=p_i s_i s_j\hat{p}_j\left[g_j-g_i\right]_+$, for all $i,j\in\mathcal{N}$. Then, for all $z\in\mathcal{N}$,

$$\begin{aligned}\frac{\partial W}{\partial p_z} &= \frac{1}{2}\sum_{j\in\mathcal{N}} s_z s_j \hat{p}_j \left[g_j - g_z\right]_+^2 - \frac{1}{2}\sum_{i\in\mathcal{N}} p_i s_i s_z \left[g_z - g_i\right]_+^2 \\ &\quad + \sum_{i\in\mathcal{N}}\sum_{j\in\mathcal{N}} \xi_{ij}\left(\frac{\partial g_j}{\partial p_z} - \frac{\partial g_i}{\partial p_z}\right) \\ &= \frac{1}{2}\sum_{k\in\mathcal{N}} s_z s_k \left(\hat{p}_k \left[g_k - g_z\right]_+^2 - p_k \left[g_z - g_k\right]_+^2\right) \\ &\quad + \sum_{j\in\mathcal{N}}\sum_{i\in\mathcal{N}} (\xi_{ij} - \xi_{ji})\frac{\partial g_j}{\partial p_z}.\end{aligned}$$

By the fact that $\mathbf{p}(t) \in \mathcal{P}(t)$, for all times $t \geq 0$ [see Claim i)], it holds that $\hat{p}_j = \left[\hat{p}_j\right]_+$, for all $j \in \mathcal{N}$. Hence, from (5.14a) it follows that $\sum_{i\in\mathcal{N}}(\xi_{ij} - \xi_{ji}) = \dot{p}_j$. In consequence,

$$\begin{aligned}\nabla_{\mathbf{p}} V^\top \dot{\mathbf{p}} &= \sum_{z\in\mathcal{N}} \dot{p}_z \frac{\partial W}{\partial p_z} + \sum_{z\in\mathcal{C}} \dot{p}_z \frac{\partial S_z(b_z, p_z)}{\partial p_z} \\ &= \frac{1}{2}\sum_{z,k\in\mathcal{N}} \dot{p}_z s_z s_k \left(\hat{p}_k \left[g_k - g_z\right]_+^2 - p_k \left[g_z - g_k\right]_+^2\right) \\ &\quad + \sum_{z\in\mathcal{N}}\sum_{j\in\mathcal{N}} \dot{p}_z \dot{p}_j \frac{\partial g_j}{\partial p_z} + \sum_{z\in\mathcal{C}} \dot{p}_z \frac{\partial S_z(b_z, p_z)}{\partial p_z}.\end{aligned}$$

From the fact that $g_\ell = 0$ and Assumption 5.3.2, it holds that

$$\begin{aligned}\sum_{z\in\mathcal{N}}\sum_{j\in\mathcal{N}} \dot{p}_z \dot{p}_j \frac{\partial g_j}{\partial p_z} &= -\sum_{z\in\mathcal{C}}\sum_{j\in\mathcal{C}} \dot{p}_z \dot{p}_j (1-\alpha)\frac{\partial h_j(\mathbf{p})}{\partial p_z} \\ &\leq -(1-\alpha)\mu \sum_{z\in\mathcal{C}} \dot{p}_z^2 \quad \text{[c.f. Remark 5.3.1].}\end{aligned}$$

Therefore,

$$\begin{aligned}\nabla_{\mathbf{p}} V^\top \dot{\mathbf{p}} &\leq \frac{1}{2}\sum_{z,k\in\mathcal{N}} \dot{p}_z s_z s_k \left(\hat{p}_k \left[g_k - g_z\right]_+^2 - p_k \left[g_z - g_k\right]_+^2\right) \\ &\quad - (1-\alpha)\mu \sum_{z\in\mathcal{C}} \dot{p}_z^2 + \sum_{z\in\mathcal{C}} \dot{p}_z \frac{\partial S_z(b_z, p_z)}{\partial p_z}.\end{aligned}$$

Here, by replacing $\dot{p}_z = \sum_{i\in\mathcal{N}}(\xi_{iz} - \xi_{zi})$ and following the procedure in [4, Proof of Theorem 2] with the fact that $\xi_{iz} s_z s_k = \xi_{iz} s_i s_k$, for all $z, k, i \in \mathcal{N}$, it can be shown that

$$\frac{1}{2}\sum_{z,k\in\mathcal{N}} \dot{p}_z s_z s_k \left(\hat{p}_k \left[g_k - g_z\right]_+^2 - p_k \left[g_z - g_k\right]_+^2\right) \leq 0.$$

Thus, $\nabla_{\mathbf{p}} V^\top \dot{\mathbf{p}} \leq \sum_{z\in\mathcal{C}} \left(\dot{p}_z \partial S_z(b_z, p_z)/\partial p_z - (1-\alpha)\mu \dot{p}_z^2\right)$. On the other hand,

$$\begin{aligned}\nabla_{\mathbf{b}} V^\top \dot{\mathbf{b}} &= \sum_{z\in\mathcal{C}}\sum_{j\in\mathcal{N}} \dot{b}_z \dot{p}_j \frac{\partial g_j}{\partial b_z} + \sum_{z\in\mathcal{C}} \dot{b}_z \frac{\partial S_z(b_z, p_z)}{\partial b_z} \\ &\quad - \sum_{z\in\mathcal{C}} (B_z - b_z)\dot{b}_z \\ &= -\sum_{z\in\mathcal{C}} \dot{b}_z \dot{p}_z \frac{\alpha}{B_z} + \sum_{z\in\mathcal{C}} \dot{b}_z \frac{\partial S_z(b_z, p_z)}{\partial b_z} \\ &\quad - \sum_{z\in\mathcal{C}} (B_z - b_z)\dot{b}_z,\end{aligned}$$

and it trivially holds that $\nabla_{\mathbf{s}} V^\top \dot{\mathbf{s}} = 0$ [due to (5.14b)]. Thus,

$$\begin{aligned}
\dot{V} &= \nabla_{\mathbf{b}} V^\top \dot{\mathbf{b}} + \nabla_{\mathbf{p}} V^\top \dot{\mathbf{p}} + \nabla_{\mathbf{s}} V^\top \dot{\mathbf{s}} \\
&\leq \sum_{z\in\mathcal{C}} \frac{\partial S_z(b_z,p_z)}{\partial b_z}\dot{b}_z + \sum_{z\in\mathcal{C}} \frac{\partial S_z(b_z,p_z)}{\partial p_z}\dot{p}_z - \sum_{z\in\mathcal{C}} \frac{\alpha}{B_z}\dot{b}_z\dot{p}_z \\
&\quad - \sum_{z\in\mathcal{C}} (1-\alpha)\mu\dot{p}_z^2 - \sum_{z\in\mathcal{C}} (B_z - b_z)\dot{b}_z \\
&\leq -\sum_{z\in\mathcal{C}} \left(\zeta_z(b_z,p_z) + (B_z - b_z)\dot{b}_z\right) \quad \text{[by Assump. 5.3.3]} \\
&\leq 0,
\end{aligned}$$

where the last inequality follows from Assumptions 5.3.1 and 5.3.3 and the fact that $b_z \leq B_z$ during the flows of the HDS, for all $z \in \mathcal{C}$. Besides, $\dot{V} = 0$ if and only if $b_z = B_z$ and $p_z = 0$, for all $z \in \mathcal{C}$. Therefore, $V(\cdot,\cdot,\cdot)$ strictly decreases along the flow trajectories of the system.

We now proceed to analyze the discrete-time change of $V(\cdot,\cdot,\cdot)$ under the jump updates of the system. We remark that the restriction for $\mathcal{C}_c(t)$ to be constant over time together with Assumption 5.3.1 imply that the state variable s_i can only jump from $s_i = 1$ to $s_i = 0$, for any CS $i \in \mathcal{C}$, i.e., jumps from $s_i = 0$ to $s_i = 1$ are not possible under the considered setup. As such, suppose that a jump from $s_z = 1$ to $s_z = 0$ occurs at an arbitrary CS $z \in \mathcal{C}$. Then,

$$\begin{aligned}
&V\left(\mathbf{b},\mathbf{p}^+,\mathbf{s}^+\right) - V\left(\mathbf{b},\mathbf{p},\mathbf{s}\right) \\
&\quad = W\left(\mathbf{b},\mathbf{p}^+,\mathbf{s}^+\right) - W\left(\mathbf{b},\mathbf{p},\mathbf{s}\right) - S_z(b_z,p_z) - \beta\bar{W} \\
&\quad < 0 \quad \text{[by construction of } \beta \text{ and } \bar{W}\text{]}.
\end{aligned}$$

Here, we have used Assumptions 5.3.1 and 5.3.3 to assert that $S_z(b_z, p_z^+) = 0$ [since $p_z^+ = 0$ by (5.12a)]. Given that the jump occurs at an arbitrary CS, we conclude that $V(\cdot,\cdot,\cdot)$ strictly decreases over the jumps of the system.

Marshalling all the conclusions above, it follows by [5, Theorem 3.19] that Claim ii) holds.

Finally, to prove Claim iii) we further restrict the analysis to the times $t \geq 0$ where the HDS flows. For such times the state vector $\mathbf{s}$ is constant, and so without loss of generality, we let $s_i = 1$, for all $i \in \mathcal{C}$. Consequently, the sets $\mathcal{C}_a(t) = \mathcal{C}$ and $\mathcal{P} := \mathcal{P}(t)$ are constant over the flow times, and the dynamics in (5.14a) become equal to the so-called Smith-Replicator dynamics in [4]. Now, let $\mathcal{W}(\mathbf{b}) = \left\{\mathbf{p} : \mathbf{p} \in \operatorname{argmax}_{\tilde{\mathbf{p}}\in\mathcal{P}} \sum_{i\in\mathcal{C}} \tilde{p}_i g_i(b_i,\mathbf{p})\right\}$. To prove Claim iii) we remark that the set $\mathcal{W}(\tilde{\mathbf{b}})$ is asymptotically stable under the dynamics in (5.14a), where $\tilde{\mathbf{b}}$ is an arbitrary (fixed) value for $\mathbf{b}(t)$ (such a claim follows immediately from [4, Theorem 2]). Since $\tilde{\mathbf{b}}$ is arbitrary, Claim iii) holds by induction for every time t. ■

A.5 Proposition 6.4.1

Consider the mapping $M : \mathbb{R}^{Nn} \to \mathbb{R}^{Nn}$ defined as follows:

$$M : \mathbf{x} \mapsto \operatorname{proj}_{\Omega} \begin{pmatrix} \Phi_1(O_1(\mathbf{s},\mathbf{x})) \\ \vdots \\ \Phi_N(O_N(\mathbf{s},\mathbf{x})) \end{pmatrix}, \tag{A.5}$$

as the observer is a nonexpansive, the feed-forward DNNs $\Phi_i(\cdot)$ are γ_i-Lipschitz continuous due to Assumption 7.3.1, and, since the projection to a convex and compact set Ω is continuous, the map $M(\cdot)$ is γ_m-Lipschitz continuous [7].

Given the continuity of $M(\cdot)$ and the convexity and compactness of Ω, it follows from Brouwer's fixed point theorem that $M(\cdot)$ has a fixed point $\mathbf{x}^* = M(\mathbf{x}^*)$. We will argue

that (6.9) holds for the fixed point $\mathbf{x}^*$. Indeed, denoting by:

$$\mathbf{z}^* = \begin{pmatrix} \Phi_1(O_1(\mathbf{s}, \mathbf{x}^*)) \\ \vdots \\ \Phi_N(O_N(\mathbf{s}, \mathbf{x}^*)) \end{pmatrix} \tag{A.6}$$

and since $\mathbf{x}^* = \text{proj}_\Omega(\mathbf{z}^*)$ and, due to a well-known propriety of projection, we have that:

$$(\mathbf{z}^* - \mathbf{x}^*)^\top (\mathbf{x}^* - \mathbf{y}) \geq 0, \quad \forall \mathbf{y} \in \Omega \tag{A.7}$$

for an arbitrary $\mathbf{x}_i \in \Omega_i$, setting $\mathbf{y} = (\mathbf{x}_i, \mathbf{x}^*_{-i})$ into the above inequality we get that:

$$(\Phi_i(O_i(\mathbf{s}, \mathbf{x}^*)) - \mathbf{x}_i^*)^\top (\mathbf{x}_i^* - \mathbf{x}_i) \geq 0 \tag{A.8}$$

thus we have:

$$(\Phi_i(O_i(\mathbf{s}, \mathbf{x}^*)) - \mathbf{x}_i^*)^\top (\mathbf{x}_i^* - \mathbf{x}_i) \geq 0, \quad \forall \mathbf{x}_i \in \Omega_i \tag{A.9}$$

which is equivalent to (6.9). ■

References

[1] Bernstein, D. S., *Matrix Mathematics: Theory, Facts, and Formulas (Second Edition)*. Princeton University Press, 2009. DOI: doi:10.1515/9781400833344.

[2] Lee, S., Chatzipanagiotis, N., and Zavlanos, M. M., "Complexity certification of a distributed augmented lagrangian method," *IEEE Transactions on Automatic Control*, vol. 63, no. 3, pp. 827–834, 2017.

[3] Horn, R., Horn, R., and Johnson, C., *Topics in Matrix Analysis*. Cambridge University Press, 1994. [Online]. Available: https://books.google.it/books?id=LeuNXB2bl5EC.

[4] Barreiro-Gomez, J. and Tembine, H., "Constrained evolutionary games by using a mixture of imitation dynamics," *Automatica*, vol. 97, pp. 254–262, 2018. DOI: https://doi.org/10.1016/j.automatica.2018.08.014.

[5] Sanfelice, R. G., *Hybrid feedback control*. Princeton University Press, 2021.

[6] Martinez-Piazuelo, J., Quijano, N., and Ocampo-Martinez, C., "Nash equilibrium seeking in full-potential population games under capacity and migration constraints," *Automatica*, vol. 141, p. 110 285, 2022. DOI: 10.1016/j.automatica.2022.110285.

[7] Eriksson, K., Johnson, C., Estep, D., Eriksson, K., Johnson, C., and Estep, D., "Vector-valued functions of several real variables," *Applied Mathematics: Body and Soul: Calculus in Several Dimensions*, pp. 789–814, 2004.